

1988

# Computer simulation of progressive failure in soil slopes

Carlo Ernest Bertoldi  
*University of Wollongong*

---

## Recommended Citation

Bertoldi, Carlo Ernest, Computer simulation of progressive failure in soil slopes, Doctor of Philosophy thesis, Department of Civil and Mining Engineering, University of Wollongong, 1988. <http://ro.uow.edu.au/theses/1232>

Research Online is the open access institutional repository for the University of Wollongong. For further information contact Manager Repository Services: [morgan@uow.edu.au](mailto:morgan@uow.edu.au).

## **NOTE**

This online version of the thesis may have different page formatting and pagination from the paper copy held in the University of Wollongong Library.

## **UNIVERSITY OF WOLLONGONG**

### **COPYRIGHT WARNING**

You may print or download ONE copy of this document for the purpose of your own research or study. The University does not authorise you to copy, communicate or otherwise make available electronically to any other person any copyright material contained on this site. You are reminded of the following:

Copyright owners are entitled to take legal action against persons who infringe their copyright. A reproduction of material that is protected by copyright may be a copyright infringement. A court may impose penalties and award damages in relation to offences and infringements relating to copyright material. Higher penalties may apply, and higher damages may be awarded, for offences and infringements involving the conversion of material into digital or electronic form.

COMPUTER SIMULATION OF  
PROGRESSIVE FAILURE IN SOIL SLOPES

A thesis submitted in fulfilment of the  
requirements for the award of the degree of

DOCTOR OF PHILOSOPHY

from

THE UNIVERSITY OF WOLLONGONG

by

CARLO ERNEST BERTOLDI, B.E. (Hons) N.S.W. (Civil)

DEPARTMENT OF CIVIL AND MINING ENGINEERING

1988

## **STATEMENT**

I hereby certify that the work presented in this thesis has not been submitted for a degree to any other university or similar institution.

---

C.E. BERTOLDI

## ABSTRACT

This thesis is concerned with the simulation of progressive failure within soil slopes considering, as a basis, the widely accepted concept of limit equilibrium. In particular, the investigations reported here concern the influence of strain-softening on the overall safety factor, the identification of local failures and the propagation of failure within a slope. Several methods of analysis were developed and successfully implemented. A number of case histories were analysed using these methods and the influence of progressive failure evaluated. Some of these methods take the initial stress field into consideration.

Theories of progressive failure are often based on the well established mechanism of strain-softening associated with soils. The extent of strain-softening at different locations within a slope or along a slip surface is generally unknown. Complete strain-softening (a residual factor of one) along a slip surface must occur after overall failure of a slope and, if no overstress has occurred anywhere and relative deformations have been small, no strain-softening would have occurred (a residual factor of zero). These are the limiting cases and thus the overall residual factor may have a value between zero and unity. More importantly, the local residual factor (as distinct from the overall residual factor) may vary from point to point along a slip surface.

A method of simulation was developed to study the factor of safety of a slope considering any arbitrary distribution of the local residual factor along the potential slip surface. Typical distributions represent failure initiating from the crest of a slope or the toe of a slope or from somewhere in the interior. The effect of the type of shear strength distributions on the factor of safety was examined. Moreover, a relationship between the average shear strength and the factor of safety was established. Criteria for acceptability of rigorous (Morgenstern and Price type) methods of slices were highlighted.

A number of methods for simulating local failure and its propagation were developed. In these methods the excess shear stress resulting from strain-softening of failed segments of the slip surface must be redistributed to other segments. Once this redistribution occurs, more segments may fail and then further redistribution occurs. This process of progressive failure continues until no more failures occur. At that stage the factor of safety is the lowest one associated with progressive failure. In one of the methods an assumption is made on the manner of this redistribution e.g. uniform distribution over the segments or linear distribution with its maximum near the last failed segment. In other methods no such assumption is made and the new 'failed' segments are identified during successive limit equilibrium calculations, one for the stage corresponding to no failures and the other for the stage with initial local failures. Considering all the failed segments, a new analysis is made and, comparing this with the previous one, further local failures may be identified. In this way, the iterative technique enables the simulation of the progressive failure process and the associated redistribution of shear stress occurs automatically.

It is well known that an initial stress field in a slope may have a significant influence on its stability. Therefore, it was considered appropriate to develop methods of analysis of progressive failure which took a given initial stress field into consideration. Two different approaches were considered for the development of these methods. The first approach is to consider the initial stress field in the identification of local failures and then to follow up with methods similar to those mentioned in the previous paragraph. The second approach is to simulate progressive failure as a transformation from the initial stress field to the stress field associated with limit equilibrium. In the latter case two different types of analysis are required for two parts of a sloping mass at each stage of progressive failure. As the failure progression process continues, the relative size of these masses changes. The interaction between the two masses is taken into consideration by including the limiting earth pressures as extreme cases of possible interaction.

The successful implementation of all the methods is demonstrated in relation to a number of case histories. The influence of progressive failure on the stability is influenced not only by the soil shear strength and brittleness but also by slope and slip surface geometry. The initial stress field may have a significant influence on the extent of progressive failure.

## ACKNOWLEDGEMENTS

The author wishes to thank the chairman and staff of the Department of Civil and Mining Engineering at the University of Wollongong for their assistance and for study and research facilities provided during the research and computer work related to this thesis. In particular, the author wishes to thank his supervisor, Dr. R.N. Chowdhury, for the ongoing assistance and advice provided over the years and especially for his assistance in compiling the final draft of this thesis.

Special acknowledgement is made of the encouragement and help provided by Dr. G.J. Montagner of the Department of Mechanical Engineering and Dr. Y.W. Wong of the Department of Civil and Mining Engineering.

Most of the computer programming and analysis work was carried out on the University of Wollongong UNIVAC computer. The author would, therefore, like to thank the staff of the University of Wollongong Computer Centre, especially Mr. Ian Piper for his assistance with many computer related problems.

In addition, the author gratefully acknowledges the assistance of those persons who, at various stages, transferred handwritten sections of this thesis into computer files for eventual processing into this finished document.

Finally, but certainly not in the least, the author wishes to thank his wife, Manuela, and his and her families for the ongoing support and encouragement received which led to the completion of this thesis.



CONTENTS

	Page
ABSTRACT . . . . .	i
ACKNOWLEDGEMENTS . . . . .	iv
CONTENTS . . . . .	v
FIGURES . . . . .	xii
CHAPTER 1: INTRODUCTION AND SCOPE . . . . .	1-1
1.1 The Slope Stability Problem . . . . .	1-1
1.2 The Relevance of Progressive Failure . . . . .	1-2
1.3 The Range of Slope Analysis Approaches . . . . .	1-3
1.4 The Role of the Finite Element Method . . . . .	1-4
1.5 The Probabilistic Approach . . . . .	1-7
1.6 Scope of this Thesis . . . . .	1-9
CHAPTER 2: CONVENTIONAL LIMIT EQUILIBRIUM METHODS OF STABILITY ANALYSIS . . . . .	2-1
2.1 Introduction . . . . .	2-1
2.1.1 The Fellenius method or the ordinary method of slices (also known as the swedish method of slices) . . . .	2-7
2.1.2 The Bishop simplified method . . . . .	2-10
2.1.3 Janbu's method of analysis . . . . .	2-11
2.1.4 The Morgenstern-Price method . . . . .	2-13
2.2 General Comments on Limit Equilibrium Methods of Analysis .	2-15

**CHAPTER 3: PROGRESSIVE FAILURE AND THE CONCEPT OF RESIDUAL**

<b>STRENGTH</b>	<b>3-1</b>
3.1 General	3-1
3.2 Definitions of Progressive Failure	3-3
3.3 Residual Strength	3-3
3.4 Conditions Necessary for Progressive Failure	3-7
3.5 The Residual Factor	3-9
3.6 Reduction of Shear Strength	3-10
3.7 Mechanisms of Progressive Failure	3-12
3.7.1 General notes on progressive failure mechanisms	3-12
3.7.2 Bjerrum's comments on the mechanism of progressive failure	3-15
3.7.3 Skempton's approach to progressive failure	3-16
3.7.4 Bishop's approach to progressive failure	3-17
3.8 Concluding Remarks	3-19

**CHAPTER 4: SIMULATION OF VARIABLE SHEAR STRENGTH MOBILISED**

<b>ALONG A SLIP SURFACE</b>	<b>4-1</b>
4.1 Aim and Scope	4-1
4.2 Variation of Shear Strength Approach	4-2
4.2.1 Definition of residual factor in this research	4-2
4.2.2 Proposed method for generating local residual factor distributions	4-3
4.2.3 Proposed approach - variable mobilisation of $c'$ and $\phi'$	4-6
4.2.4 Types of distributions assumed	4-7
4.2.5 Basis of solution method	4-8
4.2.6 Calculation of average shear strength along failure surface	4-9

4.3	Computer Programming Considerations . . . . .	4-9
4.3.1	Program MGSTRN for general stability analysis . . . .	4-9
4.3.2	Program MGSPROG for variation of $c'$ and $\phi'$ along slip surface . . . . .	4-11
4.3.3	Program MGSDIST for calculation of average shear strength . . . . .	4-13
4.3.4	Program BISHDIST for varying $c'$ and $\phi'$ using Bishop's method of analysis . . . . .	4-15
4.3.5	Calculation of distribution parameters $a, b, c$ and $d$ .	4-16
4.3.6	A significant difficulty encountered using the programs and how this was tackled . . . . .	4-17
4.4	Slopes and Types of Analyses Considered . . . . .	4-18
4.4.1	Northolt slip in cutting . . . . .	4-18
4.4.2	Vajont slide . . . . .	4-19
4.4.3	Brilliant Cut slide . . . . .	4-20
4.4.4	Hypothetical slip number 1 . . . . .	4-21
4.5	Results and Discussion . . . . .	4-21
4.5.1	Solution admissibility - a new proposal . . . . .	4-21
4.5.2	Northolt slip in cutting . . . . .	4-22
4.5.3	The Vajont slide . . . . .	4-28
4.5.4	The Brilliant Cut slide . . . . .	4-30
4.5.5	Hypothetical slip number 1 . . . . .	4-32
4.6	Relationship between Local and Overall Residual Factor . . .	4-33
4.6.1	$R_1$ defined in terms of mobilised shear strength at a point . . . . .	4-33
4.6.2	$R_1$ defined in terms of mobilised shear strength parameters $c$ and $\phi$ at a point . . . . .	4-34
4.7	Relationship between Overall Residual Factor $R$ and Factor of Safety $F$ . . . . .	4-36
4.8	Summary and Conclusions . . . . .	4-39

**CHAPTER 5: STRAIN SOFTENING – LOCAL FAILURE AND STRESS**

<b>REDISTRIBUTION</b>	<b>5-1</b>
5.1 Introduction	5-1
5.2 Bjerrum's Approach to Strain Softening and Progressive Failure	5-1
5.3 Law and Lumb's Strain Softening Approach to Progressive Failure	5-6
5.4 Effects of Crack Propagation in Progressive Failure	5-11
5.5 Other Research Related to the Concept of Strain Softening	5-14

**CHAPTER 6: SIMULATION OF PROGRESSIVE FAILURE BY LOCALISED STRAIN**

<b>SOFTENING</b>	<b>6-1</b>
6.1 Introduction and Scope	6-1
6.2 Redistribution of Excess Shear (Method 1)	6-2
6.2.1 Description of simulation procedure: uniform redistribution of excess shear	6-3
6.2.2 Description of alternate procedure: linear redistribution of excess shear	6-7
6.2.3 Definition of propagation factor	6-11
6.2.4 Computer program STRAIN1	6-11
6.2.5 Case histories considered	6-15
6.2.6 Results and discussion	6-17
6.3 Calculation of Overall Factor of Safety by Iterative Methods (Method 2)	6-20
6.3.1 Iterative methods of analysis used	6-20
6.3.2 Computer program BSTRAIN2	6-21
6.3.3 Computer program MPSTRAIN2	6-21
6.3.4 Results and discussion	6-22
6.4 Alternate Method for Redistribution of Excess Shear (Method 3)	6-26
6.4.1 General description of method	6-26

6.4.2	Description of computer program BSTRAIN3 . . . . .	6-29
6.4.3	Description of computer program MPSTRAIN3 . . . . .	6-30
6.4.4	Results and discussion . . . . .	6-30
6.5	Redistribution of Normal and Shear Forces using the Concept of Virtual Weight (Method 4) . . . . .	6-33
6.6	General Description of Method . . . . .	6-34
6.6.1	Computer programs BSTRAIN4 and MPSTRAIN4 . . . . .	6-36
6.6.2	Results and discussion . . . . .	6-37
6.7	Summary and Conclusions . . . . .	6-37
 <b>CHAPTER 7: THE CONCEPT OF INITIAL STRESS . . . . .</b>		<b>7-1</b>
7.1	Introduction and General Comments . . . . .	7-1
7.2	Simulation of 'Failure' Development in Clays . . . . .	7-2
7.3	Other Findings Related to the Initial Stress Concept . . . . .	7-5
7.4	Initial Stresses Components . . . . .	7-7
7.4.1	Definition of conjugate stress ratio . . . . .	7-7
7.4.2	Calculation of initial stresses in an inclined slope . . . . .	7-7
7.4.3	Effective stress considerations . . . . .	7-9
 <b>CHAPTER 8: INITIAL STRESS CONSIDERATIONS IN THE SIMULATION OF PROGRESSIVE FAILURE . . . . .</b>		<b>8-1</b>
8.1	General . . . . .	8-1
8.2	Simulation of Failure Considering both Strain Softening and Initial Stresses . . . . .	8-2
8.2.1	Description of method . . . . .	8-2
8.2.2	Modification of computer program BSTRAIN2 . . . . .	8-5
8.2.3	Case histories considered for analysis . . . . .	8-6
8.2.4	Results and discussion . . . . .	8-6

8.3	Simulation of Progressive Failure by Sequential Local Failure of Soil Slices . . . . .	8-8
8.3.1	General description of method . . . . .	8-9
8.3.2	Details of methods used . . . . .	8-11
8.3.3	Use of conjugate stress ratio . . . . .	8-14
8.3.4	Direction of propagation of failure . . . . .	8-14
8.3.5	Definition of propagation factor . . . . .	8-15
8.4	Boundary Condition Considerations . . . . .	8-16
8.4.1	Different modes for treatment of boundaries . . . . .	8-16
8.4.2	Consideration of forces at boundaries . . . . .	8-17
8.4.3	Consideration of active and passive earth pressures . . . . .	8-18
8.4.4	Calculation of factor of safety considering earth pressures at the imaginary vertical boundary . . . . .	8-19
8.4.5	Results and discussion . . . . .	8-22
8.4.6	Conclusions concerning comparative study . . . . .	8-22
8.5	Calculation of Overall Factor of Safety . . . . .	8-24
8.5.1	Case histories considered . . . . .	8-25
8.5.2	Results and discussion . . . . .	8-25
8.6	Summary and Conclusions . . . . .	8-28
<b>CHAPTER 9: SUMMARY AND CONCLUSIONS . . . . .</b>		<b>9-1</b>
9.1	Introduction . . . . .	9-1
9.2	Progressive Failure Concepts . . . . .	9-1
9.3	Relationship between Shear Strength Distribution and Factor of Safety . . . . .	9-3
9.4	Progression of Failure Considering Strain Softening . . . . .	9-5
9.5	Incorporation of Initial Stresses . . . . .	9-8
9.6	Concluding Remarks . . . . .	9-11

<b>APPENDIX A: DESCRIPTION OF SLOPES USED IN CASE HISTORIES . . . .</b>	<b>A-1</b>
A.1 Northolt Slip in Cutting . . . . .	A-1
A.2 Selset Landslide . . . . .	A-4
A.3 Sudbury Hill Slip in Cutting . . . . .	A-5
A.4 The Jackfield Slide . . . . .	A-6
A.5 The Balgheim Slide . . . . .	A-7
A.6 The Vajont Slide . . . . .	A-9
A.7 The Saskatchewan Slide . . . . .	A-10
A.8 The Brilliant Cut Slide . . . . .	A-11
A.9 Hypothetical Slip Number 1 . . . . .	A-13
A.10 Hypothetical Slip Number 2 . . . . .	A-14
 <b>APPENDIX B: RESIDUAL FACTOR DISTRIBUTIONS USED IN CHAPTER 4 . . .</b>	 <b>B-1</b>
B.1 Profiles of Residual Factor Distributions . . . . .	B-1
B.2 Residual Factor Coefficients used in Equation (4.3) . . . .	B-3
 <b>APPENDIX C: ADDITIONAL INFORMATION ON COMPUTER PROGRAM MGSTRN . .</b>	 <b>C-1</b>
C.1 Brief Description of Subroutines . . . . .	C-1
C.2 Input Data Required for Program . . . . .	C-3
C.3 Column Headings for Detailed Force Output . . . . .	C-6
C.4 Schematic Layout of MGSTRN Program . . . . .	C-7
 <b>APPENDIX D: BIBLIOGRAPHY . . . . .</b>	 <b>D-1</b>

# **FIGURES**

	Page
Fig. 2.1 Forces acting on a typical slice . . . . .	2-5
Fig. 2.2 Forces acting on a typical slice using Janbu's method	2-12
Fig. 3.1 Strain softening curve suggested by Skempton . . . . .	3-4
Fig. 3.2 Idealised strain softening curve suggested by Lo and Lee . . . . .	3-5
Fig. 3.3 Shearing characteristics of clays (Skempton) . . . . .	3-6
Fig. 3.4 Stress and deformation characteristics in Lake Agassiz clay (Conlon) . . . . .	3-14
Fig. 3.5 $R_1$ distributions suggested by Bishop . . . . .	3-19
Fig. 4.1 Sample $R_1$ distribution . . . . .	4-5
Fig. 4.2 Slope cross-section with typical slice coordinates . .	4-13
Fig. 4.3 Slope cross-section with angles used in BISHDIST . . .	4-17
Fig. 4.4 Factor of safety vs. average shear strength on slip surface for Northolt slip - analysis group A . . . . .	4-23
Fig. 4.5 General form of shear strength distribution . . . . .	4-25
Fig. 4.6 Factor of safety vs. average shear strength on slip surface for Northolt slip - analysis group B . . . . .	4-28
Fig. 4.7 Factor of safety vs. average shear strength on slip surface for Vajont slide . . . . .	4-29
Fig. 4.8 Factor of safety vs. average shear strength on slip surface for Brilliant Cut slide . . . . .	4-31
Fig. 4.9 Factor of safety vs. average shear strength on slip surface for arbitrary slip surface - analysis group A	4-33
Fig. 4.10 Relationship between F and R . . . . .	4-37
Fig. 4.11 Relationship between F, $s_{av}$ and R . . . . .	4-38



Fig. 5.1	Development of continuous sliding surface by progressive failure (Bjerrum) . . . . .	5-2
Fig. 5.2	Cross-section of slope considered by Law and Lumb . .	5-7
Fig. 5.3	Forces acting on a typical slice using Law and Lumb's technique . . . . .	5-8
Fig. 5.3	Slope cross-section showing method of Romani et. al. .	5-12
Fig. 5.5	Results obtained by Romani et. al. . . . .	5-14
Fig. 6.1	Cross-section through a hypothetical failure mass with failure starting from centre of mass . . . . .	6-8
Fig. 6.2	One-dimensional representation of failure surface showing stress redistribution profile . . . . .	6-8
Fig. 6.3	Flowchart for program STRAIN1 . . . . .	6-13
Fig. 7.1	Changes in stress during excavation (from Duncan and Dunlop) . . . . .	7-3
Fig. 7.2	Effect of initial stress on development of failed regions (from Dunlop and Duncan) . . . . .	7-4
Fig. 7.3	Development of failure zones in overconsolidated and normally consolidated clay layers (Dunlop and Duncan)	7-5
Fig. 7.4	In-situ stresses within a natural slope . . . . .	7-8
Fig. 8.1	Typical slope cross-section showing propagation of failure . . . . .	8-9
Fig. 8.2	Slope cross-section during progression of failure using tension crack approach . . . . .	8-17
Fig. 8.3	Slope cross-section showing boundary forces considered	8-18
Fig. 8.4	Slope cross-section showing active and passive earth pressure components . . . . .	8-20
Fig. 8.5	Boundary force considerations for progressive failure starting from bottom of slope . . . . .	8-23
Fig. 8.6	Boundary force considerations for progressive failure starting from top of slope . . . . .	8-23
Fig. 8.7	Variation in factor of safety with different modes of propagation (Northolt slide) . . . . .	8-26

Fig. 8.8	Variation in factor of safety with different values of K (Northolt slide) . . . . .	8-27
Fig. 8.9	Variation in factor of safety with different modes of propagation (Vajont slide) . . . . .	8-29
Fig. 8.10	Variation in factor of safety with different values of K (Vajont slide) . . . . .	8-29
Fig. 8.11	Variation in factor of safety with different modes of propagation (hypothetical slip 1) . . . . .	8-30
Fig. 8.12	Variation in factor of safety with different values of K (hypothetical slip 1) . . . . .	8-30
Fig. A.1	Northolt slip in cutting . . . . .	A-2
Fig. A.2	Selset landslide . . . . .	A-4
Fig. A.3	Sudbury hill slip in cutting . . . . .	A-5
Fig. A.4	Jackfield slide . . . . .	A-7
Fig. A.5	Balgheim slide . . . . .	A-8
Fig. A.6	Vajont slide eastern central slope . . . . .	A-9
Fig. A.7	Saskatchewan slide . . . . .	A-11
Fig. A.8	Brilliant Cut slide . . . . .	A-12
Fig. A.9	Hypothetical slip number 1 . . . . .	A-13
Fig. A.10	Hypothetical slip number 2 . . . . .	A-15

## CHAPTER 1

### INTRODUCTION AND SCOPE.

#### 1.1 THE SLOPE STABILITY PROBLEM.

In the study of soil mechanics it is often necessary to assess the stability of slopes or to predict the likelihood of failure of a body of soil with a sloping surface. The soil mass under consideration may be part of a natural slope or it may be a man-made slope such as a cutting or embankment. The assessment of stability is important both from the point of view of identifying potentially unstable areas or zones in existing slopes and for the design of new slopes. For engineers it is often necessary to consider the integrity and future performance of slopes associated with planned engineering constructions.

Since the earliest attempts at the mathematical and numerical analysis of the stability of earth slopes, engineers have been plagued with inconsistencies and discrepancies in the results obtained. There have been difficulties concerned with the modelling of specific situations and uncertainties with respect to relevant soil properties to be incorporated in any analysis. For example, an engineer must decide whether and when to use a 'total stress' type of analysis rather than an 'effective stress' one. Decisions must be made about the magnitudes of shear strength parameters which will be mobilised in the field. The results of laboratory tests on small samples or a limited number of field tests often form the basis of these decisions. Moreover, in each test the mobilised shear stress is a function of strain, and interpretation of the 'failure shear stress' is largely left to the judgement of the geotechnical engineer.

The difficulties faced by slope engineers are not limited to complex slope stability problems. Even apparently 'straight forward' cases of failure have not been successfully explained by existing methods of analysis. Therefore, the accuracy of these methods in simulating field behaviour has to be questioned. Moreover, many cases have been reported of slopes which had at some stage been analysed and classified as 'safe' but which did, in fact, fail.

## 1.2 THE RELEVANCE OF PROGRESSIVE FAILURE.

Existing methods of slope stability analysis have not proved to be sufficient for a complete understanding of the performance of slopes and of the factors influencing their stability. Conventional methods of analysis are still popular and widely accepted; yet their limitations are increasingly being emphasised in the literature. The development and use of stress analysis methods such as the finite element method has, in some cases, facilitated slope engineering. Probabilistic methods have also been developed to supplement conventional methods of analysis. Yet, conventional limit equilibrium remains the dominant basis of most studies related to slopes.

These methods tend to take a 'snapshot' or 'static' perspective whereby an analysis is performed for assumed conditions existing at a certain instant in time without sufficient consideration of (a) the spatial differences and local effects within a soil mass, (b) the changes which may occur as a result of stress concentrations and localised failures, and (c) time-dependent characteristics which may influence stability within the design period or life of a slope.

Most importantly, all limit equilibrium methods assume that 'failure' or the assumed condition of 'limit equilibrium' occurs simultaneously within a soil mass. Thus the factor of safety is regarded explicitly or by implication to be constant over the extent of the surface forming the lower boundary of the potential sliding mass. Thus 'progressive effects' are either ignored completely or given inadequate consideration.

The need to consider progressive effects is highlighted by tests which have shown that significant soil properties (such as the shear strength parameters of the soil along an actual slip surface) have values after failure which are different to those measured before failure. Cases have been documented where post-failure values of the shear strength parameters of the soil were significantly lower than the corresponding pre-failure values. Also, the shear strength values mobilised at different points along a slip plane have been measured as increasing or decreasing in a particular direction.

Such evidence would tend to support some form of progressive mechanism which is responsible for these changes in shear strength, spatially and over time. The concept of 'progressive failure' may explain some of the slips or landslides or failures of slopes which were predicted to be safe or stable on the basis of conventional stability analyses.

Many investigators have regarded it as highly likely that shear failure does not occur simultaneously over the entire slope. One may visualise a number of small or localised failures at different locations and the progression of this local failure from one location to another within the slope. After a significant length of the failure surface has been involved in some sort of progressive mechanism, the overall factor of safety of the slope may reduce to unity and there could be a slide or slip.

### 1.3 THE RANGE OF SLOPE ANALYSIS APPROACHES.

At this stage it is relevant to consider very briefly the different slope analysis approaches which are available to the geotechnical engineer today. With this background, the scope of this thesis will then be outlined.

First of all, one must distinguish between the two main approaches to analytical geomechanics available today, i.e.,

(a) the deterministic approach,

and (b) the probabilistic approach.

The conventional deterministic approach has held sway in geomechanics from the very beginning of individual developments which led to the consolidation of soil mechanics as a discipline in its own right. In respect of slope stability analyses, the significant deterministic methods have been as follows:

- (a) Plasticity solutions
- (b) Limit Equilibrium methods
- (c) Stress Analysis methods and especially the Finite Element method of stress deformation analysis.

There are very few plasticity solutions relevant to real slope stability problems and most attention has been devoted to limit equilibrium methods. A separate chapter is, therefore, devoted to these methods. In the following section a very brief reference is made to the role of the finite element method in slope analysis. Further consideration will, however, be given to the stress deformation approach while discussing the role of initial stress state in the performance of slopes in chapter 7. After introducing the finite element method, a brief reference to probabilistic methods will be made before outlining the scope of this thesis.

#### 1.4 THE ROLE OF THE FINITE ELEMENT METHOD.

The assumption of linear elasticity has often been made to obtain solutions to geomechanics problems. The application of such solutions is valid in some situations but only under working loads considering high factors of safety. Few elastic solutions are available for slope stability problems and, in any case, results of analyses of slope stability problems on the basis of linear elasticity would be of limited value. The behaviour of any real soil is non-linear and

stress-dependent. For geomechanics problems involving collapse or failure of a soil mass, plasticity solutions have proved to be useful. However, as stated earlier, few solutions relevant to real slope stability problems have been obtained.

Against this background, the development of the finite element method of stress deformation analysis was a major benefit to research and practice in geomechanics. The finite element approach is a versatile tool of numerical analysis which has developed rapidly and which has been applied with great success in all branches of engineering. In fact, stress-deformation analysis is the aim of only one class of finite element methods.

For stress-deformation problems related to any continuum, the finite element method can handle complex geometrical configurations and boundary conditions, any number of material types, anisotropy, non-linearity and stress-dependent behaviour. Therefore, its value in geomechanics cannot be over-emphasised. A continuum is subdivided into a number of elements separated by imaginary lines or planes and joined together at a number of nodal points forming the corners of the elements. A choice may be made about the shape of the elements and their sizes can vary from one region of the continuum to another.

The displacement formulation is popular in structural and geomechanics problems and in this formulation a choice is made as to the variation of displacement within each element. The boundary loads, the body forces, and boundary deformation conditions are specified. The results for stresses, strains and displacements are obtained for the whole region.

The accuracy of the results depends not only on the choice of element sizes and shapes and the assumed displacement functions but also on the manner in which the material behaviour has been idealised. For example, a soil mass may be idealised as a linearly elastic material and the formulation would then have the great advantage of simplicity. One could consider complex geometry and many soil layers and even anisotropy without significant changes to the basic formulation. However, as stated earlier, elastic solutions are often of very limited value in geomechanics and this is particularly true

for slope stability problems.

With further developments in the finite element method, and advances in the understanding of soil behaviour, the way has been opened up for more realistic studies of stresses and deformations and earth media. The effects of various stress paths or loading sequences can be considered. Also, incremental loading and unloading can be simulated. These features of any stress-deformation approach are of great value in geomechanics where body forces are often the most important. Many studies have been made to follow the growth of failure zones within a soil mass either on the assumption of soil behaviour as elastic-plastic or on the basis of some non-linear stress-strain relationships. The feasibility of modelling discontinuities and discontinua in general has also been investigated.

The rapid development of computers has facilitated the application of the finite element method. As the versatility and sophistication of the finite element formulation is improved, the need for powerful or fast computation increases. Even if the availability of a powerful computer is taken for granted, there are serious limitations to the use of such sophisticated methods of analysis. The more versatile and comprehensive the formulation, the greater is the input data required. For linear-elastic, isotropic analysis only two elastic parameters are required to model each type of soil but for a material with transverse isotropy, for example, this number increases to five.

To model soil as a non-linear material whose behaviour is stress-dependent as well, the number of parameters, even for the isotropic assumption, is significantly greater than that for an elastic material. Often there is not enough data available to obtain the values of required parameters. The success of the finite element approach also depends on the accuracy of the deformation parameters which are required in addition to the shear strength parameters. In limit equilibrium slope stability analyses, on the other hand, deformation parameters are not required at all. Moreover, quantitative information about the initial stress state is of key importance in finite element analyses of natural slopes and excavations. Again, this is not required for conventional limit



equilibrium calculations. The usefulness of an initial stress approach in modelling progressive change in stability on the basis of a limit equilibrium type analysis will, however, be discussed in the concluding part of this thesis.

Although the finite element approach allows step-by-step simulation of slope formation, the simulation of slip surface formation and critical equilibrium has not been demonstrated. Even the prediction of overall slope failure is not easy. Moreover, the calculation of an overall safety factor for the general case of a 'stable slope' still requires some form of limit equilibrium calculation after the stresses and deformations have been computed on the basis of a finite element analysis. A refined and comprehensive analysis may enable the growth of 'failed' zones to be simulated. Yet, because of complexity and also because of the quantity and quality of input data required, such an approach is seldom feasible in most slope stability work.

Even in situations where there are enough resources available for performing significant finite element studies and for obtaining relevant data based on comprehensive investigations, limit equilibrium slope stability analyses are still considered essential. Therefore, at best, finite element studies, which are indeed very useful, may be used to supplement limit equilibrium studies.

## 1.5 THE PROBABILISTIC APPROACH.

During the last two decades there has been an increasing recognition of uncertainties in geotechnical engineering. Geotechnical parameters may be regarded as random variables and not single-valued quantities or constants. The parameter values used in conventional deterministic studies are single-valued estimates of these variables based on available data and engineering judgement. The factor of safety of a slope calculated on the basis of these single-valued estimates is itself a random variable. Therefore, a factor of safety greater than unity does not indicate absolute stability. In fact, an interpretation of the calculated values of the

factor of safety requires a different perspective from the one of deterministic soil mechanics. There is an increasing acceptance that the framework of statistics and probability can prove to be very useful. Such a framework allows a logical analysis of various uncertainties which may be due to many factors such as:-

- (a) Spatial variability of soil properties.
- (b) Spatial variability of pore water pressures.
- (c) Testing errors in both field and laboratory tests.
- (d) Modelling errors for geotechnical parameters.
- (e) Idealisations required in development of geotechnical models and methods of analysis and related uncertainties in choice of model.

According to Yuceman, Tang and Ang [115] there are three main types of applications of statistics and probability in geotechnical engineering.

1. Statistical methods for estimating soil parameters for the development of empirical relations for various soil properties. Fitting probability distributions to soil data and performing regression analyses on soil properties are two of the more common examples of this type of application.
2. Probabilistic methods for calculating the probability of failure of a structure such as a soil slope and hence also the probability of success or reliability.
3. Concepts and methods relevant to statistical decision theory.

Slope stability studies have been carried out over a number of years within the framework of statistics and probability, and recent developments have been reported by Chowdhury [30]. It is interesting

to note that limit equilibrium slope stability models are almost invariably the basis for probabilistic formulations. Therefore, further development of limit equilibrium methods will also facilitate the improvement and development of probabilistic approaches related to slope stability. The feasibility and scope of progressive failure studies on a probabilistic basis has been demonstrated by Chowdhury and A-Grivas [32], Tang, Chowdhury and Sidi [100], and Chowdhury [30],[31].

The subject of this thesis is simulation of progressive failure and it is treated within a deterministic framework. The time is not yet ripe to dispense with the conventional framework for complex phenomena involving slope stability and especially progressive failure. However, these developments are relevant to probabilistic approaches as well which will no doubt be influenced in their own development. It must be emphasised that at this point in the development of soil mechanics, deterministic and probabilistic studies are regarded as complementary.

## 1.6 SCOPE OF THIS THESIS.

For several decades, significant work has been carried out by researchers in areas of geomechanics related to the phenomena of 'progressive failure'. Basic concepts have been explained and attempts have been made to study the possible influence of progressive failure on slope stability. However, few detailed limit equilibrium studies have been made which incorporate the simulation of progressive failure.

The main aims of the work reported in this thesis have been as follows:

- (a) to review limit equilibrium methods.
- (b) to review the principles and concepts relevant to the understanding of progressive phenomena related to slopes.

- (c) to study the influence of mobilisation of shear strength along a slip surface on the computed factor of safety assuming widely differing distributions of mobilised shear strength between the limits of 'peak' and 'residual' shear strength.
- (d) to discuss approaches for simulation of progressive failure and to develop detailed methods and procedures for their implementation within the framework of limit equilibrium.
- (e) to consider the relevance of the initial stress state to slope stability and to develop simple limit equilibrium type procedures for simulating progressive failure taking the initial stress state into consideration.
- (f) to analyse well-documented case histories on the basis of progressive failure concepts.

A major part of this work has been concerned with the development of computer programs for slope stability analysis with provision for simulating progressive failure and stress redistribution. Both so called 'simplified' and 'rigorous' limit equilibrium methods have been used as a basis for the development of these computer programs. Based on these proposed methods, simulations have been carried out for well-known cases of slope failure and the results are discussed where appropriate. The main conclusions are again reviewed in the concluding chapter of this thesis.

The use of stress-deformation methods such as the finite element method is relevant to slope stability and progressive failure as discussed in an earlier section. However, further development of the stress-deformation approach is outside the scope of this thesis.

The work presented in this thesis was not concerned with time effects such as

- (a) the time rate of any shear strength decrease that may occur in some soils, or
- (b) the rate at which pore pressure equilibrium occurs in excavated slopes.

Consequently the prediction of time to failure is outside the scope of this thesis. Using the methods described here, it would certainly be feasible to simulate the factor of safety as a function of completed slope height and of pore water pressure which fluctuates with time. These would be legitimate extensions of this thesis and, in that sense, the work is relevant to time-related aspects of analyses related to slope stability and progressive failure.

In this context it is relevant to mention that aspects related to time of failure have been considered by several investigators e.g. Lo and Lee [61],[62] Skempton [90], Nelson and Thompson [69] and Sidharta [84].

The case histories used in this thesis are essentially those in which 'effective stress' type analyses are unquestionably appropriate. Thus the work is directly relevant to the study and simulation of slope stability in the 'long-term' and transient pore-pressures are, therefore, not considered here. However, the extension to the study of 'short-term' slope stability problems is feasible. Finally, this thesis is not concerned with search techniques for theoretical critical slip surfaces.

The concept of strain-softening is of fundamental importance to the understanding of progressive failure and, as such, both the 'peak' shear strength parameters and the 'residual' shear strength parameters are required for interpretation of progressive failure studies. In some cases, the lower bounds for shear strength parameters may be higher than their 'residual' values. Care is required in distinguishing between alternative studies in which different sets of shear strength parameters relevant to the same soil mass have been used for comparison. Several stress-redistribution techniques have been suggested and again it is necessary to distinguish between these.

Finally results have, in some cases, been obtained based on both a simplified (Bishop) and a rigorous (Morgenstern and Price) method of analysis. It is necessary to mention all these alternatives in the very beginning to emphasise the scope of the thesis and to facilitate its study.

## CHAPTER 2

### CONVENTIONAL LIMIT EQUILIBRIUM METHODS OF STABILITY ANALYSIS.

#### 2.1 INTRODUCTION.

Conventional methods of slope stability analysis are based on the concept of 'limit equilibrium' which essentially involves considerations, for a body of sloping soil, of the balance between resisting forces and disturbing forces (or between resisting moments and disturbing moments). Under certain circumstances a sloping soil mass may be on the verge of failure, a state referred to as one of 'critical' or 'limiting' equilibrium. However, in general, a slope may be stable under certain conditions and unstable under other conditions. The concept of 'limit equilibrium' is applicable regardless of the degree of safety of a soil mass under the assumed conditions. Therefore, it may be invoked for all possible equilibrium states. The aim of any method of analysis based on this concept is to get a quantitative measure of safety or of the balance between resisting and disturbing forces.

In every method of analysis based on this concept a 'free body' is considered. This is the relevant sloping body separated from the rest of the soil mass by an assumed continuous rupture surface generally called a 'slip surface'. The soil along this surface is assumed to behave as a rigid plastic material satisfying the Mohr-Coulomb failure criterion. With known body forces and any other forces acting on the free body a 'solution' may be obtained after making certain assumptions.

The main aim of the solution is to estimate the magnitude of a 'safety factor' (or 'factor of safety') for the 'free body' under consideration. The shear stresses are calculated from the applied

forces and the shear strength is calculated on the basis of (a) the normal forces acting on the slip surface, and (b) the shear strength parameters of the soil. The 'factor of safety' is generally defined as the ratio of the available shear strength to that required for exactly balancing the shear stress (or just maintaining stability). In most methods of analysis, the factor of safety is assumed to be constant all along the slip surface [58]. Various intuitive simplifying assumptions are often made and the assumption of a single rupture surface of simple shape is one of them.

Originally, methods based on the concept of limit equilibrium were developed as two-dimensional methods of analysis. Although some interesting papers on three-dimensional methods of analysis have been published, practical applications and research developments are primarily based on simple two-dimensional considerations especially for slopes composed of soil. Fredlund [44], in his review of analytical methods for slope analysis, cited results by various authors which showed that in three-dimensional analyses, the factors of safety were generally greater than in the two-dimensional case, sometimes by as much as 40%. He said that this implied that results from two-dimensional back-analyses will overestimate the strength and can lead to unsafe situations when these values are used in design. Azzouz et. al. [5], similarly found that the end effects considered in a three-dimensional stability analysis increase the factor of safety by between 7% and 30% and again, neglecting these three-dimensional effects tends to overestimate the back-calculated shear strength.

Based on observation, assumed slip surfaces of cylindrical shape in soil quickly replaced the concept of planar slip surfaces (planar slip surfaces are still relevant, however, to failures along discontinuities .. especially in rock). Slip surfaces of circular and log-spiral shape were also originally considered. In recent decades, however, most methods have been developed either for circular slip surfaces or for non-circular slip surfaces of arbitrary shape.

There are a number of implicit assumptions in these methods of analysis and according to Lo [60] the following are the most important, at least in the original context of the development of



these methods.

1. At the moment of incipient failure, every point along the failure surface, whether circular or non-circular, simultaneously attains the maximum strength, drained or undrained, as the drainage conditions dictate.
2. The undrained or drained strengths are isotropic. ie. they are independent of the direction of the applied stresses on the plane of failure.
3. The distinction in the time element between 'short-term' and 'long-term' stability refers to the drainage condition only.

Various methods of slope analysis exist which use the concept of limit equilibrium. Basically, they fall into one of the following three categories.

- (a) The friction circle method
- (b) The wedge or sliding block methods
- (c) The methods of slices

In each category, many potential failure surfaces can be considered individually in order to locate the position of the 'critical' slip surface. The critical surface is defined as one having the lowest factor of safety and, therefore, represents the surface on which failure is most likely to occur. Various techniques have been developed for automatically locating this critical slip surface. Examples of such techniques are reported by Celestino and Duncan [A9], Siegel, Kovacs and Lovell [104], and Fredlund [44].

The friction circle method consists of a procedure whereby the resultant cohesive force along a circular slip surface is replaced by a force of the same magnitude parallel to the chord of the failure arc acting at a certain distance from the centre of the circle of failure. For each trial surface equilibrium is considered either analytically or graphically. The factor of safety is defined as the ratio of the

available unit cohesion to the value of cohesion required for equilibrium. A complete description of the friction circle method is available in most literature on soil mechanics and will not be presented here as it is not relevant to this research. Several simplified methods were developed using the friction circle method (Taylor 1937,1948 , Frohlich 1951) in which assumptions were made about the distribution of normal stresses but the use is limited to cases of constant angle of internal friction over the whole failure surface. Essentially, the method is suitable only for homogeneous soils.

In the method of wedges the potential sliding mass is divided into two or more wedges by line boundaries and the conditions for force equilibrium are considered for each wedge in turn. Assuming a value for the factor of safety (say 1.0) and considering the equilibrium of the first wedge (in the two wedge case) the value of the interface force is obtained. Knowing this force, the equilibrium of the second wedge is then checked. If the forces in this wedge are not in equilibrium then the initial factor of safety estimate must be incorrect. Thus, a new assumption of the factor of safety is made and a further analysis is carried out until all wedges are in equilibrium at which point the final factor of safety is obtained. As the number of wedges increases, so does the complexity of the computational procedure.

Perhaps the most widely used of the limit equilibrium methods is the method of slices. There are actually a number of methods of analysis which come under this classification. The methods of Fellenius, Bishop, Janbu, and Morgenstern and Price are the most commonly used while others such as Sarma's method and Spencer's method are also well known. Every one of the methods in this group can handle non-homogeneous soil masses. However, some methods are suitable for slip surfaces of circular shape only while others are suitable for surfaces of arbitrary shape as well.

The method of slices was first developed by Fellenius [42] and Taylor [102],[80] , and widely used versions have since been developed by Bishop [12], Janbu [51],[52],[53] , Morgenstern and Price [68] and various others.

Basically, the method of slices consists of dividing the failure mass up into a series of vertical slices and then considering the equilibrium of each of these slices individually. This method is of great advantage where more than one soil type exists within the failure mass or where the failure mass is not circular in shape. Figure 2.1 shows a typical slice with all the forces taken into account when considering equilibrium for the slice.

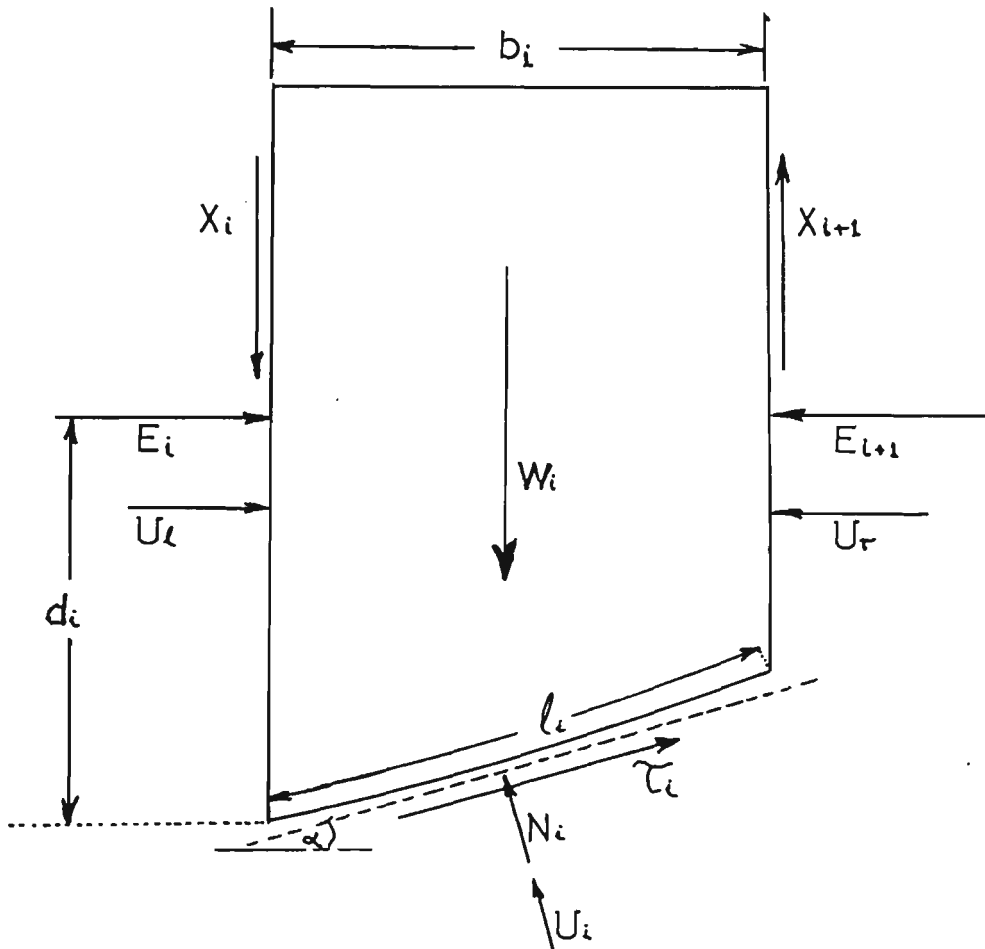


Figure 2.1 Forces Acting on a Typical Slice

The forces in figure 1 are defined as follows.

- $X_i$  = resultant of shear stresses along slice side
- $E'_i$  = resultant of normal effective stresses along slice side
- $T_i$  = resultant of shear stresses along base of slice
- $N'_i$  = resultant of normal effective stresses along base of slice
- $U_i$  = resultant of pore water pressure along left side of slice

$U_r$  = resultant of pore water pressure along right side of slice

$U_i$  = resultant of pore water pressures along base of slice

The pore water pressures are generally assumed to be known as are also the shear strength parameters. Thus for a sloping soil mass with  $n$  vertical slices the following unknowns exist.

For Force Equilibrium:

Number	Description of Unknowns
-----	-----
$n$	resultant normal forces $N'_i$ on base of each slice
1	safety factor which relates $T_i$ to $N'_i$
$n-1$	resultant normal forces, $E'_i$ , on each slice interface
$n-1$	angles $\theta_i$ which relate $X_i$ to $E'_i$
----	
$3n-1$	

For Moment Equilibrium:

$n$	coordinates $a_i$ locating the resultant $N_i$ on each slice base (distance from centre of base to where $N_i$ acts)
$n-1$	coordinates $d_i$ which define the point of application of forces $E_i$
----	
$2n-1$	

This gives a total of  $5n-2$  unknowns.

Three equations of equilibrium can be written for each slice and thus we have  $3n$  equations in total. This leaves only  $2n-2$  unknowns. If the slices are made so thin that  $a_i$  can be taken as zero we then have only  $n-2$  extra unknowns. For statical determinacy a further  $n-2$  assumptions must be made and the resulting factor of safety will thus depend on the reasonableness of the assumptions made.

The most usual assumptions made concern the forces that act against the sides of the slices (interslice forces or sidewall forces). Certain limitations exist on the way in which these assumptions are made and acceptability criteria for solutions should include the following:-

1. the shear forces on the sides of the slices cannot exceed the shear resistance of the soil.
2. the normal side forces  $E'_1$  should fall within the central third of the slice height.

There are some methods generally known as 'rigorous' methods in which the aim is to satisfy all the statical equilibrium equations and therefore suitable assumptions are made to achieve that aim while satisfying reasonable acceptability criteria. However, there are a number of well known methods which give reasonably 'correct' answers for most problems although all statical equilibrium equations are not satisfied (the word 'correct' is used here in the sense that the answers are very close to those obtained with the so-called rigorous methods in which all the equilibrium equations are satisfied). The most widely used methods in both categories are discussed in the following sub-sections.

### 2.1.1 The Fellenius Method or the Ordinary Method of Slices (also known as the Swedish Method of Slices).

In this method the interslice or sidewall forces  $T$  and  $E$  are ignored. In other words, the normal and tangential forces on the base of each slice depend only on the slice weight.

Summing the forces normal to the base of the slice we obtain

$$N'_1 + U'_1 = W_1 \cos \alpha_1 \quad (2.1)$$

or

$$N'_1 = W_1 \cos \alpha_1 - U_1$$

$$= W_i \cos \alpha_i - u_i l \quad (2.2)$$

For a circular surface of sliding the factor of safety is defined as

$$F = \frac{M_R}{M_D} = \frac{\text{Moment of Resisting forces}}{\text{Moment of Driving forces}} \quad (2.3)$$

where moments are taken about the centre of the failure arc.

For a non-circular surface of sliding however, the factor of safety can be approximated as

$$F = \frac{SF_R}{SF_D} = \frac{\text{Sum of Resisting forces}}{\text{Sum of Driving forces}} \quad (2.3a)$$

Therefore, again considering a circular surface of rupture, the factor of safety  $F$  thus becomes equal to the ratio of the moment of the shear strength along the failure surface to the moment of the weight of the failure mass.

In equation (2.3) above the moments  $M_D$  and  $M_R$  may be defined as

$$M_D = r \sum_{i=1}^n W_i \sin \alpha_i \quad (2.4)$$

and

$$M_R = r \sum_{i=1}^n (c' + \sigma'_i \tan \phi') l_i \quad \text{in general, which can simplify to}$$

$$M_R = r (c' L + \tan \phi' \sum_{i=1}^n N'_i) \quad \text{for homogeneous soil.} \quad (2.5)$$

$$\text{since } N'_i = \sigma'_i l_i$$

where  $r$  = radius of failure arc

$n$  = number of slices  
 $c'$  = cohesion intercept of soil using effective stresses  
 $\phi'$  = angle of shearing resistance using effective stresses  
 and  $L$  = the total curved length of the failure surface

Thus, for homogeneous and non-homogeneous soil the respective expressions for  $F$  are:

$$F = \frac{c'L + \tan\phi' \sum N'_i}{\sum W_i \sin\alpha_i} \quad (2.6)$$

and

$$F = \frac{\sum (c'l_i + \tan\phi' \cdot N'_i)}{\sum (W_i \sin\alpha_i)} \quad (2.6a)$$

Combining equations (2.1) and (2.6) we obtain

$$F = \frac{c'L + \tan\phi' \sum (W_i \cos\alpha_i - u_i l_i)}{\sum W_i \sin\alpha_i} \quad (2.7)$$

Similarly, for non-homogeneous soil the expression is:

$$F = \frac{\sum [c'l_i + \tan\phi' (W_i \cos\alpha_i - u_i l_i)]}{\sum (W_i \sin\alpha_i)} \quad (2.7a)$$

Because of ignoring the interslice forces, the factor of safety is in error. The error may be as low as 10% - 15% to as high as 60% for deep slip surfaces and high pore water pressure. Usually the error is on the conservative side.

Despite the errors, the method is still used in some situations due to its simplicity, the fact that the error is on the safe side, and also because hand calculations are possible. The method should be used only for preliminary calculations and should not be relied upon for deep slip surfaces with high pore water pressure. Designs based

on this method may be highly conservative and, in some cases, the results can be very misleading.

### 2.1.2 The Bishop Simplified Method.

Bishop [12] introduced a simplified method of slope stability analysis based on the assumption of a slip surface of circular shape. He calculated the normal stress on any slice base by considering the vertical equilibrium of that slice while ignoring the tangential inter-slice forces  $T_i$ . On this basis, he derived the following equation for the effective normal force  $N'_i$  on the base of any slice:-

$$N'_i = \frac{W_i - u_i b_i - (1/F)c' \cdot b_i \tan \alpha_i}{\cos \alpha_i \left[ 1 + (\tan \alpha_i \cdot \tan \phi')/F \right]} \quad (2.8)$$

Combining equations (2.6) and (2.8) we get

$$F = \frac{\sum [c' \cdot b_i + (w_i - u_i b_i) \tan \phi'] / M_i(\alpha)}{\sum W_i \sin \alpha_i} \quad (2.9)$$

where

$$M_i(\alpha) = \cos \alpha_i \left[ 1 + (\tan \alpha_i \cdot \tan \phi')/F \right] \quad (2.10)$$

The above equation for  $F$  is somewhat more involved than that for the Fellenius Method and involves an iterative solution as  $F$  appears on both sides of the equation. However, convergence is very rapid. Bishop also used a rigorous method in which the values of normal and shear forces on the sides of each slice may be found by successive approximation. The factor of safety using his simplified method was found to be very much in agreement with his rigorous method.



The Bishop simplified method gives values of  $F$  within the range given by rigorous methods except for deep failure circles when  $F$  is less than one. In cases where deep failure occurs the angle  $\alpha$  of the slice base near the toe of the slope becomes negative. From the above equations it can be seen that when  $\alpha$  is negative the denominator of equation (2.8) can become negative or zero, leading to errors or computational difficulties.

In order for the solution obtained by Bishop's simplified method to be regarded as an admissible solution the factor of safety against sliding on the vertical sections should also be satisfactory.

Bishop also suggested that for cases where errors have already been introduced into the estimate of stability by testing and sampling procedures then the approximate method will suffice but in cases where considerable care is exercised at each stage then a more rigorous method may be necessary.

### 2.1.3 Janbu's Method Of Analysis.

Janbu [51] developed a numerical method of slices, for slip surfaces of arbitrary shape, using overall horizontal equilibrium as a stability criterion and calculated the factor of safety as

$$F = \frac{\sum b_i s_i \sec^2 \alpha_i}{\sum (W_i + \Delta T_i) \tan \alpha_i} \quad (2.11)$$

where

$$s_i = \frac{c' + \left[ (W_i + \Delta T) / b_i - u_i \right] \tan \phi'}{1 + \tan \alpha_i \cdot \tan \phi' / F} \quad (2.12)$$

and

$\Delta T$  is the difference of tangential or shear forces on two successive slices as shown in figure 2.2 .

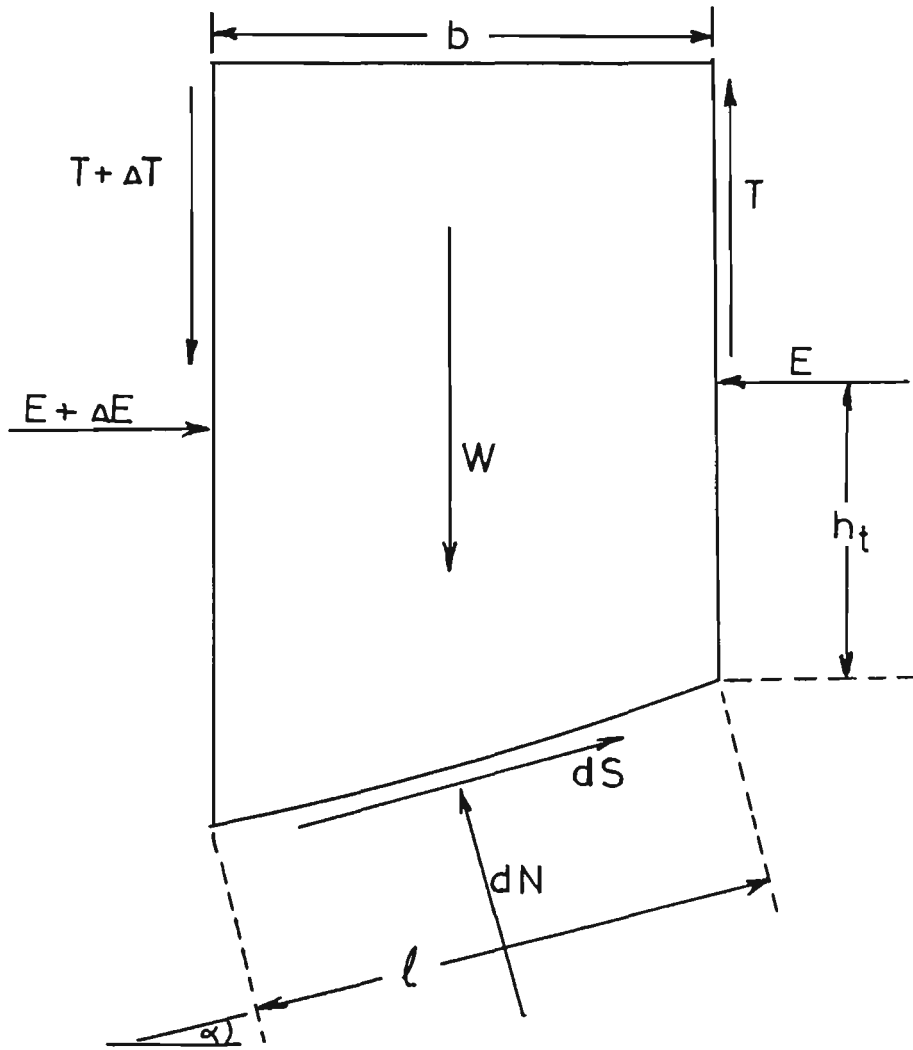


Figure 2.2 Forces Acting on a Typical Slice Using Janbu's Method

An initial assumption is made regarding the magnitude and position of the inter-slice forces. As in the simplified Bishop method an initial approximation for  $F$  must be made and this leads to an improved value each iteration until a final value is converged upon. The interslice forces are then calculated from

$$dE = (W + dT) \tan \alpha - (s \cdot b / F) \cdot \sec^2 \alpha \quad (2.13)$$

and

$$T = -E \cdot \tan \alpha_t + h_t \cdot dE / b \quad (2.14)$$

where

$dE$  is the difference of normal sidewall forces on two successive slices

and  $\alpha_t$  and  $h_t$  define the direction and position of the line of thrust.

The procedure is then repeated until two consecutive iterations yield almost identical results. Janbu gave a simplified version of his method which does not require iterative calculations.

A check must be made to ensure that the position of the line of thrust is not such that tension is implied in a significant portion of the sliding mass. If this is so then the solution may not be acceptable.

The big advantage of the Janbu method over other exact methods such as the Morgenstern-Price method is the simplicity of the calculations and the fact that a computer is not always necessary. A disadvantage, however, is that while Janbu's numerical solution can be applied to elongated shallow slip surfaces, it is in error when applied to deep slip surfaces. This is especially the case with Janbu's simplified method. Janbu's method considers the force and moment equilibrium of every single slice but for the sliding mass as a whole it considers only force equilibrium and remains unbalanced for moments (as shown by Nonveiller [70]).

Janbu's simplified method is easier to use but correction factors are required to be applied depending on the geometry of the slip surface. The multiplying factor is 1.0 for very shallow slip surfaces and as high as 1.2 for deep slip surfaces.

#### 2.1.4 The Morgenstern-Price Method.

The method of analysis of Morgenstern and Price, being very complex and involving a large number of equations, is not presented here in any detail. Full descriptions of the method are given by Morgenstern and Price [68], Hamel [45] and Chowdhury [29]. However, a very brief description of the method is given here to allow comparisons with the methods already described.

In order to make the problem statically determinate, an assumption is made by Morgenstern and Price regarding the relationship between the normal force on the side of any slice,  $E_i$ , and the shear force on the same slice side,  $T_i$ . This relationship is assumed as follows

$$T = \lambda \cdot f(x) \cdot E \quad (2.15)$$

where  $\lambda$  = a constant parameter to be determined from the solution  
and  $f(x)$  = an arbitrary specified function

Moment equilibrium is considered about the base of each slice,  $i$ , assuming that each slice is very thin. Conditions of equilibrium are applied in the directions normal and tangential to the base of the slice. Combining these equations with the Coulomb-Terzaghi failure criterion will then lead to a further set of equations. A number of linear and polynomial approximations are then made within each slice to give an expression in terms of  $dE/dx$  and  $x$ . Integrating this equation over a slice from  $x_i$  gives an expression for  $E$ .

Combining equations (2.15) and the above mentioned equation for moment equilibrium about the slice base and integrating with respect to  $x$  gives an expression for  $M$ , the moment about the slice base. Using the boundary conditions an iterative procedure is started where assumed values of  $\lambda$  and  $F$  are needed to calculate  $E$  and  $M$  at the end of the first slice. This leads to values of  $E$  and  $M$  for each slice. The procedure is repeated until equations (2.16) are satisfied and the correct values of  $\lambda$  and  $F$  are thus found. A computer is essential to obtain this solution.

$$E(x_0) = 0, M(x_0) = 0, E(x_m) = 0, M(x_m) = 0 \quad (2.16)$$

As stated earlier, the Morgenstern-Price method, unlike the methods previously mentioned, satisfies all conditions of statical equilibrium, although the results are still dependent on the assumptions made i.e. (a) the fact that  $\lambda$  is assumed constant, and (b) the form of the function  $f(x)$  which is specified by the user.

## 2.2 GENERAL COMMENTS ON LIMIT EQUILIBRIUM METHODS OF ANALYSIS.

As has been noted earlier in this chapter, some limit equilibrium methods, including the ordinary method of slices, Bishop's simplified method, and the wedge method do not satisfy all the conditions of equilibrium. Wright, Kulhawy and Duncan [113] pointed out, as have many other authors, that most equilibrium methods involve the assumption that the factor of safety is the same for each slice even though this is not really true except at failure when  $F = 1$ . Because the soil is assumed to behave as a perfectly plastic or rigid plastic material, limit equilibrium methods of analysis would not be expected to simulate the actual behaviour of slopes except perhaps at failure when, as mentioned above, the factor of safety is equal to unity.

Ching and Fredlund [25] pointed out a number of difficulties or limitations when using limit equilibrium methods of analysis. These problems arise mainly in the numerical procedure as a result of the interslice force assumptions and geometric conditions imposed on the stability computations. These difficulties are summarised as follows:-

- (a) When the variable  $m_\alpha$  approaches zero or becomes negative, unreasonable normal forces and misleading results may be computed. The solution is to restrict inclinations of the slip surface to values indicated by classical earth pressure theory.
- (b) In highly cohesive slopes, negative normal forces (indicating tension) can be computed thus causing uncertainties in the results. This is particularly true in relatively shallow slices. The solution is to assume a tension crack zone.
- (c) Convergence problems can arise as a result of using an inappropriate interslice force function. The solution is to use a side force assumption more consistent with the geometry of the slope and the stress distribution within the soil mass.

Wright, Kulhawy and Duncan [113] developed a stability analysis methodology using internal stresses determined by performing finite element analyses. For a number of slopes with wide variations in geometry and shear strength parameters they investigated the following:-

1. the variations of normal stress and factor of safety along the shear surface.
2. the overall factor of safety for each slope.

Since they simulated only built-up slopes, no assumption was necessary in respect of initial stress states. This would have been necessary for excavations or natural slopes. Using the Bishop's simplified method for comparison, they concluded as follows.

1. Normal stress distributions were very nearly the same for flat slopes and large values of  $\lambda_{c\phi}$   
 where  $\lambda_{c\phi} = (\gamma.H.\tan\phi)/c$   
 and where  $H$  = slope height  
 and  $\gamma$  = unit weight of soil
2. Although the variations of normal stress and factor of safety along the shear surface are not the same, in general the average values of  $F$  were very nearly the same. For all cases studied, the difference was found to be between 0% and 8% .
3. Since the two methods involve a substantially different approach, the close agreement in  $F$  indicates that the assumptions involved in Bishop's simplified method (and thus Janbu's method and Morgenstern and Price's method) do not lead to large errors in comparison to a method in which stresses are computed exactly by the versatile finite element method.

Fredlund [44] presented a review of general limit equilibrium theory and discussed and compared a number of well-known methods of analysis including those mentioned above. He gave comparisons of

calculated factors of safety using the various methods. Fredlund also stated that limit equilibrium methods fall short of a complete solution in that no consideration is given to kinematics and that equilibrium conditions are only satisfied in a limited sense (e.g. failure conditions are not ensured at the interslice surfaces).

In conclusion, although limit equilibrium methods of stability analysis have certain limitations (e.g. inability to calculate strains and deformations), their simplicity and ease of use compared to finite element or probabilistic methods certainly keep them among the most widely used of all stability analysis methods. These methods are especially welcome in the more practical situations where users do not always have the necessary expertise required for complex methods. Also, as has been mentioned above, the error involved in using limit equilibrium methods of analysis is not great and is usually on the safe side. This is especially true of the more rigorous methods such as the Morgenstern-Price method, the Janbu method, and in some cases the Bishop simplified method. The bulk of the research in this thesis was based on the limit equilibrium concept of analysis. Methods mentioned previously have been used as a basis for the relevant developments. These methods are:-

1. the Bishop Simplified method,      and
2. the Morgenstern-Price method.

## **CHAPTER 3**

### **PROGRESSIVE FAILURE AND THE CONCEPT OF RESIDUAL STRENGTH.**

#### **3.1 GENERAL.**

This chapter is devoted to a discussion of the concepts which have been introduced to understand the progressive failure of soil slopes. Attention has been drawn to previous studies concerning the significance of soil brittleness and residual shear strength. Different analytical approaches involving simulation of local failure and stress redistribution are discussed in chapter 5.

Conventional methods of stability analysis described in the previous chapter are usually adequate for most cases of slope analysis. However, analyses by various authors have shown that in many instances conventional methods of analysis do not adequately explain failures which have already occurred and predictions of failure or stability may not be successful. There are a number of recorded cases of failures in slopes where the factor of safety calculated by conventional methods of analysis prior to failure was greater than one.

For a slope in a perfectly plastic material (e.g. rigid-plastic or even elastic-plastic) limit equilibrium methods would be expected to prove highly reliable. However, real soils behave in ways which show marked departures from the assumption of perfect plasticity. Most soils are strain-softening to some degree and many soils exhibit a 'brittle' behaviour in undrained or drained deformation or both. Therefore, there may be discrepancies in the results of limit equilibrium studies. Often these discrepancies can be attributed to progressive failure phenomena.



In comparison to limit equilibrium methods, the finite element method can be used to obtain valuable information on the state of stresses and strains within the soil mass. It does not, however, show directly the stability condition of the slope. On the other hand, limit equilibrium methods give a factor of safety as a direct measure of the stability of the slope but fail to account for the constitutive relationships of the soil or the effects of initial stresses.

In all problems of slope stability, bearing capacity and earth pressure, even in ideally homogeneous soils, the state of limiting equilibrium is associated with a non-uniform mobilization of shearing resistance and thus with progressive failure (e.g. Bishop [13], Taylor [80]). Moreover, progressive failure should be considered not only in its spatial manifestation but also as a time-dependent process.

Bjerrum [18] also attributed certain slope failures to processes involving some mechanism of progressive failure. He pointed out cases of slides in weathered clay where the average shear stress along the failure surface due to gravity force was much less than the shear strength of the clay. Such a slide would have occurred along a slip surface which was already formed and on part of which the shear strength was less than the peak. The slip plane must thus be formed by progressive failure preceeding the actual slide (the existence of pre-existing slip surfaces had been ruled out on the basis of investigation and consideration of geotechnical and geological factors). Bjerrum stated that as the shear stresses due to gravity force are lower than the shear strength, a progressive failure can only be explained by taking into account the internal stresses in the mass.

Chandler [24] cited case records which demonstrate that post-excavation pore pressure recovery in London clay and other heavily overconsolidated clays may involve a time period of many years, consistent with low values of coefficient of swelling. Therefore, the process of swelling is a major contributory factor in the occurrence of delayed failures in cutting slopes of brown London clay in cases where time delays prior to failure are less than or equal to 50 years. Beyond that period, long term pore pressures have

become established and other factors must control the occurrence of slope failures.

### 3.2 DEFINITIONS OF PROGRESSIVE FAILURE.

As early as 1936 Terzaghi [105] presented a definition of progressive failure in which he implied that the time element was necessary for progressive failure to occur. Later (1948) Terzaghi and Peck [106], Taylor [80] and (in 1967) Bishop [13] appeared to consider progressive failure in the context of a spreading of failed or overstressed zones in space. The definition given by Terzaghi and Peck [106] is presented here in detail as follows. "The term progressive failure indicates the spreading of the failure over the potential surface of sliding from a point or line towards the boundaries of the surface. While the stresses in the clay near the periphery of this surface approach the peak value, the shearing resistance of the clay at the area where the failure started is already approaching the much smaller 'ultimate' value. As a consequence the total shearing force that acts on a surface of sliding at the instant of complete failure is considerably smaller than the shearing resistance computed on the basis of the peak values."

James [50] defined progressive failure as a simultaneous (or quasi-simultaneous) decay in both the  $c'$  and the  $\phi'$  parameters preceding actual failure. Lo [60], however, defined progressive failure as the process of successive failure of individual soil elements in a soil mass. This process spreads in space and requires time to occur. While time aspects may not always be important under some conditions, an understanding of spatial progression of failure is most essential.

### 3.3 RESIDUAL STRENGTH.

In his studies on the long-term stability of clay slopes, Skempton [88] stated that as clay is strained, it builds up an

increasing shearing resistance. Under a given effective pressure, however, there is a definite limit to the resistance a clay can offer and this is the peak strength  $s_p$ . If displacement is continued the resistance, or strength, of the clay decreases and this 'strain softening' continues until a certain 'residual strength'  $s_r$  is reached. The decrease of shear strength to a residual value is associated with relative displacements along a slip plane or discontinuity. This process is displayed in figure 3.1. The peak and residual strengths are defined as follows.

$$s_p = c'_p + \sigma'_p \tan \phi'_p \quad (3.1)$$

$$s_r = c'_r + \sigma'_r \tan \phi'_r \quad (3.2)$$

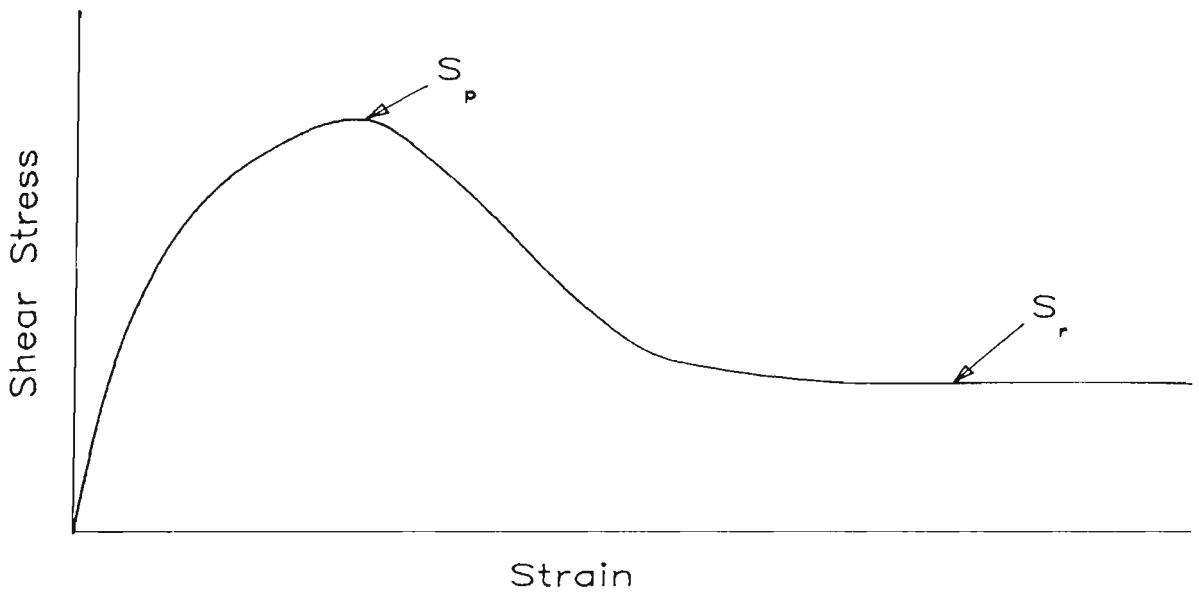


Figure 3.1 Strain Softening Curve Suggested by Skempton.

The idealisation of such a relationship as a brittle strain-softening material as shown in figure 3.2 is often convenient for analysis (e.g. Lo and Lee [62]) and has been adopted for use in this thesis.

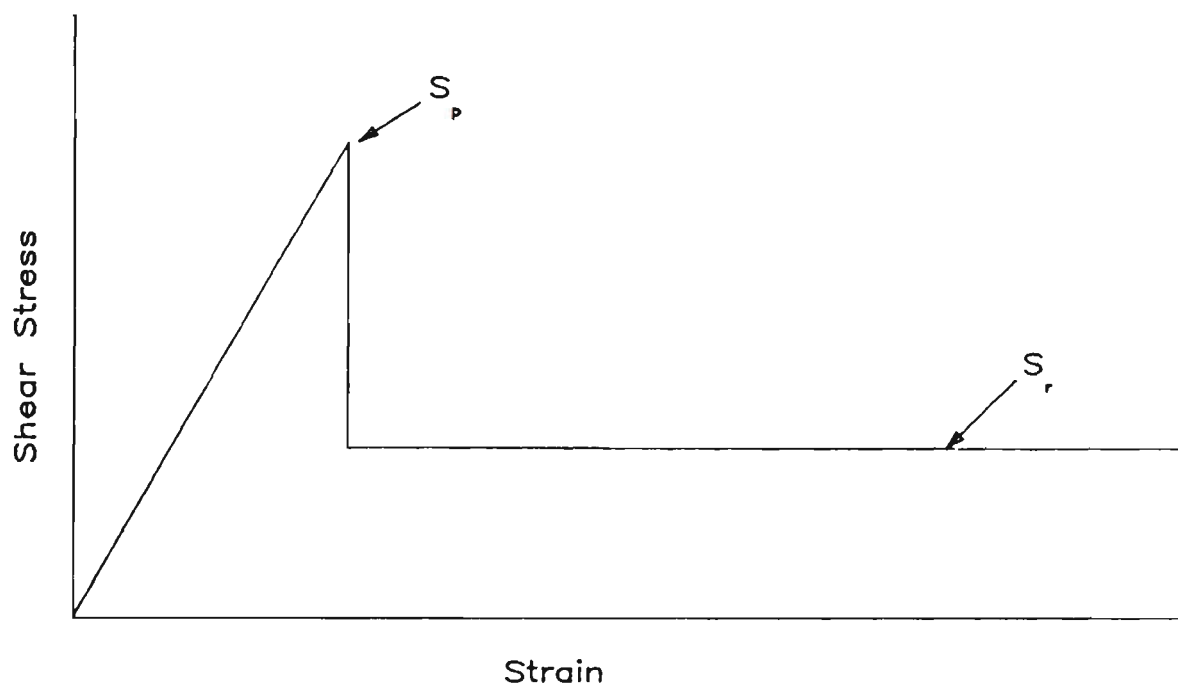


Figure 3.2 Idealised Strain Softening Curve Suggested by Lo & Lee.

Skempton [88] noted that during the shearing process, over-consolidated clays tend to expand, especially after passing the peak. Part of the drop in strength is due to an increase in water content. Thin bands or domains are developed in which the flakey clay particles are orientated in the direction of shear and the strength is further reduced. Skempton also suggested that the residual strength of a clay, under any given effective pressure, is the same whether the clay has been normally or over-consolidated. Thus  $\phi'_r$  should be the same for normally or over-consolidated clay (as shown in figure 3.3).

Skempton [89] stated that for a certain clay, the moisture content at its 'critical state' is the same no matter what its consolidation history was. After this critical state is reached, no amount of deformation will alter the moisture content (constant stress and volume are attained). The 'critical state' corresponds to the strength of a normally consolidated clay. It is possible in some over-consolidated clays that a more aggressive reduction in strength occurs before first-time slides take place, as against the very small

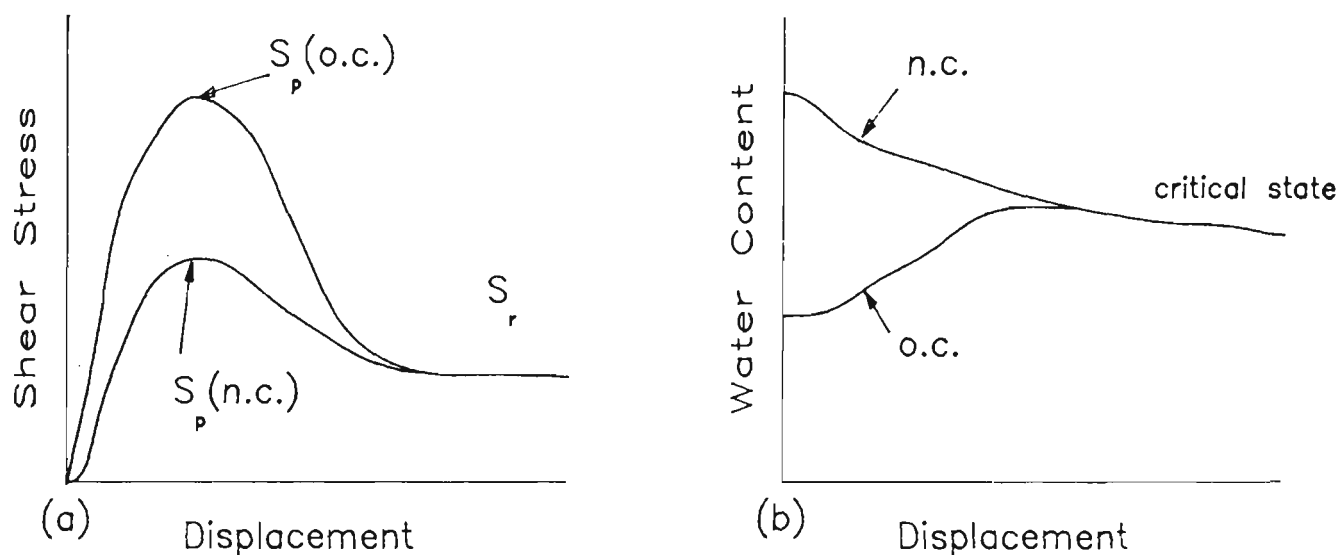


Figure 3.3 Shearing Characteristics of Clays (Skempton)

reduction in most over-consolidated clays. Also, in all clays, the residual strength will be reached only after a continuous principal shear surface has developed and this state appears to be attained after mass movements of the order of several feet (in the field).

Crawford and Eden [36] pointed out that Skempton dealt mainly with insensitive, overconsolidated clays which tend to expand during shear, especially after the peak strength is reached. The increasing water content caused by this expansion, together with the particle reorientation, local overstressing and time effects lead to a reduced strength at high strains which may precede slope failure. Sensitive clays, however, can exist in nature at rather high void ratios as a result of their bonded nature when highly over-consolidated. Under increasing or sustained shearing stresses the bonds are broken down and the structure collapses, decreasing the volume. If the pore water drainage is poor due to low permeability, pressures build up till the effective stresses on the failure plane approach zero. This is the state thought to exist on the failure plane of a flow slide.

Bishop [16] indicated that residual strength should correspond to extremely large displacements within the soil mass. Lo and Lee [63], however, used the term residual strength to designate the slowly decreasing strength in the post-peak range corresponding to moderately large displacements in the field. From back analyses of landslides involving Lias clay Chandler [23] found that residual strength decreases with increasing normal stress.

Tavenas and Leroueil [101], while investigating cuts in slopes, suggested that the residual strength situation is only relevant to the case of failure along a pre-sheared sliding surface.

### 3.4 CONDITIONS NECESSARY FOR PROGRESSIVE FAILURE.

At this stage it is necessary to consider the conditions under which progressive failure is most likely to occur. Skempton and LaRochelle [66] suggested that fissures in the soil may adversely influence the strength of heavily over-consolidated clays and shales in the following ways.

1. Open fissures may form portion of the failure surface across which the shear resistance is zero.
2. Closed fissures may form portion of the failure surface across which only the residual strength is mobilised.
3. Fissures (closed or open) adversely influence stresses within the slope. This increases the likelihood of progressive failure.

Also, open fissures might increase the rate of swelling and stress redistribution.

Bjerrum [18] concluded that the development of a surface of sliding by progressive failure is possible in over-consolidated plastic clays provided the following conditions are satisfied.

- (a) internal lateral stresses are large enough to cause stress concentrations in front of an advancing sliding surface, where the shear stresses are greater than the peak shear strength.
- (b) the clay contains a sufficient amount of recoverable strain energy to produce the necessary expansion of the clay in the direction of sliding to strain the clay in the zone of failure.
- (c) the residual shear strength is relatively low compared with the peak shear strength.

Skempton and Petley [96] showed that for tests performed on over-consolidated clays, the strength along principal slip surfaces in landslides and tectonic shear zones, is at, or very close to, the residual. Along minor shears, however, with somewhat irregular surfaces on which the relative movements have been small, the strength is appreciably above the residual.

Since residual conditions are reached slightly more rapidly under low stress levels than under high, Peck [71] and James [50], hypothesized that in larger landslides the slip zones in the toe area, will exhibit a lower strength than further back into the slipping mass, where the stress level is higher. Lo and Lee [62] stated that conditions pertinent to the occurrence of progressive failure in slopes are

- (a) brittleness of soil
- (b) non-uniformity in distribution of shear stresses and sometimes
- (c) deterioration of strength with time due to softening, change of ground water conditions or rheological effects.

### 3.5 THE RESIDUAL FACTOR.

It is now convenient to introduce some form of measure of the extent to which progressive failure has actually progressed. If progressive failure is generally acknowledged as a progressive decrease of the shear strength from the peak to the residual value (this process may be a function of time, space or both) then a 'residual factor' is defined which gives an indication of the extent of progressive failure.

Skempton [88] defined the residual factor  $R$  as the amount by which the average strength has fallen from the peak to the residual (equation 3.3). In other words,  $R$  is the proportion of the total slip surface in the soil along which the strength has fallen to the residual value (equation 3.3a). Bishop [14], however, defined a local residual factor,  $R_l$  (similar to that defined by Skempton but varying along the slip surface) to denote the proportional drop from the peak to the residual strength at any point along the surface.

The overall residual factor of Skempton's may be expressed as

$$R = \frac{s_p - s_{av}}{s_p - s_r} \quad (3.3)$$

or

$$R = \frac{L_r}{L} \quad (3.3a)$$

In contrast, the local residual factor is expressed as follows

$$R_l = \frac{s_p - s_i}{s_p - s_r} \quad (3.4)$$

where

$s_p$  is the peak shear strength,  
 $s_r$  is the residual shear strength,



- $s_i$  is the actual shear strength at point  $i$ ,  
 $s_{av}$  is the average shear strength along the slip surface,  
 $L$  is the total length of the slip surface, and  
 $L_r$  is the length of slip surface over which the shear strength has fallen to the residual value.

### 3.6 REDUCTION OF SHEAR STRENGTH.

Skempton [88],[89] made the following comments on the role of strength reduction in progressive failure with particular reference to his investigation of slides in London clay:

- (a) After a slide has taken place, the shear strength of soil along the slip surface is equal to the residual value.
- (b) First-time slides in slopes in non-fissured clays correspond to strengths only slightly less than the peak.
- (c) First-time slides in fissured clays correspond to strengths well below the peak.
- (d) Some form of progressive failure must be operative to take the clay past the peak. Possibly, a non-uniform stress to strength ratio along the slip surface or fissures acting as stress concentrators and leading to a softening of the clay mass may be responsible.
- (e) In natural slopes in London clay the strength had fallen to the residual value.
- (f) On pre-existing shear surfaces the residual strength obtains.

Skempton and Hutchinson [94] analysed the stability of structures and natural slopes in the London clay and concluded that the strength of highly over-consolidated, fissured clays dropped to the normally consolidated value. That is, the effective cohesion approached zero

as a consequence of open fissures and the softening effect facilitated by the fissures.

Bjerrum [19] suggested that the combined effect of weakening and softening could be taken into account by assuming that the cohesion intercept would approach zero while the friction angle would remain the same as for an intact clay. This concept was also invoked by James [50] who found that the loss in strength before actual failure was almost entirely due to a loss in terms of the parameter  $c'$  as suggested originally by deLory [39] and quoted by Skempton [89]. During this phase the value of parameter  $\phi'$  remains at, or very near to, the peak value since the effect of weathering on this parameter within engineering time scales is generally negligible.

Skempton [91] stated that the post-peak drop in drained strength of an intact overconsolidated clay may be considered as being due, firstly, to an increase in water content (dilatancy) and secondly, to re-orientation of clay particles parallel to the direction of shearing. In normally consolidated clays, the post-peak drop in strength is due entirely to particle re-orientation.

Rivard and Lu [78] calculated factors of safety close to 1.0 based on measured embankment and foundation strengths and observed pore pressures thus strengthening the case for the use of normally consolidated strength for soils with structural discontinuities. In addition to the presence of structural discontinuities, softening of the clay may be a contributing factor in reducing the strength to the normally consolidated value. These structural discontinuities are difficult to observe in soft clays, whereas they are readily apparent in stiff soils, thus in soft clays special attention should be devoted to searching for structural defects.

Skempton [88] said that in clays where no fissures or joints exist the decrease in strength from the peak to the residual state is small or even negligible. However, much of his research experience was with cuttings in fissured London clay and he did not analyse many examples of failures in intact or non-fissured clays. He did emphasise that, if failure has already occurred, any subsequent movements on the existing slip surface will be controlled by the

residual strength, no matter what type of clay is involved.

From tests carried out on overconsolidated blue marl, Sotiropoulos and Cavounidis [97] suggested the possibility that 'portions of clayey soil mass, when sheared, may pass to the softening side of the stress-strain curve without ever reaching the peak strength of the material exhibited by different portions of the same mass'. They further suggested that this behaviour may be due to the existence of small, non-apparent fissures. In relating this type of behaviour to the process of progressive failure, Sotiropoulos and Cavounidis concluded that 'if part of a clay slope is characterised by this behaviour, a slide may be initiated without the shear stress exceeding what normally would be expected to be the peak strength value'.

### 3.7 MECHANISMS OF PROGRESSIVE FAILURE.

#### 3.7.1 General Notes On Progressive Failure Mechanisms.

Taylor [80], while considering primarily the shearing resistance of sands in an effective stress context, associated progressive failure with the redistribution of shear stress along a potential failure surface. No mention was made, however, regarding the direction of propagation of progressive failure. Thomson and Tweedie [107], while investigating the Edgerton landslide found strong evidence to suggest that failure was progressing from a scarp at the top of the slide down towards the toe. Field evidence indicated that the lower part of the failure surface had reactivated an old failure surface, whereas the scarp area represented a first-time slide. Analyses of the failure indicated that residual angles of shearing resistance were being mobilised along the other, pre-sheared part of the failure surface due to old landslides. Along the latter portion of the failure surface the soil parameters yielding the most reasonable factor of safety were a peak angle of shearing resistance and a cohesion very much less than that determined from laboratory testing.

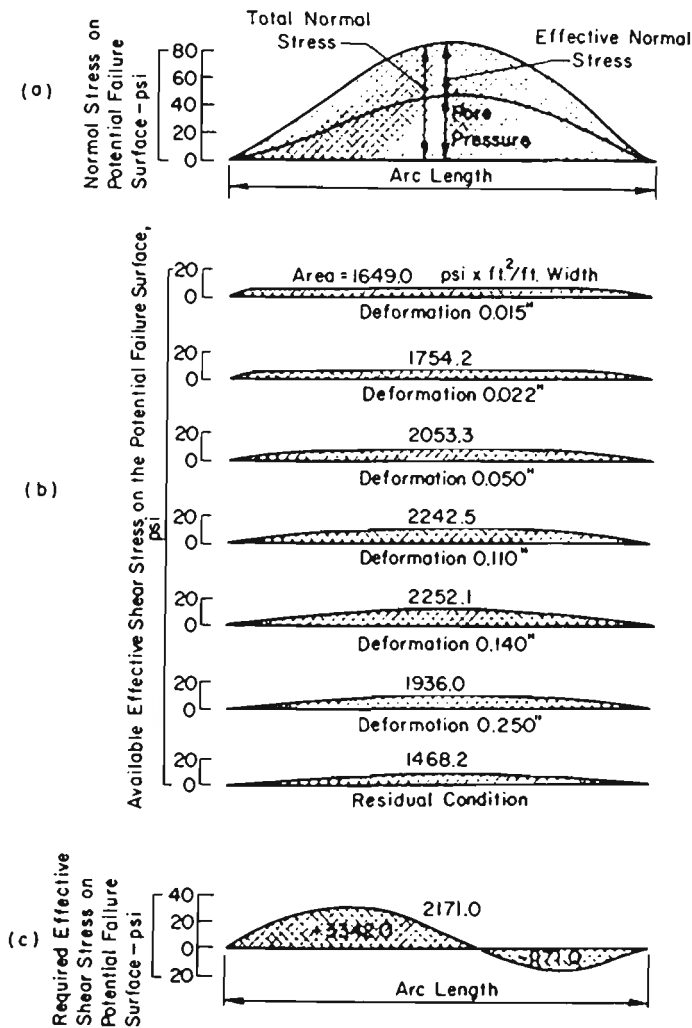
Wilson [111], in field studies aimed at investigating the mechanisms associated with progressive ground movements, made a number of important observations. Using inclinometers to measure relative displacements, he found that in progressive landslides in excavated slopes, failure tended to start at the toe of the slope, progressing upwards to the crest. In slides where fill is added to the upper part of the slope, however, Wilson found that the opposite happens and rupture develops and progresses downwards from the crest to the toe of the slope.

Peck [71] presented the results of a series of tests carried out by R.J.Conlon on clays from Winnipeg in the bed of old glacial lake Agassiz and his important observations concerning progressive failure (based on these results) are summarised below.

Assuming that failure occurs along a circular arc with no deformation or distortion of the sliding mass, relative deformations can be achieved along the failure surface, of sufficient magnitude for shear strength to drop to a residual value. The peak shear strength obviously cannot be mobilised simultaneously along the surface of sliding because normal pressure varies along the surface of sliding and the strain necessary to reach the peak strength depends on the normal pressure (see figure 3.4).

In as much as real soils are deformable and compressible, the displacement along the surface of sliding is not uniform from one end to the other. Near the upper portion of the surface, the shearing forces are somewhat greater than the shearing resistances corresponding to any amount of deformation. Therefore, the support of slices along the upper surface of sliding requires the development of forces between slices. Part of the load is transferred down the mass through inter-slice forces. Part is carried by the tensile resistance between the slices and those higher up. The transfer of the load from the upper slices to those below involves a compressive strain roughly parallel to the slope.

Conlon set forth a quantitative procedure for estimating the available shearing resistance along the surface of sliding. He took the shearing resistance on the upper portion of the failure surface



(a) DISTRIBUTION OF NORMAL PRESSURE ALONG TYPICAL POTENTIAL CIRCULAR FAILURE ARC THROUGH LAKE AGASSIZ CLAY, ASSUMING NO REDISTRIBUTION DUE TO SHEARING STRESSES WITHIN SLIDING MASS; (b) TOTAL SHEARING RESISTANCE MOBILIZED AT VARIOUS UNIFORM DEFORMATIONS ALONG POTENTIAL SLIP SURFACE; AND (c) REQUIRED SHEAR STRESS ALONG POTENTIAL FAILURE ARC IF STRESSES WITHIN SLIDING MASS ARE IGNORED (FROM R. J. CONLON)

Figure 3.4 Reproduced from Peck [71]

equal to the residual value, the shearing resistance on the central zone of maximum normal stress at the peak value, and the shearing resistance for the lower portion of the failure surface consistent with the shear deformation for the peak shearing resistance for the maximum normal stress.

Tavenas and Leroueil [101] in their investigations with cut slopes, found no fundamental difference between the mechanism involved in the accidental failure of natural slopes and the delayed failure of

cut slopes.

Athanasiau [4] proposed a method of slope stability analysis whereby the non-linear stress-strain behaviour of the soil adjacent to the sliding surface can be simulated. He considered only horizontal forces on each side of the slices in the soil mass. Before failure, the state of stresses could be approximately described by the horizontal forces (which remain larger than the vertical ones). Assuming failure to start by a discontinuity in the slope (resulting in the removal of lateral support) his results show that this release of horizontal stresses at the toe of the slope induces shear stresses on the slip surface leading to progressive shear strength concentration and release, meaning progressive failure.

### 3.7.2 Bjerrum's Comments On The Mechanism Of Progressive Failure.

Bjerrum [18] stated that, in the process of progressive failure in slopes in unweathered clay, when a slip face has developed over a certain length and the resistance against horizontal displacement of the whole block above the slip plane has been reduced so much, that it cannot resist the active earth pressure of the soil mass above, progressive failure will develop into a massive slide. In excavations in deep deposits of heavily over-consolidated plastic clays, the progressive failure can also start as follows.

When an excavation is made, a reduction in the overburden pressure will occur and the ratio of horizontal to vertical stress will increase in the clay beneath the bottom of the excavation. "At a certain depth of the excavation, this ratio can exceed the critical value at which shear stress equals peak shear strength and a passive shear failure will occur. This results in a heave at the bottom of the excavation, followed by a horizontal movement of the clay next to the excavation. This causes a decrease in the horizontal thrust of the clay, leading to a local concentration of shear stresses in the clay beneath the slope. If these shear stresses exceed the peak shear strength, progressive failure will proceed and finally, a continuous failure surface will be formed." In both of the above cases, the

movement of the slope will be predominantly horizontal. Refer to figure 5.1 in chapter 5.

### 3.7.3 Skempton's Approach To Progressive Failure.

Skempton [88], modified his earlier ideas that the strength along the slip surface at the time of failure, is at some places peak and some places residual, the point of demarcation being described by Skempton's residual factor. He argued that stiff, fissured clays possibly undergo a loss in strength in cuttings, tending towards the fully softened value which may be regarded as approximately equal to the ultimate value of the soil in the normally consolidated state. The softened strength is also approximately equal to the critical state strength. In such clays, there must be a mechanism of progressive failure and/or softening which takes them past the peak and just before a first-time slide occurs, there is a softened shear zone with many minor shears. Some over-consolidated clays may exhibit a more aggressive reduction in strength, before a first-time slide takes place.

Residual strength is only reached (in all clays), after a continuous principal shear surface has developed, corresponding to mass movements in the order of several feet in the field. Skempton [90] later confirmed some of his earlier findings and made further comments as follows.

1. The shear strength of brown London clay for first-time slides is considerably less than the peak, so some progressive failure mechanism appears to be involved.
2. The in-situ strength is given approximately by the 'fully softened' value and also by the lower limit of the strength measured on structural discontinuities.
3. The residual strength is much smaller than this. Residual strength is mobilised after the slip has occurred and large (1 to 2 metres) displacements have taken place.

4. Slides in London clay generally occur many years after the cutting is made.

The main reason for this last point is the very slow rate of pore pressure equilibration, despite the fissured structure of the clay. That is, when a cutting is made, the mass of overlying soil is decreased, which leads to an immediate reduction in pore pressure due to the development of negative excess pore pressure. It had been postulated earlier that, due to the presence of fissures, the pore pressures would very rapidly increase to equilibrium values. However, this is not so. Detailed studies based on field observations of pore water pressure over many years (at sites where piezometers have been installed) revealed (Skempton [90] ) that, in some slopes, negative pore pressures still existed many years after cutting and that pore pressure equilibrium was not reached for decades. Therefore, the presence of fissures does not necessarily lead to a high value of soil mass permeability in the field. It may be that the fissures are not perfectly inter-connected for drainage to occur.

#### 3.7.4 Bishop's Approach To Progressive Failure.

Bishop [13] postulated that, in a short-term analysis in terms of undrained strength, failure may be expected to commence within the soil mass and propagate towards the surface in both directions. In a long-term analysis, where effective strength parameters are used and the shear strength is a function of normal stress, this failure might, in contrast, be expected to begin at the surface, possibly, at both toe and crest and propagate inwards into the soil mass (see case 2 in figure 3.5). Detailed case studies were, however, not analysed.

It should be noted that in the case of a cut or natural slope, the stresses and hence the initiation of progressive failure will be influenced by the state of stress in the ground before excavation or before erosion.



Associated with the limiting or critical equilibrium state leading to the first-time sliding of a slope in overconsolidated soil, Bishop [14] proposed that for some part of the slip surface the drained peak strength will be mobilised while the post-peak and pre-peak strengths will be operative over the remainder of the slip surface. A small further displacement will then bring the whole surface into the peak and post-peak states. At this point of complete failure the strength at all points will lie between the two limits of the peak and residual states.

As mentioned earlier in this chapter, Bishop proposed a local residual factor  $R_1$  which varies along the slip surface and which denotes the proportional drop from the peak to the residual strength at any point along the surface. The shear strength mobilised at a point on the failure surface may be represented using Bishop's local residual factor, by the following expression

$$s = s_p - R_1(s_p - s_r) \quad (3.5)$$

It is noted that a local residual factor of zero implies a mobilised shear strength equal to the peak value whereas a local residual factor of one implies a mobilised shear strength equal to the residual value. The distribution of  $R_1$  varies along the rupture surface and actual values in practice are mainly speculative. Although some part of the surface must have an  $R_1$  value of zero, it is less certain that some part exists where  $R_1$  equals one especially in first-time slides.

Ring shear tests on undisturbed samples of London clay have shown that while the initial drop in strength is rather rapid, relative displacements of earth masses of the order of 30 centimetres are required before residual strengths are approached. However, tests in the laboratory may not be an effective method of determining the strains and deformations required to decrease shear strength to residual values. The determination of the distribution of  $R_1$  based on laboratory tests is also difficult with the equipment and techniques available at the present time. Bishop considered the two distributions shown in figure 3.5. One distribution implies

progressive failure to commence at the toe of the slope (see case 1, figure 3.5) and progress upward while the other implies failure to start simultaneously at the top and the toe of the slope and progress along the rupture surface towards the central region (see case 2, figure 3.5).

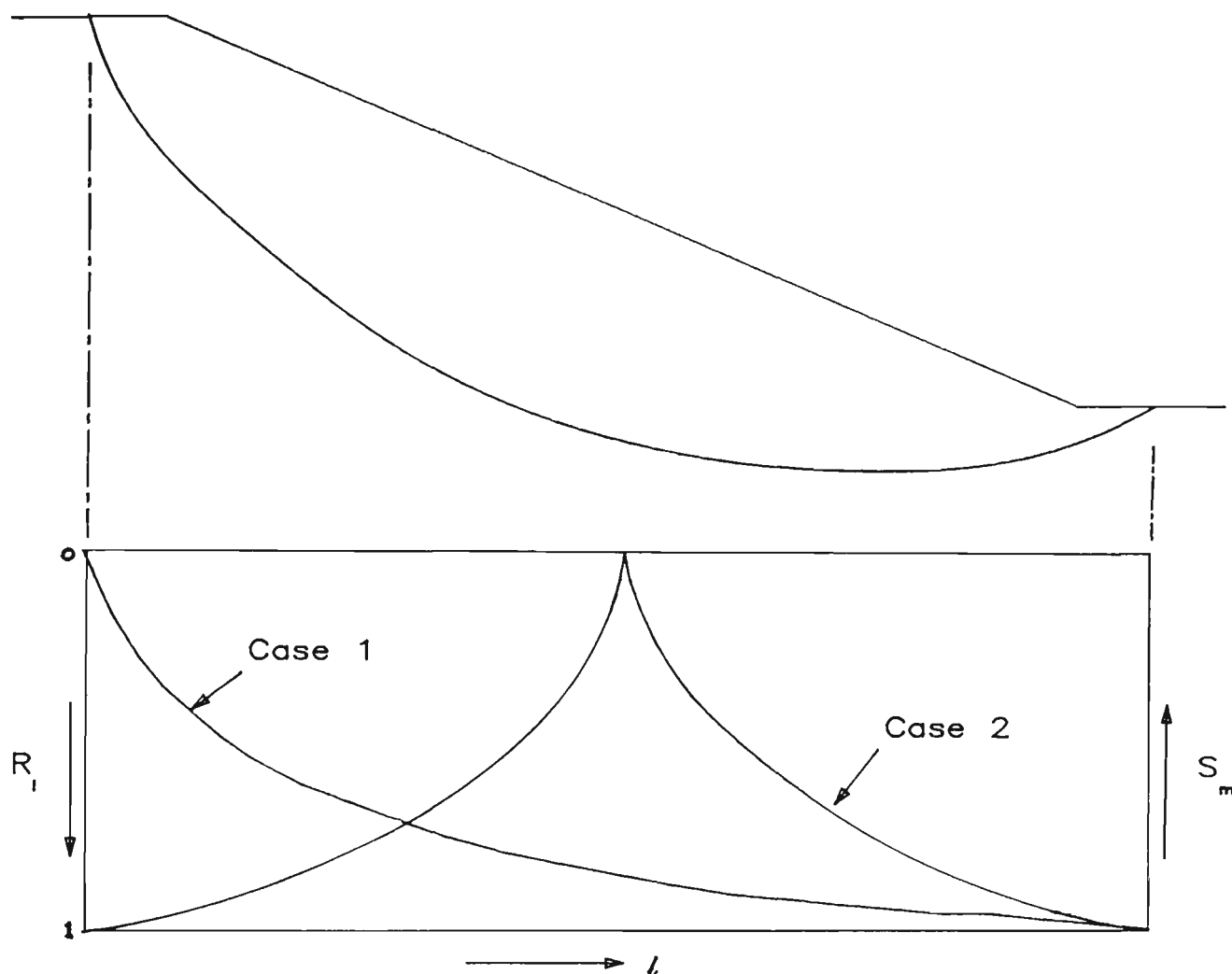


Figure 3.5  $R_i$  Distributions Suggested by Bishop.

### 3.8 CONCLUDING REMARKS.

A review of publications concerning previous and continuing research leads one to the firm conclusion that slides in soil slopes involve some form of progressive failure and that soil brittleness (strain-softening behaviour) is of paramount importance in many failures. It is necessary to develop analytical techniques which simulate the propagation of failure within a slope. Some approaches which have been suggested in the past are discussed in chapter 5.

## CHAPTER 4

### SIMULATION OF VARIABLE SHEAR STRENGTH MOBILISED ALONG A SLIP SURFACE.

#### 4.1 AIM AND SCOPE.

In the previous chapter, a number of approaches to the problem of progressive failure were discussed. In particular, the description of a mechanism of progressive failure presented by A.W.Bishop [13],[14] was discussed in which Bishop suggested that in a slope in over-consolidated clay, at the point of complete failure, the strength at all points along the failure surface will lie between the limiting values of the peak and residual states. Bishop also went on to suggest two possible distributions for the shear strength mobilised along the slip surface at the time of failure.

As well as the distributions suggested by Bishop, which varied gradually over the length of the failure surface, some different distributions were implied by Skempton [88] and Lo and Lee [62] who considered part of the slip surface to be at the peak and part at the residual value of shear strength at the instant of failure. This would imply an abrupt drop from the peak to the residual value at some point along the slip surface. This then leaves part of the failure surface at peak strength while the remainder is at the residual value.

The primary objective of the present chapter is to study the significance of variable shear strength distributions along the failure surface. The distribution may have any form provided the shear strength at any point on the slip surface is between the peak and residual values. There may be a gradually varying shear strength (i.e. a smooth distribution) or there may be an abrupt drop of shear strength at some point on the slip surface.

Several distributions have been assumed to describe the variation of shear strength along the slip surface. For each distribution, the limit equilibrium factor of safety and the average shear strength along the failure may be calculated. An important and specific aim of the work presented in this chapter is thus to determine the relationship, if any, between the assumed shear strength distribution, the calculated average shear strength along the failure surface and the resulting factor of safety obtained by limit equilibrium stability analyses. Another aim is to study the results in the light of proposed acceptability criteria for a particular method of analysis and to propose new criteria if necessary.

This chapter deals with an important aspect of progressive failure, namely, the variable mobilisation of shear strength along a slip surface which would be associated with different modes of failure progression. However, the analytical procedures developed for the relevant studies are based firmly on limit equilibrium concepts and new or additional assumptions are not necessary to carry out the analyses. On the other hand, the development of a limit equilibrium state (or a failure state where critical equilibrium is reached) may be regarded as **non-simultaneous** because of the variable mobilisation of shear strength. This is the major distinction between the analyses reported here and those which might be made in conventional studies. Although the analyses deal with homogeneous soil, non-uniform strength mobilisation implies a form of non-homogeneity as regards the analysis procedure presented here.

## 4.2 VARIATION OF SHEAR STRENGTH APPROACH.

### 4.2.1 Definition of Residual Factor in this Research.

In order to represent shear strength distributions in this chapter, the concept of a residual factor will be used. Whereas Skempton [88] defined his residual factor as the proportion of the failure surface over which the strength has fallen to the residual value, Bishop [14],[13] defined a local residual factor,  $R_1$ , as the proportional drop in strength from the peak to the residual state at

any point along the failure surface.

For the purpose of the work presented in this chapter, the local residual factor defined by Bishop will be used. As mentioned above, and in greater detail in the previous chapter, this local residual factor is considered to be a function of the position along the failure surface.

#### 4.2.2 Proposed Method for Generating Local Residual Factor Distributions.

Bishop considered distributions of mobilised shear strength which are consistent with failure progression either from the toe or from somewhere in the interior of the slope. In this chapter, a wider range of distributions is considered since failure may start from the crest or toe of the slope or anywhere in the interior. The shear strength distribution (and thus the  $R_1$  distribution) need not be of the form suggested by Bishop and may have any arbitrary form. Distributions where shear strength varies linearly from the peak to the residual value in either direction or, even where no variation exists and the peak strength or the residual strength is obtained throughout the failure surface are, of course, included. Also, cases where shear strength may fall sharply from the peak to the residual value in either direction (as suggested by Skempton [88] and Lo and Lee [62],[63] are also included. Detailed descriptions of distributions of shear strength used will be given later in this chapter.

It is now necessary to find a relationship between the local shear strength  $s$  and the local residual factor  $R_1$  and also to derive an expression for the residual factor  $R_1$  in terms of the horizontal distance along the failure surface. The value of the residual factor  $R_1$  is given by

$$R_1 = \frac{s_p - s}{s_p - s_r} \quad (4.1)$$

where  $s_p$  and  $s_r$  are the peak and residual values of shear strength respectively. Therefore,

$$s = s_p - R_1(s_p - s_r) \quad (4.2)$$

Now in order to represent a number of distributions of  $R_1$  which may be straight lines, exponential curves or combinations of both,  $R_1$  is defined by the following general equation.

$$R_1 = ae^{bx} + cx + d \quad (4.3)$$

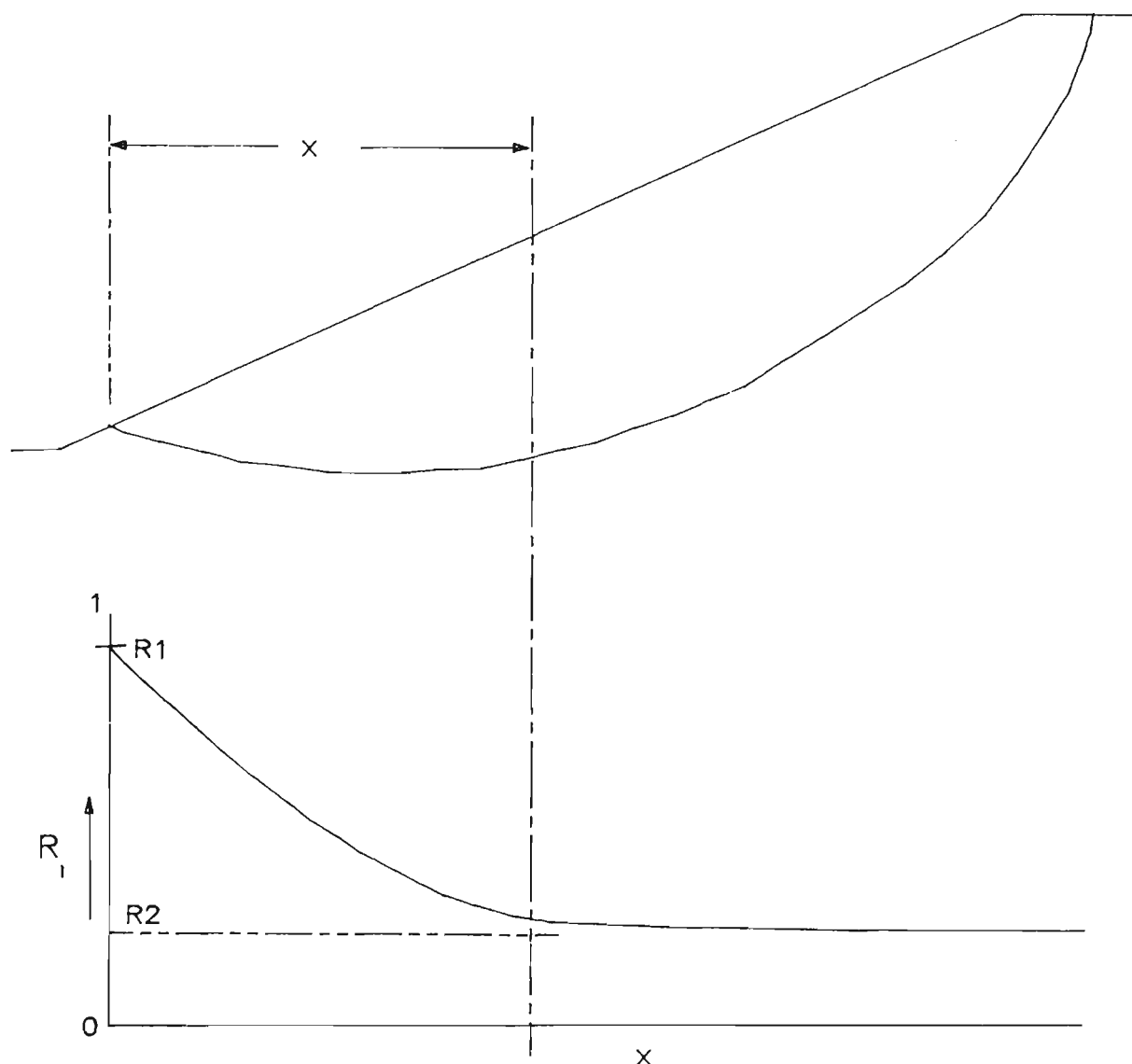
where  $x$  is the horizontal distance from the toe end of the assumed or known failure surface to the point in question on the same surface and where  $a, b, c$ , and  $d$  are constants.

Figure 4.1 shows just a sample distribution for  $R_1$ .  $R_1$  and  $R_2$  are the values of the local residual factor at the toe and crest of the slope respectively. In this diagram  $R_1$  is greater than  $R_2$ , indicating that the shear strength at the toe is less than the shear strength at the crest and thus failure has started from the toe end. When  $R_1$  is less than  $R_2$ , the shear strength at the toe is greater than the shear strength at the crest of the slope and failure is assumed to start from the crest. In other words, the point of initiation of failure can usually be located by the point with the highest value of  $R_1$  (and thus the lowest value of shear strength).

It is useful to consider the expanded form of equation (4.2) as follows:-

$$s = c'_p + \sigma'_n \tan \phi'_p - R_1 [(c'_p - c'_r) + \sigma'_n (\tan \phi'_p - \tan \phi'_r)] \quad (4.4)$$

where  $c_p$ ,  $\phi_p$ ,  $c_r$  and  $\phi_r$  are known and a distribution for  $R_1$  may be assumed. However, in general,  $\sigma'_n$  is not known in advance because it is a part of the particular limit equilibrium solution. Therefore it is difficult, if not impossible, to simulate the distribution of mobilised shear strength  $s$  even if the  $R_1$  is known or assumed. To overcome this obstacle, the approach described in the following section is proposed in this thesis.

Figure 4.1 Sample  $R_i$  Distribution

Now consider that the mobilised values of the shear strength parameters at any point are  $c'$  and  $\phi'$  and the normal stress at that point is  $\sigma'_n$ . Then, for that point, the mobilised shear strength could be written in the form

$$s = c' + \sigma'_n \tan \phi' \quad (4.5)$$

It may be noted that the values of  $c'$  and  $\phi'$  can not be determined from the single equation (4.4) even if  $\sigma'_n$  were known.

Finally, it may also be noted that the distribution of  $\sigma'_n$  from a limit equilibrium solution which incorporates variable shear strength mobilisation will, in general, be different from the

distribution obtained from a solution which assumes simultaneous failure.

#### 4.2.3 Proposed Approach - Variable Mobilisation of $c'$ and $\phi'$ .

Prior knowledge or the assumption of  $c'$  and  $\phi'$  values in limit equilibrium methods is essential for their implementation. In the Morgenstern-Price method, as with most limit equilibrium methods of analysis, the overall factor of safety and the normal stresses on each slice along the failure surface are calculated using known values of shear strength parameters  $c'$  and  $\phi'$  along with various other parameters, and not directly from the local shear strength  $s$ . Given a distribution for  $s$ , the overall factor of safety cannot be calculated, as it depends on values of  $c'$  and  $\phi'$  and these cannot uniquely be calculated from known values of  $s$  using the Mohr-Coulomb equation. Therefore, the following procedure has been developed. The local shear strength  $s$  at any point along the failure surface is defined by equation (4.5). The local values of the mobilised shear strength parameters may be defined in terms of their respective peak and residual values as

$$c' = c'_p - R_1(c'_p - c'_r) \quad (4.6a)$$

$$\phi' = \phi'_p - R_1(\phi'_p - \phi'_r) \quad (4.6b)$$

where  $R_1$  is the local residual factor for both  $c'$  and  $\phi'$  defined in the same way as the residual factor for the shear strength  $s$ . Its distribution may assume a general form such as the polynomial equation suggested in equation (4.3). Also,  $c'_p$ ,  $\phi'_p$ ,  $c'_r$  and  $\phi'_r$  are the peak and residual values respectively of the shear strength parameters.

In this work, the same value of  $R_1$  is used for both  $c'$  and  $\phi'$ . In other words,  $c'$  and  $\phi'$  vary along the slip surface according to the same distribution curve between their respective peak and residual values. Nevertheless, it would be quite feasible (without significant additional effort) to incorporate different



arbitrary distributions of  $c'$  and  $\phi'$ .

#### 4.2.4 Types of Distributions Assumed.

A wide range of  $R_1$  distributions was chosen as shown in Appendix B. The distributions, however, fall into two major categories.

1. Failure starting from the bottom of the slope, that is,  $R_1$  is 1 at the toe and  $R_1$  is 0 at the top of the slope, which indicates that residual conditions have been reached at the toe first.
2. Failure starting from the top of the slope, that is,  $R_1$  is 1 at the top and  $R_1$  is 0 at the bottom, indicating that residual conditions have been reached first at the top.

Within these two categories, many sub-categories exist, where  $R_1$  has a constant value of 1 or 0 throughout, where the distribution is broken up into more than one part, and where distributions may be linear, exponential, or a combination of both. These can be seen in appendix B. The distributions suggested by Bishop [14] are included (distributions A1 and L1) as are some similar to those of Lo and Lee [62] where a sudden drop from peak to residual conditions is assumed (distributions Q and R).

Work by various authors, including James [50] and Peck [71], has shown that in many cases failure is more likely to start from the bottom of the slope. This is because residual conditions are reached slightly more rapidly under low stress levels than under high levels, and the toe, or bottom of the slip surface, is under lower stress levels than further into the slope. Thus more emphasis has been placed on distributions where failure is assumed to start from the bottom of the slope, although a number of cases of failure starting from the top are also considered. The results are then compared to see if it can be determined which case is the more critical.

#### 4.2.5 Basis of Solution Method.

As mentioned earlier, the stability analyses procedure developed for the studies reported in this chapter is based on the limit equilibrium approach. Of the various limit equilibrium methods, the four described in chapter two were considered, and the one most suited to the requirements of this research, was found to be the Morgenstern-Price method although the Bishop's simplified method was used for slopes having circular surfaces of sliding. The Janbu method was eliminated due to the fact that it gives increased errors as the depth of the failure surface increases.

Not all solutions obtained by this method, however, may be regarded as admissible for the general limiting equilibrium problem. Morgenstern and Price defined an admissible solution as one which gives a reasonable distribution of normal force  $N$ , along the failure surface. A reasonable distribution of  $N$ , was defined as one which does not require a potential sliding mass to sustain internal forces which it is physically incapable of sustaining. Other criteria for the admissibility of a solution to a soil slope stability problem have been given by Morgenstern and Price [68], Bailey [7] and Whitman and Bailey [109] as,

1. There must be no effective tensile stresses on the sides of slices.
2. The shear stresses on the sides of slices must be less than those which would exist if a condition of limiting equilibrium existed on these surfaces.

Hamel [14] also discussed the acceptability of solutions and developed specific criteria or guidelines as discussed in subsequent sections.

#### 4.2.6 Calculation of Average Shear Strength Along Failure Surface.

The average shear strength  $s_{av}$  along the failure surface at the time of failure will be defined as,

$$s_{av} = \frac{\sum_{i=1}^n (c'_i + \sigma'_i \tan \phi'_i) \Delta L_i}{L} \quad (4.7)$$

where  $c'_i$  = local effective cohesion intercept for slice  $i$  ,  
 $\sigma'_i$  = effective normal stress on base of slice  $i$  ,  
 $\phi'_i$  = local effective angle of shearing resistance for slice  $i$  ,  
 $\Delta L_i$  = curved length of base of  $i^{th}$  slice along failure surface ,  
 $L$  = total length (curved) of failure surface,  
 and  $n$  = number of slices.

### 4.3 COMPUTER PROGRAMMING CONSIDERATIONS.

#### 4.3.1 Program MGSTRN for General Stability Analysis.

A computer program to perform the numerical calculations of the Morgenstern-Price method of stability analysis was developed by Bailey [7] and presented by Hamel [45] for General Analytics Inc. As a detailed description of this computer program, called MGSTRN, is presented by Hamel [45], only a brief outline of the program will be given here.

The main program MGSTRN calls eleven subprograms which actually perform the various calculations. The relationship of these subprograms to the main program and to each other is shown schematically in appendix C. The individual subroutines are also briefly described in appendix C. Also, details of the input data and required input formats, and also, details of column headings and formats for detailed force output, appear in appendix C.

It should be noted that two versions of MGSTRN were written by Bailey. These will be called MGSTRN1 and MGSTRN2. MGSTRN1 is a conversational, time-sharing program, with input solicited by the computer through a remote teletype. The program asks questions regarding input data and is better suited for persons not familiar with the type and format of the input required. MGSTRN2 is a batch program, where all data is read in from a data file, without conversing with the user. Output is then automatically directed to the output device selected. In this research, emphasis was given to the extension of MGSTRN2, the batch version of MGSTRN. The main development for the work reported in this chapter was the incorporation of different distributions of mobilised values of the shear strength parameters implying different progressive failure modes.

From the detailed output obtained from MGSTRN, checks must be made to ensure that the criteria for an admissible solution are satisfied. These criteria are stated in terms of stresses, while the solution of Morgenstern's equations and the output of MGSTRN, gives only forces. Hamel [45], recommended the following criteria for purposes of evaluating Morgenstern-Price solutions to soil slope stability problems.

1. The effective normal forces on the sides and bases of slices should be compressive.
2. The height of the point of application of each of the effective normal side forces, should be between  $0.25H$  and  $0.65H$ , where  $H$  is the height of the slice side.
3. The average friction angle required on the side of each slice when full cohesion is mobilized, should be less than 80% of the average available friction angle along that surface.

The results obtained are examined in the light of these criteria and recommendations for revised criteria are then given.

#### 4.3.2 Program MGSPROG for Variation of $c'$ and $\phi'$ Along Slip Surface.

The computer program MGSTRN performs all calculations involving the Mohr-Coulomb shear strength parameters  $c'$  and  $\phi'$  using a constant value for both  $c'$  and  $\phi'$ , which is input as soil data in the subroutine MTYPIN as described in the previous section. A variation of MGSTRN called MGSPROG (standing for progressive failure by Morgenstern-Price method), was developed to handle the form of progressive failure simulation obtained by varying  $c'$  and  $\phi'$  throughout the failure mass.

Firstly, instead of reading in data as  $c'$  and  $\phi'$  as was previously done in MTYPIN, two additional parameters are read. We now input  $c'_p$ ,  $c'_r$ ,  $\phi'_p$  and  $\phi'_r$  through MTYPIN. Thus the format required for the input of soil data becomes,

Quantity	Input Symbol	Format
First Line :		
Soil Number	ns	F4.0
Total Unit Weight	$\gamma$	F8.3
Peak Cohesion Intercept	$c'_p$	F8.3
Residual Cohesion Intercept	$c'_r$	F8.3
Peak Friction Angle	$\phi'_p$	F5.0
Residual Friction Angle	$\phi'_r$	F5.0
Pore Pressure Ratio	$r_u$	F5.1
Capillary Head Ratio	$r_c$	F4.1
Second Line:		
a	BI(1)	G14.0
b	BI(2)	G14.0
c	BI(3)	G14.0
d	BI(4)	G14.0

(place 99. on new line at end of soil data).

The parameters a,b,c,d are the coefficients of the  $R_1$  equation (4.3).

In MTYPIN, the soil parameters are given new names.

$n_s$  becomes  $K$  ,  
 $\gamma$  becomes  $SOIL(K,1)$  ,  
 $c'_p$  becomes  $SOIL(K,2)$  ,  
 $c'_r$  becomes  $CSNRL(K)$  ,  
 $\phi'_p$  becomes  $SOIL(K,3)$  ,  
 $\phi'_r$  becomes  $PHIRL(K)$  ,  
 $r_u$  becomes  $RU(K)$  or  $SOIL(K,4)$  ,  
 $r_c$  becomes  $SOIL(K,5)$  ,

If only one soil is considered, then  $K$  is always 1. If not, then  $K$  is equal to the soil number (=1,2,3,...etc.).

In the subroutine NEWFSZ, which does most of the detailed calculations involving  $c'$  and  $\phi'$ , the local values of  $c'$  and  $\phi'$  are defined for each slice,  $i$ , for all  $n$  slices.

$$c'_i = c'_p - (R_1)_i (c'_p - c'_r) \quad (4.8)$$

and

$$\phi'_i = \phi'_p - (R_1)_i (\phi'_p - \phi'_r) \quad (4.9)$$

where

$$(R_1)_i = ae^{b \cdot XRL} + c \cdot XRL + d \quad (4.10)$$

and  $XRL$  is the function (decimal from 0 to 1.0) of the horizontal distance from  $X_1$  (x co-ordinate of first point on failure surface) to  $X_n$  (x co-ordinate of last point on failure surface) of the centre of slice  $i$  and is defined as;

$$(XRL)_i = \frac{(X_i + X_{i+1})/2 - X_1}{X_n - X_1} \quad (4.11)$$

These co-ordinates are explained in figure 4.2 .

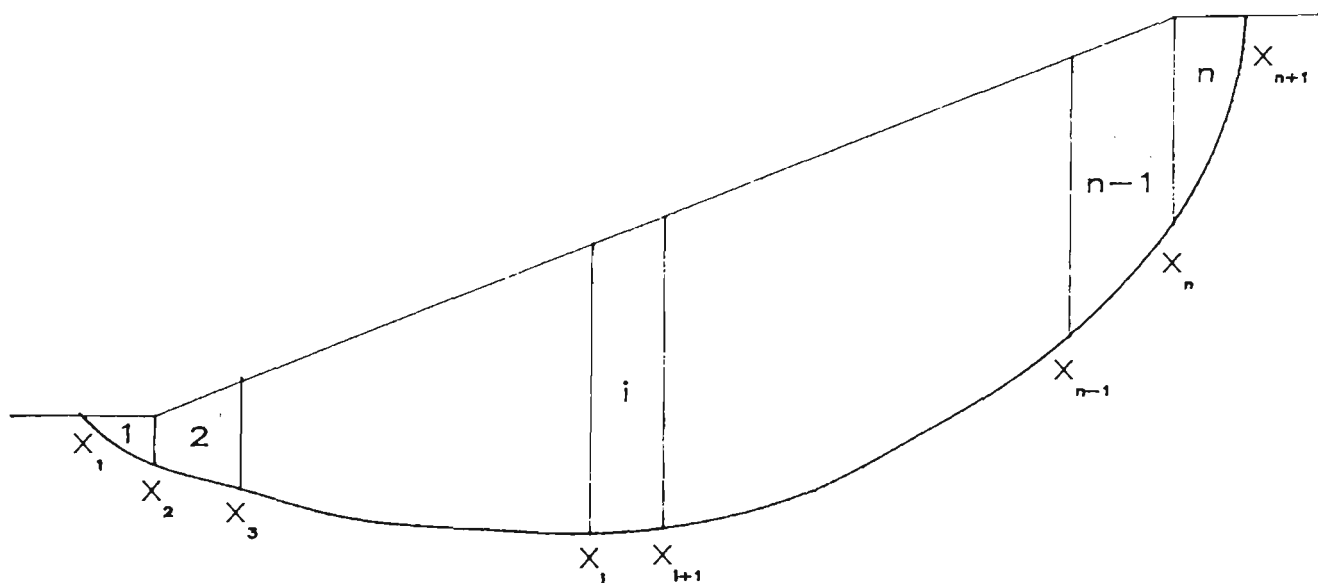


Figure 4.2 Slope Cross Section with Typical Slice Coordinates

Again as with program MGSTRN, two versions of program MGSPROG exist. The first, MGSPROG1, is a conversational, time sharing version, while the second, MGSPROG2, is a batch version with no user interaction. As with MGSTRN, the MGSPROG2 version was used to obtain the results in this chapter. MGSPROG1 was used mainly in error checking work, requiring user interaction, but is much too slow with large amounts of input data.

#### 4.3.3 Program MGSDIST for Calculation of Average Shear Strength.

Program MGSPROG described above, does not calculate the average shear strength  $s_{av}$ . Therefore, a similar program called MGSDIST was created to calculate the value of  $s_{av}$ . MGSDIST also has an extra subroutine called FACTOR, which calls special plotting routines to draw a cross-section of the slope and plot the points of application of each of the effective normal side forces, to check for the second admissibility criteria specified by Hamel. FACTOR also causes plots

of the  $R_1$  distribution and resulting  $\sigma'_i$  and  $s_i$  distribution along the failure surface. The value of  $s_{av}$  is calculated in subroutine OUTPUT using equation (4.7) after values of  $\sigma'$  for each slice have been calculated. Equation (4.7) may be rewritten as follows.

$$s_{av} = \frac{\sum_{i=1}^n s_i \cdot \Delta L}{L} \quad (4.12)$$

where

$$s_i = c'_i + \sigma'_i \tan \phi'_i \quad (4.13)$$

and where  $c'_i$  and  $\phi'_i$  are calculated in subroutine NEWFSZ, (using equations (4.8) and (4.9)) and  $\sigma'_i$  is calculated earlier in OUTPUT.

$\Delta L$  is calculated from the geometry of the failure surface as

$$\Delta L = \left[ (X_{i+1} - X_i)^2 + (Y_{i+1} - Y_i)^2 \right]^{0.5} \quad (4.14)$$

The values of  $c'_{av}$  and  $\phi'_{av}$  are calculated as mentioned above by the following equations.

$$c'_{av} = \frac{\sum_{i=1}^n c'_i \cdot \Delta L}{L} \quad (4.15)$$

$$\phi'_{av} = \frac{\sum_{i=1}^n \phi'_i \cdot \Delta L}{L} \quad (4.16)$$



#### 4.3.4 Program BISHDIST for Varying $c'$ and $\phi'$ Using Bishop's Method of Analysis.

BISHDIST is a program (written in FORTRAN) which was developed on the basis of Bishop's simplified method of analysis to determine the factor of safety of slopes with circular surfaces of sliding. The program has the capability for arbitrary variation of the Mohr-Coulomb shear strength parameters  $c'$  and  $\phi'$  along the failure surface and for calculation of the average shear strength acting along that failure surface at the time of failure. In order to do this, peak and residual values of the parameters must be input to the program, along with the other soil and slope data as follows. Refer to figure 4.3 for explanation of some of the following parameters.

Symbol	Description
R	Slip circle radius
D	Sector angle, $\delta$
BE	Slope angle, $\beta$
SN	Number of strips to be taken
G	Unit weight of soil, $\gamma$
CPK	Peak values of cohesion $c'_p$
CRL	Residual value of cohesion, $c'_r$
RU	Pore Pressure Ratio, $r_u$
PHPK	Peak value of angle of shearing resistance, $\phi'_p$
PHRL	Residual value of angle of shearing resistance, $\phi'_r$

The above data may be input on a single line, with each data element separated by a blank or comma. To describe the distribution of  $c'$  and  $\phi'$  along the failure surface, the parameters a,b,c and d of the  $R_1$  equation (4.3) must be input to the program. This distribution data is read in as follows:

Symbol	Description
DI	Distribution Number
BI(1)	A
BI(2)	B
BI(3)	C

BI(4)

D

Again, these values may be input on one line, each separated by blanks or commas. If more than one distribution is used, the above data is repeated for each distribution, using the respective distribution number DI for each one. At the end of all distribution data, a number greater than 20 must be input to signal the end of the distribution data. If N distributions are used (and thus the highest value of DI is N), the program then divides the slope sector angle  $\delta$  into N equal subsectors, thus dividing the length of the failure surface into N equal lengths, each having a different location and  $R_1$  value. Equations (4.8), (4.9) and (4.10) are then used to evaluate local values  $c'_i$ ,  $\phi'_i$  and  $(R_1)_i$ . However, in this case, the parameter  $(XRL)_i$  is defined as the fraction (decimal from 0 to 1.0), obtained by dividing the angle  $\theta$  by the sector angle  $\delta$ , where  $\theta$  is the angle made by that fraction of the failure arc, exhibiting residual conditions as shown in figure 4.3. The value of  $XRL_i$  is thus given by the expression

$$(XRL)_i = \theta_i / \delta \quad (4.17)$$

The average shear strength along the failure surface is then calculated using equation (4.12) where, in this case,

$$\Delta L = \Delta \theta \cdot R \quad (4.18)$$

and

$$\Delta \theta = \theta_i - \theta_{i-1} \quad (4.19)$$

#### 4.3.5 Calculation of Distribution Parameters a,b,c and d.

In order to input the  $R_1$  distributions shown in appendix B into the programs MGSPROG, MGSDIST and BISHDIST, it was necessary to calculate the coefficients a,b,c and d of equation 4.3. This was done with the aid of a curve fitting program called CURFIT, which used the method of least squares to obtain the equation of the line of best fit (in the form  $y = ae^{bx} + cx + d$ ) of a number of points.

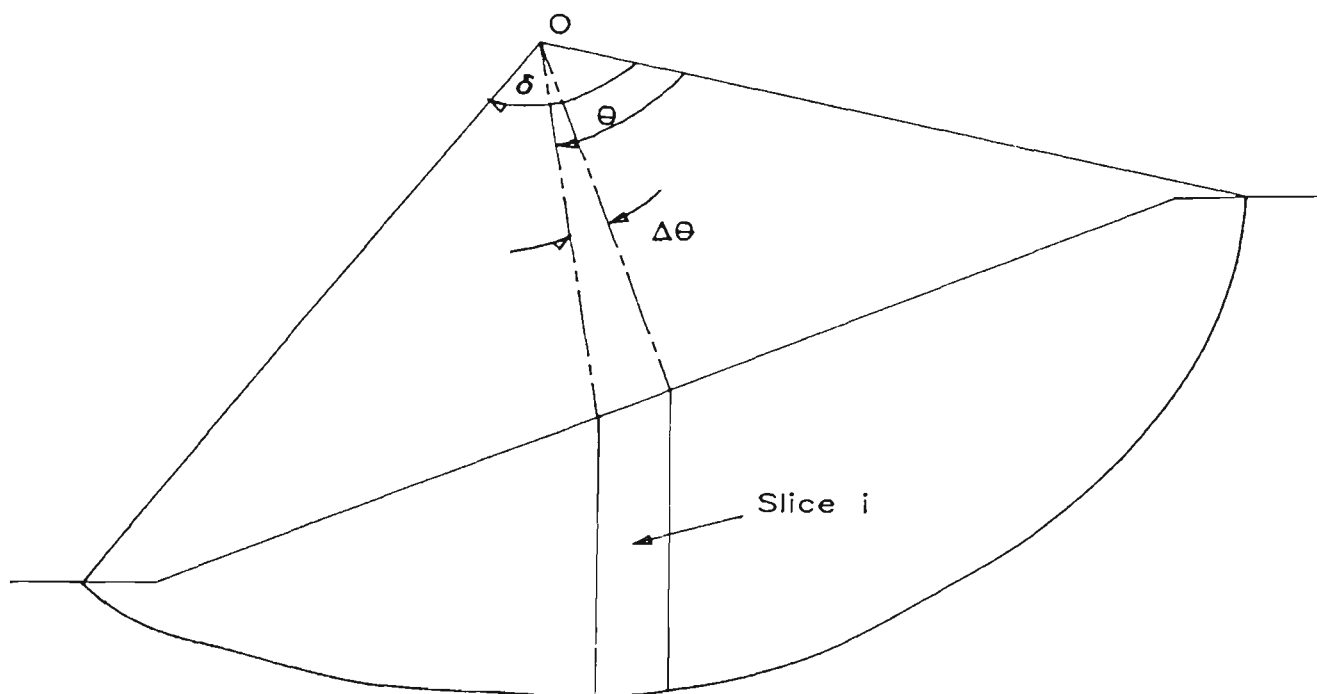


Figure 4.3 Slope Cross Section with Angles Used in BISHDIST

For each of the distributions shown in appendix B, the curve was accurately drawn on graph paper and the x and y co-ordinates of up to 50 points were measured and input into program CURFIT, which gave as results the values of a,b,c and d for that distribution. The resulting values of these coefficients for each distribution are also given in appendix B.

#### 4.3.6 A Significant Difficulty Encountered Using the Programs and How this was Tackled.

When using the Morgenstern-Price programs MGSPROG and MGSDIST, a

problem was encountered in cases where the  $R_1$  distribution was not the same throughout the failure mass (i.e. where discontinuous distributions were used). In cases such as distribution D2, H2, K2, Q and R, there are in fact two distributions for  $R_1$  within the soil mass. As a strength distribution is herein assumed to be a property of the soil along the failure surface, the problem is overcome by assuming that a different type of soil exists for each different  $R_1$  distribution within the failure mass. The values of a, b, c and d are then input as soil parameters. All other soil parameters remain the same as for the original soil, so in fact, only the value of  $R_1$  will change as a 'new soil' is encountered.

#### 4.4 SLOPES AND TYPES OF ANALYSES CONSIDERED.

For the analyses carried out in this chapter it was decided to use three well-known slip case histories. These were the Northolt Slip in cutting, the Vajont Slide, and the Brilliant Cut slide. As well as these three cases, a fourth example was also analysed. This case will be referred to as Hypothetical Slip Number 1 (HS1) and consists of a simple slope of uniform inclination, homogeneous soil and an assumed circular failure surface. The reason for using slope HS1 is to eliminate any effects of irregularities in slope geometry on the results obtained. Full descriptions of these four slopes are presented in appendix A.

The first three slopes were analysed using programs MGSPROG and MGSDIST. Slope HS1, however, was analysed both by the above two programs and also by program BISHDIST to allow direct comparison of results obtained using the two different methods of stability analysis.

##### 4.4.1 Northolt Slip in Cutting (Henkel [48], Skempton [88]).

For the purpose of this research, the slope geometry used is as shown in appendix A. However, the actual slip surface is used rather

than the approximated circular surface used by Skempton. Also, the shear strength parameters consistent with a factor of safety of 1.0 (as given by Skempton [88]) were used. These parameters are

$$\begin{aligned}\phi_p &= 18^\circ & \phi'_r &= 9.5^\circ \\ c'_p &= 6.7 \text{ kPa} & c'_r &= 0\end{aligned}$$

Two series of analyses were performed on the Northolt slip. The first of these is denoted by the name 'Series A' and consists of a large number of individual runs of programs MGSPROG and MGSDIST, each corresponding to one of the  $R_1$  distributions presented in appendix B. In these analyses, a constant pore-pressure ratio of 0.34 is used for the slope.

'Series B' is a series of analyses aimed at observing the influence of the pore-pressure ratio  $r_u$  on the relationship between the factor of safety obtained and the value of average shear strength along the failure surface. Pore-pressure values of 0, 0.34 and 0.68 were used as well as a fourth case, in which the position of the piezometric surface was assumed to be known. This case gave a value of average  $r_u$  of approximately 0.35).

#### 4.4.2 Vajont Slide (Broili [21], Lo, Lee And Gelinas [64]).

The slope geometry and shear strength parameters used for the Vajont slope are presented in appendix A. The shear strength parameters are varied in a number of ways for each  $R_1$  distribution used. These strength variations are as follows.

- (a)  $c'$  remains constant at the peak value, while  $\phi'$  varies between the peak and residual values,

- (b) both  $c'$  and  $\phi'$  vary between the peak and residual values,
- (c)  $c'$  remains constant at the residual value, while  $\phi'$  varies between the peak and residual values,
- (d)  $c'$  varies between the peak and residual values, while  $\phi'$  remains constant at the peak value,
- (e)  $c'$  varies between the peak and residual values while  $\phi'$  remains constant at the residual value.

#### 4.4.3 Brilliant Cut Slide (Ackenheil [1], Hamel [45],[46]).

In both the previous cases, the soil was taken to be uniform throughout the length of the failure surface. The Brilliant Cut failure mass on the other hand, encompasses five approximately homogeneous zones of soil or rock material. It was chosen to enable a study of the relationship between the resulting factor of safety for the slope and the  $R_1$  distributions and calculated shear strengths in a case where the soil is not uniform throughout the slope (and hence also non-uniform in shear strength along the slip surface).

Having calculated the value of  $R_1$  for various points along the failure surface, the local values of  $c'$  and  $\phi'$  are then found using equations (4.5) and (4.6). The peak and residual values of  $c'$  and  $\phi'$  in these equations vary from one soil to another and thus the respective values must be used depending on the soil existing on the failure surface at the point being considered. For the purpose of this work the soil and rock parameters given in appendix A are used.

For studies concerning the two previous examples, a constant side-force function assumption was used for the Morgenstern-Price method. For studies concerning this case history, two alternatives were used. These two side-force assumptions are (1) constant, and (2) full sine wave added to a trapezoid function (see Hamel [45]). Experience had shown that the other side force function assumptions

described by Hamel did not produce feasible results.

#### 4.4.4 Hypothetical Slip Number 1.

As mentioned earlier, a hypothetical slope stability problem was also used as an example. The slope geometry and soil parameters used are as shown in appendix A.

As with the Northolt Slip, a number of analyses were carried out with the aim of gaining some insight into the effect of pore water pressure on the relationship between the average shear strength obtained along the failure surface and the resulting factor of safety. In order to do this a number of different analyses were carried out, each using a different value of pore pressure ratio  $r_u$ . The values of  $r_u$  used were 0, 0.25, 0.34 and 0.68.

Two sets of analyses were performed. The first is based on the Morgenstern-Price method of analysis as for the previous case histories, while the second is based on the Bishop simplified method. Program MGSDIST was used for the first series which is denoted series A while program BISHDIST was used for the second series denoted series B. For both series, all the above values of  $r_u$  were used. Furthermore, five distributions of shear strength parameters  $c'$  and  $\phi'$  were considered. These five correspond to  $R_1$  distributions A1, B, M, N and P shown in appendix B.

### 4.5 RESULTS AND DISCUSSION.

#### 4.5.1 Solution Admissibility - A New Proposal.

This section contains the results of the analyses described earlier in this chapter. These results are presented in graphical form. The resulting factors of safety should be evaluated for admissibility using the three admissibility criteria stated earlier. These admissibility criteria should also serve as a measure of the

acceptability of the  $R_1$  distributions used.

In order to facilitate the evaluation of the overall admissibility of a given result for a particular slope, the following reliability factor  $\omega$  is defined. For each of the three admissibility criteria noted earlier, the number of slices within the slope which satisfy that particular criteria  $N_s$  is divided by the total number of slices in the slope  $N_t$ . The three results are averaged and expressed as a percentage as shown in equation (4.20) below.

$$\omega = (100/3) \sum (N_s)_i / N_t \quad (4.20)$$

The procedure suggested above is only an approximate one and gives a reasonable indication of the reliability of any given result. However, it cannot be used as a cut and dry rule for assessing the admissibility of a solution. It can be said, however, that solutions with reliability factors of, say, over 60% are fairly reliable whereas solutions with factors under 20% may be disregarded. This conclusion is based on experience of the author.

#### 4.5.2 Northolt Slip in Cutting.

As mentioned in the previous section, the first of the two series of analyses performed on the Northolt Slip involved a large number of  $R_1$  distributions used in conjunction with the Morgenstern-Price method of stability analysis.

The calculated values of average shear strength and their corresponding values of factor of safety were plotted against each other as shown in figure 4-4. From an analysis of this plot it is evident that a definite relationship exists between the factor of safety,  $F$  for the slope and the average shear strength,  $S_{av}$  along the failure surface. This relationship is of linear form.



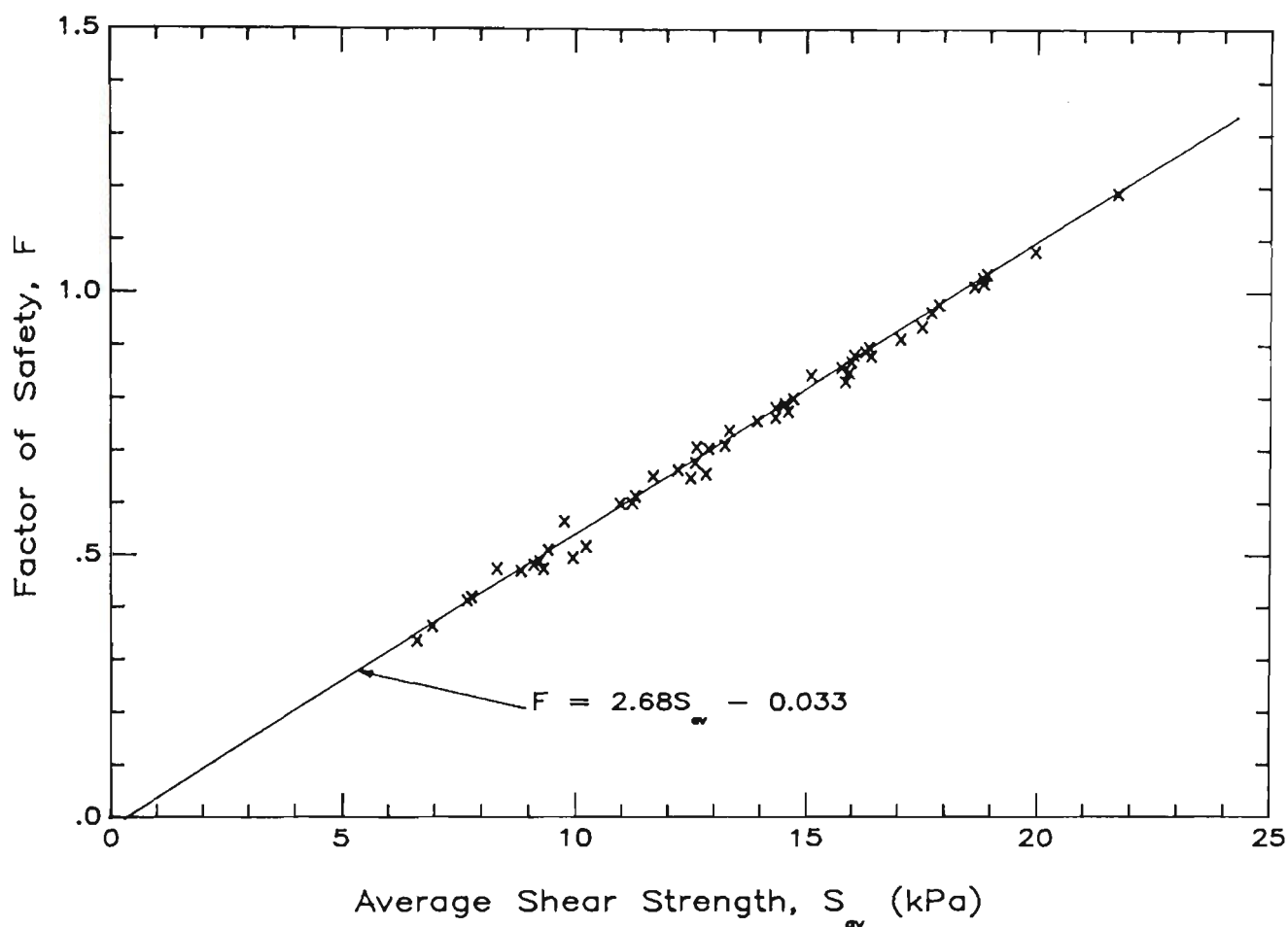


Figure 4.4 Factor of Safety vs. Average Shear Strength on Slip Surface for Northolt Slip — Analysis Group A

Although some degree of scatter is evident in the plot, this scatter is relatively low and a line of best fit is easily drawn through the given points. The equation for this straight line was found to be

$$F = 2.68 S_{av} + \varepsilon \quad (4.21)$$

where  $\varepsilon \approx -0.03$

The constants in the equation (i.e. 2.68 and -0.03) are mainly a reflection of this particular slope and slip surface geometry.

Primarily, this empirical equation serves to indicate that, for this particular slope, given this specific set of soil data, a given relationship exists between  $F$  and  $S_{av}$  irrespective of which distribution of  $R_1$  is used for  $c'$  and  $\phi'$ . The resulting factor of safety, therefore, depends only on the value of the average shear strength over the failure surface, regardless of the mode or direction of failure progression. In an absolutely accurate solution, one might expect the straight line shown in figure 4.4 (i.e.  $\varepsilon \approx 0$ ).

Earlier in this chapter, it was pointed out that the results presented here are attributed to various distributions of  $c'$  and  $\phi'$ . Not much mention has yet been made, however, of the actual distribution of the shear strength mobilised along the failure surface, or, of its relationship to the  $c'$  and  $\phi'$  distributions used. It may be recalled that values for a distribution of shear strength could not be directly used in any limit equilibrium method of analysis since specific data on the values of the effective shear strength parameters  $c'$  and  $\phi'$  is always required. Therefore, the distribution of mobilised shear strength is obtained from the known local values of  $c'$  and  $\phi'$ , and values are then obtained from the actual solution for  $\sigma'$  along the failure surface ( $\sigma'_n$  is the value of the effective normal stress on the base of a soil slice).

The above mentioned shear strength distributions were plotted and examined. In general, it was noted that the resulting shear strength distributions bear little resemblance to the assumed  $R_1$  distributions for  $c'$  and  $\phi'$ . In other words, the manner in which  $c'$  and  $\phi'$  are mobilised along the slip surface as a consequence of some mechanism of progressive failure does not have a significant influence on the form of the spatial distribution of mobilised shear strength along the slip surface.

The most prevalent type of shear strength distribution was found to be as shown in figure 4.5. It is worthy of note that the value of  $s$  decreases towards both ends of the slip surface and may approach zero. This is not surprising considering that the normal effective stress  $\sigma'$  approaches zero at the extreme boundaries of the failure surface, and that the value of  $s$  then depends only on the value of  $c'$  which, in many of the above examples, is taken as zero. This factor

would suggest that the  $R_1$  distributions given by Bishop and presented in figure 3.4 may be somewhat unrealistic and not relevant to the limit equilibrium method of slope analysis. If Bishop's distributions were to be taken, not as shear strength distributions, but as distributions of the shear strength parameters  $c'$  and  $\phi'$ , then they are certainly feasible in a progressive failure context. For ' $\phi = 0$ ' situations, the conclusions will be different. However, this thesis is concerned primarily with effective stress slope stability analyses.

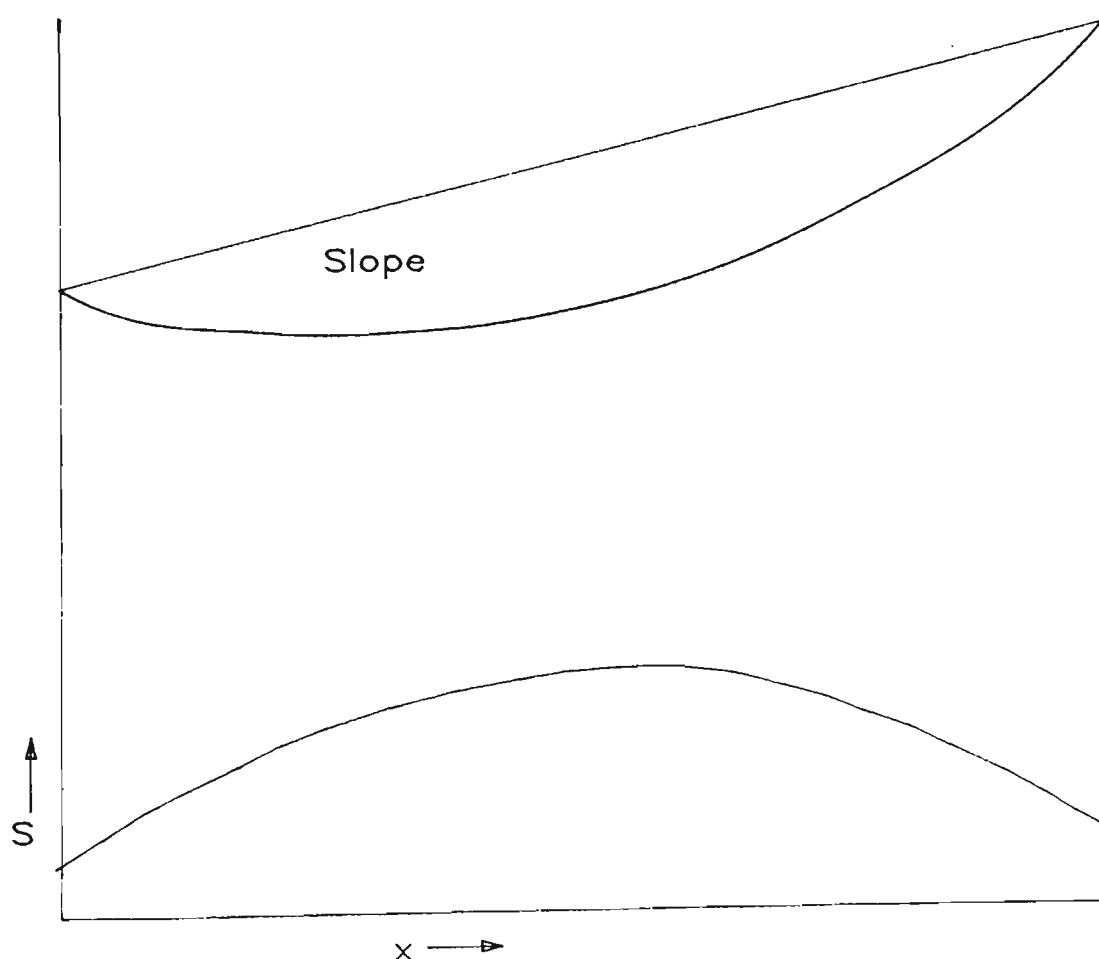


Figure 4.5 General Form of Shear Strength Distribution

As a further comment on Bishop's proposed distributions, it is worth comparing the results obtained by similar but opposite distributions. In other words, comparing the results of distributions B, Q and O (where failure appears to start at the toe of the slope) to those of B2, R and P (where failure is assumed to start at the crest)

shows a slightly lower factor of safety for the latter. It could be said that in cases where local failure starts at the crest of the slope, the chances of overall slope failure are greater. Also, cases where local failure is assumed to start near the centre of the slope and proceed outwards were found to yield low factors of safety compared to cases where local failure started from the toe or where local failure started from both the toe and crest of the slope simultaneously.

It would therefore appear that while the variations in the factors of safety were small and may have been due largely to the geometrical properties of the slope, local failures starting from the crest of the slope or from the centre of the slope are most likely to cause overall slope failure.

The Reliability Factor  $\omega$  gives a measure of the extent to which the admissibility criteria given by Hamel [45] are satisfied. Most values of  $\omega$  were found to be between 30% and 60% with a few as low as 27% or as high as 73%. It must be remembered that the three admissibility criteria were presented firstly by Morgenstern and Price [68] and later reviewed by Hamel [14], with the view of developing guidelines for the acceptability of solutions obtained by the Morgenstern-Price method of slope stability analysis. Since the Morgenstern-Price method is a limit equilibrium method and the assumption made in all limit equilibrium methods is that the factor of safety,  $F$  is constant throughout the Slope (an assumption which is actually true only at failure when  $F=1$ ), then the admissibility criteria can be said to apply only in the region of  $F=1$ . Thus if  $F$  is less than say 0.6, or much greater than 1.0, then  $\omega$  would be expected to be low. This is supported by the fact that cases in which  $F$  lies between the limits of 0.95 and 1.15 have  $\omega$  values between 56% and 73%, while for cases where  $F$  is less than 0.5,  $\omega$  is usually less than 30%.

From this, it would appear that the reliability factor  $\omega$  can only be effectively used as a measure of admissibility if the solution lies in the region of  $F=1$ . However, the value of  $\omega$  is never higher than 73%, which means that the admissibility criteria are never fully satisfied. Upon a more detailed investigation of the results, it is found that criterion number 1, which states that the effective normal

forces on the sides and bases of slices should be compressive, is satisfied most of the time (that is, only a few slices exist in each analysis, where the criterion is not satisfied). Looking at criterion number 2, it is found that the height of the point of application of each of the effective normal side forces, lies between  $0.25H$  and  $0.65H$  (where  $H$  is the height of the slice) in less than half of the total number of slices. Also the third criterion, which states that the average friction angle required on the side of each slice when full cohesion is mobilized, should be less than 80% of the average available friction angle along that surface, is only satisfied to a certain degree (about 80% of slices for  $F=1.0$ ).

It would seem that of the three criteria given, the first can be taken as a fair indication to acceptability, the third should be looked into in more detail and the second can be said to be unacceptable for consideration, as it seems highly unlikely that it would ever be satisfied to a reasonable degree except under ideal conditions.

To facilitate analyses in the following sections, the number of  $R_1$  distributions used was reduced to ten only. This was done in order to save time and reduce the number of calculations. Many of the distributions give similar results and thus can be eliminated. Those distributions were chosen which gave the widest range of results, the least repetition of results and the largest variation of distribution shapes. They are A2, B1, M, P, H2, K1, K2, Q and R, as described in appendix B.

The second series of analyses performed on the Northolt Slip was, as mentioned earlier, an attempt to observe the effects of different pore water pressure values on the relationship between the factor of safety  $F$  and the average shear strength mobilised along the failure surface  $s_{av}$ . To do this, four sets of analyses were carried out using values of pore-pressure ratio equal to 0, 0.34 and 0.68 for the first three respectively while providing an assumed piezometric surface for the fourth. Only the ten  $R_1$  distributions mentioned above are used in these analyses. The results of these analyses were plotted and are shown in figure 4.6.

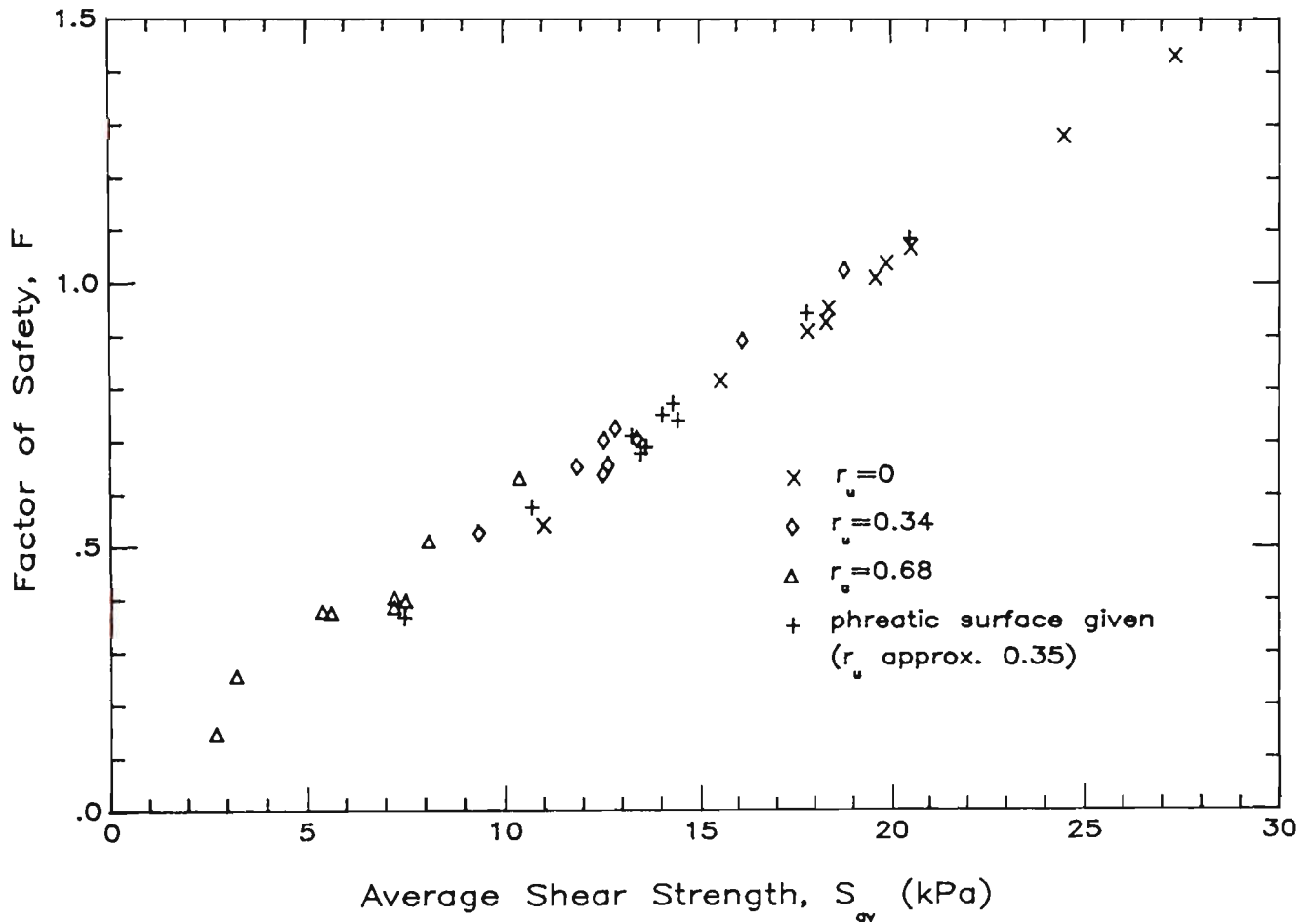


Figure 4.6 Factor of Safety vs. Average Shear Strength for Northolt Slip — Analysis B

#### 4.5.3 The Vajont Slide.

Based on the factors mentioned in the previous section, only ten  $R_1$  distributions were used with the Vajont Slide. However, for each of these distributions, a number of combinations of the shear strength parameters is used. These combinations are as follows.

- (a)  $c'$  remains constant at the peak value while  $\phi'$  varies between the peak and residual values,
- (b) both  $c'$  and  $\phi'$  vary between their peak and residual values,

- (c)  $c'$  remains constant at the residual value while  $\phi'$  varies between its peak and residual values,
- (d)  $c'$  varies between the peak and residual values while  $\phi'$  remains constant at its peak value,
- (e)  $c'$  varies between the peak and residual values while  $\phi'$  remains constant at the residual value.

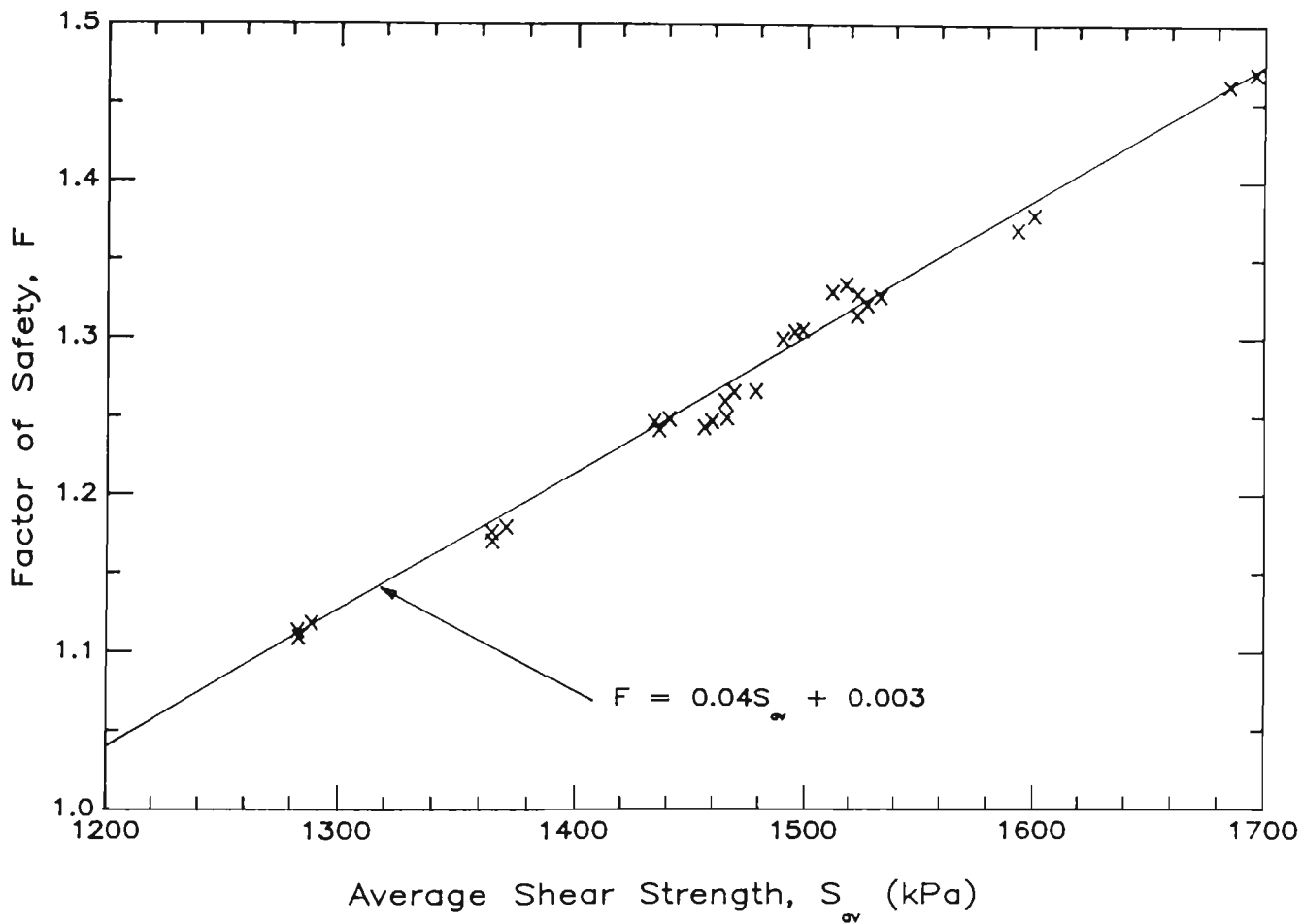


Figure 4.7 Factor of Safety vs. Average Shear Strength Along the Slip Surface for the Vajont Slide.

Figure 4.7 displays the resultant factors of safety plotted against their respective values of  $s_{av}$ . Apart from a slightly higher degree of scatter, it is seen that the relationship between  $F$

and  $s_{av}$  is very similar to that obtained with the Northolt Slip. The curve of best fit is again linear and is described by the expression

$$F = 0.0414s_{av} + \varepsilon$$

where  $\varepsilon \approx 0.003$

Once again, this relationship confirms that the value of  $F$  is not directly related to the type of distribution used but to the average shear strength mobilised along the failure surface which is, of course, influenced not only by the distribution but also by the pore water pressure, the normal stress, and peak and residual shear strength parameters

#### 4.5.4 The Brilliant Cut Slide.

The same series of distributions and combinations of shear strength parameters as was used with the Vajont Slide was also used with the Brilliant Cut Slide. Two series of analyses were performed however. As well as using side-force assumption 1 in the Morgenstern-Price program MGSDIST, a second side force assumption, 7 is used in order to obtain an indication of the effect on the analysis results of using a different assumption.

As pointed out earlier, the Brilliant Cut Slide is an example of a failure mass encompassing a number of soil or rock materials. It is not uniform like the previous slopes analysed and therefore gives some indication of the behaviour of the  $F$  vs  $s_{av}$  relationship in a slope where the distribution curve for  $c'$  and  $\phi'$  varies according to the soil type encountered.

Hamel [45] used two side-force assumptions in attempting to evaluate the stability of the slope and the same two side-force assumptions are used here (1 and 7). He concluded that the solution obtained using side-force assumption 1 was acceptable by the acceptability criteria which he defined, but that the solution



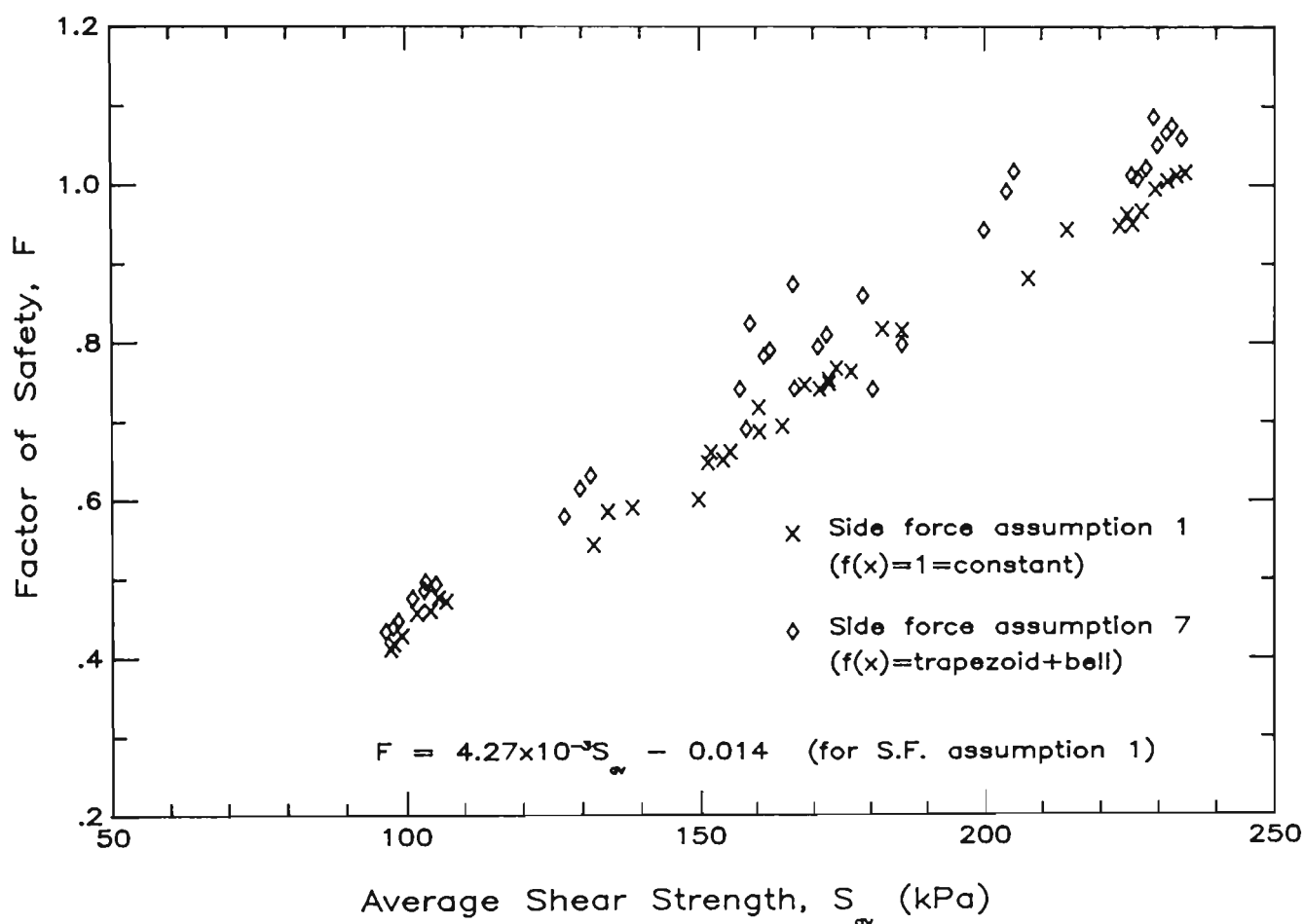


Figure 4.8 Factor of Safety vs. Average Shear Strength for Brilliant Cut Slide

obtained from side-force assumption 7 was not. By comparing the two sets of results, which are displayed in figure 4.8, it can be seen that there is a large degree of scatter in the results obtained using side-force assumption 7 while only a small amount of scatter exists in the set of results obtained using side-force assumption 1. The relationship based on a constant side force assumption is again linear and can be expressed as

$$F = 4.3 \times 10^{-3} S_{av} + \varepsilon$$

where  $\varepsilon \approx -0.014$

The above observations reinforce the decision made earlier to use

side-force assumption 1 as the standard assumption throughout this research. They also support the findings of the previous two cases analysed.

#### 4.5.5 Hypothetical Slip Number 1.

As was mentioned in the previous section two further series of analyses were carried out on Hypothetical Slip number 1. The first, series A, was based on the Morgenstern-Price method of analysis to calculate the factor of safety of a number of cases. A number of  $R_1$  distributions was used, each with three different pore pressure values. The second, series B, uses the same  $R_1$  distributions and pore-pressure values, but this time Bishop's simplified method was used to perform the stability analyses.

The results of these analyses are shown in figure 4.9. Apart from the fact that the results obtained by the Morgenstern-Price method have, in general, a higher degree of scatter when plotted than those results obtained by the Bishop simplified method, the line of best fit of the Morgenstern-Price results appears to be slightly higher and to the left of the Bishop method results. Also, the data from the three sets of analyses using the three different values of pore-pressure ratio appears to lie on the same line. This implies that pore-water pressure has no effect on the relationship between the factor of safety and the average shear strength. It is well known that the factor of safety  $F$  decreases as  $r_u$  increases, but the average mobilised shear strength decreases by a proportionate amount so as to leave the relationship between the two unchanged. Also, the relationship between  $F$  and  $s_{av}$  is again linear as has been found to be the case in earlier analyses.

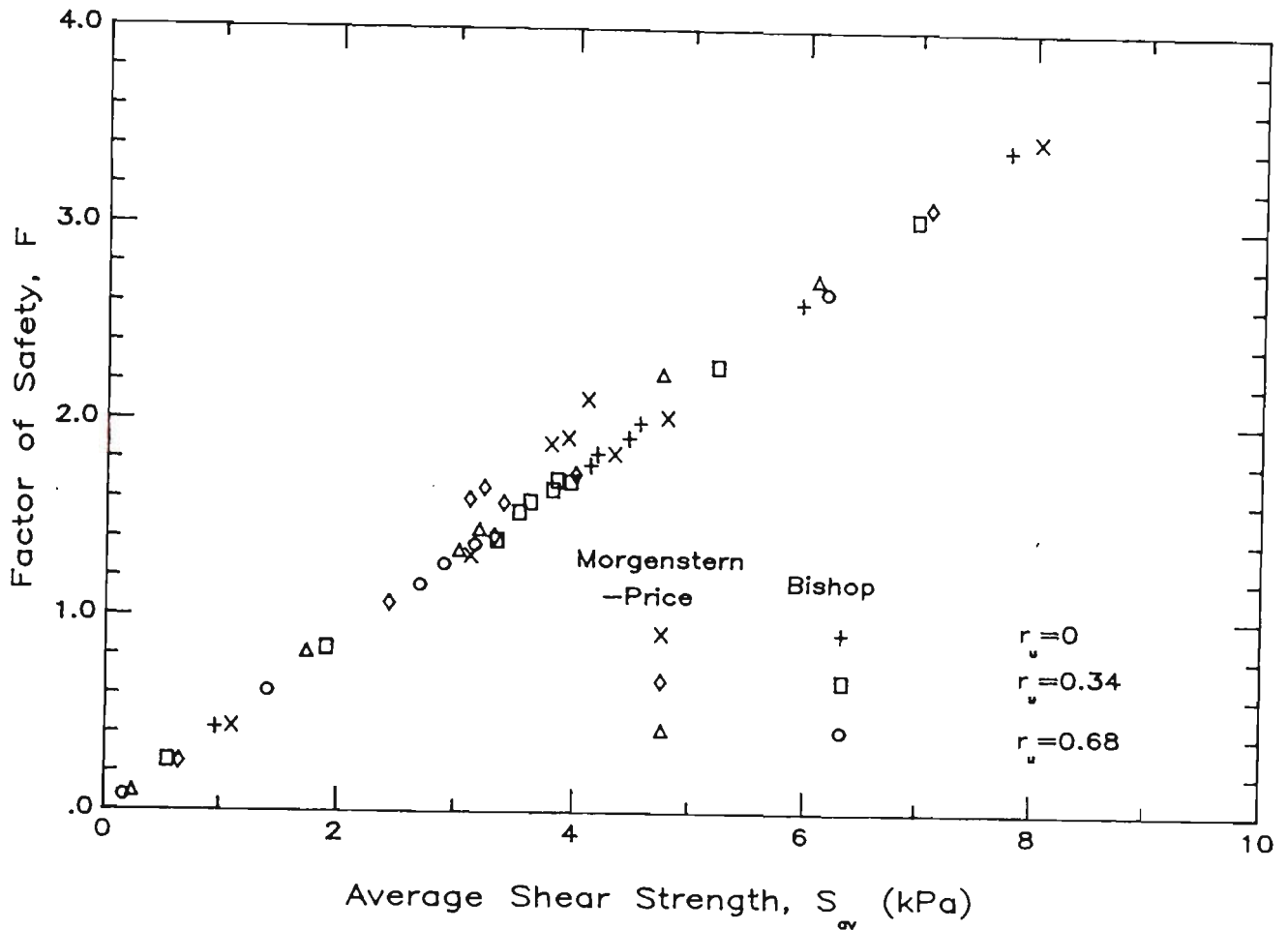


Figure 4.9 F.o.S vs. Average Shear Strength for Arbitrary Circular Slip Surface (Analysis A) – Sample Problem with Uniform Slope and Homogeneous Soil.

#### 4.6 RELATIONSHIP BETWEEN LOCAL AND OVERALL RESIDUAL FACTOR.

##### 4.6.1 $R_1$ Defined in Terms of Mobilised Shear Strength at a Point.

The shear strength mobilised at a point is given by equation (4.2) and is reproduced below

$$s = c'_p + \sigma'_n \tan \phi'_p - R_1 \left[ (c'_p - c'_r) + \sigma'_n (\tan \phi'_p - \tan \phi'_r) \right] \quad (4.4)$$

The average shear strength over a slip surface is given by

$$s_{av} = \frac{1}{L} \int s \, dl \quad (4.22)$$

and substituting for  $s$ , we have

$$s_{av} = s_p - \frac{(s_p - s_r)}{L} \int R_1 \, dL \quad (4.23)$$

Substituting this in the Skempton equation for residual factor, i.e. in the equation

$$R = \frac{s_p - s_{av}}{s_p - s_r}$$

we have the simple result

$$R = \frac{1}{L} \int R_1 \, dl \quad (4.24)$$

#### 4.6.2 $R_1$ Defined in terms of Mobilised Shear Strength Parameters $c$ and $\phi$ at a Point.

The local mobilised shear strength at a point is given by

$$s = c + \sigma \tan \phi$$

where, in terms of the local residual factor  $R_1$

$$c = c_p - R_1(c_p - c_r)$$

$$\phi = \phi_p - R_1(\phi_p - \phi_r)$$

Substituting these values and integrating over the length of the slip surface, the average shear strength becomes

$$s_{av} = c_p - \frac{c_p - c_r}{L} \int R_1 dl + \int \sigma' [\tan\{\phi_p - (\phi_p - \phi_r)R_1\}] dl \quad (4.25)$$

Considering the two limiting cases  $R_1=0$  and  $R_1=1$ .

For  $R_1=0$  and  $s_{av}=s_p$  the above equation reduces to

$$s_p = c_p + \sigma'_{av} \tan \phi_p$$

For  $R_1=1$  and  $s_{av}=s_r$  the equation becomes

$$s_r = c_r + \sigma'_{av} \tan \phi_r$$

Noting the general expression for  $s_{av}$ , the integration of the second term would depend only on the actual  $R_1$  distribution. However, the integration of the last term is dependent on the distribution of the effective normal stress as well as that of  $R_1$ . Therefore, the  $s_{av}$  is theoretically indeterminate. Accordingly, a simple theoretical relationship between  $R$  and  $R_1$  can not be derived.

It may be noted also that in the Skempton residual factor equation

$$R = \frac{s_p - s_{av}}{s_p - s_r}$$

$s_p$  and  $s_r$  can not be regarded as constants since  $\sigma'$  varies over the length of the slip surface. However, from the two limiting cases derived above, it would be quite in order to express  $s_p$  and  $s_r$  in terms of the average effective normal stress so that

$$R = \frac{c_p + \sigma'_{av} \tan \phi_p - s_{av}}{(c_p - c_r + \sigma'_{av} (\tan \phi_p - \tan \phi_r))} \quad (4.26)$$

To determine the value of the average residual factor, it would first be necessary to carry out the appropriate limit equilibrium analysis with the known  $R_1$  distribution. From this analysis, both the average shear strength and the average normal stress can be calculated. Knowing these values, the value of the overall residual factor would then be known.

#### 4.7 RELATIONSHIP BETWEEN OVERALL RESIDUAL FACTOR R AND FACTOR OF SAFETY F.

In the ideal case, the overall factor of safety would be directly proportional to the average shear strength. i.e.

$$F = K \cdot s_{av}$$

where K is a constant for a given slope and slip surface and represents the inverse of the average shear stress over a slip surface. Knowing the overall residual factor R we get

$$s_{av} = s_p - R(s_p - s_r) \quad (4.27)$$

and by definition of R we arrive at the expression

$$F = Ks_p - RK(s_p - s_r) \quad (4.28)$$

The values of  $s_p$ ,  $s_r$  and R depend on the average normal stress. Moreover, the value of R also depends on the local residual factor distribution. Therefore, there is no unique relationship between the factor of safety and the residual factor R. In general, it is obvious that as R increases, F will decrease. Assuming for simplicity that R can be varied independently without significantly

influencing  $s_p$  and  $s_r$ , the variation of  $F$  with  $R$  is linear, decreasing from  $F=Ks_p$  at  $R=0$  to  $F=Ks_r$  at  $R=1$  (see figure 4.10). In general, however, the relationship will be non-linear since variation in  $R$  reflects a change in the average normal stress and hence in the values of peak and residual shear strength based on the average effective normal stress. In this context, it is interesting to note that Lo and Lee [62] and Chowdhury and DeRooy [33] found the relationships between  $F$  and  $R$  to be somewhat non-linear using finite element and limit equilibrium procedures respectively. In both cases, very simple  $R_1$  distributions were assumed by the authors i.e.  $R_1=1$  over part of the slip surface and  $R_1=0$  over the remaining part.

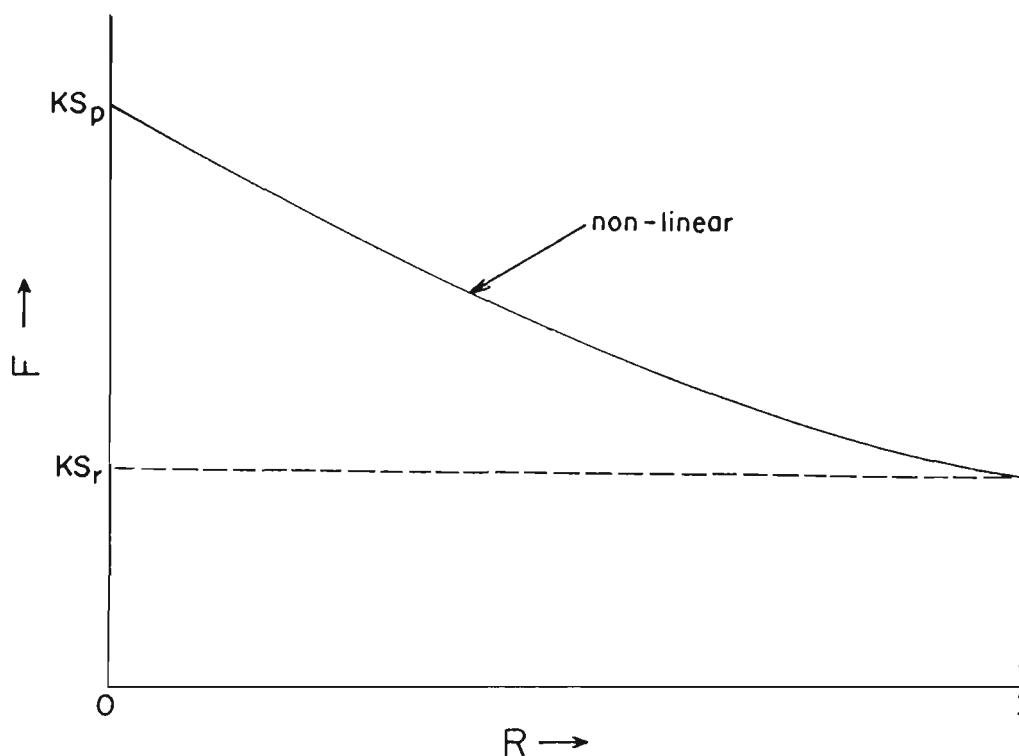


Figure 4.10 Relationship between  $F$  and  $R$ .

#### ' $\phi=0$ ' Situation.

For problems in which the shear strength is independent of the normal effective stress (saturated clay under short-term undrained conditions), the relationship between  $F$  and  $R$  will be linear. The average shear strength is given by

$$s_{av} = c_{u_p} - (c_{u_p} - c_{u_r}) \frac{1}{L} \int R_l dl$$

Using the result obtained in equation (4.24) we have

$$s_{av} = c_{u_p} - (c_{u_p} - c_{u_r})R$$

This result could also have been obtained directly from (4.26) or (4.27). Moreover, from equation (4.28)

$$F = Kc_{u_p} - RK(c_{u_p} - c_{u_r})$$

Thus both the average shear strength and the factor of safety are linear functions of the overall residual factor as shown in figure 4.11.

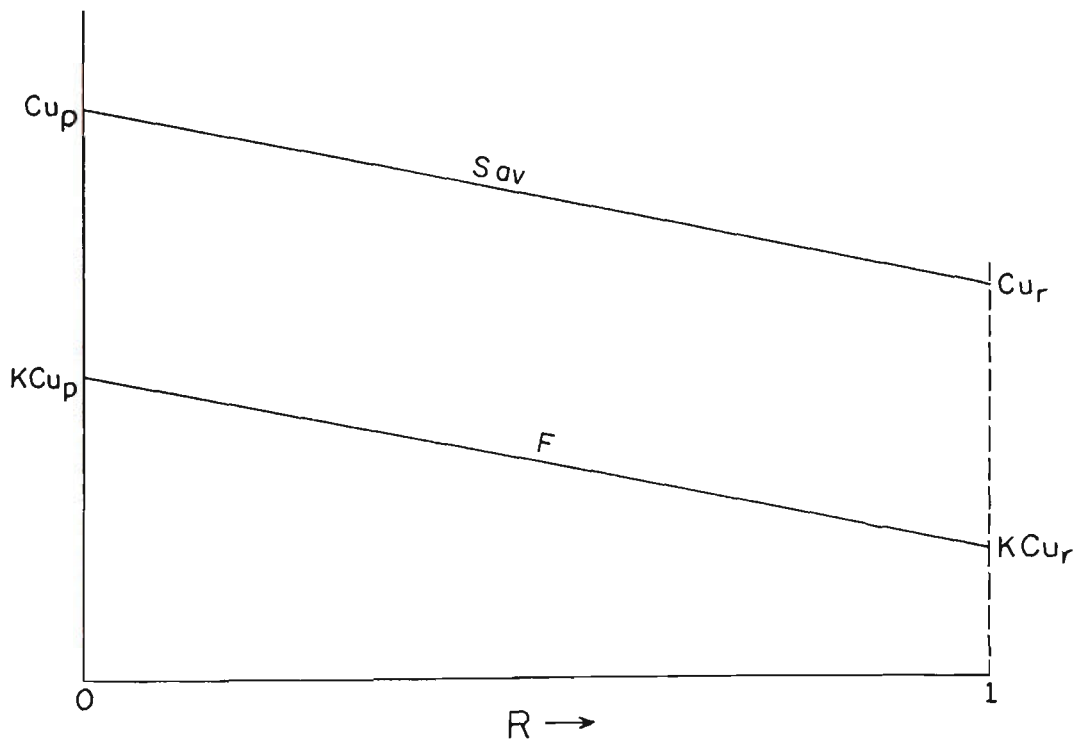


Figure 4.11 Relationship between  $F$ ,  $s_{av}$  and  $R$ .



#### 4.8 SUMMARY AND CONCLUSIONS.

During progressive failure the shear strength along the potential slip surface may vary gradually from a peak value to a residual value. The distribution of mobilised shear strength will depend primarily on the mode and direction of failure progression. However, the exact nature of the distribution of mobilised shear strength parameters can not be determined. Therefore, it is useful to generate a number of distributions and study the results of stability analyses based on them. It should be noted that an arbitrary distribution of mobilised shear strength parameters may be associated with the instant of complete slope failure or sliding. However, even if complete sliding does not occur, a slip surface may have propagated and there may be sufficient movements and deformations associated with progressive decrease of shear strength. Accordingly, arbitrary distributions of mobilised shear strength parameters can be expected in slopes which are currently stable but which may have suffered some degree of deformation and distortion.

Various distributions of the local residual factor  $R_1$  were generated to simulate the mobilisation of shear strength parameters  $c'$  and  $\phi'$  along a slip surface. New procedures were developed so that stability analyses could be carried out within the framework of limit equilibrium using any arbitrary distribution of the local residual factor. These procedures can handle slip surfaces of circular shape as well as slip surfaces of arbitrary shape. The new generalised procedures were found to be feasible and proved successful for all the problems that were analysed.

One aim of the analyses was to determine whether the shape of a distribution of  $R_1$  has any influence on the overall factor of safety. However, the factor of safety was found to be directly proportional to the average mobilised shear strength regardless of other factors. This result appears intuitively reasonable for simulation of slope stability in homogeneous soil when progressive effects are ignored. However, for analyses which include progressive effects leading to the non-uniform mobilisation of shear strength parameters, such a simple and neat relationship could not have been predicted without the new procedures for analysis established in this

thesis.

In the ideal case, the straight line relating  $F$  to  $s_{av}$  would pass through the origin. Computed results show a small intercept on the X or Y axes even though a rigorous limit equilibrium approach (Morgenstern-Price) is used as the basis for the development of the new analysis procedures. The results of the analyses by any method would be unacceptable if the intercept were significant and the following criterion is proposed on the basis of experience gained so far.

$$F = Ks_{av} + \varepsilon, \quad \varepsilon \leq 0.05$$

This may be regarded as a criterion for the acceptability of the solution method.

The three criteria proposed by Hamel [45] for the admissibility of the Morgenstern and Price solution were also examined. The first criterion requiring that the effective normal forces on the sides and bases of slices be compressive was almost always satisfied. The second criterion, which required that the point of application of the effective normal side forces should lie between  $0.25H$  and  $0.65H$  ( $H$  being the slice height) was found to be very stringent and was not satisfied for all the slices.

A 'reliability factor'  $\omega$  was proposed as a measure of the extent to which any given solution satisfies those criteria and this factor has been defined in equation (4.20). Considering all the slices into which a slope has been divided, the reliability factor never approached 100% and was generally below 80%. On the basis of experience, the satisfaction of the first of Hamel's three criteria is a good yardstick of the admissibility of a solution.

Keeping everything else constant, the value of the factor of safety  $F$  decreases linearly with increase in porewater pressure ratio  $r_u$  because such an increase leads to a corresponding decrease in the average shear strength. Analyses were carried out to study the influence of  $r_u$  on the relationship between  $F$  and  $s_{av}$  and this influence was found to be insignificant. In other words, for a given

fixed value of mobilised shear strength,  $F$  changes very little even if  $r_u$  changes significantly.

In general, the mobilised shear strength is of the form shown in figure 4.5 regardless of the type of distribution chosen for the local residual factor  $R_1$ . This form does not resemble the distributions of mobilised shear strength suggested by Bishop [14] which are unrealistic. It is not appropriate to apply an arbitrary distribution of the residual factor to the shear strength. However, as proposed in this thesis, such distributions may be assumed for the shear strength parameters  $c'$  and  $\phi'$ . If the distributions of  $R_1$  were intended for  $c'$  and  $\phi'$ , such distributions have indeed been shown to be feasible in respect of progressive failure along slip surfaces in slopes. However, other types of distributions of the residual factor  $R_1$  are equally feasible.

Based on the relationship that the factor of safety is directly proportional to the average shear strength, it has been shown that the factor of safety decreases with an increase in the residual factor  $R$ . The relationship is expected to be non-linear in the general case and linear under ' $\phi=0$ ' conditions.

The average shear strength  $s_{av}$  and the overall residual factor  $R$  may be related to the local residual factor  $R_1$ . The relationships are, in general, not simple except for the case where  $R_1$  is applied to the mobilised shear strength.

## CHAPTER 5

### STRAIN SOFTENING: LOCAL FAILURE AND STRESS REDISTRIBUTION.

#### 5.1 INTRODUCTION.

A considerable amount of research has been carried out by various authors on the subject of strain softening in soils. This chapter presents a brief summary of some different approaches to the associated concepts of strain softening, local failure of soil elements, and redistribution of excess shear stresses along rupture surfaces.

#### 5.2 BJERRUM'S APPROACH TO STRAIN SOFTENING AND PROGRESSIVE FAILURE.

Bjerrum [18] presented an explanation for the mechanism of a progressive slope failure. He noted that it is world-wide experience from slides in over-consolidated plastic clays and clay shales, that the average shear stress along the failure surface is much smaller than the shear strength measured in relevant shear tests in the laboratory. Bjerrum stated that this finding holds true for slides in fresh cuts as well as for slides in natural slopes.

Bjerrum also stated that under certain conditions, slides in over-consolidated plastic clays and clay shales are preceded by the development of a continuous failure surface by a mechanism of progressive failure. He then postulated a possible mechanism which explored how a progressive failure can occur and how it can lead to the development of a continuous sliding surface. Bjerrum's postulation is presented here in some detail.

In order to illustrate the principles involved, Bjerrum considered the simplified case of a small section of a uniform stable slope of inclination  $\alpha$  as shown in figure 5.1(a). Attention was centred on the stresses existing on a surface parallel to the ground surface at a depth  $z$ .

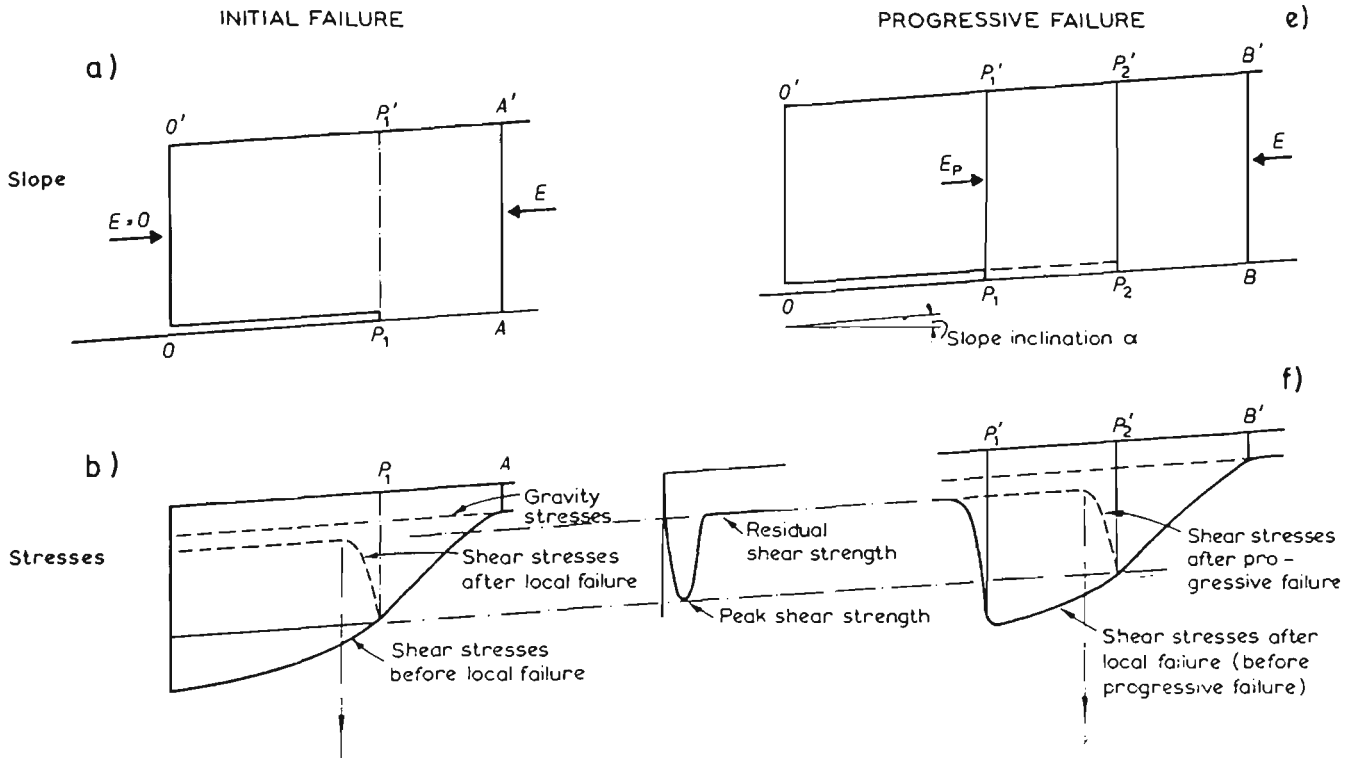


Figure 5.1 Development of Continuous Sliding Surface by Progressive Failure (Bjerrum)

Consider the equilibrium of the section  $OAA'O'$  in figure 5.1(a). Since originally the only shear stresses existing along  $OA$  are those produced by the gravity force of the block, the shear stress is thus given by

$$\tau = \gamma z \sin \alpha \cos \alpha \quad (5.1)$$

Since the slope is stable, the above shear is less than the peak shear strength of the clay.

In order to initiate a progressive failure, a discontinuity of some type must exist somewhere in the slope. Assuming that a cut with vertical walls is made down to a depth  $z$  adjacent to the considered section, removal of the lateral support on  $O'O$  by excavation, produces a redistribution of the internal stresses in the block  $OAA'O'$ . If  $AA'$  is sufficiently far from  $OO'$  so that the lateral stresses on  $AA'$  are unaltered, equilibrium of  $OAA'O'$  is only maintained if the shear force along  $OA$  increases, by the amount  $E$ , the total internal lateral earth pressure on  $AA'$ . In other words,

$$E = \int \tau_E dl \quad (5.2)$$

The additional shear stresses are not uniformly distributed. However, we know that the maximum will be at  $O$  (see figure 5.1(b)). If we let  $k$  be the concentration factor which expresses the ratio between the maximum and the average stress on plane  $OA$ , we find that the maximum shear stress due to  $E$  is therefore

$$(\tau_E)_{\max} = k.E/(OA) \quad (5.3)$$

The total shear stress at point  $O$  is then

$$\tau_o = \gamma z \sin\alpha \cos\alpha + k.E/(OA) \quad (5.4)$$

This equation is deduced on the basis of equilibrium conditions only, assuming that shear stresses are not greater than the shear strength.

It is now necessary to determine whether the excavation will initiate progressive failure. This depends on whether the maximum value of  $\tau$  is greater than the peak shear strength of the clay and this in turn depends on the value of the magnitude of  $E$ . Provided that the value of  $E$  is large enough for the theoretical value of  $\tau$  to be greater than the peak shear strength, a local failure will occur.

Local failure will start at point O and proceed as far as the shear stresses exceed strength (up to  $P_1$  in figure 5.1(b)). The occurrence of shear failure at the base of block  $OO'P_1P_1$  will mean that

1. a reduction of shear stresses on  $OP_1$  will occur from the theoretical value above to the peak shear strength.
2. the internal lateral stresses in the block of clay  $OO'P_1P_1$  will diminish.

Due to the elastic behaviour of clay, this lateral unloading causes the clay to expand towards the excavation by sliding on the newly-formed failure plane  $OP_1$ . The resulting differential strain across the failure zone is governed by the recoverable strain energy of the clay and if this is large enough the strain will be sufficient to reduce  $s$  from the peak to the residual value.

Provided that  $s_r$  is low compared to  $s_p$ , the failure surface and consequent strain will cause a larger reduction of shear stresses along  $OP_1$  and a corresponding increase of shear stress on the surface to the right of  $P_1$ . Thus progressive failure is initiated and the slip plane has advanced to point  $P_1$ . Next, investigate in a similar manner the conditions for further advancement beyond point  $P_1$  in figure 5.1(e).

The above procedure is repeated, considering the equilibrium of block  $P_1BB'P_1'$ . Section  $BB'$  is so far from  $P_1P_1'$ , that the lateral stresses on  $BB'$  are unaffected by what happened on the left of  $P_1$ . Again, consider the shear stresses along the base of the block. Now, the additional shear stresses, due to the lateral stresses in the clay, are dependent on the difference between the lateral forces  $E$  and  $E_p$  acting on the upslope and downslope sections of the block respectively. The maximum  $\tau$  is now at  $P$  and equals

$$\tau_{\max} = \gamma z \cos\alpha \cdot \sin\alpha + (E - E_p)/(P_1 B) \quad (5.5)$$

If  $\tau_{\max}$  is greater than  $s_p$ , the local failure will develop into a

progressive failure. The smaller the value of  $E_p$ , the greater the likelihood of failure progressing. The maximum value that  $E_p$  can have is

$$(E_p)_{\max} = OP_1 (s_r - \gamma z \cos \alpha \cdot \sin \alpha) \quad (5.6)$$

Bjerrum concluded that if  $s_r$  is so low, or the inclination of the slope is so high, that the block of clay resting on an already-formed slip plane will slide downhill, the maximum value that  $E_p$  can have will be very small. Thus  $\tau_{\max}$  at  $P_1$  will be approximately equal to  $\tau_{\max}$  at  $O$  when initial failure occurred and the failure surface will proceed from  $P_1$  to  $P_2$ .

If conditions do not change in the upslope direction, the progressive failure continues to proceed uphill, gradually leading to the development of a continuous sliding surface along which the shear resistance is reduced to the residual value. On the other hand, if  $s_r$  is greater than  $\gamma z \cdot \cos \alpha \cdot \sin \alpha$ , (e.g. if  $s_r$  is so high or the inclination so low, that if the block is cut loose at its base, it has no tendency to slide downhill), the value of  $E_p$  gradually increases up the slope and progressive failure will come to a halt at a certain distance from the excavation.

Bjerrum also concluded that in order for progressive failure to start, leading to the development of a continuous failure surface, there must be a discontinuity somewhere in the clay mass, or at its boundary, where failure can be initiated and the deformations required for a further development can be produced.

Bjerrum arrived at the following conclusions on the process of progressive failure.

1. The development of a continuous failure surface by progressive failure is only possible if there exist, or can develop, local shear stresses exceeding  $s_p$ . Thus, the danger of local failure increases with the ratio  $P_H/s_p$  where  $P_H$  is the lateral internal stress.



2. The advance of a failure zone must be accompanied by local differential strain in the zone of shear failure, sufficient to strain the clay beyond failure.
3. The clay must show a large and rapid decrease in shear strength with strain after the failure strength has been mobilized, so that the shear resistance in the failure zone will not obstruct the movement required to obtain the differential strain and thus, to move the zone of stress concentration into the neighbouring zone of unfailed clay. The ratio  $s_p/s_r$  expresses the degree of strain softening in the clay.

Finally, Bjerrum made the following general comments on the process of progressive failure.

- (a) Different over-consolidated clays will not have equal susceptibilities to progressive failure.
- (b) The more over-consolidated the clay, the greater the content of recoverable strain energy and the greater the danger of progressive failure.
- (c) The steeper the slope and the deeper the cut which initiates failure, the more favourable are the conditions for progressive failure.

It should be noted that Bjerrum's approach is limited to propagation of failure along a predominantly planar slip surface.

### 5.3 LAW AND LUMB'S STRAIN SOFTENING APPROACH TO PROGRESSIVE FAILURE.

Law and Lumb [58] proposed a limit equilibrium method of analysis for the study of progressive failure in slope stability under a long term condition. By dividing the soil mass into a number of vertical slices, the soil at the base of each slice can be tested for local

failure. Once local failure has taken place the post-peak strength is assumed to be operative. This then initiates a redistribution of interslice forces and leads to some further local failure. Law and Lumb state that with this method, realistic available strengths along the slip surface can be evaluated and a final factor of safety (expressed in terms of the actual available reserve of strength) can be evaluated. Law and Lumb based their analysis on effective stresses and assumed that post-peak strengths are given by a friction angle equal to the peak value and a zero cohesion. Consider the section through a slope of height  $H$  and slope  $\theta$  together with a circular slip surface and a typical slice of mean height  $h$  and width  $b$  as shown by Law and Lumb and presented in figure 5.2.

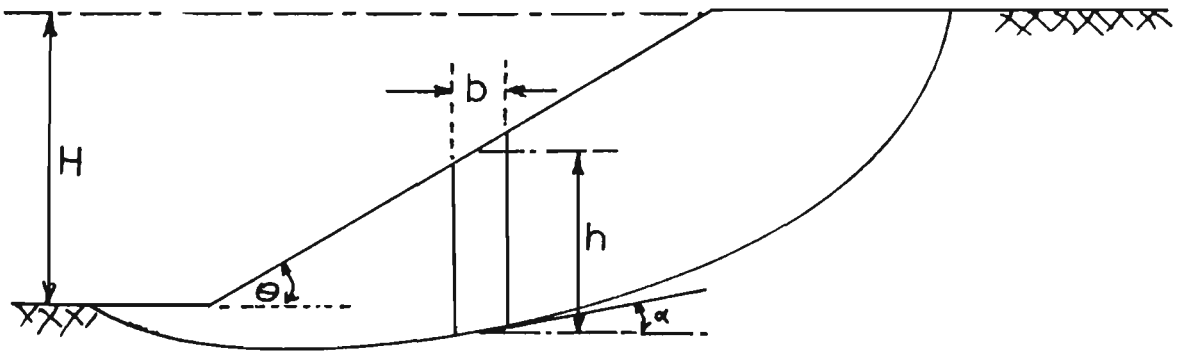


Figure 5.2 Cross-section of Slope considered by Law and Lumb

Law and Lumb presented the following method of analysis. Taking moments about the mid-point of the base of the slice in figure 5.3, we obtain

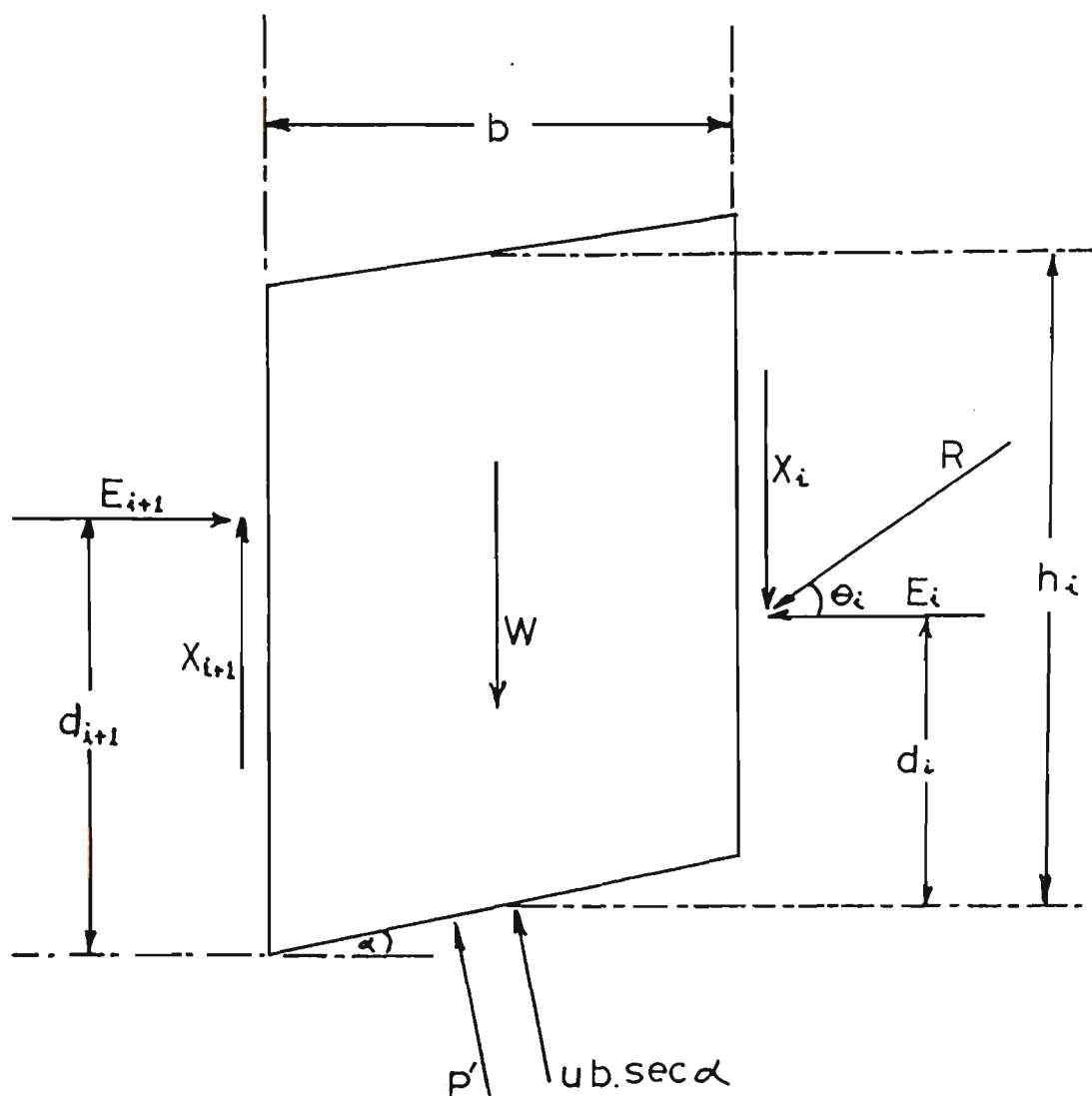


Figure 5.3 Forces Acting on a Typical Slice using Law and Lumb's Technique

$$E_{i+1} = E_i \cdot \frac{d_i + (\tan \alpha - \tan \theta_i) b/2}{d_{i+1} + (\tan \theta_{i+1} - \tan \alpha) b/2} \quad (5.7)$$

Resolving forces parallel to the base, the shear force on the slice base is found to be

$$T = E_i (\cos \alpha + \sin \alpha \tan \theta_i) - E_{i+1} (\cos \alpha + \sin \alpha \tan \theta_{i+1}) + W \sin \alpha \quad (5.8)$$

Therefore  $S_p$ , the available maximum shear resistance based on the Coulomb equation is obtained by resolving forces vertically, hence

$$S_p = [c'_p b + [W(1 - r_u) + (X_i - X_{i-1})] \tan \phi'_p] / m'_a \quad (5.9)$$

where  $c'_p$ ,  $\phi'_p$  are the peak values of the cohesion and angle of internal friction of the soil in terms of effective stress.

$$r_u = ub/W \quad (\text{Morgenstern and Price, 1960}) \quad (5.10)$$

and

$$m'_a = \cos\alpha + \tan\phi'_p \cdot \sin\alpha \quad (5.11)$$

By comparing  $T$  and  $S_p$ , Law and Lumb recognised the existence of local failure. Law and Lumb assumed the process of local failure to occur when, at some location, the shear stress due to the effect of gravity and pore pressure has exceeded the maximum available soil strength. This assumes that, prior to any local failure, the resultant of all the interslice forces acting on a slice is zero. The condition for local failure is thus expressed as

$$Wsina > [c'_p b + W(1-r_u)\tan\phi'_p] / m'_a \quad (5.12)$$

Once local failure takes place, the slice is in limiting equilibrium and the stress mobilized at the base is equal to the post-peak resistance of the soil. Law and Lumb assumed that immediately after reaching peak value, the soil resistance would drop abruptly to the final post-peak value, hence

$$S_r = [c'_r b + [W(1-r_u) + (X_i - X_{i+1})]\tan\phi'_r] / (m'_a)_r \quad (5.13)$$

where

$$(m'_a)_r = \cos\alpha + \tan\phi'_r \cdot \sin\alpha \quad (5.14)$$

Owing to a decrease in resistance in the failed slice, additional forces are transmitted to neighbouring slices. This leads to the second process of local failure. Thus for propagation of local failure, the following must be true for a slice to be deemed to have failed locally.

$$T > S_p \quad (5.15)$$

where  $T$  and  $S_p$  are given by equations (5.8) and (5.9) respectively. This procedure is continued until the last slice is reached or no more slices fail.

Law and Lumb's procedure for calculating side forces is not presented here but their expression for side force is

$$E_{i+1} = \frac{D_i + E_i [1 + \tan(\alpha - \phi'_r) \tan \theta_i]}{1 + \tan(\alpha - \phi'_r) \tan \theta_{i+1}} \quad (5.16)$$

where

$$D_i = W(1 - r_u) \tan(\alpha - \phi'_r) + W \cdot r_u \tan \alpha - Q \quad (5.17)$$

and

$$Q = c'_r \cdot b \cdot \sec^2 \alpha / (1 + \tan \phi'_r \tan \alpha)$$

Law and Lumb define a new safety factor, the final safety factor  $F_f$ , as the ratio of the overall available strength to the actual shear stress required for equilibrium. Hence,

$$F_f = \frac{\sum S_p + \sum S_r}{\sum T} \quad (5.18)$$

By considering equilibrium of the soil mass above the slip surface, the above equation can be expressed as

$$F_f = \frac{1 + \sum (S_p - S_r)}{\sum W \sin \alpha} \quad (5.19)$$

The interslice forces throughout the soil mass are considered for redistribution of the excess shear stress. The results for example problems are shown in table 5.1 which is reproduced from Law and Lumb's paper. This table contains a summary of soil data and factors

of safety for three case records.

The three slopes concerned are the Selset slide, which took place in boulder clay in England, the Northolt slip in cutting in London clay, and the Sudbury Hill slide in brown London clay. Appendix A contains details of these three slopes.

---

Table 5.1  
SUMMARY OF LAW AND LUMB'S SLIDE CASE RECORDS

	Selset	Northolt	Sudbury
$\phi'_p$ (deg)	32.0	20.0	20.0
$c'$ (kN/m <sup>2</sup> )	8.6	12.0 *	12.0 *
$\gamma$ (kN/m <sup>3</sup> )	21.8	18.8	18.8
H(m)	12.8	6.5 #	7.0
$r_u$	0.35	0.25	0.30
F **	1.14	1.67	1.75
$F_r$	0.63	0.64	0.73
$F_f$	1.0	1.0	1.0

---

\* From Henkel (1957) and Chandler and Skempton (1974).

# Actual height of the slip.

\*\* Safety Factor from the Bishop simplified method using peak strength.

$F_r$  is the safety factor from Bishop and Morgenstern (1960) using post-peak strength.

$F_f$  is the final safety factor obtained by Law and Lumb.

#### 5.4 EFFECTS OF CRACK PROPAGATION IN PROGRESSIVE FAILURE.

Romani et. al. [79], noted that most current slope stability procedures ignore the effects of cracking prior to total failure of the soil mass or treat them in an empirical manner. They presented a method for evaluating the effects of crack propagation in soil bodies

with sloping boundaries. The following assumptions were applied.

- (a) the body is a linear elastic material
- (b) the problem is two-dimensional only
- (c) the most critical sliding surface progresses along a circular path which passes through the toe of the slope.

Romani et. al. presented a method which, briefly explained, is as follows.

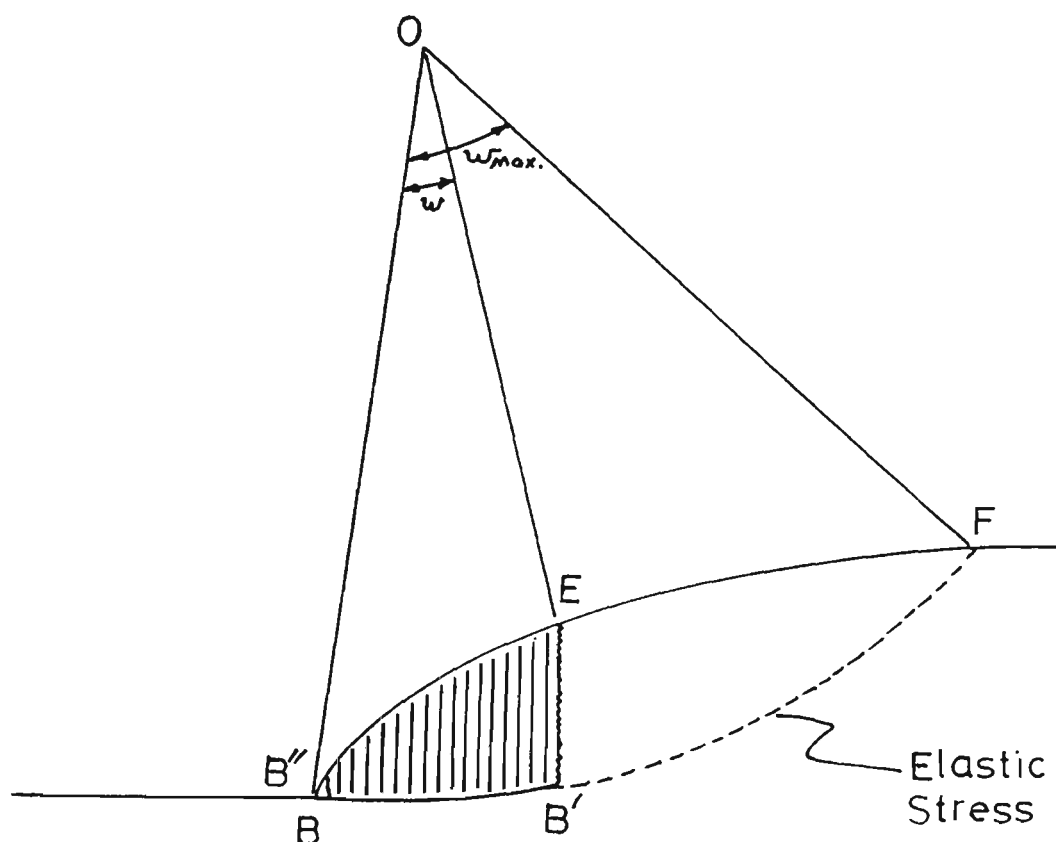


Figure 5.4 Slope Cross-section Showing Method of Romani et. al.

Referring to figure 5.4, a slit is assumed to start at point B. When the slit has progressed to point B', the line of discontinuity B'E appears above it. Having assumed a circular crack, BB'B'', the material above this crack defined by the body BB'EB'', is taken

as a rigid body and its stability is analysed by the method of slices. The region to the right, B'FE, is assumed to be in a condition of elastic stress.

This mixed approach is required due to surface BB'B'', which constitutes a surface of discontinuity of stress vectors and causes elastic stresses to be undetermined along that surface. The resisting and driving forces of each part are calculated and the factor of safety is defined as

$$F = \frac{S_{\sigma} + S_C + S_{BB'}}{D_{\tau} + D_{BB}} \quad (5.20)$$

where

$$S_{\sigma} = \tan \phi_p \int \sigma \, ds \quad (5.21)$$

$$S_C = c_a \int ds \quad (5.22)$$

$$S_{BB'} = \sum (c_p + N \cdot \tan \phi_p) \quad (5.23)$$

$$D_{\tau} = \int \tau \, ds \quad (5.24)$$

$$D_{BB'} = \sum (W \sin \alpha) \quad (5.25)$$

and where

$$\sigma = \sigma_y \cos^2 \theta + \sigma_x \sin^2 \theta + \tau_{xy} \sin 2\theta \quad (5.26)$$

and

$$\tau = [(\sigma_y - \sigma_x)/2] \sin 2\theta - \tau_{xy} \cos 2\theta \quad (5.27)$$

where  $\theta$  is the inclination of the plane on which  $\sigma$  and  $\tau$  act.

The results obtained by Romani et.al. are shown in figure 5.5. These results show that local failures starting at the crest of the slope are potentially more dangerous than local failures starting at the toe of the slope. Romani used the Bishop Simplified Method for



the solution of the failed section of the slope.

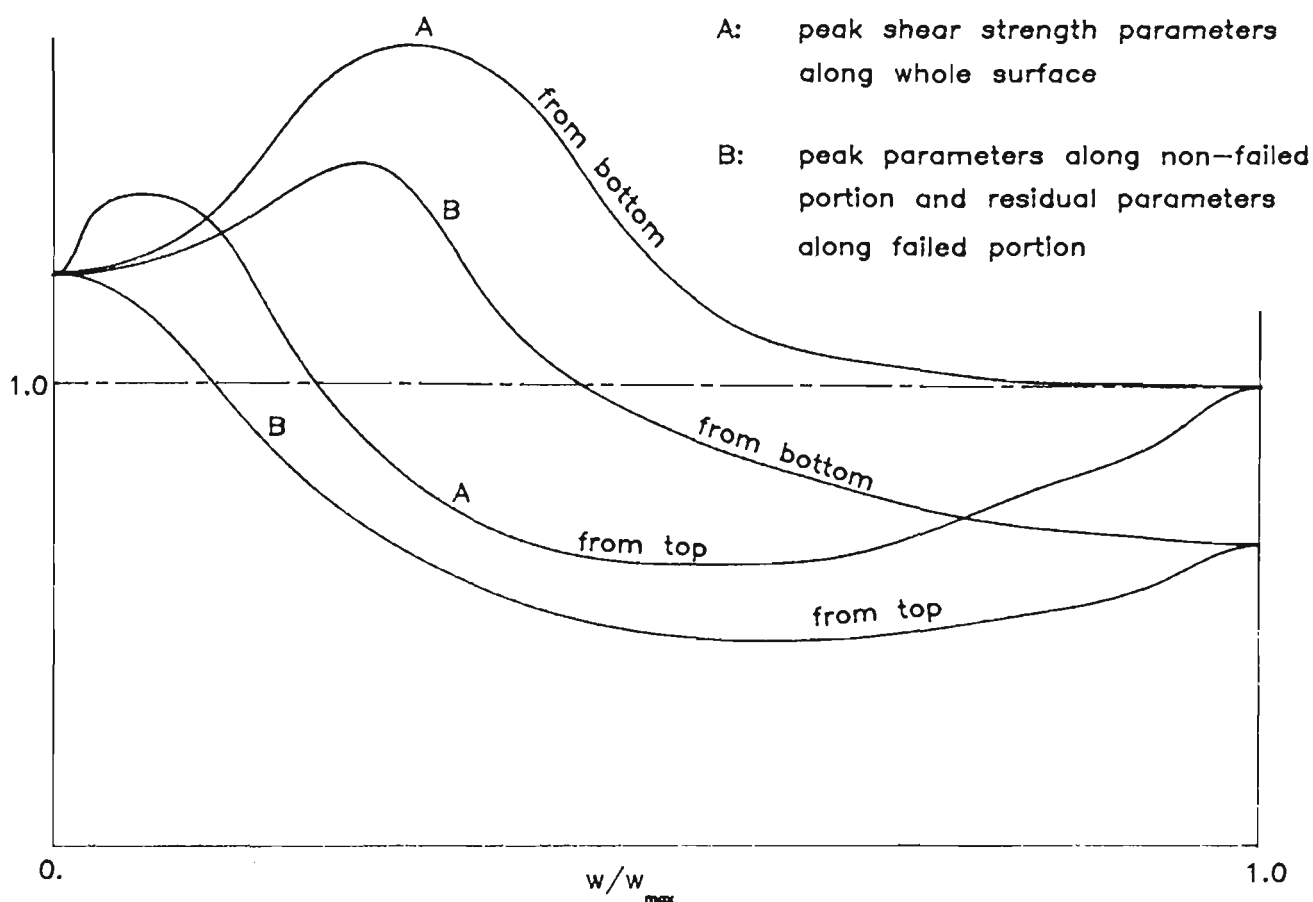


Figure 5.5 Results Obtained by Romani et. al.

## 5.5 OTHER RESEARCH RELATED TO THE CONCEPT OF STRAIN SOFTENING.

The level of uncertainty in the shear strengths of materials along a shear surface may not necessarily be the same. Thus the assumption of identical factors of safety everywhere along a shear surface is not realistic (refer to Bishop [13],[14] and Chowdhury [29]). Chugh [34] presented a procedure for calculating a variable factor of safety along a shear surface within the framework of the limit equilibrium method. He stated that the idea of incorporating a variable factor of safety in a slope stability analysis follows very closely the idea used for the variable interslice force inclination in that a characteristic shape for its variation along a shear surface is predefined and the solution procedure is required to calculate a

scalar factor which scales the characteristic.

Chugh defined the  $F$  value at any point along the slip surface as the ratio of available shear strength to the driving shear stress at that point. He thus stated that since  $\sigma'_n$  and  $\tau$  (induced) values fall on one curve and there may be several curves (one for each material) the ratio of mobilised shear strength to shear stress induced is different, and hence the factor of safety along the shear surface is varying.

Tavenas and Leroueil [101], in their investigations with cut slopes, found that as a result of the dissipation of negative pore pressures, the effective stress condition at any point in the slope progressively moves towards the limit state. The shear strength which governs the initiation of local failure at any point in a slope cut in intact clay corresponds to an effective stress condition on the limit state curve. The time-dependent displacement of the limit state combines with the time-dependent modification of the effective stress condition in the slope to result in a delayed failure.

At any point in the slope, the strength mobilised at the onset of local failure is in the limit state. Following local failure, strain softening occurs and the effective stress condition tends towards the critical state. Along with this, local failure can be initiated in neighbouring clay elements as a result of shear stress transfer from the strain softening clay. Full failure of the slope occurs when the loss of strength in those areas which have already failed cannot be compensated by the reserve resistance in the other non-failed areas.

Foerster and Georgi [43] presented a method of analysis which incorporated a progressive mechanism of failure as a function of time. Using the finite element method, they formulated an iterative procedure whereby the state of stress in elements was compared to a predefined value, that of the residual strength. By failing elements where the stress value exceeded the residual strength and by stress redistribution a situation was obtained whereby general failure of the structure occurred. Their analyses showed that the extent of the overstressed zone increases with time.

Sallfors and Larsson [80] stated that in a slope where the factor of safety against failure is low, consolidation and creep will result in the redistribution of stresses with time. They showed that this redistribution of stresses has an effect on the preconsolidation pressure and also results in a rotation of the principal stresses. The shear strength and the anisotropy is thereby also affected.

Reddy and Venkatakrishna Rao [77] suggested that only the points along the failure surface are in critical equilibrium and, at other points above the failure surface, the mobilised shear strengths are less than those at critical equilibrium. Using the method of characteristics, they assumed that mobilised shear strength varies with depth and treated the whole soil mass as a series of layers and obtained a series of factors of safety for different heights in a given slope. They found their results to be in fair agreement with and slightly lower in value than similar results obtained by the friction circle method.

Nelson and Thompson [69] presented a theory of creep failure to explain the relationship between creep, strain softening, and time-dependent failures in overconsolidated clays. They based their theory on the principle that time-dependent irreversible strains (creep) have the same detrimental effect on a soil's internal bonds as do the plastic strains associated with strain softening during a triaxial test.

They hypothesised that 'interparticle bonds form at points of high local stress during application of large consolidation pressures. Such bonds are the primary cause of the peak strengths observed in overconsolidated clays. Under conditions of sustained shear stress, plastic deformations occur across these bonds resulting in their deterioration', thereby causing 'irreversible time-dependent deformations recognised as creep and a corresponding reduction of the peak strength toward the residual strength of the soil.

Also, Nelson and Thompson reported that laboratory tests have shown that 'some critical strain exists at which point all of the internal bonds in the soil will have failed' and 'the shear strength of the soil will have been reduced to its residual strength. If, at

this point, the applied stress were greater than the residual strength, equilibrium would not be maintained and the tertiary stage of creep would begin'.

Nelson and Thompson reasoned that at low stress states, just above the residual strength, the number of bonds which must fail before tertiary creep begins is greater than at high stress states, therefore indicating that the critical strain should increase for lower stresses.

This finding was supported by Ter-Stepanian [104] who, while studying creep in clays, found that failure takes place only at high stress levels and comparatively short stress age. Thus failure is much less likely to occur at slightly lower stress levels.

Sidharta [38] developed a practical engineering method to predict, by means of a creep-failure approach, the time to failure of a slope of moderately to heavily overconsolidated clay after a cut or excavation. He considered the potential for progressive failure to occur due to the simultaneous accumulation of creep strain and decrease in strength due to dissipation of negative excess porewater pressure. The analysis uses a limit equilibrium approach and Bishop's simplified method of analysis was used for circular slip surface cases.

Sidharta used a value of shear strength between the peak and residual values and defined a residual factor similar to that defined by Skempton. He assumed stress redistribution to begin after the first point on the critical failure surface reaches the post-peak (strain-softening) side of the stress-strain curve. He simulated progressive failure starting from a number of points within the failure mass and found that regardless of where the progressive failure is assumed to be initiated, as long as the average initial deviator stress is held constant, the predicted time to failure was about the same. His model used data on Brown London clay and considered the clay to be homogeneous.

Bernander [10] stated that deformations and the time factor must be taken into account when analysing slopes in strain rate softening materials.

Wu et.al [114] investigated a number of slopes in soft shales containing discontinuities in the form of slickensides. They measured the shear strengths of the intact shales and slickensides and performed stability analyses to calculate the shear strength of the shale in the failed slopes. They attempted to estimate the effect of slickensides and stress redistribution on the reduction of shear strength below its peak value.

They suggested that the residual strength is a limiting strength where an appreciable portion of the surface may follow slickensides or local shear zones. Also, in the cases of slopes that failed, neither slickensides nor local failure alone would have reduced the overall shear strength sufficiently to induce slope failure. Failure in these cases was caused by the combined effect of large slickensides intensity and local failure.

Andrei and Athanasiu [3] considered the mechanism of progressive mobilisation of shear strength in developing a method of slope stability analysis using Janbu's method as its basis. They determined a relationship between the assumed displacement of the material along the proposed surface of sliding and the factor of safety.

## CHAPTER 6

### SIMULATION OF PROGRESSIVE FAILURE BY LOCALISED STRAIN SOFTENING.

#### 6.1 INTRODUCTION AND SCOPE.

In the previous chapter, a number of approaches to the problem of progressive failure were discussed. These approaches varied basically in the mechanism considered responsible for the initiation of the process of progressive failure. Bjerrum [18] argued that a discontinuity of some type must exist in the slope in order to initiate a progressive failure and emphasised the role of lateral stress. Romani et. al. [79] assumed that a crack-type discontinuity would facilitate the initiation of the process of progressive failure

Law and Lumb [58], on the other hand, approached the problem from a different angle. They considered the stress state at the base of a number of soil slices to determine whether conditions were favourable for local failure to occur. Once overstress in terms of Mohr-Coulomb failure criteria had occurred, the assumption was made that failure had occurred locally and that conditions on the bases of 'failed' slices corresponded to those obtained when the residual strength of the soil was reached. The excess shear stress remaining was then redistributed by a complex procedure as discussed in the previous chapter.

The primary objective of this chapter is to present new methods for the simulation of stress redistribution associated with local failure and strain-softening within a slope. Specifically, possible local failure and strain-softening is considered along the bases of individual slices. However, in the methods proposed here consideration of interslice forces is not required for stress redistribution although either simplified or rigorous methods are used

to calculate safety factors for a slope iteratively. Thus for the calculation of each safety factor, due consideration may be given to interslice forces and to force and moment equilibrium. However, simulation of the redistribution of stress associated with progressive failure does not require the consideration of these interslice forces. Therefore, the methods proposed are easy to use in comparison to others that have been suggested in the past.

In order to explain the salient features of the proposed methods and to demonstrate their implementation, a number of case histories of slope failures were analysed and the results are presented in this chapter. These include the three case records referred to in the previous chapter (i.e. Northolt, Selset and Sudbury Hill) as well as the Jackfield slide (England), the Balgheim slide (Germany), the Vajont slide (Italy), the Saskatchewan slide (Canada), the Brilliant Cut slide and two hypothetical slides. Details of all these appear in appendix A. Reasons for the introduction of the two hypothetical slides are also given in appendix A.

## 6.2 REDISTRIBUTION OF EXCESS SHEAR (METHOD 1).

As defined by Law and Lumb, a local failure is initiated when at some location, the shear stress due to the effect of gravity and pore pressure has exceeded the maximum available soil strength. 'Once local failure takes place, the slice is in limiting equilibrium and the stress mobilised at the base is equal to the post-peak resistance of the soil' [58]. In other words the shear strength on the slice base has dropped to the residual value. Since the shear stress cannot exceed the available shear strength, the excess stress must be transmitted to the unfailed slices.

Whereas Law and Lumb transmit these excess stresses by a complex procedure which incorporates the excess stresses into newly calculated interslice forces, the technique presented here attempts to simplify the solution of the problem by neglecting interslice forces altogether. The excess shear is transmitted to the unfailed slices by distributing it across the unfailed length of the failure surface.

Part of the excess shear is added to the shear stress already existing at the base of each unfailed slice. The exact process of redistribution will be described later in this chapter.

This entire procedure is then repeated until no further local failure occurs anywhere along the failure surface. A detailed description of the proposed technique is given in the following sections.

### 6.2.1 Description Of Simulation Procedure: Uniform Redistribution Of Excess Shear.

The following is a step by step description of the procedure involved in this simulation. It should be noted that effective forces, rather than stresses, are used throughout the following sections.

Step 1: Calculate the shear force and shear strength on the base of each slice:- From equation (5.8) and neglecting interslice forces we obtain the shear as

$$T_i = W_i \sin \alpha_i \quad (6.1)$$

The shear strength is given by the expression

$$(S_p)_i = \frac{c'_p b_i + W_i (1-r_u) \tan \phi'_p}{m'_\alpha} \quad (6.2)$$

where

$$m'_\alpha = \cos \alpha_i + \sin \alpha_i \tan \phi'_p \quad (6.3)$$

The peak factor of safety is then calculated as



$$F = \frac{\sum_{i=1}^n (S_p)_i}{\sum_{i=1}^n T_i} \quad (6.4)$$

Step 2: Check for local failure:- Local failure is deemed to occur on any slice where the mobilised shear force calculated equals, or exceeds, the calculated shear strength. Thus, local failure occurs on any slice where

$$T_i \geq (S_p)_i \quad (6.5)$$

where  $T_i$  and  $(S_p)_i$  are described in equations (6.1) and (6.2). If no slices satisfy this condition (i.e. if no local failure occurs), then the previously calculated factor of safety is taken as the final factor of safety.

Since the occurrence of local failure is only checked on one slice at the time and the stresses and strengths on slices are dependent on the width and position of a slice, it is possible that by combining into one slice, two adjacent slices, one of which has failed locally while the other has not, overall local failure of the combined slice may occur. The following procedure is thus followed for each slice,  $i$ , where local failure is deemed to have occurred.

If slice  $i-1$  has not failed, the combined slice consisting of slices  $i$  and  $i-1$  is tested for local failure. Local failure for the combined slice is said to occur if

$$T_{i-1} + T_i > S_{i-1} + S_i \quad (6.6)$$

where  $T$  and  $S$  are defined by equations (6.1) and (6.2). If local failure occurs, part of the excess shear force on slice  $i$  is redistributed to slice  $i-1$ . The amount of redistributed shear force is equal to

$$\Delta T = S_{i-1} - T_{i-1} \quad (6.7)$$

Thus, the shear forces on the two slices become

$$(T_i)_{\text{new}} = (T_i)_{\text{old}} - \Delta T$$

and

$$(T_{i-1})_{\text{new}} = (T_{i-1})_{\text{old}} + \Delta T \quad (6.8)$$

This ensures that both slices will individually fail when tested by equation (6.5). This procedure is repeated for slice  $i+1$ .

**Step 3: Reduce strength on failed slices to post-peak value:-** On all slices where local failure has occurred, the soil strength parameters are assumed to have fallen from their peak values to their residual values. That is,  $c' = c'_r$  and  $\phi' = \phi'_r$  on all failed slices. Therefore, on all slices where local failure has occurred, the shear strength is expressed as:

$$(S_r)_j = \frac{c'_r b_j + W_j(1-r_u)\tan\phi'_r}{m'_{ar}} \quad (6.9)$$

where

$$m'_{ar} = \cos\alpha_j + \sin\alpha_j \tan\phi'_r \quad (6.10)$$

Also, as the mobilized shear force cannot exceed the available shear strength, the mobilized shear force on each failed slice will be set to equal the residual shear strength on the base of that slice.

$$\text{i.e. } (T_f)_j = (S_r)_j \quad (6.11)$$

where

$$(T_f)_j = \text{mobilized shear force on a failed slice } j$$

**Step 4: Redistribute the excess shear force:-** The problem now exists to account for all the excess forces which have been taken from the failed slices. The excess forces must be redistributed throughout the unfailed slices to maintain equilibrium in the soil mass. As the excess shear force derived from any failed slice  $j$  is given by

$$e_j = T_j - (T_f)_j \quad (6.12)$$

and the total excess shear force to be redistributed is given by the expression

$$e_t = \sum_{j=1}^m e_j = \sum_{j=1}^m [T_j - (T_f)_j] \quad (6.13)$$

where  $m$  is the number of failed slices.

The total excess shear force is assumed to be redistributed uniformly over the unfailed length of failure surface. For an unfailed slice  $i$ , the amount of excess shear force distributed to it is,

$$\Delta T_i = \frac{e_t l_i}{L_u} \quad (6.14)$$

where  $l_i$  = length of base of unfailed slice  $i$ .  
and  $L_u$  = total unfailed length of slip surface.

Thus, the new mobilized shear force on the base of unfailed slice  $i$  becomes

$$T_i = (T_i)_{old} + \Delta T_i \quad (6.15)$$

or

$$T_i = (T_i)_{old} + (e_t l_i) / L_u \quad (6.16)$$

**Step 5: Calculate the new Factor of Safety:-** The new factor of safety is then calculated as the sum of the shear resistance on the base of all (failed and unfailed) slices divided by the sum of the shear forces acting on the base of all slices, and is expressed as;

$$F = \frac{\sum_{i=1}^n (S_p)_i + \sum_{j=1}^m (S_r)_j}{\sum_{i=1}^n T_i + \sum_{j=1}^m (T_f)_j} \quad (6.17)$$

for  $n$  unfailed slices and  $m$  failed slices;

The top left expression denotes the sum of the shear strengths (peak) on bases of unfailed slices; the right expression denotes the sum of the shear strengths (residual) on bases of failed slices; the bottom left expression denotes the sum of the mobilised shear forces on bases of unfailed slices; and the bottom right expression denotes the sum of the mobilised shear forces on bases of failed slices.

Having found the new value of  $F$ , the procedure then returns to step number 2 above and stops only when no further slices satisfy the criteria for local failure in step 2.

#### 6.2.2 Description Of Alternate Procedure: Linear Redistribution Of Excess Shear.

In the previous section, it was assumed that the excess shear force obtained after local failure is distributed uniformly over the unfailed length of the failure surface. As an alternative to this redistribution profile, a second case is investigated where the excess shear force is assumed to be distributed linearly over the unfailed length of the failure surface.

The assumption is made that local failure is most likely to occur at some point along the failure surface somewhere between the toe of the slope and the crest. At a certain stage in time, there will exist a zone within the failure mass within which local failure has spread. Figure 6.1 shows a cross-section through a hypothetical failure mass where local failure has progressed along the shown failure surface from some point within the area designated as the 'failure zone', outwards in both directions to points P1 and P2 on the boundaries as shown.

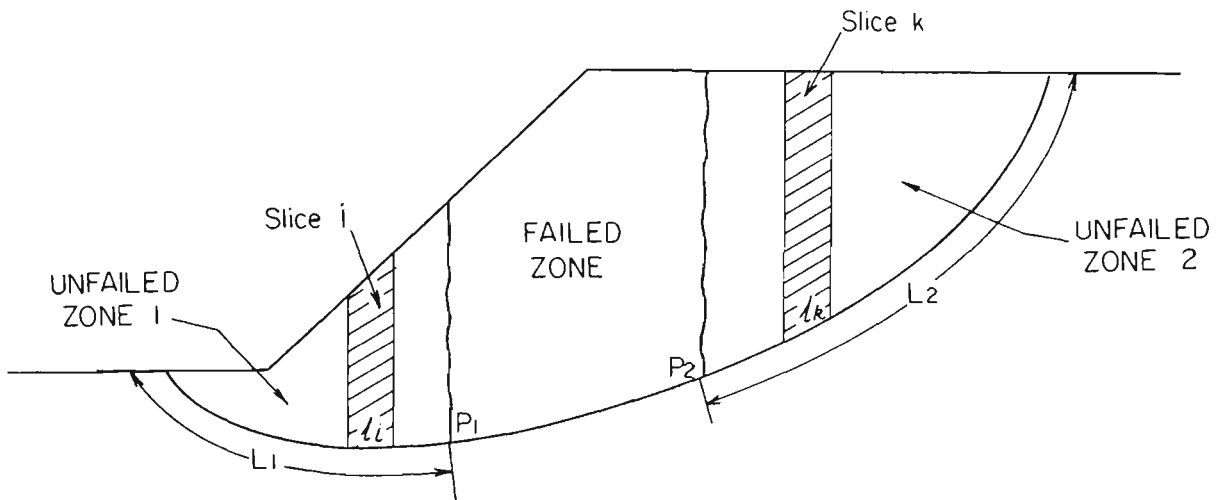


Figure 6.1 Cross-section through a Hypothetical Failure Mass with Failure Starting from Centre of Mass.

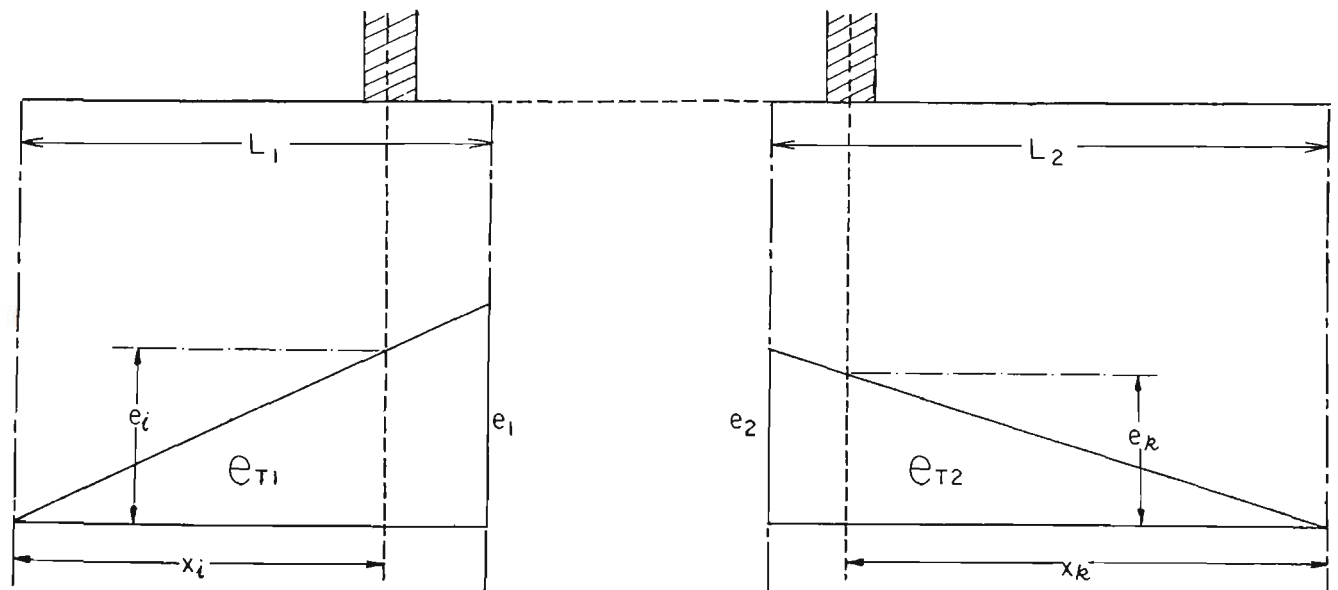


Figure 6.2 One-dimensional Representation of Failure Surface showing Stress Redistribution Profile.

Having calculated  $e_t$  and representing the failure surface in a one-dimensional diagram, the redistribution profile appears as shown in Figure 6.2. In some cases, however, the zone referred to as the 'failure zone' in figures 6.1 and 6.2 may contain some slices which have not yet failed. It is altogether possible that there may be no clearly defined failure zone, but only a zone where there exists a number of failed slices with unfailed slices dispersed throughout. For such a situation, a 'centre of failure' is located. This centre of failure is simply the centre of gravity of all the failed slices. All unfailed slices to the left of the centre of failure are treated as belonging to 'unfailed zone 1' while all unfailed slices to the right of the centre of failure are treated as belonging to 'unfailed zone 2'.

As shown in figure 6.2, the largest amount of redistributed shear force is in the immediate vicinity of the failed zone. The amount of shear force being added to the unfailed slices is assumed to decrease linearly with unfailed distance from the centre of failure, falling to zero at the extreme ends of the slip surface. Therefore, the excess shear force added to an unfailed slice  $i$  in unfailed zone 1 is given by:

$$\Delta T_i = e_i l_i \quad (6.18)$$

where  $l_i$  is the curved length of the base of slice  $i$ .

and

$$e_i = e_1 x_i / L_1 \quad (6.19)$$

where  $x_i$  is the curved length of the slip surface from the extreme boundary of the slip surface (here the toe) to the midpoint of slice  $i$ , and  $L_1$  is the total length of slip surface in unfailed zone 1, and

$$e_1 = 2(e_t)_1 / L_1 \quad (6.20)$$

where  $(e_t)_1$  is that part of the total excess shear force distributed over the slip surface of zone 1 and is given by:

$$(e_t)_1 = \frac{e_t \cdot L_1}{L_1 + L_2} \quad (6.21)$$

$e_t$  being the total excess shear force given by equation (6.13) and  $L_2$  the total length of slip surface in unfailed zone 2. Thus equation (6.18) becomes

$$\Delta T_i = \frac{2e_t x_i l_i}{L_1(L_1 + L_2)} \quad (6.22)$$

Similarly for unfailed zone 2, the excess shear force to be added to an unfailed slice is given by

$$\Delta T_k = \frac{2e_t x_k l_k}{L_2(L_1 + L_2)} \quad (6.23)$$

Therefore, the new modified shear force on the base of an unfailed slice,  $i$  in unfailed zone 1 becomes

$$T_i = (T_i)_{old} + \Delta T_i$$

or

$$T_i = (T_i)_{old} + \frac{2e_t x_i l_i}{L_2(L_1 + L_2)} \quad (6.24)$$

and for an unfailed slice  $k$  in unfailed zone 2

$$T_k = (T_k)_{old} + \frac{2e_t x_k l_k}{L_2(L_1 + L_2)} \quad (6.25)$$

The overall procedure involved is the same as that described in the previous section. Step 4, however, is replaced by the above procedure for linearly redistributing excess shear force.

### 6.2.3 Definition Of Propagation Factor.

As an indication of the extent to which progressive failure has occurred, a factor is introduced here which shall be called the 'Propagation Factor'. This propagation factor is defined as the fraction of the total length of the assumed failure surface over which local failure has occurred. More specifically, the propagation factor is defined as that fraction (expressed as a decimal between 0 and 1) derived by dividing the sum of the base lengths of all slices in the failure mass where local failure has occurred by the sum of the base lengths of all the slices in the failure mass. This is expressed as

$$PF = \frac{\sum_i^n (l_f)_i}{\sum_i^N l_k} = \frac{\sum_i^n (l_f)_i}{L} \quad (6.26)$$

where  $(l_f)_i$  = the base length of a failed slice  $i$ .

$l_k$  = the base length of any slice  $k$ ,

$n$  = the number of failed slices,

$N$  = the total number of slices,

and  $L$  = the total curved length of the failure surface.

### 6.2.4 Computer Program STRAIN1.

As the calculations involved in the simulation of progressive failure using method 1 are highly repetitive, and therefore time consuming, the process is greatly facilitated by the use of a digital computer. Also, the degree of accuracy is greatly increased by using a computer since random errors, which would normally occur due to the large number of calculations, are eliminated.



Written in FORTRAN 77, the computer program STRAIN1 was developed and run on the UNIVAC 1100 computer at the University of Wollongong. Figure 6.3 contains a flowchart which describes the internal structure of the main program.

The program is capable of handling both cases of excess shear distribution detailed above. A parameter called the 'shear force distribution option' (1 = uniform and 2 = linear distribution of excess shear) is read in as data and this parameter controls the internal operation of the program according to the required distribution method. As each new value of the factor of safety is calculated, the program also calculates the corresponding value of the propagation factor. These two values, along with detailed data for each soil slice, are printed as output from the program after each new factor of safety is calculated. The detailed slice data includes values of shear force and shear resistance on the base of each slice as well as an indicator which tells if the slice has undergone local failure. Once the final factor of safety is obtained, final values of the factor of safety and the propagation factor are output as well as values of the peak and residual factors of safety, and the value of the factor of safety before shear redistribution commenced (ie. after the first set of slices have failed locally but before any excess shear has been redistributed). Subroutine SPARAM, which reads in the soil parameter data and the slope geometry data, also calculates other necessary soil data such as angles of slice bases and toplines, slice weights and the pore water pressure acting on the base of each slice.

In calculating the pore-water pressure acting on the base of each slice, subroutine SPARAM considers two options. If the value of the pore-pressure ratio read from the data file is less than 1.0 the pore-water pressure,  $u$  for each slice base is calculated from this value of  $r_u$  using the following expression.

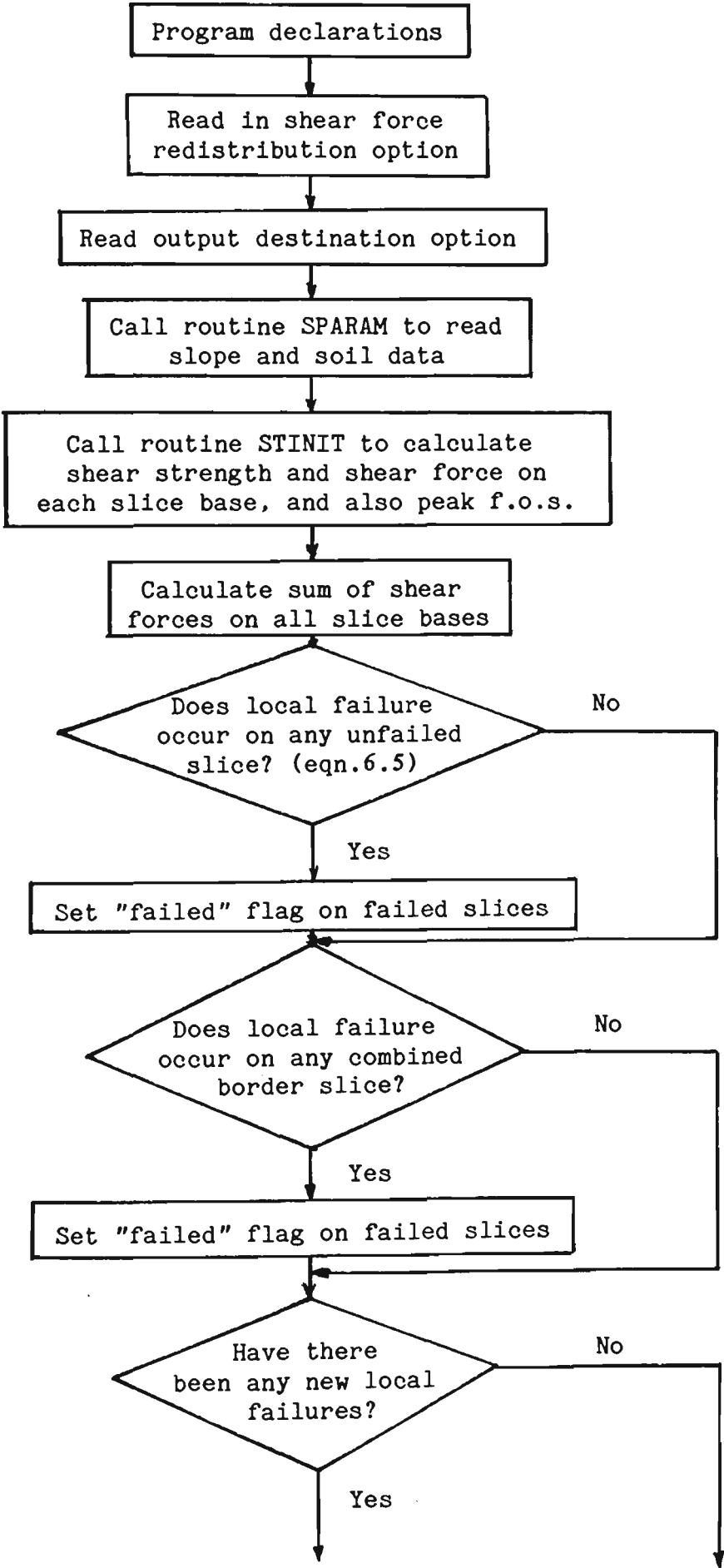
$$u_i = \gamma z_i r_u \quad (6.27)$$

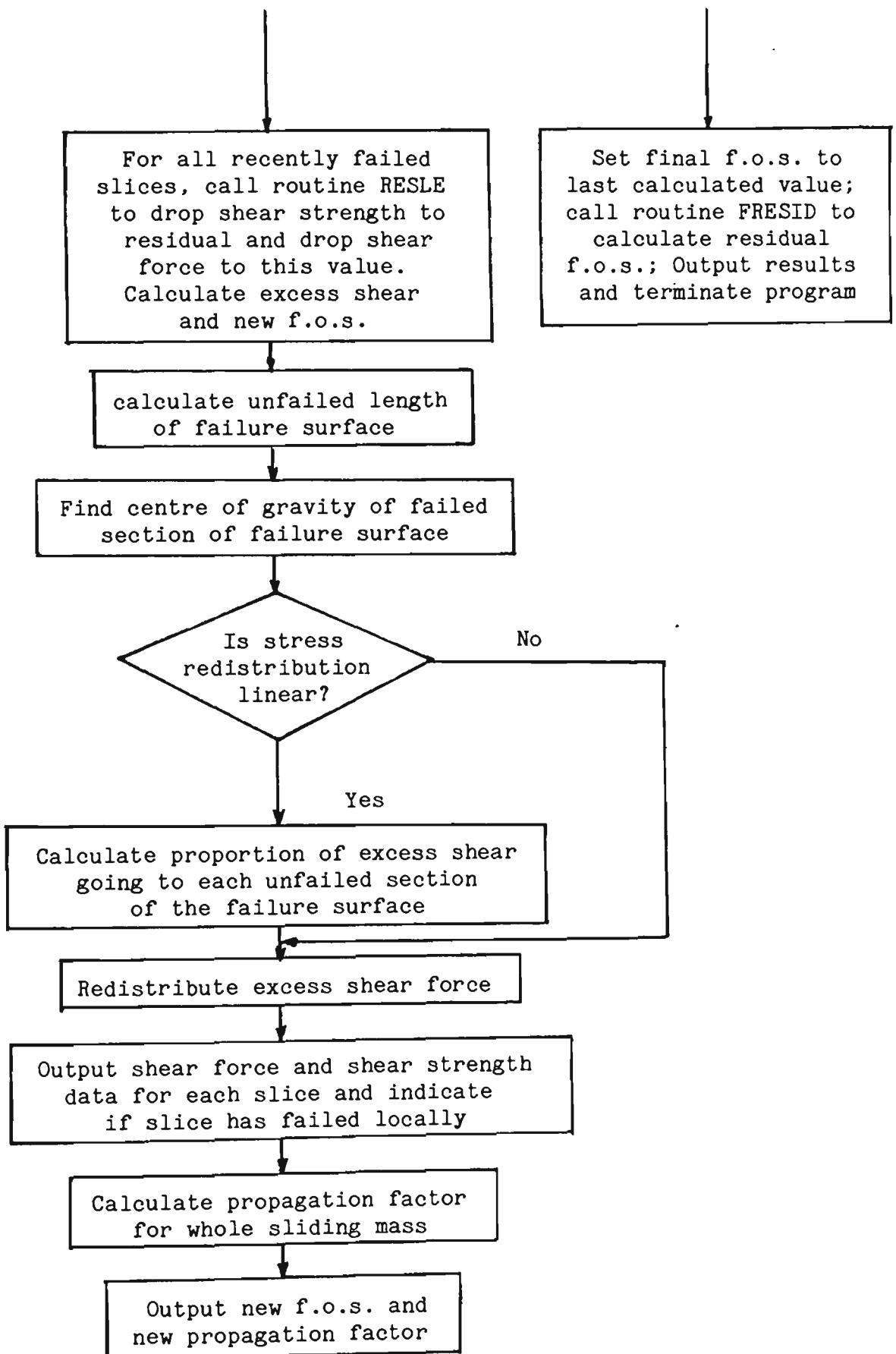
where  $\gamma$  = unit weight of soil

and  $z_i$  = height of midpoint of slice  $i$ .

If, on the other hand, the given value of  $r_u$  is greater than 1.0,

Figure 6.3 Flowchart for Program STRAIN1.





this indicates that the phreatic surface co-ordinates are specified and the pore-water pressure for each slice base is calculated from the height of the phreatic surface at that slice. The pore-water pressure on the base of a slice  $i$  is given by

$$u_i = \gamma_w z_i \quad (6.28)$$

where  $\gamma_w$  = unit weight of water ,  
and  $z$  = height of phreatic surface above slice base ,

Subroutine STINIT calculates the peak shear strengths on the bases of each soil slice and the initial (peak) factor of safety using equation (6.17). Subroutine FRESID is identical to subroutine STINIT except that residual values of shear strength parameters are used instead of peak values. Therefore, the residual value of the factor of safety is calculated instead of the peak value, again using equation (6.17).

Finally, subroutine RESLE performs a similar function to subroutine STINIT except that it differentiates between slices where local failure has occurred and those where it has not. If local failure has occurred, the shear strength is calculated using residual shear strength parameters  $c_r$  and  $\phi_r$ , whereas if local failure has not occurred peak values of shear strength parameters are used.

#### 6.2.5 Case Histories Considered.

As mentioned earlier in this chapter, the simulation technique presented above was applied to a number of case histories in order to study the feasibility of the proposed method. There were a total of ten case histories used, each of which is described in detail in appendix A. The relevant soil data for each of the slopes described is also presented in appendix A.

At this stage a mention must be made of the shear strength parameters assumed to exist on the failure surface at the time of failure. It is understood, from the previous sections, that at the time of overall failure there may exist parts of the failure surface along which peak conditions prevail while at other points residual conditions exist. No mention has been made however, about the actual values of the residual shear strength parameters of the soils concerned.

When considering the value of the residual cohesion intercept  $c'_r$  it is widely accepted that this value is given by the fully softened strength value of zero. The residual value of the effective angle of shearing resistance, however, is subject to greater debate. Various authors (including Law and Lumb [58]) argue that this residual value of  $\phi'$  should equal its peak value. The majority, on the other hand, regard the fully softened value of  $\phi'$  to be somewhat lower than the peak value.

In order to attempt to verify the results obtained by Law and Lumb, and also to obtain results for the case histories as analysed by Skempton, Henkel, Romani and other authors, two separate sets of analyses are performed on the ten slopes described in appendix A.

The first of these, named 'system A', uses the following combination of shear strength parameters.

- (a) peak  $c'$  and  $\phi'$  as given in appendix A ,
- (b) residual value of  $c'$  equal to zero ,
- (c) residual value of  $\phi'$  equal to the peak value.

The second system, 'system B', uses the following combination of shear strength parameters.

- (a) peak  $c'$  and  $\phi'$  as given in appendix A ,

- (b) residual value of  $c'$  equal to zero ,
- (c) residual value of  $\phi'$  is less than the peak value and is as given in appendix A.

As well as the two systems of shear strength parameters mentioned above, three of the case histories were also analysed using a number of different pore-water pressure conditions. The Northolt slip is firstly analysed using a pore-pressure ratio of 0.25 as used by Law and Lumb. Secondly, a pore-pressure ratio of 0.34 is applied to this slip as this is the average value quoted by Skempton as existing along the failure surface. Thirdly, the piezometric surface obtained from the soil data presented by Skempton is used directly in calculating the pore water pressure on the base of each slice.

Similarly an  $r_u$  value of 0.35 was used for the Selset slide and a value of 0.30 for the Sudbury Hill slide. As well as this, a piezometric surface is defined for both slides. The main object of this dual analysis is to allow comparisons between

- (a) the results obtained by previous investigators and the results obtained in this chapter, and
- (b) the more realistic results obtained by using the given piezometric surface to calculate pore-water pressure.

#### 6.2.6 Results And Discussion.

Table 6.2 contains the results obtained using program STRAIN1 and the theoretical procedure described in method 1. Results for both system A and system B are shown. The meanings of the symbols in the table are as follows.

- $F_p$  is the peak factor of safety for the slope.
- $F_r$  is the residual factor of safety for the slope.
- $F_b$  is the factor of safety obtained just prior to the commencement of stress redistribution.
- $PF_b$  is the value of the propagation factor when the factor of safety is equal to  $F_b$ .
- $F_c$  is the final factor of safety with uniform stress redistribution.
- $PF_c$  is the propagation factor value after uniform stress redistribution.
- $F_l$  is the final factor of safety with linear stress redistribution.
- $PF_l$  is the propagation factor value after linear stress redistribution.

It would appear from the results in table 6.2 that no clear-cut conclusions can be reached regarding the feasibility of the proposed method applied to the given case histories. Certain trends can, however, be observed and these will be discussed here. A more comprehensive discussion will be presented at the conclusion of this chapter and a number of conclusions will be drawn there.

The most obvious point to note is that, in all cases where the resulting factors of safety due to constant and linear redistribution of excess shear, respectively, are not equal, the factor of safety obtained by linearly redistributing excess shear is lower than the other. In other words,  $F_l$  is less than or equal to  $F_c$ .

Some slopes (Balgheim, Hypothetical Slope 1) show no drop in  $F$  from the peak value. Others (Jackfield, Hypothetical Slope 2) show a small drop in factor of safety after the initially overloaded slices have failed but produce no further reduction in  $F$  upon redistributing excess shear in any manner. The results for system B data showed, in general, lower values of factor of safety as would be expected since lower values of  $\phi'$  are used. In certain cases, however, no local failure was noticed and, as in the case of system A, no drop in  $F$  from the peak value was observed.

TABLE 6.2

Results from Program STRAIN1 (Method 1).  
 Limit Equilibrium method of slices including provision for  
 Strain Softening and Stress Redistribution.

(a) Using shear strength parameters as per system A.

Slide	$F_p$	$F_r$	$F_b$	$PF_b$	$F_c$	$PF_c$	$F_1$	$PF_1$
Northolt								
ru=.25	1.57	.93	1.37	.40	1.29	.52	1.29	.52
ru=.34	1.46	.82	1.21	.47	1.21	.47	.82	1.00
P.S.	1.47	.83	1.23	.41	1.19	.52	.83	1.00
Selset								
ru=.35	1.03	.82	.93	.55	.82	1.00	.82	1.00
P.S.	.97	.76	.87	.55	.73	1.00	.76	1.00
Sudbury								
ru=.30	1.91	.98	1.64	.32	1.55	.43	1.37	.62
P.S.	1.91	.98	1.77	.16	1.67	.29	1.47	.51
Jackfield	2.03	1.55	2.01	.06	2.01	.06	2.01	.06
Balgheim	1.38	.73	1.38	.00	1.38	.00	1.38	.00
Saskatchewan	1.16	.86	1.11	.87	1.08	.88	.86	1.00
Vajont	1.23	1.22	1.22	.69	1.22	.74	1.22	.74
Hyp.1	3.00	.98	3.00	0.	3.00	.00	3.00	.00
Hyp.2	2.20	.73	1.89	.25	1.89	.25	1.89	.25

(b) Using shear strength parameters as per system B.

Slide	$F_p$	$F_r$	$F_b$	$PF_b$	$F_c$	$PF_c$	$F_1$	$PF_1$
Northolt								
ru=.25	1.57	.75	1.31	.40	1.14	.59	.75	1.00
ru=.34	1.46	.66	1.14	.47	.66	1.00	.66	1.00
P.S.	1.47	.67	1.16	.41	1.05	.59	.67	1.00
Selset								
ru=.35	1.03	.77	.91	.55	.77	1.00	.77	1.00
P.S.	.97	.72	.85	.55	.72	1.00	.72	1.00
Sudbury								
ru=.30	1.91	.79	1.58	.32	1.38	.51	.79	1.00
P.S.	1.91	.79	1.73	.16	1.32	.55	.79	1.00
Jackfield	2.03	1.17	2.00	.06	2.00	.06	2.00	.06
Balgheim	1.38	.69	1.38	.00	1.38	.00		
Saskatchewan	1.16	.49	1.03	.87	.49	1.00	.49	1.00
Vajont	1.23	.99	1.10	.69	1.03	.88	.99	1.00
Hyp.1	3.00		3.00	.00	3.00	.00	3.00	.00
Hyp.2	2.20	.65	1.87	.25	1.87	.25	1.87	.25



In cases where a number of values of the pore-pressure ratio were used, or where the phreatic surface was used to indicate pore-pressure levels, the results obtained showed nothing unexpected. Factors of safety obtained using phreatic surface points to indicate pore-pressure levels corresponded very closely to factors of safety obtained using corresponding average  $r_u$  values.

### 6.3 CALCULATION OF OVERALL FACTOR OF SAFETY BY ITERATIVE METHODS (METHOD 2).

#### 6.3.1 Iterative Methods Of Analysis Used.

As an alternative to calculating the overall factor of safety as shown in the previous section from equation (6.17), it was decided to investigate the consequences of calculating the overall factor of safety using some more rigorous methods of stability analysis. The first method of stability analysis considered is the Bishop simplified method. This method is used because of its simplicity in application and its suitability to many of the case histories used.

Since Bishop's method of analysis is only applicable to slopes with circular slip surfaces, it is therefore necessary to use a more general, rigorous method such as that of Morgenstern and Price for slopes not exhibiting a circular surface of sliding. It is also of interest to compare the results obtained by these two methods of analysis. Therefore, both of the above mentioned methods of analysis will be used on each of the ten case histories analysed.

The overall procedure remains basically the same as that described in the previous section. In step 5 of the procedure described, however, rather than using equation (6.17) to calculate the new factor of safety a complete limit equilibrium analysis is performed in the form of either the Bishop simplified method or the Morgenstern-Price method. From this analysis the new factor of safety is obtained.

The analysis is performed using the current local values of shear strength parameters  $c'$  and  $\phi'$ . In other words, all slices where local failure has occurred are treated as having residual shear strength parameters while all others are treated as being at the peak condition.

### 6.3.2 Computer Program BSTRAIN2.

Program BSTRAIN2, standing for Bishop Strain-softening Method 2, is again very similar to program STRAIN1 described in the previous section. It is in fact a modified version of program STRAIN1. Due to this fact, a detailed description of the program will not be presented here.

The major difference between the two above mentioned programs occurs within subroutines STINIT, FRESID and RESLE which perform the same functions as they do in program STRAIN1, except that in this case the factor of safety calculated within each is found using Bishop's simplified method of analysis rather than equation (6.17).

### 6.3.3 Computer Program MPSTRAIN2.

Program MPSTRAIN2 is an extension of program MGSTRN2 described in chapter 4. The basic structure of MPSTRAIN2 remains the same as for MGSTRN2. Routines CNSTNT and MTYPIN are called as in MGSTRN2 except that in this case MTYPIN reads in both peak and residual values of the shear strength parameters  $c'$  and  $\phi'$ . MSLOPE, FRBODY, FBGEOM and FUNCTN are then called followed by routine SOLUTN which calculates the initial, peak factor of safety of the slope under consideration.

Following this, comes the major difference between program MPSTRAIN2 and its predecessor. A new routine named STRAIN is called to perform the strain-softening simulation. In actual fact, STRAIN is identical to the main body of program BSTRAIN2, with two exceptions. Firstly, there is no need to call routine SPARAM to read soil data and

slope geometry data as this has already been done in routines MTYPIN and FRBODY. Secondly, instead of using the Bishop simplified method to obtain values of the factor of safety for the slope, subroutine SOLUTN is called to perform this task. Once the situation is reached (as for program BSTRAIN2) where no further soil elements, or slices, fail then results are printed out and control is transferred back to the main program of MPSTRAIN2.

#### 6.3.4 Results And Discussion.

As for the method described in the previous section, the results from trial runs using method 2 are presented here in tabular form. Two complete sets of results are presented. The first was obtained using program BSTRAIN2 and the second using program MPSTRAIN2. These two sets of results are shown in tables 6.3 and 6.4 respectively. The symbols shown have the same meanings as for program STRAIN1 (method 1) described earlier and will not be repeated here.

Again, as with the results presented in the previous section, no distinct conclusions can be reached by observing the results in this section. Similar trends to those observed in the previous section are observed here in that  $F_1$  is generally smaller than (if not equal to)  $F_c$ . Also, the same slopes show no drop in factor of safety from the peak value as in the previous section. This is also true for those slopes which show an initial drop in factor of safety after overloaded slices have failed but which show no further drop in factor of safety after stress redistribution has taken place. Finally, similar observations were made regarding the relationship between the results obtained using system A data and those obtained using system B data.

Comparisons between the results obtained from program STRAIN1 using method 1 and program BSTRAIN2 using method 2 produced the following observations. It is noted that in most cases, the factor of safety produced by program STRAIN1 was less than that produced by program BSTRAIN2. This observation also holds true for calculated values of the peak factor of safety, thus indicating that these differences in  $F$  are not due to the method of simulating progressive

TABLE 6.3

Results from Program BSTRAIN2 (Method 2).  
Bishop Simplified method Extended and Updated for  
Strain Softening and Stress Redistribution.

(a) Using shear strength parameters as per system A.

Slide	$F_p$	$F_r$	$F_b$	$PF_b$	$F_c$	$PF_c$	$F_l$	$PF_l$
Northolt								
ru=.25	1.65	.92	1.40	.40	1.32	.52	1.32	.52
ru=.43	1.52	.79	1.23	.47	1.23	.47	.79	1.0
P.S.	1.54	.81	1.26	.41	1.21	.52	.81	1.0
Selset								
ru=.35	1.04	.77	.91	.56	.77	1.0	.77	1.0
P.S.	.97	.69	.84	.56	.69	1.0	.69	1.0
Sudbury								
ru=.30	1.99	.98	1.69	.32	1.58	.43	1.40	.62
P.S.	1.99	.98	1.83	.16	1.72	.29	1.50	.51
Jackfield	2.12	1.60	2.09	.06	2.09	.06	2.09	.06
Balgheim	1.43	.70	1.43	.00	1.43	.00	1.43	.00
Saskatchewan	1.28	.76	1.18	.87	1.14	.88	.76	1.0
Vajont	1.31	1.30	1.30	.69	1.30	.74	1.30	.74
Hyp.1	3.55	.98	3.55	.00	3.55	.00	3.55	.00
Hyp.2	2.34	.69	1.98	.25	1.98	.25	1.98	.25

(b) Shear strength parameters as per system B.

Slide	$F_p$	$F_r$	$F_b$	$PF_b$	$F_c$	$PF_c$	$F_l$	$PF_l$
Northolt								
ru=.25	1.65	.72	1.33	.40	1.15	.58	.72	1.0
ru=.34	1.52	.63	1.15	.47	.63	1.0	.63	1.0
P.S.	1.54	.64	1.18	.41	1.06	.59	.64	1.0
Selset								
ru=.35	1.04	.71	.88	.56	.71	1.0	.71	1.0
P.S.	.97	.64	.81	.56	.64	1.0	.64	1.0
Sudbury								
ru=.30	1.99	.76	1.62	.32	1.40	.51	.78	1.0
P.S.	1.99	.77	1.79	.16	1.34	.55	.77	1.0
Jackfield	2.12	1.18	2.08	.06	2.08	.06	2.08	.06
Balgheim	1.43	.66	1.43	.00	1.43	.00	1.43	.00
Saskatchewan	1.28	.22	1.04	.87	.22	1.0	.22	1.0
Vajont	1.31	.99	1.22	.69	1.04	.89	.99	1.0
Hyp.1	3.55	.81	3.55	.00	3.55	.00	3.55	.00
Hyp.2	2.36	.61	1.96	.25	1.96	.25	1.96	.25

TABLE 6.4

Results from Program MPSTRAIN2 (Method 2).  
Based on Morgenstern-Price method Extended for  
Strain Softening and Stress Redistribution.

(a) Using shear strength parameters as per system A.

Slide	$F_p$	$F_r$	$F_b$	$PF_b$	$F_c$	$PF_c$	$F_l$	$PF_l$
Northolt								
ru=.25	1.59	.87	1.31	.40	1.26	.47	1.23	.52
ru=.34	1.47	.75	1.14	.47	1.06	.59	.75	1.0
P.S.	1.54	.81	1.25	.41	1.20	.47	.81	1.0
Selset								
ru=.35	1.05	.79	.93	.56	.79	1.0	.79	1.0
P.S.	1.10	.84	.98	.56	.84	1.0	.84	1.0
Sudbury								
ru=.30	2.00	.99	1.70	.32	1.52	.51	1.41	.62
P.S.	2.02	1.01	1.86	.16	1.78	.25	1.53	.51
Jackfield	2.12	1.61	2.09	.06	2.09	.06	2.09	.06
Balgheim	1.45	.68	1.45	.00	1.45	.00	1.45	.00
Saskatchewan								
Vajont	1.38	1.37	1.37	.65	1.37	.73	1.37	.70
Hyp.1	3.55	.98	3.55	.00	3.55	.00	3.55	.00
Hyp.2	2.17	.64	1.77	.25	1.77	.25	1.77	.25

(b) Using shear strength parameters as per system B.

Slide	$F_p$	$F_r$	$F_b$	$PF_b$	$F_c$	$PF_c$	$F_l$	$PF_l$
Northolt								
ru=.25	1.59	.68	1.25	.40	1.09	.59	.68	1.0
ru=.34	1.47	.59	1.08	.47	.59	1.0	.59	1.0
P.S.	1.54	.64	1.18	.41	1.04	.59	.64	1.0
Selset								
ru=.35	1.05	.73	.90	.56	.73	1.0	.73	1.0
P.S.	1.10	.77	.95	.56	.77	1.0	.77	1.0
Sudbury								
ru=.30	2.0	.78	1.64	.32	1.42	.51	.78	1.0
P.S.	2.02	.79	1.82	.16	1.42	.51	.79	1.0
Jackfield	2.12	1.19	2.07	.06	2.07	.06	2.07	.06
Balgheim	1.45	.64	1.45	.00	1.45	.00	1.45	.00
Saskatchewan								
Vajont	1.38	1.04	1.21	.65	1.13	.86	1.15	.80
Hyp.1	3.55	.98	3.55	.00	3.55	.00	3.55	.00
Hyp.2	2.17	.58	1.75	.25	1.75	.25	1.75	.25

failure used but are due simply to the method used for calculating the factor of safety for a slope. It is interesting to note, however, that calculated values of the residual factor of safety which are less than 1.0 in value are found to be greater when using program STRAIN1. We can therefore conclude that calculated values of the factor of safety  $F$  obtained from program STRAIN1 appear to be closer to 1.0 than the values obtained using program BSTRAIN2.

In virtually all cases, the values of the propagation factor  $PF$  obtained by programs STRAIN1 and BSTRAIN2 are identical. This reinforces the suggestion made earlier that the two simulation methods produce the same results. It can be seen that the two simulation techniques induce the same amount of local failure in the slopes tested and that any discrepancies in calculated values of the factor of safety  $F$  are due entirely to differences in the methods of calculating  $F$ .

When comparing results obtained by the two programs based on method 2, BSTRAIN2 and MPSTRAIN2, the following points are noted. The values of the factors of safety obtained by the program MPSTRAIN2 appear, in general, to be slightly higher than those obtained by program BSTRAIN2. Values of the propagation factor  $PF$ , on the other hand, seem to be the same in most cases, again emphasizing the point that differences in the final factor of safety are due mainly to differences in the methods used for calculating  $F$ . In this case, the more rigorous Morgenstern-Price method used in program MPSTRAIN2 would be expected to give the more reliable results. It is also noted that the largest differences in values of  $PF$  obtained by the two different programs, occur in slopes where the failure surface is of irregular shape and where the Bishop simplified method used in program BSTRAIN2 is the least reliable.

Due to the close correlation between values of  $PF$  obtained from the two programs BSTRAIN2 and MPSTRAIN2, it can be said that the method of simulation presented in this section appears to give valid results. The main discrepancies seem to be in areas where the Bishop simplified method of slope analysis is not expected to give reliable results and program MPSTRAIN2 results should therefore be used in such cases.

#### 6.4 ALTERNATE METHOD FOR REDISTRIBUTION OF EXCESS SHEAR (METHOD 3).

A method of simulating progressive failure is presented here which, while similar to the methods presented in the previous two sections in its detection of local failure on the base of a soil slice, is inherently different in its approach to the calculation and subsequent redistribution of excess shear forces over the failure surface.

##### 6.4.1 General Description Of Method.

Again, making use of the Bishop simplified method for limit equilibrium analyses, the following procedure is derived for method 3.

Step 1: Perform a limit equilibrium analysis on the slope and obtain an initial (peak) factor of safety,  $F_p$ .

Step 2: Calculate the mobilised shear force on the base of each slice,  $i$ , using the expression

$$\begin{aligned} (M_i)_0 &= \frac{(T_i)_p}{F_0} \\ &= \frac{c'_i l_i + (W_i \cos \alpha_i - u_i l_i) \tan \phi'_p}{F_0} \end{aligned} \quad (6.29)$$

Note that for the first iteration,  $F_0 = F_p$ .

Step 3: Check for local failure:- Each unfailed slice is checked for local failure. Local failure is deemed to have occurred if the shear force on the base of the slice is greater than the available shear strength on the slice base (i.e. if the inequality expressed in equation (6.5) is satisfied). The shear force on the base of the slice is given by equation (6.1) while in this case the available shear strength on the slice base is given by

$$(S_p)_i = c'_p l_i + (W_i \cos \alpha_i - u_i l_i) \tan \phi'_p \quad (6.30)$$

Expanding this, we obtain a new inequality which must be satisfied before local failure can occur on any slice. This inequality is

$$W_i \sin \alpha_i > c'_p l_i + (W_i \cos \alpha_i - u_i l_i) \tan \phi'_p \quad (6.31)$$

STEP 4: Reduce strength on failed slice to post-peak value:- The shear strength parameters of the soil on the base of all slices where local failure has just occurred are dropped to their residual values. The shear strength on the base of a slice where local failure is said to have occurred is given by the expression in equation (6.32) below.

$$(S_r)_i = c'_r l_i + (W_i \cos \alpha_i - u_i l_i) \tan \phi'_r \quad (6.32)$$

Step 5: Calculate new F and mobilised shear force:- As the shear strength on a failed slice falls to the residual value, the shear force acting on the slice base also falls to a value equal to the residual shear strength and the excess force given by  $T_p - T_r$  has to be redistributed. This redistribution process occurs automatically while performing a new equilibrium analysis. This new limit equilibrium analysis is performed using the updated values of shear strength parameters for the soil on each slice (i.e., peak values on unfailed slices and residual values on failed slices). A new factor of safety,  $F_1$ , is thus found.

For each unfailed slice, i, a new value of the mobilised shear force is obtained as follows,

$$\begin{aligned} (M_i)_1 &= \frac{(T_i)_p}{F_1} \\ &= \frac{c'_p l_i + (W_i \cos \alpha_i - u_i l_i) \tan \phi'_p}{F_1} \end{aligned} \quad (6.33)$$



Step 6: Calculate excess shear forces:- Since the factor of safety has fallen due to the drop to the residual value of the shear strength on some of the slices as described above, the value of the mobilised shear force will now be higher on each unfailed slice than before. The excess shear force on each unfailed slice,  $i$ , after the first iteration is thus expressed as

$$(e_i)_1 = (M_i)_1 - (M_i)_0 \quad (6.34)$$

Step 7: Check for local failure on unfailed slices:- The total shear force tending to cause local failure on an unfailed slice  $i$  is now equal to

$$T_i = W_i \sin \alpha_i + (e_i)_1 \quad (6.35)$$

Therefore, combining equations (6.5) and (6.34), local failure is said to occur if

$$W_i \sin \alpha_i + (e_i)_1 \geq (S_p)_i \quad (6.36)$$

where  $(S_p)_i$  is given by equation (6.30).

The procedure now returns to step 4 and steps 4 through to 7 are repeated until no further slices fail in step 7. At this stage the factor of safety is recorded as the final factor of safety.

Generalising the equations described in steps 5, 6 and 7 above, let us assume that  $k$  iterations have occurred resulting in a modified factor of safety equal to  $F_k$ .

In step 5, for an unfailed slice  $i$ , the new value of mobilised shear force is given by

$$(M_i)_k = \frac{(T_i)_p}{F_k}$$

$$= \frac{c'_p l_i + (W_i \cos \alpha_i - u_i l_i) \tan \phi'_p}{F_k} \quad (6.37)$$

In step 6, the excess shear force on an unfailed slice  $i$  becomes

$$(Me_i)_k = (M_i)_k - (M_i)_0 \quad (6.38)$$

Finally in step 7 the total shear force tending to cause local failure on unfailed slice  $i$  is given as

$$T_i = W_i \sin \alpha_i + (Me_i)_k \quad (6.39)$$

and the inequality which must be satisfied before local failure can occur becomes

$$W_i \sin \alpha_i + (Me_i)_k \geq S_{pi} \quad (6.40)$$

or

$$W_i \sin \alpha_i + (Me_i)_k \geq c'_p l_i + (W_i \cos \alpha_i - u_i l_i) \tan \phi'_p \quad (6.41)$$

#### 6.4.2 Description Of Computer Program BSTRAIN3.

As with methods 1 and 2, the procedure described above is greatly aided by the use of a computer program. Program BSTRAIN3 was written (also in FORTRAN 77 on the University of Wollongong Univac 1100 computer) to perform the procedure described above in method 3. Program BSTRAIN3 calls two subroutines. These are SPARM2 and FACSAF. SPARM2 is virtually identical to SPARAM in programs STRAIN1 and BSTRAIN2. The differences exist only in the internal storage allocation. Routine FACSAF is a general purpose routine which performs a Bishop's simplified limit equilibrium analysis on the slope in question. It is basically the same as subroutines FRESID and

STINIT in structure.

#### 6.4.3 Description of Computer Program MPSTRAIN3.

As with method number 2, a corresponding program using the Morgenstern-Price method of stability analysis was developed and given the name MPSTRAIN3. Since it closely resembles program MPSTRAIN2, it will not be described in detail.

The program structure is identical to that of program MPSTRAIN2 except for subroutine STRAIN which is the routine performing the actual strain softening. Subroutine STRAIN in program MPSTRAIN3, therefore, uses the simulation procedure described in method 3 above and used by program BSTRAIN3. As with its counterpart in program MPSTRAIN2, the current routine STRAIN does not call routine SPARAM to read soil and slope data, and calls routine SOLUTN to calculate the limit equilibrium factor of safety using Morgenstern and Price's method of analysis. Again, routine STRAIN closely resembles the main body of program BSTRAIN3.

#### 6.4.4 Results And Discussion.

The results of a number of analyses carried out using the simulation procedure outlined in this section are presented below. Table 6.5 contains the results of a series of analyses using program BSTRAIN3 while table 6.6 contains a similar set of results for program MPSTRAIN3. The results presented here differ from those presented earlier in this chapter in that only one final factor of safety is calculated whereas previously two values,  $F_c$  and  $F_1$ , were obtained. This factor of safety is denoted by  $F_f$ . The corresponding value of the propagation factor at the point where the final factor of safety is reached is represented by the symbol  $PF_f$ .

TABLE 6.5

Results from Program BSTRAIN3 (Method 3).  
Bishop Simplified method Extended and Updated for  
Strain Softening and Stress Redistribution.

(a) Using shear strength parameters as per system A.

Slide	$F_p$	$F_r$	$F_b$	$PF_b$	$F_f$	$PF_f$
Northholt						
ru=.25	1.65	.92	1.42	.34	1.37	.41
ru=.34	1.52	.79	1.24	.41	1.42	.41
P.S.	1.54	.81	1.26	.41	1.26	.41
Selset						
ru=.35	1.03	.77	.94	.47	.94	.47
P.S.	.97	.69	.85	.51	.81	.64
Sudbury						
ru=.30	1.99	.98	1.83	.17	1.79	.21
P.S.	1.99	.98	1.87	.13	1.87	.12
Jackfield	2.12	1.60	2.09	.06	2.09	.06
Balgheim	1.43	.70	1.43	.00	1.43	.00
Saskatchewan	1.28	.76	1.20	.86	1.20	.86
Vajont	1.31	1.30	1.30	.59	1.30	.59
Hyp.1	3.55	.98	3.55	.00	3.55	.00
Hyp.2	2.36	.69	2.15	.14	2.15	.14

(b) Using shear strength parameters as per system B.

Slide	$F_p$	$F_r$	$F_b$	$PF_b$	$F_f$	$PF_f$
Northholt						
ru=.25	1.65	.72	1.35	.34	1.28	.41
ru=.34	1.52	.63	1.16	.41	1.16	.41
P.S.	1.54	.64	1.18	.41	1.18	.41
Selset						
ru=.35	1.04	.71	.91	.47	.88	.56
P.S.	.97	.64	.82	.51	.76	.68
Sudbury						
ru=.30	1.99	.78	.80	.17	1.75	.21
P.S.	1.99	.77	1.84	.13	1.79	.16
Jackfield	2.12	1.18	2.08	.06	2.08	.06
Balgheim	1.43	.66	1.43	.00	1.43	.00
Saskatchewan	1.28	.22	1.07	.86	1.07	.86
Vajont	1.31	.99	1.17	.59	1.12	.69
Hyp.1	3.55	.81	3.55	.00	3.55	.00
Hyp.2	2.36	.61	2.14	.14	2.14	.14

TABLE 6.6

Results from Program MPSTRAIN3 (Method 3).  
Based on Morgenstern-Price method Extended for  
Strain Softening and Stress Redistribution.

(a) Using shear strength parameters as per system A.

Slide	$F_p$	$F_r$	$F_b$	$PF_b$	$F_f$	$PF_f$
Northolt						
ru=.25	1.59	.87	1.35	.34	1.30	.41
ru=.34	1.47	.75	1.18	.41	1.18	.41
P.S.	1.54	.81	1.28	.38	1.25	.41
Selset						
ru=.35	1.05	.79	.95	.47	.95	.47
P.S.	1.10	.84	1.00	.47	1.00	.47
Sudbury						
ru=.30	2.00	1.00	.84	.17	1.80	.20
P.S.	2.02	1.00	1.90	.13	1.88	.15
Jackfield	2.12	1.60	2.09	.05	2.09	.05
Balgheim	1.45	.68	1.45	.00	1.45	.00
Saskatchewan						
Vajont	1.38	1.37	1.37	.55	1.37	.55
Hyp.1	3.55	.98	3.55	.00	3.55	.00
Hyp.2	2.17	.64	1.93	.14	1.93	.14

(b) Using shear strength parameters as per system B.

Slide	$F_p$	$F_r$	$F_b$	$PF_b$	$F_f$	$PF_f$
Northolt						
ru=.25	1.59	.68	1.29	.34	1.23	.41
ru=.34	1.47	.59	1.12	.41	1.12	.41
P.S.	1.45	.64	1.20	.38	1.18	.41
Selset						
ru=.35	1.05	.73	.93	.47	.91	.51
P.S.	1.10	.77	.98	.47	.98	.47
Sudbury						
ru=.30	2.00	.78	1.81	.17	1.76	.21
P.S.	2.02	.79	1.87	.13	1.80	.19
Jackfield	2.12	1.19	2.08	.05	2.08	.05
Balgheim	1.45	.64	1.45	.00	1.45	.00
Saskatchewan						
Vajont	1.38	1.04	1.25	.55	1.21	.66
Hyp.1	3.55	.81	3.55	.00	3.55	.00
Hyp.2	2.17	.57	1.92	.14	1.92	.14

From the results shown in tables 6.5 and 6.6 the following observations were made. The final factor of safety  $F_f$  is, in the majority of cases, greater than  $F_c$  obtained from programs BSTRAIN1 and BSTRAINS2. Consequently, the value of  $PF_f$  is considerably less than the value of  $PF_c$ . Also, there appears to be less tendency for the value of the factor of safety to decrease past  $F_b$ , and it is noted that  $F_b$  is slightly higher using program BSTRAIN3 than using BSTRAIN2.

Comparing the results of programs BSTRAIN3 and MPSTRAIN3 the same observations are made as for previous sections. The main differences in values of factor of safety are due simply to the method used to calculate the factor of safety (i.e. Bishop's simplified method or Morgenstern-Price method) and not on the simulation process used. The fact that, in most cases, the values of PF obtained from the two programs BSTRAIN3 and MPSTRAIN3 are identical reinforces this observation.

#### 6.5 REDISTRIBUTION OF NORMAL AND SHEAR FORCES USING THE CONCEPT OF VIRTUAL WEIGHT (METHOD 4).

In method 3, which was described in the previous section, a procedure for simulating progressive failure using strain softening was described. As a slice of soil in a failure mass was said to have failed locally by satisfying the inequality in equation (6.5), the shear strength of the soil in that slice was assumed to have dropped to its residual value and the shear force was also dropped to equal the shear strength. A process was then described whereby the excess shear force was redistributed throughout the unfailed soil mass and a new factor of safety calculated.

However, the shear force is not the only force acting on the base of a slice. In order to maintain equilibrium, the normal force on the base of each slice should also be considered and redistributed after local failure. This section describes a method of simulating progressive failure along a surface of sliding, taking into account both shear and normal forces on the base of each individual slice.

## 6.6 GENERAL DESCRIPTION OF METHOD.

The procedure described herein is very similar to that described in the previous section for method 3. Basically, the difference is that instead of calculating and redistributing the mobilised shear strength along the failure surface, a quantity known as the virtual weight of a soil slice is calculated and redistributed in a manner similar to that used to redistribute the excess mobilised shear force in the previous method. The procedure, which again uses the Bishop simplified method of limit equilibrium analysis, is as follows.

**Step 1: Calculate peak factor of safety:-** As with the previous method a limit equilibrium analysis is performed on the slope in question and an initial (peak) factor of safety,  $F_p$ , is obtained.

**Step 2: Calculate virtual weight for each slice:-** If we consider a slice  $i$  and assume it has a virtual weight  $(W_i)_0$  such that

$$F_0 = F_p = \frac{c'_p l_i + [(W_i)_0 \cos \alpha_i - u_i l_i] \tan \phi'_p}{(W_i)_0 \sin \alpha_i} \quad (6.42)$$

We can obtain an expression for the virtual weight  $(W_i)_0$  of each slice as

$$(W_i)_0 = \frac{c'_p l_i - u_i l_i \tan \phi'_p}{F_0 \sin \alpha_i - \cos \alpha_i \tan \phi'_p} \quad (6.43)$$

**Steps 3 and 4: Locate local failure and reduce strength:-** These steps are identical to Steps 3 and 4 described in the previous section. Each slice is checked for local failure and if local failure has occurred the shear strength is dropped to its residual value.

**Step 5: Calculate new value of virtual weight for each slice:-** Calculate a new value for the factor of safety by performing another limit equilibrium analysis on the slope using the modified values of shear strength for each slice. Having found  $F_1$  we can then also

calculate the new value of the virtual weight  $(W_i)_1$  for each slice. Thus for an unfailed slice  $i$ ,

$$(W_i)_1 = \frac{c'_p l_i - u_i l_i \tan \phi'_p}{F_1 \sin \alpha_i - \cos \alpha_i \tan \phi'_p} \quad (6.44)$$

Step 6: Calculate excess virtual weight for each slice:- As  $F_1$  is less than  $F_0$ , due to the reduced shear strength on slices where local failure has occurred, then  $(W_i)_1$  is greater than  $(W_i)_0$ . Therefore each unfailed slice  $i$  has an excess virtual weight equal to

$$(W_{e_i})_1 = (W_i)_1 - (W_i)_0 \quad (6.45)$$

Step 7: Calculate modified slice weight:- When considering local failure on an unfailed slice  $i$  we now consider a modified value of the slice weight. This modified value is defined as

$$(W_m)_1 = W_i + (W_{e_i})_1 \quad (6.46)$$

where  $W_i$  is the actual slice weight.

Thus substituting  $(W_m)_1$  for  $W_i$  in equation (6.31) we now obtain the following inequality which must be satisfied in order for local failure to occur on an unfailed slice  $i$ .

$$(W_m)_1 \sin \alpha_i > c'_p l_i + [(W_m)_1 \cos \alpha_i - u_i l_i] \tan \phi'_p \quad (6.47)$$

Again, as in method 3, the procedure now returns to step 4 and steps 4 through to 7 are repeated until no further slices fail in step 7. At this stage the factor of safety is the final factor of safety.

Again, generalising the equations described in steps 5, 6 and 7 above, assuming that  $k$  iterations have occurred resulting in the  $k^{\text{th}}$  value of the factor of safety equal to  $F_k$  we obtain the following expressions:



In step 5, for an unfailed slice  $i$  the new value of virtual weight is

$$(W_i)_k = \frac{c'_p l_i - u_i l_i \tan \phi'_p}{F_k \sin \alpha_i - \cos \alpha_i \tan \phi'_p} \quad (6.48)$$

In step 6, the excess virtual weight after  $k$  iterations is given by

$$\begin{aligned} (W_e)_k &= (W_i)_k - (W_i)_0 \\ &= \frac{c'_p l_i - u_i l_i \tan \phi'_p}{F_k \sin \alpha_i - \cos \alpha_i \tan \phi'_p} - \frac{c'_p l_i - u_i l_i \tan \phi'_p}{F_0 \sin \alpha_i - \cos \alpha_i \tan \phi'_p} \end{aligned} \quad (6.49)$$

Finally in step 7, the modified slice weight becomes

$$(W_m)_k = W_i + (W_e)_k \quad (6.50)$$

where  $W_i$  is the actual slice weight. The inequality which must be satisfied for local failure to occur thus becomes

$$(W_m)_k \sin \alpha_i > c'_p l_i + [(W_m)_k \cos \alpha_i - u_i l_i] \tan \phi'_p \quad (6.51)$$

#### 6.6.1 Computer Programs BSTRAIN4 And MPSTRAIN4.

Two programs, BSTRAIN4 and MPSTRAIN4, were used to obtain results from the case histories used to verify the feasibility of the method described in this section. As with the previous method (method 3) the two programs mentioned above make use of the Bishop simplified method and the Morgenstern-Price method of stability analysis respectively. These programs are thus very similar to program BSTRAIN3 and MPSTRAIN3 described in the previous section and differ only in the actual

procedure for simulating the progression of local failure. Due to this, no description of the two programs will be presented here.

#### 6.6.2 Results And Discussion.

As with the previous section, the following results are from a number of analyses carried out using the simulation procedure described in this section. Again, two sets of results are presented. Table 6.7 contains the results of the simulation as obtained by using program BSTRAIN4 and table 6.8 contains corresponding results obtained from program MPSTRAIN4.

Again, from the results obtained by the two programs BSTRAIN4 and MPSTRAIN4 using method 4 and shown in tables 6.7 and 6.8, similar observations are made to those for method 3 in the previous section. As a matter of fact, the same comments can be applied to the results of programs BSTRAIN4 and MPSTRAIN4 using method 4 as were made for programs BSTRAIN3 AND MPSTRAIN3 using method 3. There is even less of a tendency for the value of the factor of safety to decrease past  $F_b$  than there was using method 3. It can therefore be said that the redistribution of shear forces by this method is not very effective towards initiating local failure along the unfailed portion of the failure surface.

#### 6.7 SUMMARY AND CONCLUSIONS.

From the results presented in this chapter a number of conclusions can be reached. The values of propagation factor corresponding to the final factor of safety obtained using methods 3 and 4 are lower than the values obtained using methods 1 and 2. The values of the final factor of safety are thus higher using methods 3 and 4. In fact, they are never as low as 1. In most cases, there is no drop in the value of the factor of safety from the peak value. Where the factor of safety does drop below 1.0 the relevance of the results is dubious as the peak factor of safety in those cases is

TABLE 6.7

Results from Program BSTRAIN4 (Method 4).  
Bishop Simplified method Extended and Updated for  
Strain Softening and Stress Redistribution.

(a) Using shear strength parameters as per system A.

Slide	$F_p$	$F_r$	$F_b$	$PF_b$	$F_f$	$PF_f$
Northolt						
ru=.25	1.65	.92	1.42	.34	1.42	.34
ru=.34	1.52	.80	1.24	.41	1.24	.41
P.S.	1.54	.81	1.26	.41	1.26	.41
Selset						
ru=.35	1.04	.77	.94	.47	.94	.47
P.S.	.97	.69	.65	.51	.84	.56
Sudbury						
ru=.30	1.99	.98	1.83	.17	1.83	.17
P.S.	1.99	.98	1.87	.13	1.87	.13
Jackfield	2.12	1.60	2.09	.06	2.01	.23
Balgheim	1.43	.70	1.43	.00	1.43	.00
Saskatchewan	1.28	.76	1.20	.86	1.20	.86
Vajont	1.31	1.30	1.30	.59	1.30	.59
Hyp.1	3.55	.98	3.55	.00	3.55	.00
Hyp.2	2.36	.69	2.15	.14	2.15	.14

(b) Using shear strength parameters as per system B.

Slide	$F_p$	$F_r$	$F_b$	$PF_b$	$F_f$	$PF_f$
Northolt						
ru=.25	1.65	.72	1.35	.34	1.35	.34
ru=.34	1.52	.63	1.16	.41	1.16	.41
P.S.	1.54	.64	1.18	.41	1.18	.41
Selset						
ru=.35	1.04	.71	.91	.47	.91	.47
P.S.	.97	.64	.82	.51	.81	.56
Sudbury						
ru=.30	1.99	.78	1.80	.17	1.80	.17
P.S.	1.99	.77	1.84	.13	1.84	.13
Jackfield	2.12	1.18	2.08	.06	1.81	.34
Balgheim	1.43	.66	1.43	.00	1.43	.00
Saskatchewan	1.23	.22	1.07	.86	1.07	.86
Vajont	1.31	.99	1.17	.59	1.14	.64
Hyp.1	3.55	.81	3.55	.00	3.55	.00
Hyp.2	2.36	.61	2.14	.14	2.14	.14

TABLE 6.8

Results from Program MPSTRAIN4 (Method 4).  
Based on Morgenstern-Price method Extended for  
Strain Softening and Stress Redistribution.

(a) Using shear strength parameters as per system A.

Slide	$F_p$	$F_r$	$F_b$	$PF_b$	$F_f$	$PF_f$
Northolt						
ru=.25	1.59	.87	1.35	.34	1.35	.34
ru=.34	1.47	.75	1.18	.41	1.18	.41
P.S.	1.54	.81	1.28	.38	1.28	.38
Selset						
ru=.35	1.05	.79	.95	.47	.95	.47
P.S.	1.10	.84	1.00	.47	1.00	.47
Sudbury						
ru=.30	2.00	.96	1.84	.17	1.84	.17
P.S.	2.02	1.01	1.90	.13	1.90	.13
Jackfield	2.12	1.61	2.09	.05	1.92	.40
Balgheim	1.45	.68	1.45	.00	1.45	.00
Saskatchewan						
Vajont	1.38	1.37	1.37	.55	1.37	.55
Hyp.1	3.55	.98	3.55	.00	3.55	.00
Hyp.2	2.17	.64	1.93	.14	1.93	.14

(b) Using shear strength parameters as per system B.

Slide	$F_p$	$F_r$	$F_b$	$PF_b$	$F_f$	$PF_f$
Northolt						
ru=.25	1.59	.68	1.29	.34	1.29	.34
ru=.34	1.47	.59	1.12	.41	1.12	.41
P.S.	1.54	.64	1.20	.38	1.18	.41
Selset						
ru=.35	1.05	.73	.93	.47	.91	.51
P.S.	1.10	.77	.98	.47	.98	.47
Sudbury						
ru=.30	2.00	.78	1.81	.17	1.81	.17
P.S.	2.02	.79	1.87	.13	1.87	.13
Jackfield	2.12	1.19	2.08	.05	1.35	.81
Balgheim	1.45	.64	1.45	.00	1.45	.00
Saskatchewan						
Vajont	1.38	1.04	1.25	.55	1.23	.64
Hyp.1	3.55	.81	3.55	.00	3.55	.00
Hyp.2	2.17	.57	1.92	.14	1.92	.14

extremely close to 1.0 .

It would therefore appear that, for the case histories considered, methods 3 and 4 are not very successful at initiating and propagating local failure, method 4 being the least successful. Methods 1 and 2, on the other hand, seem to be much more effective in simulating the propagation of the zone of strain softening after local failure along the assumed surface of sliding. Since methods 1 and 2 are basically the same method and differ only in the fact that method 1 uses a less refined procedure for calculating the factor of safety, we can hence concentrate on method 2 which appears to give the most feasible results.

Considering the results obtained in method 2 using the shear strength parameters as per system A (these shear strength parameters correspond to those used by Law and Lumb [58]) and comparing them to the results obtained by Law and Lumb, the following comments can be made. Law and Lumb applied their technique to only three case histories all of which were assumed to have circular surfaces of sliding. These three case histories are the Northolt, Selset and Sudbury Hill slides. Firstly, the Selset slide is a bad example to demonstrate strain softening as its peak factor of safety was found to be 1.05 using a pore pressure ratio value of 0.35. For the Northolt slide, using an  $r_u$  value of 0.25, and the Sudbury Hill slide, using an  $r_u$  value of 0.30, the final factors of safety calculated using a linear stress redistribution profile were 1.23 and 1.41 respectively, corresponding to propagation factors of 0.52 and 0.69 respectively. It is feasible to suppose that by using a more severe stress redistribution profile, perhaps an exponential distribution, local failure may have propagated further to give a final factor of safety closer to 1. However, comparing these results with those obtained using shear strength parameters as per system B, it can be seen that sufficient strain, softening can be induced in the latter to bring the factor of safety down below 1.

Although, by using the shear strength parameters according to system B, a larger number of slopes give factors of safety below 1.0, a certain number of cases show no significant change (or none at all) when using different stress redistribution profiles or shear strength

parameters. These cases, namely the Jackfield, Balgheim, Vajont, Hyp.1 and Hyp.2 slides, show very little tendency towards stress redistribution on the basis of limit equilibrium even though the Balgheim slope and the two hypothetical slopes have residual factors of safety less than 1. It would thus appear that the proposed method does not function for these cases, the reason perhaps being the geometry of the slopes in question.

It is known that in cases where the failure surface is parallel to the top surface, especially if the failure surface is shallow, then the chances of strain softening occurring using limit equilibrium methods of analysis are very low. In such cases, the final factor of safety will be approximately (if not exactly) equal to the peak factor of safety. This is exactly what would be expected in the case of the Jackfield and Balgheim slopes. It is not, therefore, an error in the proposed method, but more precisely, a limitation of the limit equilibrium method of analysis. The obvious next step would be to investigate alternatives to the limit equilibrium approach.

It may not be necessary to discard the limit equilibrium methods entirely in order to present a technique which accurately predicts the likelihood of the soil mass to fail. It may, in fact, be possible to extend the method of analysis to incorporate certain factors which are not considered by conventional limit equilibrium methods. One such factor, and one which has been considered of increasing significance in recent years, is the initial stress state of the soil in the slope prior to the commencement of strain softening. The following chapters will attempt to investigate this initial stress state and the consequences of incorporating its influence in the progressive failure simulation techniques presented herein.

## CHAPTER 7

### THE CONCEPT OF INITIAL STRESS.

#### 7.1 INTRODUCTION AND GENERAL COMMENTS.

In recent years consideration of initial stresses in the analysis of stress conditions in soil masses has been given increasing importance. This is especially so in the case of over-consolidated clays or soils where the consolidation history of the soil mass determines, to a large extent, the ratio and magnitude of the horizontal and vertical stresses within it. In this chapter, reference is made to a number of investigations concerned with initial stresses in soils and rocks. Some research results which concern the initial stress conditions existing in soil and rock masses and their influence on ground conditions are summarised. From the findings of various research investigators some understanding may be achieved regarding the role of stress conditions in the development of progressive failure in soil slopes.

Evidence of stress conditions in which the magnitudes of the stresses in the horizontal direction were found to be much greater than the magnitudes of stresses in the vertical direction has been reported by various authors. Petersen [74] in his studies of the Bearpaw shale at Saskatchewan, in Canada, estimated that the horizontal stresses in the shale were about 1.5 times as great as the overburden pressure at a point approximately 20 metres beneath the ground surface. Skempton [87] showed that, for London clay, the ratio of the horizontal stresses to the vertical effective stresses, varied with depth from about 1.5 at a depth of 30 metres to approximately 2.5 at a depth of 3 metres. Skempton concluded, therefore, that near the surface, the horizontal pressure was sufficiently near the maximum passive pressure to cause failure of the clay. Langer [57] also gave

evidence of horizontal stresses of the order of three times the overburden pressure. Bjerrum [18] showed that high initial lateral stresses could result in large shear stresses at the base of an excavated slope, and thus increase the likelihood of progressive failure. Among others, Chowdhury [26] has referred to a number of publications concerned with the existence, importance and role of initial stresses in soil and rock slopes.

In their analyses of embankments, Brown and King [22] considered different potential slip surfaces for both excavated and built-up slopes. In their analyses, the actual incremental process of slope construction was simulated. The effects of the initial state of stress on the embankment stresses in linearly elastic materials was studied in detail. They showed that in a built-up slope, the maximum shear stresses in the foundation material are influenced by the ratio of horizontal stresses to vertical overburden stresses. Brown and King also pointed out that the possibility of failure originating was more likely in embankment slopes.

## 7.2 SIMULATION OF 'FAILURE' DEVELOPMENT IN CLAYS.

Duncan and Dunlop [40] developed a method of analysis of slopes excavated in materials with low and high initial horizontal stresses representative of either (a) normally consolidated or (b) heavily over-consolidated clays. They included the effects of various initial stress conditions by simulating the excavation of a slope in an initially horizontal deposit of clay in a series of incremental steps. Referring to figure 7.1, the initial stresses on a slope to be excavated are represented by  $\sigma_0$ . On the inclined surface, these initial stresses include both shear and normal components.

Excavation of the slope was simulated by Duncan and Dunlop by applying changes in the stresses  $\Delta\sigma$  to the excavated surface. Application of these changes in stress, which are equal in value and apposite in sign to the initial stresses  $\sigma_0$ , results in a stress-free condition on the excavated surface. The applied changes in stress are resisted only by the remaining material in the slope and



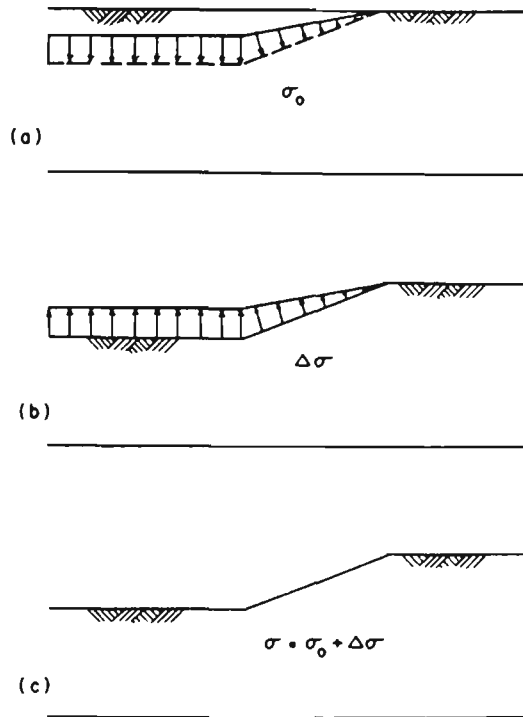


Figure 7.1 Changes in Stress during Excavation (from Duncan and Dunlop [40]).

they induce changes in stress away from the excavated surface which may be calculated by the finite element method. These changes in stress are then added to the initial stress values to obtain the combined or final stresses.

For purposes of analysis the real soil was represented by a homogeneous, linear elastic, isotropic material. The effects of nonlinear stress-dependent behaviour and the role of stress concentration due to fissures were ignored. They noted that field investigations had shown that the horizontal stresses in heavily over-consolidated clays may exceed the overburden pressure by 50% or even more in some cases.

Duncan and Dunlop concluded that the higher the horizontal stresses before construction, the lower the factor of safety corresponding to the development of local failure around the slope. Therefore, the existence of high horizontal stresses in heavily over-

consolidated clays and shales increases the probability of progressive failure occurring in these materials.

In a later paper, Dunlop and Duncan [41] demonstrated how the analytical procedure described briefly above may be used to calculate displacements, strains and stresses around slopes even after local failure has developed. By simulating the excavation of the slope in a series of steps or layers beginning from a horizontal surface, Dunlop and Duncan made the following observations.

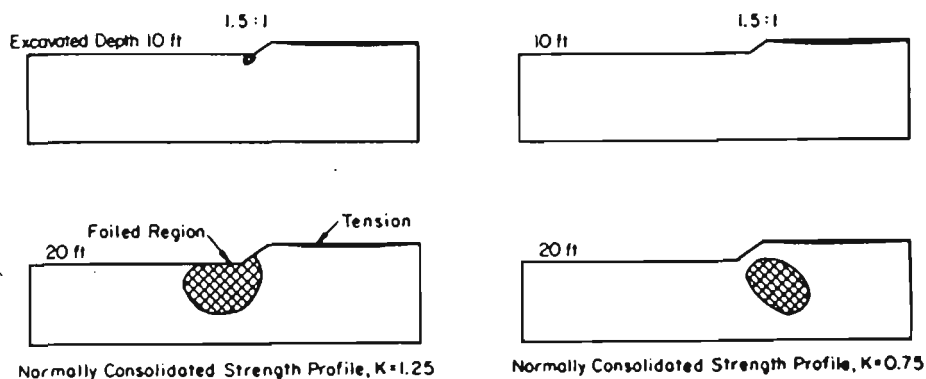
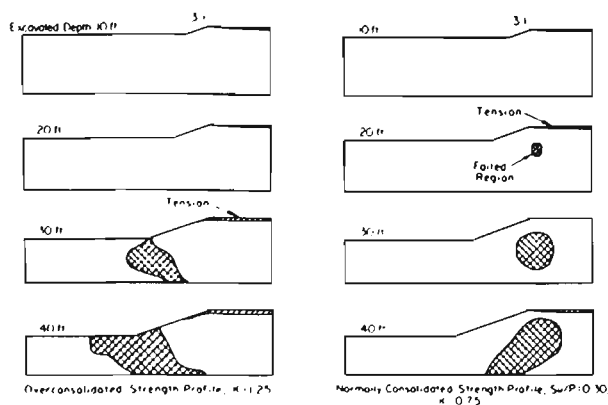
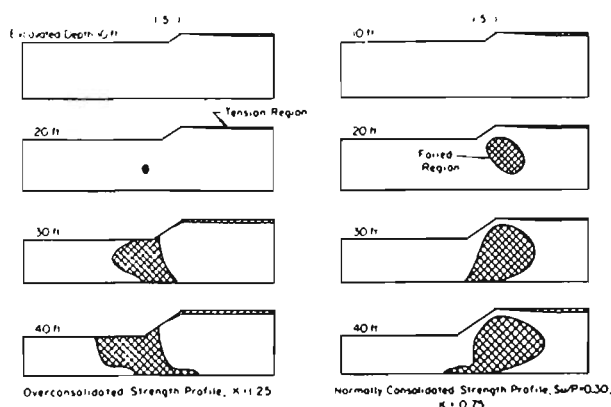


Figure 7.2 Effect of Initial Stress on Development of Failed Regions (from Dunlop and Duncan [41]).

1. Around excavations having high initial horizontal stresses, the failure zone develops first near the toe of the slope, subsequently progressing back beneath the slope. When the initial stresses are low, however, the failure zone develops first beneath the slope crest, subsequently progressing downward and towards the slope (see figure 7.2).
2. Around excavations with initial stresses and strength profiles representative of normally consolidated clays, failure begins beneath the slope. As excavation continues, the failure zone extends upwards toward the slope crest and downwards toward the toe of the slope (see figure 7.3).



(a) —DEVELOPMENT OF FAILURE ZONES AROUND 3:1 SLOPE IN OVERCONSOLIDATED AND NORMALLY CONSOLIDATED CLAY LAYERS



(b) —DEVELOPMENT OF FAILURE ZONES AROUND 1.5:1 SLOPE IN OVERCONSOLIDATED AND NORMALLY CONSOLIDATED CLAY LAYERS

Figure 7.3 From Dunlop and Duncan [41].

3. Around excavations with initial stress and strength profiles representative of over-consolidated clays, failure was found to begin beneath the bottom of the excavation. As excavation continues, the failure zone extends both upwards to the base of the excavation and downwards to the bottom layer (refer to figure 7.3).

### 7.3 OTHER FINDINGS RELATED TO THE INITIAL STRESS CONCEPT.

Vaughan and Kwan [108] stated that there is no general theory relating soil properties to both stress history and a varying initial

structure. Stress history is linked with in-situ stress but few attempts have been made to relate the degree of weathering directly to engineering properties, and no attempt seems to have been made to relate it to in-situ effective stress.

Vaughan and Kwan attempted to predict the effective stress changes and in-situ effective stresses in a residual soil by considering weathering as a weakening process which involves decreasing unit weight, strength and stiffness. They found that the combination of low horizontal stress with decreasing shear strength due to weathering is likely to cause shear failure, particularly in slopes. During shear failure, disintegration and particle wastage, horizontal stress is likely to tend towards the value given by the active earth pressure coefficient.

Kirkpatrick, Khan and Mirza [56], in their studies on overconsolidated clays, produced results which showed that compared with in-situ soils, stress-relieved samples suffered appreciable loss of strength and increase in failure strain and produced considerably different effective stress paths to failure. This behaviour was more pronounced with increasing sample age and was more acute for kaolin than for the less permeable illites.

Bernander and Olofsson [11] found that certain parameters such as the brittleness index, deviatoric strain at peak strength and the initial stress level greatly affect the mechanism of progressive failure. They proposed a method of solution which takes into account the relevant deformations in the soil mass. They suggested that this approach and the results obtained by the analyses convincingly explain the formation, propagation and final configuration of major landslides in Sweden.

## 7.4 INITIAL STRESSES COMPONENTS.

### 7.4.1 Definition Of Conjugate Stress Ratio.

The conjugate stress ratio,  $K$ , is defined as the ratio of initial horizontal normal stresses to initial vertical normal stresses at a point within a soil mass. For a horizontal soil mass, assuming that the vertical stresses are due entirely to the weight of the overburden, the magnitudes of these vertical and horizontal stresses is given by Taylor [80] as

$$\sigma_v = \gamma z \quad (7.1a)$$

$$\sigma_h = k\gamma z \quad (7.1b)$$

where  $\gamma$  is the unit weight of the soil and  $z$  is the depth below the soil surface of the point in question (otherwise known as the height of the overburden). Note that equations (7.1) represent total and not effective stresses unless the soil is a dry soil such as cohesionless sand without a water table.

### 7.4.2 Calculation Of Initial Stresses In An Inclined Slope.

For a slope with uniform surface inclination  $\beta$ , the conjugate stresses are as follows (see figure 7.4a):-

$$\sigma_v = \gamma z \cos\beta \quad (7.2)$$

and

$$\sigma_\beta = K\gamma z \cos\beta \quad (7.3)$$

Chowdhury [26] derived the following expressions for the normal and shear stresses in a horizontal and vertical coordinate system (see figure 7.4(b)).

$$\sigma_x = K\gamma z \cos^2\beta \quad (7.4)$$

$$\sigma_z = \gamma z (1 + K \sin^2 \beta) \quad (7.5)$$

$$\tau_{xz} = K \gamma z \sin \beta \cdot \cos \beta \quad (7.6)$$

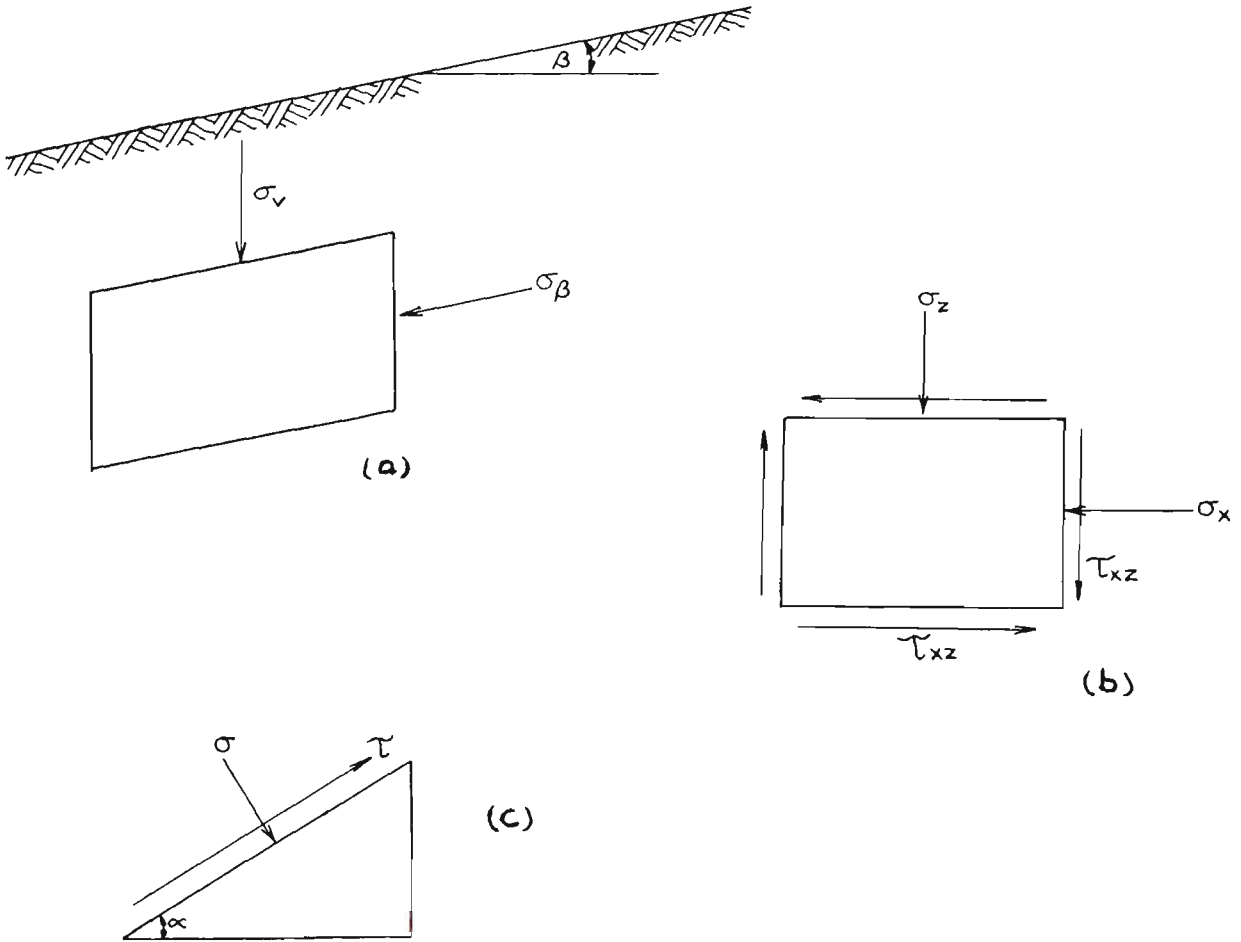


Figure 7.4 In-situ Stresses within a Natural Slope (Chowdhury).

Following from the above, expressions can be derived for the normal and shear stresses acting on a plane inclined at an angle  $\alpha$  to the horizontal as shown in figure 7.1(c). These expressions are given by equations (7.7) and (7.8) below.

$$\sigma = \gamma z \left[ \cos^2 \alpha (1 + K \sin^2 \beta) + K \sin^2 \alpha \cdot \cos^2 \beta - K \sin 2\alpha \cdot \sin \beta \cdot \cos \beta \right] \quad (7.7)$$

$$\tau = \gamma z \left[ \sin \alpha \cdot \cos \alpha (1 + K \sin^2 \beta - K \cos^2 \beta) - (\sin^2 \alpha - \cos^2 \alpha) K \sin \beta \cdot \cos \beta \right] \quad (7.8)$$

### 7.4.3 Effective Stress Considerations.

For cases where pore-water pressures exist within the slope, it is useful to define a ratio  $K_o$  of horizontal and vertical normal effective stresses. This ratio is given by the expression [26]

$$K_o = \frac{K \cos^2 \beta - r_u}{1 + K \sin^2 \beta - r_u} \quad (7.9)$$

where

$$r_u = u/\gamma z \quad (7.10)$$

and is a dimensionless pore pressure ratio.

This definition of  $K_o$  is in accord with normal geotechnical practice. It would be incorrect to define  $K_o$  as a ratio of effective conjugate stresses as conjugate stresses are resultant total stresses (involving both normal and shear components) and not normal stresses and thus the application of effective stress hypothesis to such stresses is not valid [26].

However, considering soil with a horizontal surface i.e.  $\beta=0$ , equation (7.9) becomes

$$K_o = \frac{K - r_u}{1 - r_u} = \frac{\sigma'_h}{\sigma'_v} \quad (7.11)$$

where  $\sigma'_h$  and  $\sigma'_v$  are the effective horizontal and vertical normal stresses at any point. Moreover, if the pore water pressure at the point is zero (i.e.  $\beta=0$ ,  $u=0$ ) then

$$K_o = K \quad (7.12)$$

## CHAPTER 8

### INITIAL STRESS CONSIDERATIONS IN THE SIMULATION OF PROGRESSIVE FAILURE.

#### 8.1 GENERAL.

In Chapter 6, concepts concerning strain softening of soils and associated stress redistribution were used to facilitate the simulation of progressive failure in slopes. Methods of analysis were proposed for soil slope problems with consideration for progressive failure and a series of results were obtained. Results of individual methods were compared with previously published ones for particular case histories [58] and it was also possible to assess the results obtained by alternative methods proposed. In many cases, the progressive failure resulting from strain softening was not sufficient to cause overall slope failure. However, since most of the slopes analysed had failed at some time in the past, it could be argued that the strain softening approach on its own may be insufficient for predicting or simulating overall slope failure under all conditions.

In recent years it has been found that the in-situ or initial stresses inherent in a soil mass are of considerable importance in geotechnical investigations. As detailed in Chapter 7, several authors have emphasized the considerable role of in-situ stresses in the development of failure zones within soil masses. Consequently, the initial stress state must be taken into consideration in simulating progressive failure.

Most soils are found to have some degree of anisotropy where, depending on the consolidation history of the soil mass, the stresses in one direction (usually horizontal) are greater than those in other directions. In an over-consolidated clay slope, for example, it is



commonly found that the horizontal stress is in excess of the vertical stress at any point within the mass. Cases have been reported where the horizontal effective stresses at a point within a soil mass have been found to be up to three times as great in magnitude as the vertical effective stresses at the same point.

In this chapter, the problem of progressive failure is tackled by considering the initial stresses inherent in a slope. The simulation of change in safety factor with the development of progressive failure is attempted in a number of ways. One of these methods involves the extension of techniques presented in Chapter 6 for soils in which strain softening is the most important factor for the development of progressive failure.

## 8.2 SIMULATION OF FAILURE CONSIDERING BOTH STRAIN SOFTENING AND INITIAL STRESSES.

In Chapter 6 a number of techniques were used for a strain softening soil to simulate progressive failure. It was concluded that the technique referred to as Method 2 appeared to be the most successful in simulating the process of initiation and propagation of local failure which may lead to overall failure of a given sloping soil mass. It is therefore intended to extend this technique to include initial stress considerations and to observe the effect of including these initial stresses in the analysis of the case histories considered earlier in Chapter 6.

### 8.2.1 Description of Method.

The method proposed below is similar to that described as Method number 2 in Chapter 6.

Step 1: Calculate the shear force and shear strength on the base of each slice:- The shear force on the base of a given slice  $i$  is denoted by the following expression.

$$T_i = \tau_i \cdot l_i \quad (8.1)$$

where  $\tau_i$  is the initial shear stress existing in the slope before failure starts as defined by equation (7.8), and where  $l_i$  is the length of the slice base.

The shear strength on the base of slice  $i$  is given as

$$(S_p)_i = (c_p + \sigma_i \tan \phi_p) l_i \quad (8.2)$$

where  $\sigma_i$  is the initial normal stress existing in the slope before failure occurs and is given by equation (7.7).

The factor of safety  $F$  is found from equation (6.4) as in the previous method.

**Step 2: Check for local failure:-** The procedure followed in this step is identical to the procedure described in step 2 of methods 1 and 2 in Chapter 6. In the current method, however, the values of  $S_p$  and  $T$  are obtained using the expressions given in equations (6.1) and (6.2) for normal and shear stresses respectively.

**Step 3: Reduce strength on failed slices to the post-peak value under conditions of limiting equilibrium:-** As with the methods described in Chapter 6, on all slices where local failure has occurred, the soil strength parameters are assumed to have fallen from their peak values to their residual values. In addition, the newly failed zone is assumed to behave as if it were in limiting or critical equilibrium whereas the remaining unfailed sections of the slope are still under conditions of initial stress. Therefore, on all slices where local failure has occurred, the shear strength is expressed by equation (6.9). Again, as in Chapter 6, since the mobilised shear force cannot exceed the available shear strength, the mobilised shear force on each failed slice will be set equal to the residual shear strength on the base of that slice as shown by equation (6.11).

**Step 4: Redistribute the excess shear force:-** The procedure followed in this step is again the same as that followed in step 4 of methods 1

and 2 presented in Chapter 6. It is, therefore, not repeated here.

**Step 5: Calculate the new factor of safety:-** The procedure used to calculate the new factor of safety is similar to that described in method 2 in Chapter 6. An iterative procedure is used whereby a complete limit equilibrium analysis (using Bishop's simplified method) is carried out on the slope using the last known value of the factor of safety  $F$ , and a new value of  $F$  is then calculated. This procedure continues until the difference between two successive values of  $F$  is negligible. The difference between the calculation of  $F$  in this current method and the calculation of  $F$  in method 2 of Chapter 6 is in the equation used to calculate each successive value of  $F$ .

Equation (6.17) is used to calculate the value of the factor of safety in methods 1 and 2 of chapter 6. Although this equation also holds true for the current method, it will be expressed differently since we are now dealing with two different models for simulation of stress conditions within one method of analysis, namely initial stress and limit equilibrium models. All unfailed slices are assumed to be still under conditions of initial stress, and all failed slices are assumed to be in limiting equilibrium. Therefore, the overall factor of safety may be calculated by using the expression given in equation (8.3) below.

$$F = \frac{\sum (S_p)_{is} + \sum (S_p)_{le}}{\sum T_{is} + \sum T_{le}} \quad (8.3)$$

where the terms with the 'is' subscript refer to those slices which have not yet failed and the terms with the 'le' subscript refer to those slices which have failed and which are in limiting equilibrium.

Again, as with the previous method, the procedure returns to step 2 above and halts only when no further slices satisfy the criteria for local failure in step 2.

### 8.2.2 Modification of Computer Program BSTRAIN2.

As the present method is basically similar to that referred to as method 2 in Chapter 6 and varies mainly in the equations used for the calculation of forces on slice bases, the program BSTRAIN2 which was used in the previous method can also be used here with some alterations. The program was modified to include the following additions.

1. a user specified option is read in at the start of the program to indicate whether initial stresses are to be included. This is in the form of a YES/NO answer to a generated question and initialises a flag variable in the program.
2. subroutine STINIT is modified to enable calculation of initial values of slice forces according to equations (8.1) and (8.2) incorporating equations (7.7) and (7.8). This addition to routine STINIT is used when the slope is assumed to be under initial stress conditions.
3. an 'initial stress' counterpart to routine RESLE was written and called routine RESIS. This new routine performs the iterative procedure for calculating the new factor of safety. In calculating the new value of  $F$ , subroutine RESIS uses equation (8.3) in conjunction with equations (8.1), (8.2), (7.7) and (7.8).

The overall procedure followed in program BSTRAIN2 is the same as it was in Chapter 6 except that when subroutine STINIT is called to calculate the initial values of normal and shear forces on the slice bases as well as the factor of safety  $F$ , a check is made as to whether initial stresses are to be included in the analysis. According to the result of this test the relevant parts of subroutine STINIT are processed. Secondly, in subsequent iterations, a check is again made for initial stress inclusions. If initial stresses are to be included, then subroutine RESIS is used to calculate forces on slice bases and subsequent values of the factor of safety  $F$ . If initial

stresses are not to be included, then subroutine RESLE is used as for method 2 in Chapter 6.

### 8.2.3 Case Histories Considered for Analysis.

In order to present comparative results using the present method, the nine case histories considered in Chapter 6 were analysed again by the method presented here. These case histories represent slides at Northolt, Selset, Sudbury Hill, Jackfield, Balgheim, Saskatchewan and Vajont as well as two hypothetical cases and are all fully documented in Appendix A and Chapter 6. Some of the actual cases are omitted however. For example, in the Northolt, Selset and Sudbury Hill slides only the cases where the actual phreatic surface is given are used. In addition, the shear strength parameters used here will be in accordance with system B as defined in Chapter 6. This combination of shear strength is as follows.

1. peak values of  $c'$  and  $\phi'$  as given in Appendix A.
2. residual value of  $c'$  equal to zero
3. residual value of  $\phi'$  is less than the peak value with magnitude as shown in Appendix A

### 8.2.4 Results and Discussion.

Table 8.1 shows a summary of results obtained by performing the above analytical procedure on the case histories detailed above. It is seen that in some cases (e.g. Northolt, Selset) the factor of safety obtained decreases during the process of stress redistribution. However, the other case histories show no decrease in factor of safety with stress redistribution. In other words, little or no stress redistribution occurs.

TABLE 8.1

Results from Program BSTRAIN2 using Initial Stresses.

(a) K = 1.0

Slide	F <sub>p</sub>	F <sub>r</sub>	F <sub>b</sub>	PF <sub>b</sub>	F <sub>c</sub>	PF <sub>c</sub>	F <sub>l</sub>	PF <sub>l</sub>
Northolt	1.641	0.636	1.439	0.236	0.686	1.000	0.686	1.000
Selset	1.021	0.638	0.895	0.678	0.650	1.000	0.650	1.000
Sudbury	1.976	0.770	1.976	0	1.976	0	1.976	0
Jackfield	2.210	1.182	2.234	0.076	2.234	0.076	2.234	0.076
Balgheim	2.095	0.658	2.095	0	2.095	0	2.095	0
Saskatchewan	5.148	0.928	5.148	0	5.148	0	5.148	0
Vajont	1.517	0.987	1.536	0.081	1.536	0.081	1.536	0.081
Hyp.1	3.762	0.812	3.762	0	3.762	0	1.536	0
Hyp.2	2.449	0.612	2.449	0	2.449	0	2.449	0

(b) K = 1.5

Slide	F <sub>p</sub>	F <sub>r</sub>	F <sub>b</sub>	PF <sub>b</sub>	F <sub>c</sub>	PF <sub>c</sub>	F <sub>l</sub>	PF <sub>l</sub>
Northolt	1.931	0.636	1.553	0.367	1.125	0.853	1.125	0.853
Selset	1.144	0.638	1.003	0.702	0.674	1.000	0.674	1.000
Sudbury	2.100	0.770	2.100	0	2.100	0	2.100	0
Jackfield	2.426	1.182	2.387	0.146	2.387	0.146	2.387	0.146
Balgheim	2.832	0.658	2.790	0.058	2.790	0.058	2.790	0.058
Saskatchewan	6.130	0.928	6.130	0	6.130	0	6.130	0
Vajont	1.767	0.987	1.647	0.211	1.562	0.446	1.591	0.280
Hyp.1	4.088	0.812	4.088	0	4.088	0	4.088	0
Hyp.2	2.813	0.612	2.646	0.081	1.408	0.725	1.549	0.648

(c) K = 2.0

Slide	F <sub>p</sub>	F <sub>r</sub>	F <sub>b</sub>	PF <sub>b</sub>	F <sub>c</sub>	PF <sub>c</sub>	F <sub>l</sub>	PF <sub>l</sub>
Northolt	2.286	0.636	1.714	0.506	1.533	0.719	1.347	0.853
Selset	1.275	0.638	1.111	0.741	1.076	0.876	0.700	1.000
Sudbury	2.235	0.770	1.840	0.293	0.839	1.000	0.839	1.000
Jackfield	2.674	1.182	2.586	0.206	2.586	0.206	2.586	0.206
Balgheim	4.228	0.658	4.098	0.110	4.098	0.110	4.098	0.110
Saskatchewan	7.465	0.928	7.235	0.045	7.235	0.045	7.041	0.090
Vajont	2.072	0.987	1.825	0.280	1.792	0.446	1.825	0.280
Hyp.1	4.466	0.812	4.466	0	4.466	0	4.466	0
Hyp.2	3.265	0.612	2.608	0.284	1.673	0.725	1.749	0.689

As the value of the coefficient  $K$  is increased from 1.0 to 1.5 and then to 2.0, the value of the factor of safety for the Sudbury case decreases to less than 1.0. For the other slopes, however, increasing the value of  $K$  does produce some small drop in the factor of safety but does not reduce it to anywhere near 1.0.

It appears, therefore, that the proposed method of analysis or simulation procedure does not sufficiently explain the failure of the case histories studied. It is therefore necessary to consider other possible factors and mechanisms which facilitate the development and propagation of slope failure.

One reason for the limited success of the above approach is that reorientation of principal stresses which occurs during the process of excavation of a slope (or during embankment construction) has not been considered. The method as developed here is applicable only to natural slopes with a uniform initial stress field. For built-up slopes, stress analyses using the finite element method would be required to get the true initial state of stress before the proposed method could be applied with complete success.

### 8.3 SIMULATION OF PROGRESSIVE FAILURE BY SEQUENTIAL LOCAL FAILURE OF SOIL SLICES.

Attempts were made in the previous section to evaluate strain softening effects on the propagation of local failure in a soil slope. It was found that in many cases these strain softening effects appeared not to have caused an overall failure of the slope. At this stage, it is not clear whether this lack of overall failure was due to insufficient local failure occurring or due to the method of simulating the progression of failure through the failure mass.

In order to help resolve this question, a method of simulating progressive failure was devised which assumes that the initial stress state changes to a simple gravitational stress field progressively along the potential slip surface. Thus a simulation procedure is proposed which links the initial stress state of a slope to the

conventional limit equilibrium stress field considering segments of the potential surfaces one by one to have been transformed in this way. In this approach it is therefore unnecessary to use a criterion for local failure as such because the aim is to study how the limit equilibrium factor of safety is actually reached.

### 8.3.1 General Description of Method.

Consider the slope shown in Figure 8.1 . With the potential failure surface represented by the curve BCE, it is initially assumed that the entire sliding mass BCEDB is under conditions of initial stress. At this stage the normal and shear stresses at any point within this mass are described by equations (7.7) and (7.8) respectively.

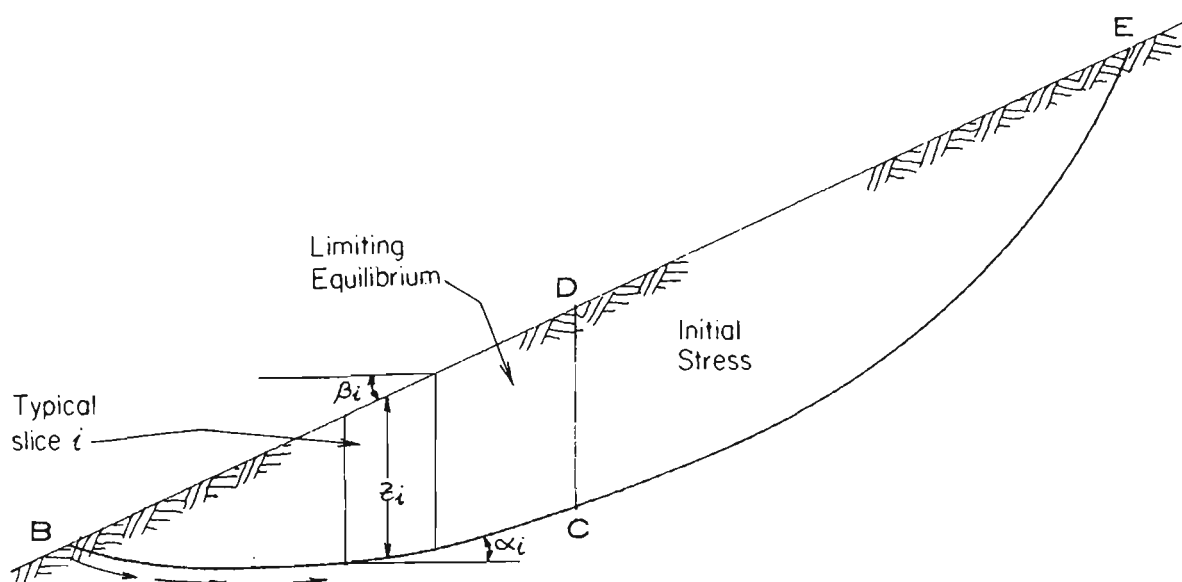


Figure 8.1 Typical Slope Cross-section showing Propagation of Failure.



A procedure similar to that described by Romani et. al. [79] and Chowdhury [29] is used. However, in this research the scope of the analysis is extended beyond that of the previous work done in this field.

As described in section 5.4, Romani et. al. presented a method of analysis which involved a crack or slit which begins at one end of the failure surface and proceeds towards the other end. At any point in time when the crack has progressed to a certain point, the part of the slope beyond that point and not yet reached by the crack is analysed under assumed conditions of elastic stress. Considering propagation from B to D, the section of the slope above the crack i.e. DCE is analysed as a rigid body using the concept of limit equilibrium. The Bishop simplified method is used for this part. The resisting and driving forces are thus calculated for each part and the overall factor of safety for the slope obtained. This is repeated for a large number of points and curves are obtained of the value of the factor of safety for failure starting from either the crest or the toe of the slope.

Chowdhury used a similar method except that the uncracked portion of the slope is considered to be under the influences only of the initial stresses inherent in the soil mass. Again the resisting and driving forces are calculated for each section and the overall factor of safety obtained. The results for variation of factor of safety obtained by Chowdhury are similar in trend to those of Romani et. al. considering the progression of the limit equilibrium stress field either from the crest or from the toe of the slope.

For this research, previous work was modified and the main improvement results from the following:-

1. Instead of using the Bishop simplified method for the section of the slope under limiting equilibrium, the Morgenstern-Price method of analysis has been used. Apart from advantages in the way of accuracy, this method allows non-circular failure surfaces to be analysed.

2. A number of ways of defining the section of the failure mass assumed to be in limiting equilibrium have been considered in the method proposed here.
3. Consideration has been given to the internal forces at the assumed boundary between the two parts of a potential failure mass, one at initial stress and the other at limiting equilibrium.

### 8.3.2 Details of Methods Used.

Failure will initiate in a natural slope either from the crest or from the toe. Divide the soil mass above the potential failure surface into a number of vertical slices as is usual with conventional limit equilibrium studies. Assume that local failure commenced at point B (figure 8.1) and has extended some distance. By local failure, it is meant that the shear stress has exceeded the peak shear strength and that the shear strength parameters  $c'$  and  $\phi'$  at that particular point have fallen to their residual values. Moreover, the soil in that part of the failure mass which has thus failed is now locally in a state of limiting equilibrium.

Consider that local failure has progressed along the potential slip surface from point B to point C (figure 8.1). Therefore, while the mass CEDC is still considered to be totally under initial stress conditions with shear strength parameters  $c'$  and  $\phi'$  at their peak values, the mass BCDB is assumed to now be under conditions of limiting equilibrium with  $c'$  and  $\phi'$  having dropped to their residual values along the surface BC. At this stage, the normal and shear stresses acting on the base of a slice  $i$  within the mass BCDB are given by the following equations in accordance with the concepts referred to in chapter 7 and, in particular, equations (7.7) and (7.8).

$$\sigma_i = \gamma z_i \left[ \cos^2 \alpha_i (1 + K \sin^2 \beta_i) + K \sin^2 \alpha_i \cdot \cos^2 \beta_i - K \sin 2\alpha_i \cdot \sin \beta_i \cdot \cos \beta_i \right] \quad (8.4)$$

$$\tau_i = \gamma z_i \left[ \sin \alpha_i \cdot \cos \alpha_i (1 + K \sin^2 \beta_i - K \cos^2 \beta_i) - (\sin^2 \alpha_i - \cos^2 \alpha_i) K \sin \beta_i \cdot \cos \beta_i \right] \quad (8.5)$$

where  $z_i$  is the height of the slice,

$\alpha_i$  is the angle of the slice base to the horizontal,

and  $\beta_i$  is the average angle of the topslope above the slice.

In order to obtain a measure of the overall stability of the combined mass, an expression is formulated to calculate the overall factor of safety for this mass. As the factor of safety of a soil or rock mass is generally defined as the ratio of the sum of the resisting forces to the sum of the driving forces in the mass, the overall factor of safety is expressed as given in equation (8.6) below.

$$F = \frac{\sum s_i}{\sum \tau_i} \quad (8.6)$$

where  $\sum s_i$  is the sum of the resisting stresses from both sections of the failure mass,

and  $\sum \tau_i$  is the sum of the driving stresses from both sections of the failure mass.

The above equation can be re-written as

$$F = \frac{\sum s_{le} + \sum s_{is}}{\sum \tau_{le} + \sum \tau_{is}} \quad (8.7)$$

where  $M$  is the number of slices which have experienced local failure.

In equation (8.7) above

$$s_{le} = c'_r + \sigma'_{le} \tan \phi'_r \quad (8.8)$$

where  $\sigma'_{le}$  is the effective normal stress on the base of the slice obtained from limit equilibrium considerations;

$$s_{is} = c'_p + \sigma'_{is} \tan \phi'_p \quad (8.9)$$

where  $\sigma'_{is}$  is the effective normal stress on the base of the slice obtained from equation (8.4);

$$\tau_{le} = \frac{c'_r + \sigma'_{le} \tan \phi'_r}{F_{le}} \quad (8.10)$$

where  $F_{le}$  and  $\sigma'_{le}$  are both found by the application of the Morgenstern-Price limiting equilibrium method; and

$\tau_{is}$  is the effective shear stress on the base of a slice obtained from equation (8.5).

At the point in time before progressive failure or transformation of stress state has started, equation (8.7) reduces to equation (8.11) below.

$$F = \frac{\sum s_{is}}{\sum \tau_{is}} \quad (8.11)$$

where  $s_{is}$  and  $\tau_{is}$  are defined by equations (8.9) and (8.5) respectively.

On the other hand if progression to 'limit equilibrium' stress state has occurred through the entire failure mass, equation (8.7) will reduce to equation (8.12) below.

$$F = \frac{\sum s_{le}}{\sum \tau_{le}} \quad (8.12)$$

where  $s_{le}$  and  $\tau_{le}$  are defined by equations (8.8) and (8.10) respectively.

### 8.3.3 Use of Conjugate Stress Ratio.

It is important to note here that while the equations for normal and shear stress on the base of any slice  $i$  (refer to equations (8.4) and (8.5)) both depend on the conjugate stress ratio  $K$ , in practice the value of  $K$  is not readily known. On the other hand  $K_o$ , the ratio of effective horizontal and vertical normal stresses, is more readily determined from measured laboratory or field data. It is this parameter  $K_o$  which is commonly encountered in geotechnical literature.

For the cases examined in this chapter, therefore, it is assumed that the value of  $K_o$  is known and is uniform throughout the failure mass. The value of  $K$  is then calculated for each slice within this mass using equation (8.13) below which is obtained as a rearrangement of equation (7.9).

$$K_i = \frac{K_o + r_u(1-K_o)}{\cos^2\beta_i - K_o \sin^2\beta_i} \quad (8.13)$$

in which  $K_i$  is the value of  $K$  for vertical slice  $i$ .

### 8.3.4 Direction of Propagation of Failure.

In the description of the method above, local failure was assumed to start at the toe of the failure surface. It is possible, however, that local failure may follow a different path.

Bishop [14] suggests that the shear strength in a slope may fall to the residual quicker at the toe of the slope or possibly at both ends simultaneously, thus suggesting that local failure may start more easily in one of these two modes. Romani et. al., [79] and Chowdhury [29] both have obtained results to indicate that failure tends to propagate, or is potentially more dangerous, when starting from the top end of the failure surface. Also, results described in Chapter 6

seem to indicate that local failure starting from some point near the centre of the slope may also be critical.

### 8.3.5 Definition of Propagation Factor.

At this stage, it is convenient to introduce a means of defining the extent to which the 'failure' or the transformation of stress has progressed. In other words, a factor, which shall be called the Propagation Factor, is introduced which describes the fraction of the total length of the failure surface which has changed from a condition of initial stress to a condition of limiting equilibrium. The propagation factor therefore indicates the fraction of the failure surface length which has experienced 'local failure'. This fraction is expressed as a decimal value between 0 and 1.

As failure can progress from more than one point at the one time, a more general definition of the propagation factor must be used. Thus, the Propagation Factor (expressed as a decimal value between 0 and 1.) is defined as that value derived by dividing the sum of the base lengths of all slices in the failure mass which have reached conditions of limiting equilibrium by the sum of the base lengths of the total number of slices. The expression for the propagation factor thus becomes;

$$PF = \frac{\sum_{i=1}^n \Delta l_{ie}}{\sum_{i=1}^N \Delta L_i} \quad (8.14)$$

where  $N$  is the total number of slices,

$n$  is the number of slices where limiting equilibrium conditions exist

$\Delta l_{ie}$  is the length of the base of slice  $i$  where limiting equilibrium conditions exist,

and  $\Delta L_i$  is the length of the base of any slice  $i$ .

#### 8.4 BOUNDARY CONDITION CONSIDERATIONS.

In order to obtain values of  $\sigma_{le}$  and  $F_{le}$  as required in equations (8.8) and (8.10) above, it is necessary to determine a method of applying a limiting equilibrium analysis to that section of the slope which is said to be under limiting equilibrium conditions. Consideration must be given to the line of separation between the two sections and to the boundary conditions existing about this line. An investigation of the normal and shear stress distributions around this line and over the whole failure mass must also be made.

##### 8.4.1 Different Modes for Treatment of Boundaries.

Two methods are considered for obtaining the factor of safety  $F_{le}$  for that part of the slope under conditions of limiting equilibrium. The first of these methods involves evaluating separately the overall factors of safety of the slope under limiting equilibrium conditions and under initial stress conditions. The overall factor of safety is then calculated as

$$F = \frac{F_{le} \cdot l_{le} + F_{is} \cdot l_{is}}{l_{le} + l_{is}} \quad (8.15)$$

The second method involves breaking up each of the two sections into its component slices and evaluating the overall factor of safety as shown previously in equation (8.7). The factor of safety for the section of the slope under limiting equilibrium conditions and the calculated stresses are derived from assuming that the failure surface extends only to the bottom of the line of separation between the two sections. The top surface includes a tension crack running down this line of separation to join the failure surface. This model, shown in figure 8.2, corresponds to the second method in accordance with equation (8.7).

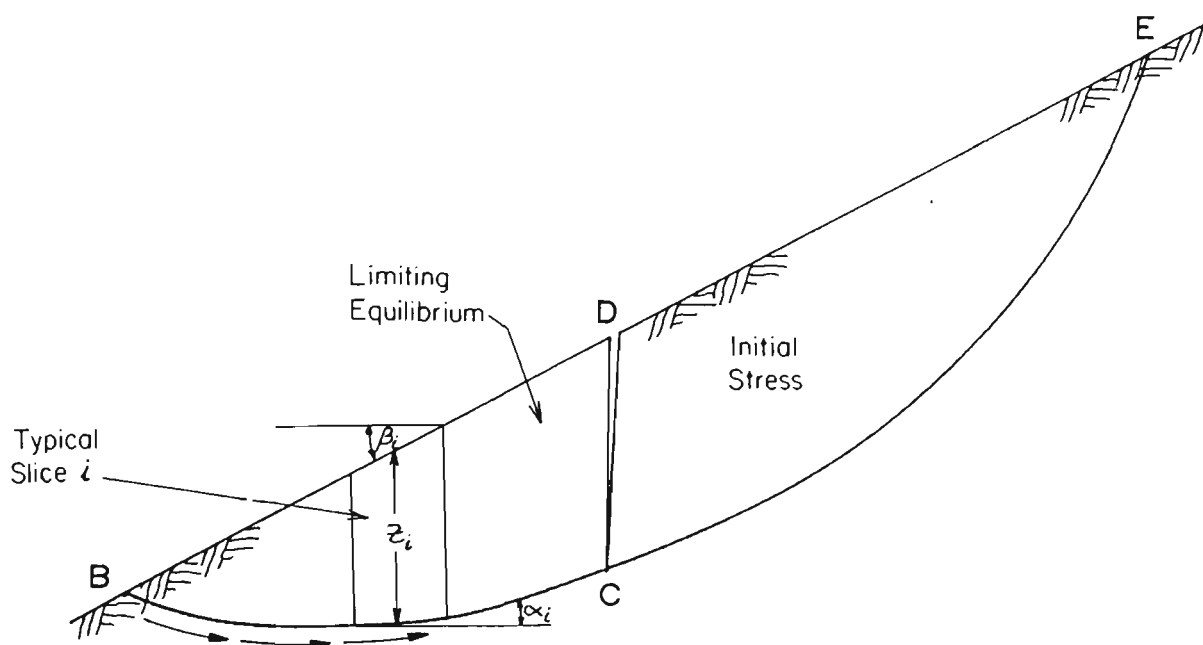


Figure 8.2 Slope Cross-section during Progression of Failure using Tension Crack Approach.

Program MGSINIT2 includes the capability for successively re-defining both the top slope profile and the failure surface so that the tension crack DC moves progressively from point B to point E or vice-versa depending on the direction of failure propagation.

#### 8.4.2 Consideration of Forces at Boundaries.

Forces at the assumed vertical boundary BD may be considered by referring to figure 8.3. Assume zone 1 to be under conditions of initial stress only while zone 2 is in a state of limiting equilibrium. A normal force  $P$  acts on the left boundary of mass BCD due to the resistance of mass ABD and with it is associated a shear force  $P_1$ . This force  $P$  is neglected in the Morgenstern-Price calculation of  $F$  for mass BCD in limiting equilibrium. Before altering the given Morgenstern-price method to include a rigorous solution taking into account the force  $P$ , it seems reasonable to estimate the effect of neglecting  $P$  altogether.





$$P_P = 0.5\gamma H^2 N_\phi + 2cHN_\phi^{0.5} \quad (8.17)$$

where  $N_\phi = \tan^2(45+\phi/2)$

Three series of trials were made on the arbitrary circular slip mass.

- i) Neglecting  $P$  and  $P_1$
- ii) Assuming  $P = P_A$  and  $P_1 = P_A \tan\phi'/F$
- iii) Assuming  $P = P_P$  and  $P_1 = P_P \tan\phi'/F$

In each case the proposed failure mass was divided into ten vertical slices of equal width and failure was assumed to propagate from the top of the slope (RHS) to the toe (LHS). Zone 2 which is assumed to be under limit equilibrium conditions becomes larger by one additional slice at a time and  $P$  and  $P_1$  are correspondingly shifted to the left one slice until the whole mass ABCDA is in limiting equilibrium.

The factor of safety for the section of the slope considered to be in limiting equilibrium was found first. For the case where no active or passive pressures were assumed to act, the calculation of  $F_{le}$  was made according to equation (2.9).

#### 8.4.4 Calculation of Factor of Safety Considering Earth Pressures at the Imaginary Vertical Boundary.

For the cases involving active or passive earth pressure as shown in figure 8.4 below, we have;

For the active pressure case three different components must be considered in equation (8.16).

$$P_A = P_1 + P_2 + P_3$$

where

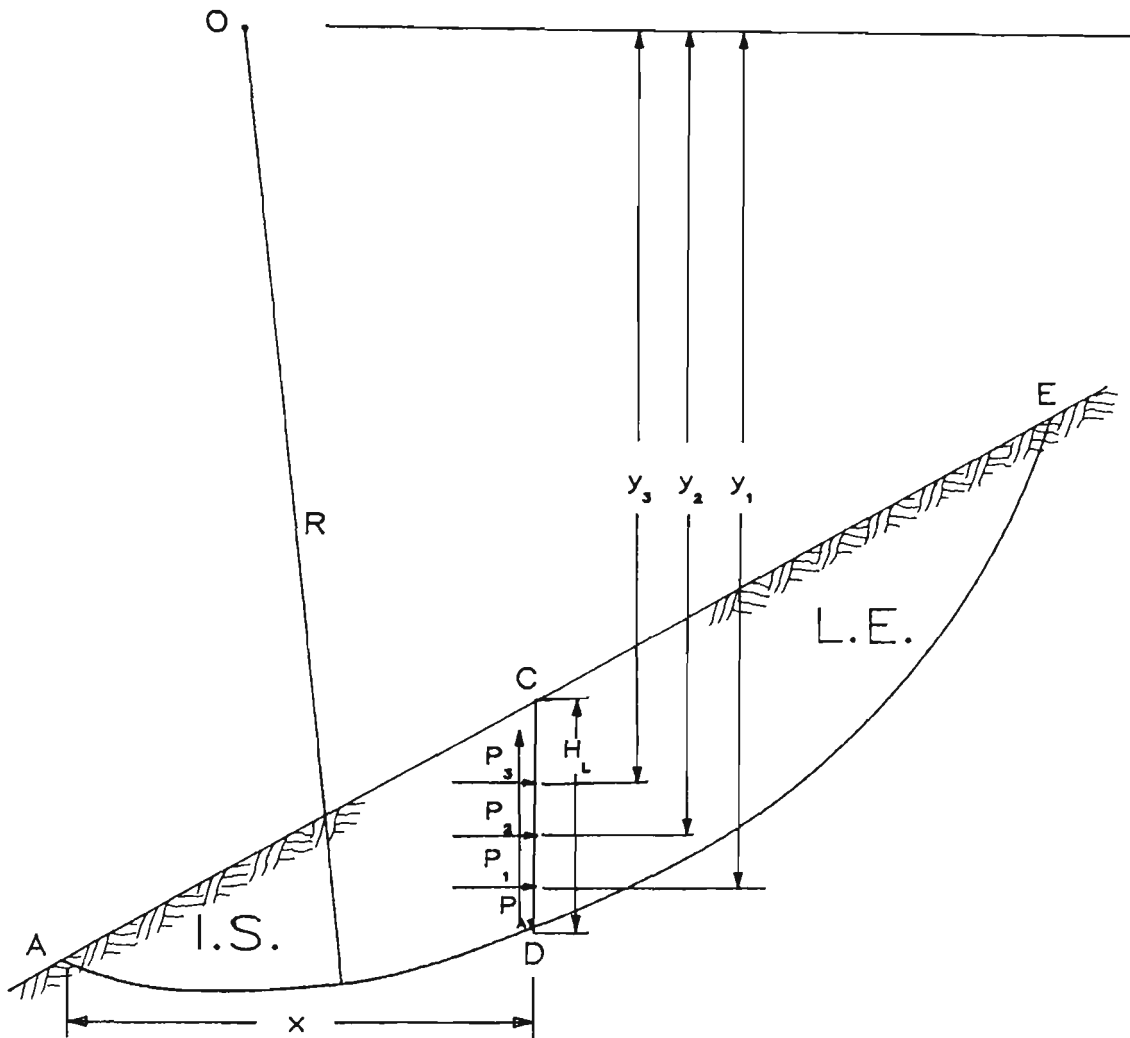


Figure 8.4 Slope Cross-section showing Active and Passive Earth Pressure Components.

$$P_1 = 0.5\gamma H^2/N_\phi \text{ and acts at one third of the height } H_L,$$

$$P_2 = 2cH/N_\phi^{0.5} \text{ and acts at the half way mark } H_L/2, \text{ and}$$

$$P_3 = 2c^2/\gamma \text{ and acts at a distance } 2cN_\phi^{0.5}/3\gamma \text{ down from point C.}$$

$$P_{A1} = P_A \tan\phi / F_{le}$$

Thus, taking moments about point O to find the factor of safety of the mass CDE we get,

$$F_{le} = \frac{\sum (RES_i)_{le} \cdot R}{\sum (MOV_i)_{le} \cdot R - P_1 y_1 + P_2 y_2 - P_3 y_3 - P_{A1} x} \quad (8.18)$$

where  $(RES_i)_{le}$  is the resisting force on slice  $i$  in the part of the slip surface which is assumed to be at limit equilibrium, and  
and  $(MOV_i)_{le}$  is the moving (or disturbing) force on slice  $i$  in that part of the slip surface which is assumed to be at limit equilibrium.

Starting with an initial value of  $F_{le}$ , the final value should be arrived at after only a few iterations.

For the passive pressure case two components must be considered. That is

$$P_p = P_1 + P_2 = P_p \text{ in equation (8.17)}$$

where

$$P_1 = 0.5 \gamma H^2 N_\phi \text{ and acts at one third of the height } H_L, \text{ and}$$

$$P_2 = 2cHN_\phi^{0.5} \text{ and acts at } H_L/2$$

$$P_{p1} = P_p \tan \phi / F_{le}$$

Again, taking moments about point O we get,

$$F_{le} = \frac{\sum (RES_i)_{le} \cdot R}{\sum (MOV_i)_{le} \cdot R - P_1 y_1 - P_2 y_2 - P_{p1} x} \quad (8.19)$$

In all three cases (i.e. active pressure, passive pressure and no pressure) the overall factor of safety for the mass ADEC is found by the expression

$$F = \frac{\sum (S'_i)_{is} + \sum (RES_i)_{le}}{\sum (\tau'_i)_{is} + \sum (MOV_i)_{le}} \quad (8.20)$$

where

$$S'_{is} = c' + \sigma'_{is} \tan \phi'$$

and  $\tau'_{is}$  and  $\sigma'_{is}$  are defined by equations (8.5) and (8.4) respectively.

#### 8.4.5 Results and Discussion.

The value of  $F$  is calculated and plotted for each point (i.e. each successive additional slice) against the propagation factor (P.F.) which is defined earlier in this chapter.

Figure 8.5 shows the relationship between the factor of safety  $F$  and the propagation factor P.F. when failure is assumed to progress from the toe of the slope up to the top. The curves show the change in the overall factor of safety under the different pressure considerations as the failure mass changes from an initial stress state to one of limiting equilibrium.

Similarly, figure 8.6 shows this relationship as failure progresses from the top of the slope down to the toe. The same three pressure options apply to the shifting boundary assumed under progression of failure.

#### 8.4.6 Conclusions Concerning Comparative Study.

From the curves in figures 8.5 and 8.6 it is clear that the factors of safety considering passive earth pressure are somewhat higher than the factors of safety considering active earth pressure or no pressure at all. The latter two, however, are nearly identical.

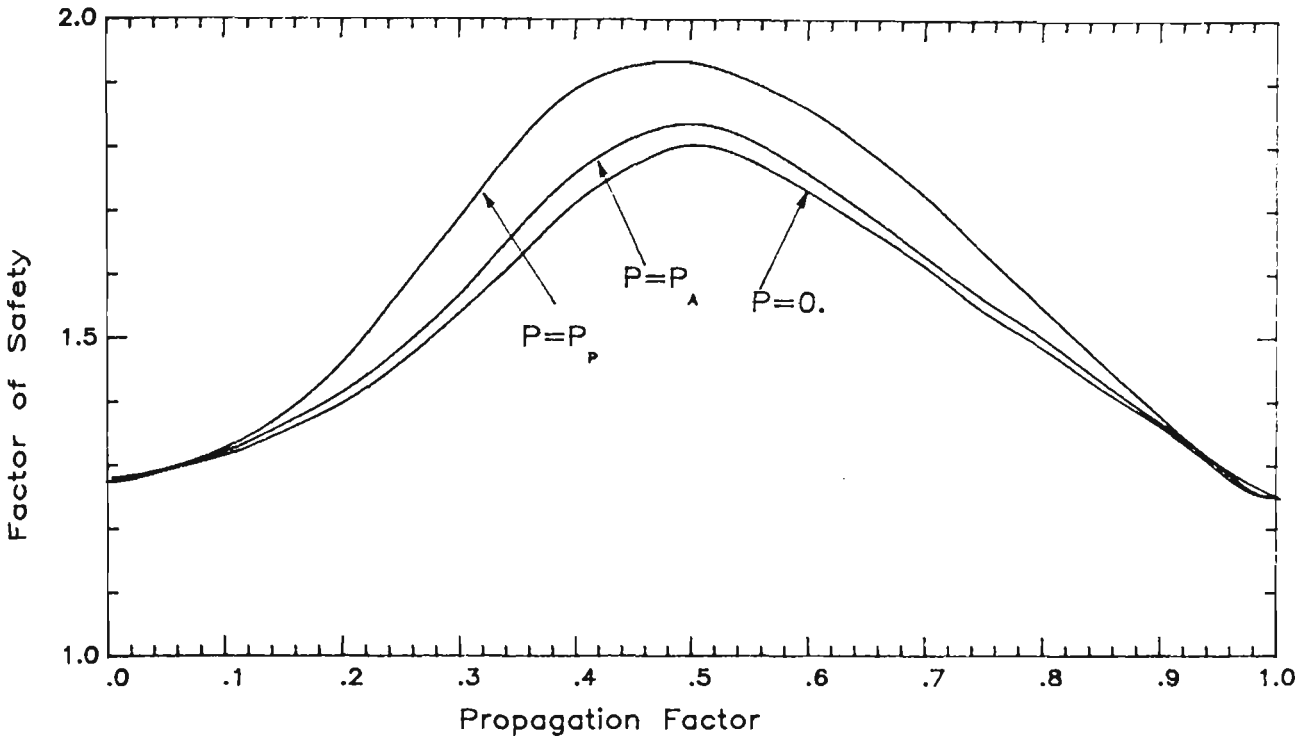


Figure 8.5 Boundary Force Considerations for Progressive Failure Starting From Bottom of Slope

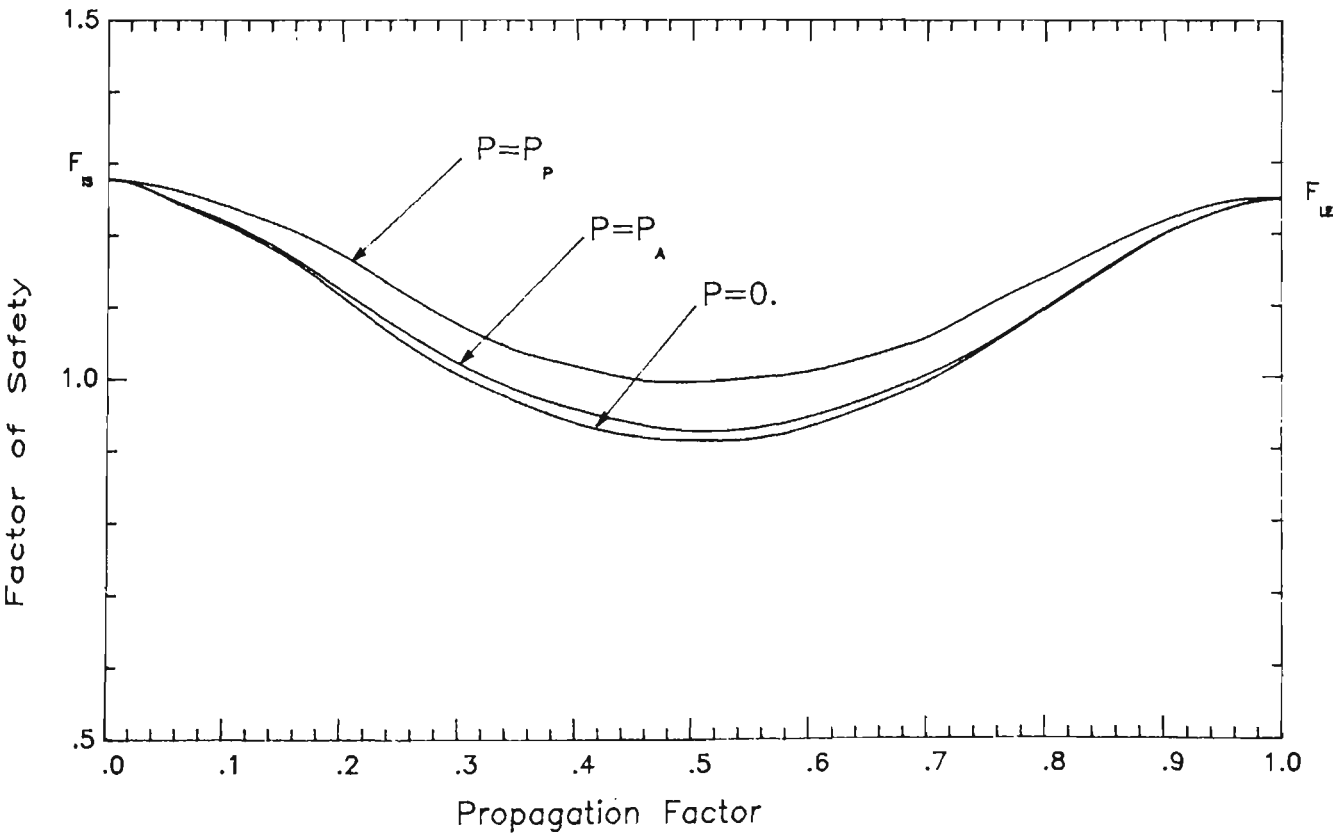


Figure 8.6 Boundary Force Considerations for Progressive Failure Starting From Top of Slope

The case with no earth pressure appears to have slightly lower values than the corresponding one considering active pressure. Thus the case with  $P=0$  is the most conservative.

The differences in results between the three alternative cases are not significant in general. Therefore, the forces  $P$  and  $P_1$  can be omitted altogether to simplify the calculations and the results are guaranteed to be conservative.

The second method for calculating the overall factor of safety (as described in section 8.4.1) appears to be attractive and has been used for the analysis of case histories as discussed in the subsequent sections.

## 8.5 CALCULATION OF OVERALL FACTOR OF SAFETY.

The calculation of the overall factor of safety is carried out using equation (8.7) as mentioned earlier. Program MGSINIT2 is used to calculate the factors of safety. The results obtained by this method will be discussed later. As stated in the previous section, the effect of any forces acting on the vertical boundary between the 'failed' and 'unfailed' slices is ignored.

In the calculation of the overall factor of safety, the effective shear stress  $\tau_{is}$  on the base of slices under initial stress conditions is given by equation (8.5). This equation contains the conjugate stress ratio  $K$ . The relationship between  $K$  and the ratio of horizontal and vertical stresses  $K_0$  was shown in equation (8.13).

It is the intention here to compare the results obtained using different values of  $K$  and  $K_0$ .

### 8.5.1 Case Histories Considered.

The slopes considered in this section are a subset of those used and described in section 8.2. A number of slopes was analysed but only the results of three are reported here as they represent a good cross-section of the results obtained. These three slopes are Northolt, Vajont and the hypothetical case number one.

### 8.5.2 Results and Discussion.

Figure 8.7 shows four curves indicating the change in the overall factor of safety of the Northolt slope as propagation of failure is simulated so that the slope mass moves from an initial stress state ( $P.F.=0$ ) to a state where it is entirely in a state of limiting equilibrium ( $P.F.=1$ ). The four curves correspond to four possible modes of failure. These are ;

1. failure starting at the toe (bottom) of the slope,
2. failure starting at the crest of the slope,
3. failure starting simultaneously from both ends of the slope,  
and
4. failure starting from the centre of the slope and progressing  
outwards.

From the four curves shown and from various other cases investigated it is obvious that failure modes (1) and (4) are unrealistic and that the factors of safety obtained are always higher than those obtained with the whole slope under either initial stress or limiting equilibrium conditions. Therefore, the curves corresponding to these methods are omitted from the subsequent figures showing the results.



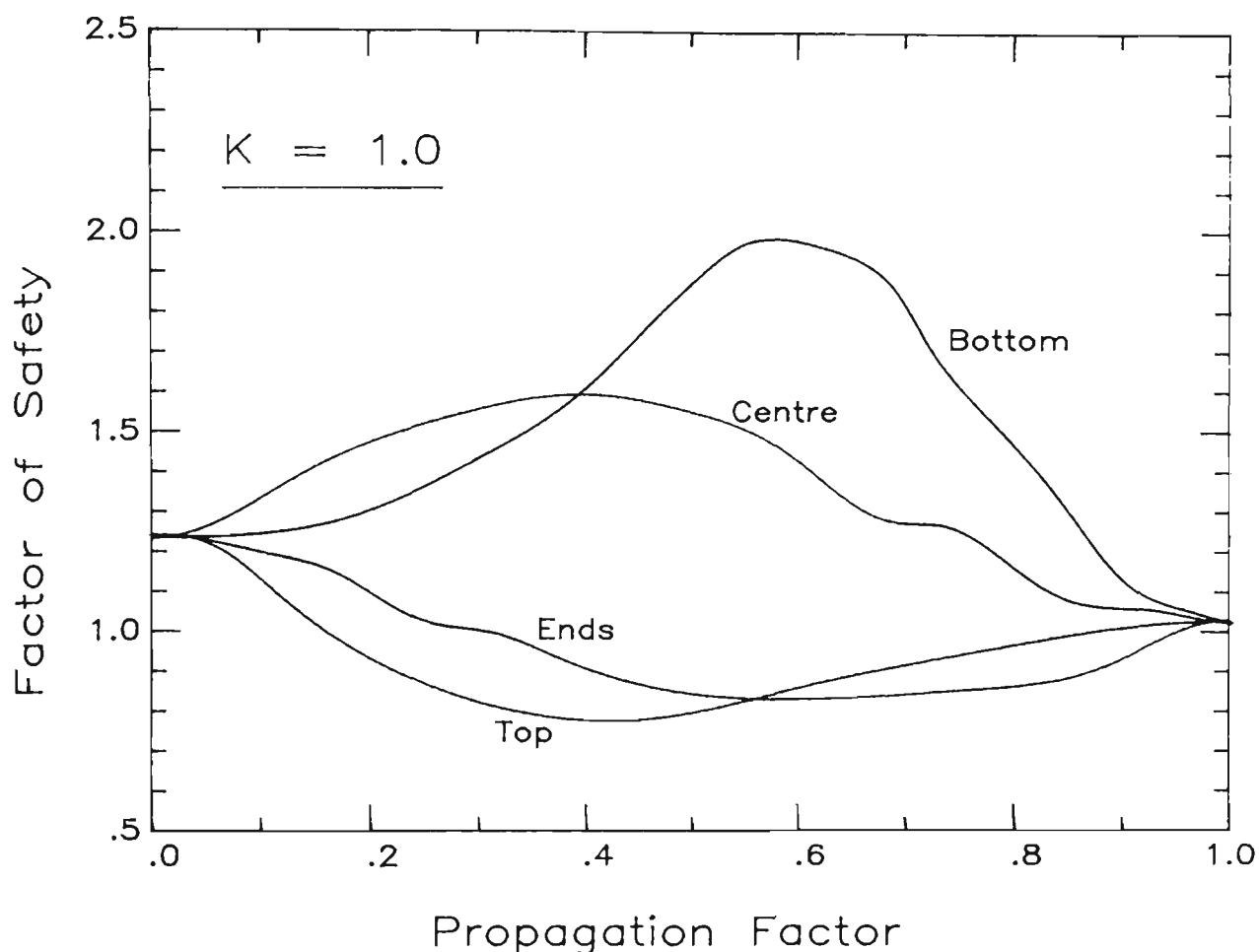


Figure 8.7 Variation in Factor of Safety with Different Modes of Failure Propagation (Northolt Slide).

It is clear, however, that the other two modes (2) and (3) both show a significant reduction in the factor of safety as failure progresses. It appears that, in some cases, there exists a point where the value of the factor of safety is lower than that of either the initial stress situation or the limiting equilibrium situation. In fact, although  $F_{le}$  and  $F_{is}$  are both greater than 1, at a point where local failure has progressed approximately 18% of the distance from the top of the slope to the toe (i.e. P.F.=0.18), the factor of safety becomes less than 1 thereby indicating overall failure of the slope. The occurrence of this gradual progressive failure may therefore explain the failure of this particular slope in which both

$F_{is}$  and  $F_{le}$  were found to be greater than 1.

By studying in detail all the results obtained, a general conclusion was reached that mode (2), where failure starts at the crest of the slope, is the most critical of all modes considered given that the factor of safety drops more rapidly and is generally lower than mode (3). Most of the results presented here are, therefore, of failure progressing from the crest of the slope.

However, overall failure in slopes may be caused by progressive local failure in either of these two modes.

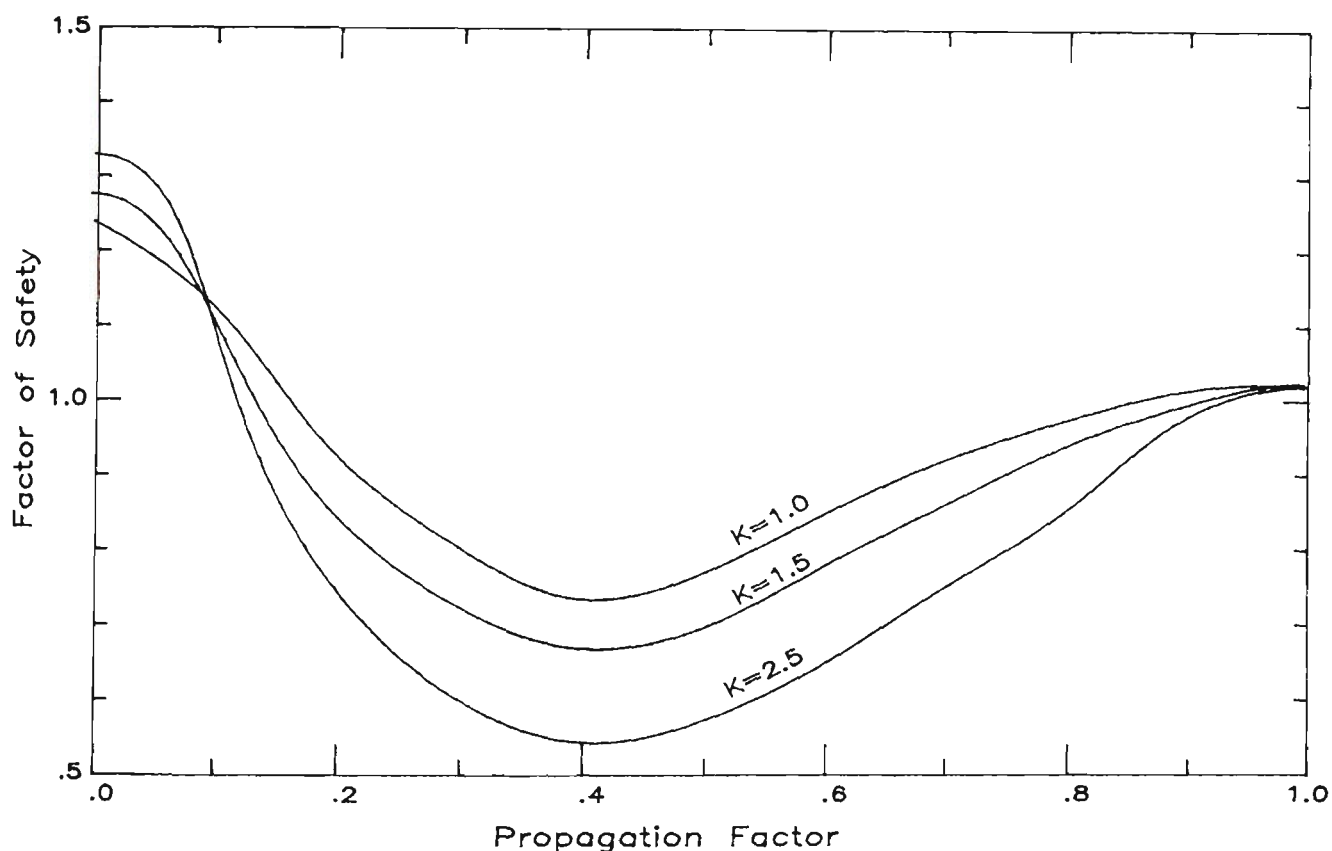


Figure 8.8 Variation in Factor of Safety for Different Values of K (Northolt Slide).

Figure 8.8 shows the variation in the curve obtained by failure mode (2) for different values of the factors  $K$  and  $K_0$ . It is evident that as  $K$  or  $K_0$  increases, the curve for factor of safety becomes more critical (i.e. the factors of safety decrease) therefore increasing the chance of overall slope failure.

Figures 8.9 and 8.10 show similar information for the Vajont slide. It is seen that although  $F_{is}$  is approximately 1.6 and  $F_{le}$  is approximately 1.1, a value of less than 1 is obtained with values of  $K$  greater than or equal to 1.5 and with failure originating from the top of the slope (mode 2).

Similarly, figures 8.11 and 8.12 describe the variation of the factor of safety with the abovementioned modes of progressive failure for the arbitrary slip circle number one. In this case,  $F_{is}$  is approximately 2.3 and  $F_{le}$  is approximately 1.26. Here, however, the curve of factor of safety values for failure starting at the top of the slope only reaches as low as 1 for values of  $K$  of 3.5 or over. Although such a state of initial stress may be rare, the analysis still demonstrates the principle that failures starting at the crest of the slope are critical and that the overall factor of safety can reduce to as low as 1, thereby initiating overall slope failure.

## 8.6 SUMMARY AND CONCLUSIONS.

From the results presented in section 8.2 it was clear that simulation of stress re-distribution following local failure and strain softening within limit equilibrium does not necessarily predict slope behaviour accurately. Considering case histories, the analyses were not fully successful in explaining how failure occurred. The modes of re-distribution of the excess stresses created as a result of local failure did produce additional local failures up to a point but did not really come close, in most cases, to causing overall failure. Primarily, this is because a uniform initial stress field is considered to exist and therefore few initial local failures occur.

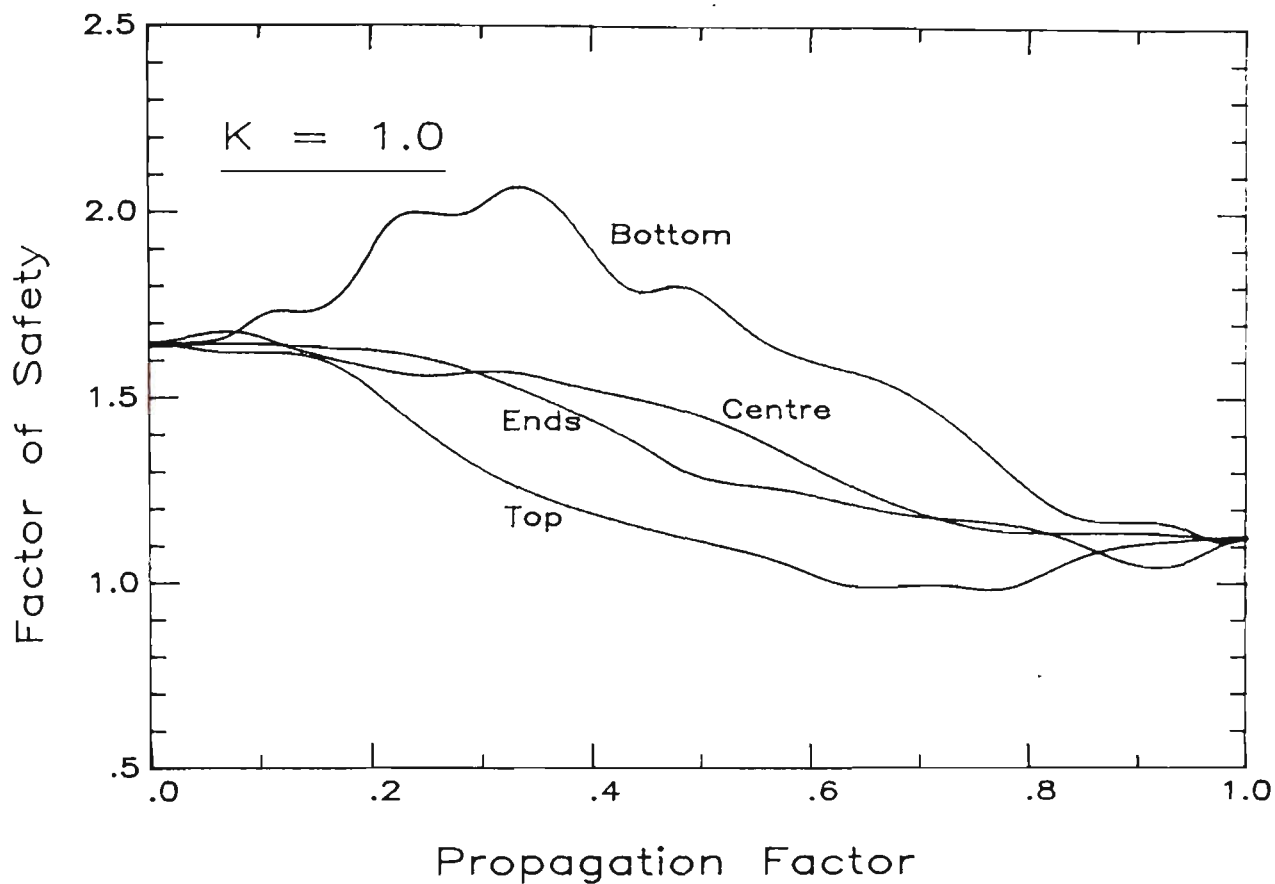


Figure 8.9 Variation in Factor of Safety with Different Modes of Failure Propagation (Vajont Slide).

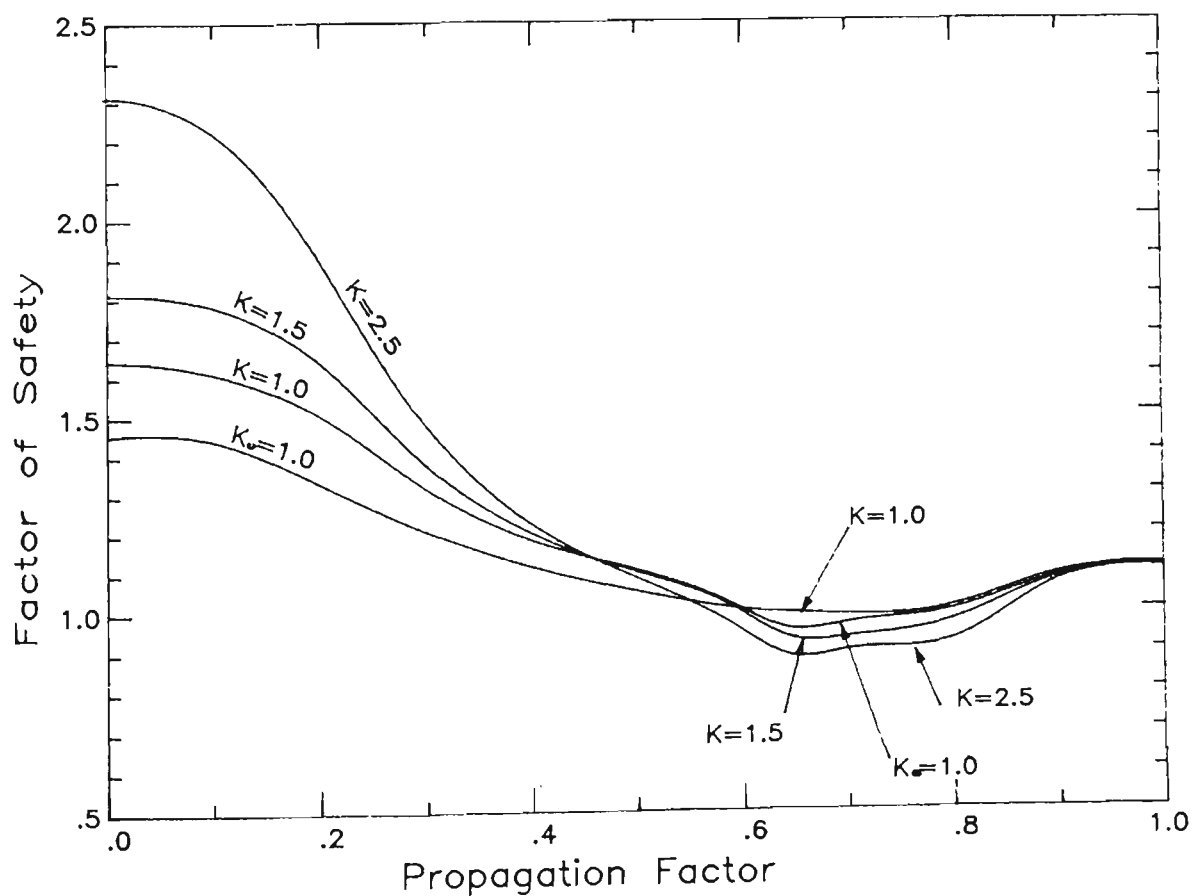


Figure 8.10 Variation in Factor of Safety for Different Values of  $K$  (Vajont Slide).

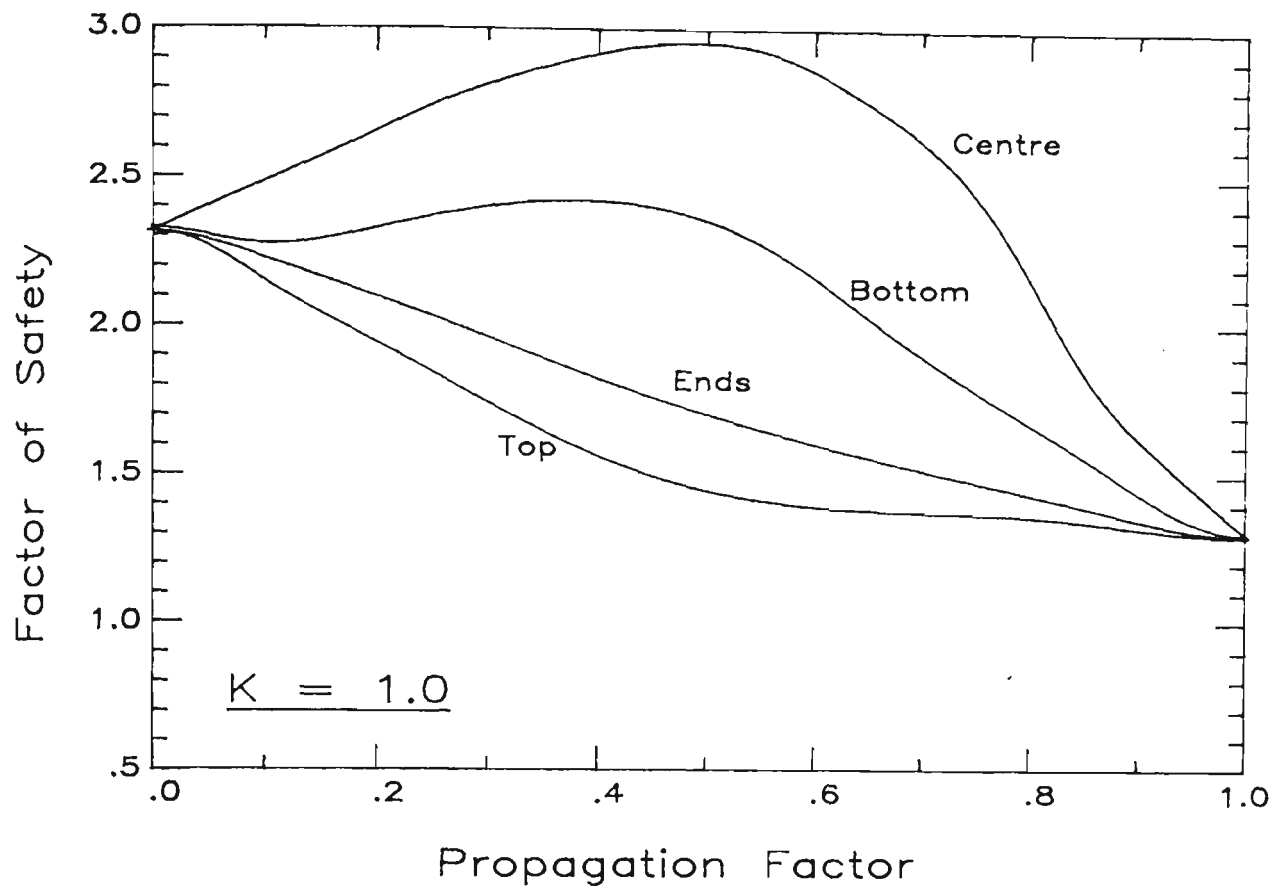


Figure 8.11 Variation in Factor of Safety with Different Modes of Failure Propagation (Hypothetical Slip 1).

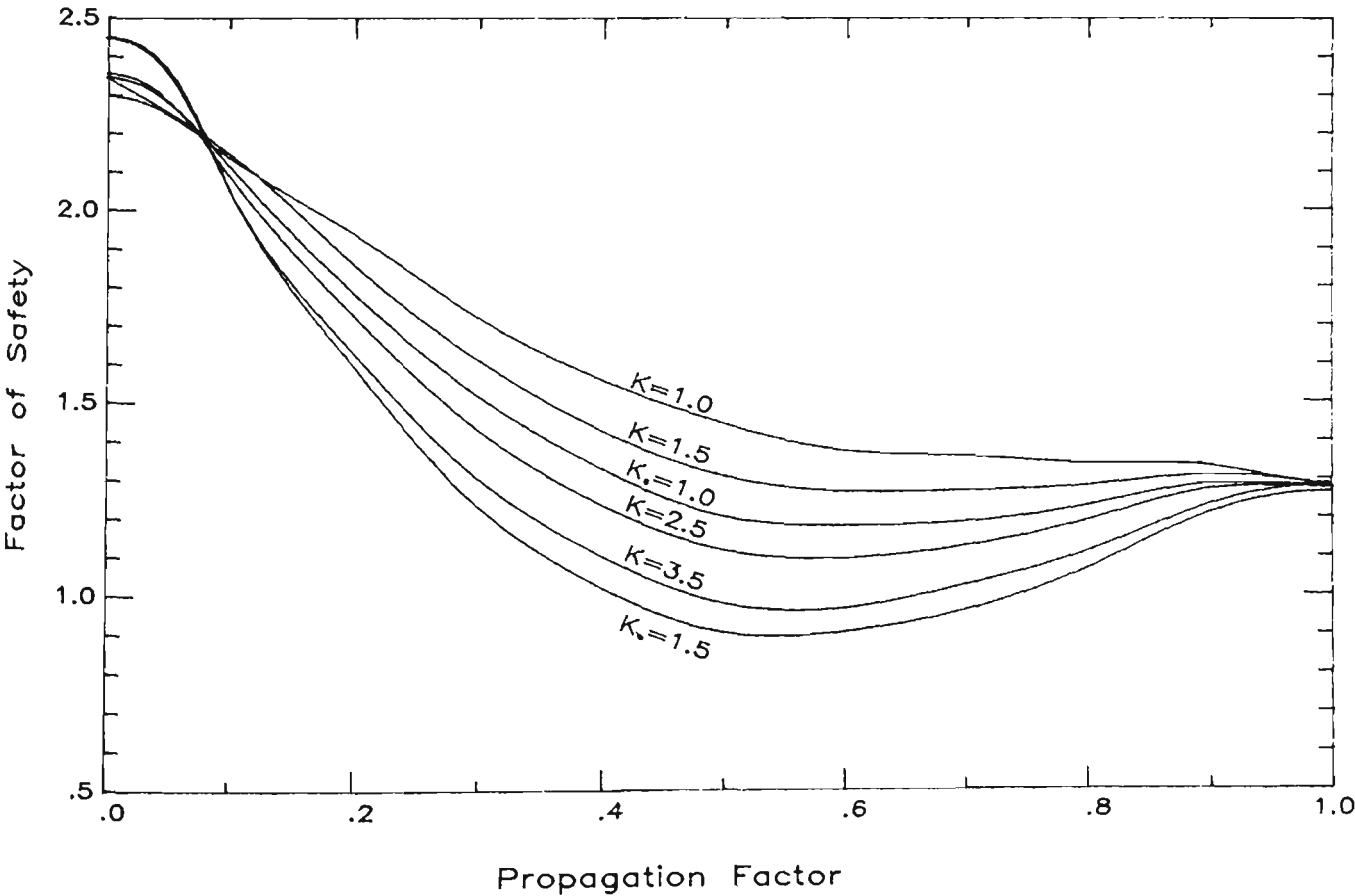


Figure 8.12 Variation in Factor of Safety for Different Values of K (Hypothetical Slip 1).

However, in the subsequent sections of this chapter, it was shown that for most case histories, if local failure was simulated as a progression from the initial stress state to a limiting equilibrium state, a stage was often reached where the overall factor of safety of the slope was reduced to a value less than or equal to 1, thus indicating overall slope failure. This occurred even though the factor of safety under both initial stress and limiting equilibrium conditions was above 1.

From the analyses made, it can be stated that progressive failure beginning at the crest of a slope and progressing down towards the toe can produce a situation where the overall factor of safety of the slope has reduced to less than or equal to 1 and thus slope failure is predicted, even if the values of  $F_{is}$  and  $F_{le}$  are both greater than 1. In some cases a conjugate stress ratio greater than 1 is required for this to occur. We can therefore say that, depending on the relationship between horizontal and vertical initial stresses in a slope, the type of progressive failure described above may explain, to a certain extent, why some slopes fail in spite of factors of safety greater than unity on the basis of conventional methods of analysis.

## CHAPTER 9

### SUMMARY AND CONCLUSIONS.

#### 9.1 INTRODUCTION.

The research reported in this thesis is primarily concerned with the simulation of progressive failure within a sloping soil mass considering alternative mechanisms of strain-softening and different modes of failure propagation. The studies have been carried out within a conventional deterministic framework and the basis for the investigations is the widely accepted limit equilibrium model. The methods reported here for analysis of progressive failure have been found suitable whether a simplified (Bishop type) or rigorous (Morgenstern-Price type) method of slices is used. However, most of the work has been carried out using the 'rigorous' approach associated with the well known Morgenstern-Price method of slope stability analysis. To the author's knowledge, this is the first time methods of analysis of progressive failure have been developed in this way and successfully implemented for a number of case histories.

The scope of the thesis is clearly outlined in chapter 1 (especially section 1.6) and conventional limit equilibrium methods of analysis have been discussed briefly in chapter 2.

#### 9.2 PROGRESSIVE FAILURE CONCEPTS.

In chapter 3, different interpretations of the term progressive failure were discussed. The relationship between any progressive failure mechanism and the concept of residual strength is of fundamental importance. At some stage during the progressive failure

process, the strength of the soil along the potential slip surface reduces from the peak value towards a residual (or fully softened) value. The manner and extent of this reduction has been a matter of some controversy.

The two most popular theories assume the following;

1. As local failure progresses and passes some location along a slip surface, the soil strength there will drop suddenly from the peak value to the residual value. Therefore, all points along the failure surface to which local failure has progressed will exhibit a residual or fully softened strength while all other points will still be at the peak value. In other words, this theory assumes a perfectly brittle material response.
2. As local failure progresses along the slip surface there will be segments of the surface where sufficient movement has taken place to reduce the strength to its residual value while other segments have suffered no movement (or local failure) and, therefore, are at the peak strength. The remaining parts of the slip surface would have values of shear strength varying between the lower limit of residual strength and the upper limit of peak strength.

The latter theory was postulated by Bishop [13] who defined a residual factor which varies along the slip surface and which denotes the proportional drop from the peak to the residual strength at any point along the surface. Bishop went on to suggest possible distributions of this residual factor, and hence of the shear strength along the slip surface, which indicate that progressive failure may start at the (a) top of the slope and progress downward, (b) toe and progress upward, or (c) both ends and progress inwards towards the centre.



### 9.3 RELATIONSHIP BETWEEN SHEAR STRENGTH DISTRIBUTION AND FACTOR OF SAFETY.

As reported in chapter 4, investigations were carried out to ascertain whether there was any relationship between the shear strength distribution existing along the slip surface and the calculated factor of safety of the soil mass. A number of distributions of the residual factor  $R_1$  was chosen to be used in conjunction with the limit equilibrium stability analysis. Although a wide range of  $R_1$  distributions was used, most of the distributions fell into two major groups:-

1. Failure starting from the bottom of the slope ( $R_1$  equal to 1 at toe and 0 at crest).
2. Failure starting from the crest of the slope ( $R_1$  equal to 1 at crest and 0 at toe).

The aim was to see whether some  $R_1$  distributions produced lower factors of safety (and therefore indicated a higher likelihood of failure) than others.

As it was not possible to directly set the shear strength values along the failure surface to match the chosen  $R_1$  distribution, it was decided to set the values of the shear strength parameters  $c'$  and  $\phi'$  to match this distribution. Expressions were derived for  $c'$  and  $\phi'$  in terms of the local residual factor (equations 4.6).

The Morgenstern-Price method of analysis was used as a basis for the simulation and calculation of the factor of safety. The calculated values of  $c'$  and  $\phi'$  were used in this analysis to arrive at a value for  $F$ . For some slopes with circular surfaces of sliding, the Bishop simplified method was also used.

The results obtained using the Morgenstern-Price method of analysis were tested for acceptability according to a number of acceptability criteria defined by Morgenstern and Price, Hamel [14] and other authors. These criteria were found to be, in general, too stringent and recommendations were made in this chapter as to their

modification.

Two computer programs were developed to perform the abovementioned analyses with the variable  $c'$  and  $\phi'$  distributions. Variations of these programs were developed to calculate the average shear strength along any potential failure surface.

Table 9.1 gives a summary of this simulation method and the computer programs used. The results obtained using this method showed that there was no correlation between the chosen  $R_1$  or shear strength distribution and the calculated factor of safety. The factor of safety was, however, found to be directly proportional to the value of the average shear strength along the slip surface. This relationship was found to be linear. In other words, it does not matter how the shear strength is distributed along the failure surface, it matters only what its average value is.

---

Table 9.1 Summary of Progressive Failure Simulation Methods Presented in Chapter 4.

---



---

Method:	Simulation of arbitrary decrease in shear strength parameters along slip surface.
Main Features:	<ul style="list-style-type: none"> <li>- allows different distributions of residual factor and therefore shear strength parameters.</li> <li>- calculates the average shear strength along the failure surface and the factor of safety of a slope corresponding to any arbitrary distribution of local residual factor.</li> </ul>
Section:	4.2.3
Programs:	MGSPROG, MGSDIST

---

#### 9.4 PROGRESSION OF FAILURE CONSIDERING STRAIN SOFTENING.

The mechanism of strain-softening and stress redistribution in slopes is considered in detail in chapters 5 and 6. Four methods developed for simulating progressive failure on the basis of these mechanisms have been presented in chapter 6.

Method 1 is based on the assumption that once local failure has occurred on the bases of one or more slices, the excess shear stress may be redistributed either uniformly or according to a linear function (with maximum near the failed slice) across the unfailed segments of the slip surface. Once a slice has failed locally, the shear strength parameters  $c$  and  $\phi$  on its base are assumed to have dropped to their residual values. The factor of safety is then found by dividing the sum of the resisting forces by the sum of the disturbing forces. The results of method 1 analyses showed that a linear function for the redistribution of excess shear stress leads to lower factors of safety than a uniform function. In some cases, however, little or no drop in factor of safety occurred as a result of redistribution of shear stress.

Method 2 is inherently similar to method 1 except that the factors of safety are determined by performing Morgenstern-price and Bishop simplified analyses on each case history considered. Residual values of the shear strength parameters were again used for failed slices in these analyses. In virtually all cases, the results obtained were almost identical to those obtained using method 1. The two simulation techniques induced the same amount of local failure and any discrepancies are due entirely to the differences in methods used to obtain the factor of safety.

Method 3 is different from methods 1 and 2 in so far as no assumption is made in advance regarding the manner in which excess shear stress will be redistributed. The mobilised shear force on each unfailed slice is recalculated after successive limit equilibrium analyses. After this, the excess shear force on each unfailed slice is determined. The total shear force tending to cause local failure on an unfailed slice is then calculated using equation (6.35) and all unfailed slices are again examined for local failure using equation

(6.36). For the case histories considered, this technique for simulating progressive failure was found to induce less local failures than the previous two methods. All factors of safety obtained were either equal to or greater than those obtained by methods 1 or 2 for a given case history.

Method 4 is different from method in that a quantity which has been termed the virtual weight of a soil slice is calculated during the iterative analysis process. This enables the excess mobilised shear force to be redistributed as in method 3. Results for the case histories considered showed even less tendency for local failure to occur than with method 3.

A summary of the four simulation methods used in chapter 6 is presented in table 9.2. The results obtained using these four methods showed that strain softening may be responsible for a certain amount of local failure leading to overall slope failure. In a number of cases, redistribution of excess shear stresses generated by local failure due to strain softening, reduced the factor of safety of the slope to below 1. In other cases, however, very little or no strain softening (and hence local failure) was obtained and therefore the factor of safety remained very near its peak value. This could have been due to the method of stress redistribution or to the geometry of these slopes as some of them fit into the category of slope geometries where strain softening by limit equilibrium is not readily achieved.

---

Table 9.2 Summary of Progressive Failure Simulation Methods Presented in Chapter 6.

---



---

Method 1:           Simulation of redistribution of excess shear stress to study propagation of local failure along slip surface. This method is based on a very simplified limit equilibrium approach.

Main Features:   - allows distribution of excess shear either uniformly or linearly (maximum near last failed slice) over unfailed slices.

- mobilised shear force attains its residual value (i.e.  $c$  and  $\phi$  drop to residual) after local failure.
- if slice does not fail it is combined with an adjacent failed slice to see if combined failure will occur.
- $F$  is found by summation of resisting and disturbing forces as per equation (6.17).

Section: 6.2

Programs: STRAIN1

---

Method 2: Simulation of redistribution of excess shear stress to study propagation of local failure along slip surface as in method 1 but using more sophisticated methods of analysis to calculate factor of safety (i.e. based on Morgenstern-Price and Bishop type methods of slices).

Main Features: -  $F$  is found by both the Bishop simplified and the Morgenstern-Price methods of analysis.

Section: 6.3

Programs: BSTRAIN2, MPSTRAIN2

---

Method 3: Simulation of redistribution of excess shear stress by recalculation of mobilised shear force.

Main Features: -  $F$  is found by both the Bishop simplified and the Morgenstern-Price methods of analysis.

- mobilised shear force on unfailed slice bases is recalculated after stress redistribution.
- successive analyses are required.
- no assumption about the type of redistribution of excess shear stress is made in advance. This happens automatically.

Section: 6.4

Programs:           BSTRAIN3, MPSTRAIN3

---

Method 4:           Simulation of redistribution of excess normal and shear forces using the concept of virtual weight.

Main Features:   - F is found by both the Bishop simplified and the Morgenstern-Price methods of analysis.  
                   - takes into account both shear and normal forces on slice bases.  
                   - a quantity designated the 'virtual weight' of each slice is calculated and local failure and excess shear redistribution are related to this changing quantity.

Section:           6.5

Programs:           BSTRAIN4, MPSTRAIN4

---

## 9.5 INCORPORATION OF INITIAL STRESSES.

In chapter 7, works by various authors were presented concerning the concept of initial stress. Although a number of different aspects of initial stress were discussed, it was generally noted that the ratio of horizontal stresses to vertical effective stresses measured in field tests could be as high as 2.5 or 3. Expressions were presented for the calculation of the normal and shear initial stresses acting on a slip surface segment of arbitrary inclination.

A number of simulation methods were introduced in chapter 8 which incorporated the initial stress concept into the propagation of local failure. The first of these methods is concerned with simulation of progressive failure considering local failure and stress redistribution as in method 2 of chapter 6 except that the initial stress state existing in the slope prior to failure is taken into

consideration. Basically, the method is identical to method 2 of chapter 6 except that the normal and shear forces on the bases of unfailed slices were calculated using initial stress expressions given in equations (8.1) and (8.2). The normal and shear forces on bases of failed slices were calculated using limit equilibrium expressions given in equations (6.9) and (6.11). The factor of safety was calculated using equation (8.3). It was shown that in cases of initial stress corresponding to a conjugate stress ratio greater than say 1.5 there was a significant reduction in the final factor of safety, sometimes to a value below 1. However, little additional strain softening occurred and the reduction in overall factor of safety was probably due only to the increased shear stresses in the slope resulting from higher values of  $K$ . This was supported by the fact that those slopes where little or no strain softening occurred using the simulation methods of chapter 6 still exhibited a similar extent of strain softening.

The situation was then considered where local failure was assumed to have extended beyond the limits achieved in the above procedures. The slope was initially assumed to be totally under initial stress conditions and as failure progressed, areas which had failed locally were then assumed to be in limiting equilibrium. A limit equilibrium analysis using the Morgenstern-Price method was carried out on the failed section of the slope. From this, the normal and shear forces on the failed slices were calculated using equations (8.8) and (8.10). For the unfailed slices, the normal and shear forces were calculated using the initial stress equations mentioned previously. The overall factor of safety for the entire slope was then calculated using equation (8.7). The interaction between the two masses of changing size was considered at each stage.

The possibility of failure starting at either the crest, toe, centre or both ends of the slope was considered. It was found that, in virtually all cases, local failure starting at the crest of the slope was potentially more dangerous than from other areas. The factor of safety reduced, as failure progressed, to a minimum value. This value, especially at higher values of  $K$  was usually less than 1 which indicated that if conditions favour the progression of local failure along an assumed slip surface, a point may be reached where

the overall factor of safety is less than or equal to 1 and the slope may fail.

Table 9.3 summarises the two simulation methods presented in chapter 8.

---

Table 9.3 Summary of Progressive Failure Simulation Methods Presented in Chapter 8.

---

Method 1: Simulation of progressive failure considering both strain softening and initial stresses.

Main Features:

- extension of method 2 from chapter 6 (see table 9.2).
- includes initial stress considerations.
- on unfailed slice bases, normal and shear forces are calculated using initial stress expressions (equations (8.1) and (8.2)).
- on failed slice bases, normal and shear stresses are calculated using limit equilibrium based expressions (equations (6.9) and (6.11)).
- $F$  is found from equation (8.3).

Section: 8.2

Programs: BSTRAIN2 (modified to incorporate initial stress considerations).

---

Method 2: Simulation of progressive failure by sequential local failure of soil slices.

Main Features:

- assumes that the initial stress state changes to a simple gravitational stress field progressively along the potential slip surface.
- assumes an imaginary boundary to separate the initial stress (unfailed) and the limit equilibrium (failed) sections of the slope.



- the overall factor of safety is calculated according to equation (8.7).
- normal and shear stresses on bases of slices in the unfailed section are found using initial stress equations.
- those on slice bases in the failed section are found by performing a Morgenstern-Price limit equilibrium analysis on the failed section and then obtaining the stresses using equations (8.8) and (8.10).

Section:           8.3, 8.5

Programs:         MGSINIT2

=====

## 9.6 CONCLUDING REMARKS.

In this thesis a number of methods of slope analysis have been presented which were developed to simulate progressive failure and to relate the extent of strain softening and stress redistribution to the overall factor of safety of a soil slope. The methods have been successfully implemented and used for the analysis of a number of case histories. In some methods an initial stress field is also taken into consideration.

The investigations reported in this thesis show that progressive failure may lead to a significant drop in the overall safety factor for some slopes but not for others. The values of shear strength parameters and the extent of soil brittleness are important but are not the only factors which determine the likelihood of failure progression. The slope and slip surface geometry may have an important influence on the extent to which redistribution of excess shear stress will lead to new local failures. An initial stress field is important and the higher the value of the conjugate stress ratio  $K$ , the lower is the value of the minimum safety factor during progression.

There is no single method of analysis which will be suitable for all situations. However, the methods developed here offer a wide choice for the simulation of progressive failure and the selection of an appropriate method would be based on the type of problem, the available data and the actual requirements of analysis.

The work reported in this thesis has also highlighted the importance of acceptability criteria for rigorous methods of analysis. The linear relationship between average shear strength along the slip surface and the factor of safety has been confirmed for a very wide range of conditions. Such a relationship may, in itself, provide the best acceptability criteria.

## APPENDIX A

### DESCRIPTION OF SLOPES USED IN CASE HISTORIES.

This appendix contains descriptions of all the soil or rock slopes referred to within this text and used as case histories in the validation of the various methods of analysis presented.

#### A.1 NORTHOLT SLIP IN CUTTING.

The analysis of a slip in a cutting at Northolt, England was carried out by Skempton, Henkel and Delory in 1955 and described by Henkel in 1957 [48] and Skempton in 1964 [88]. The excavation was made in 1936 and occurred 19 years later in 1955.

The analysis was made on a circular arc approximating to the observed slip surface. The average values of peak and residual strength were found to be 28.5 kPa and 10.3 kPa respectively. The average shear stress, and hence, the average shear strength acting along the slip surface at the time of failure was 18.2 kPa.

Consequently, Skempton calculated the value of his residual factor,  $R$  (see chapter 3), to be 0.56 and the strength parameters consistent with a factor of safety of 1.0 were found to be  $c' = 6.7$  kPa and  $\phi' = 18^\circ$ .

The Northolt slip is situated in London clay. Fissures and joints and occasional slickensides can be seen throughout the full depth of the London clay but such features are much more conspicuous in the weathered zone, characterised by the brown colour of the clay (in contrast to the blue or slatey grey colour of the unweathered

clay). These findings plus the fact that the Northolt slip is in cutting point to the clay being an overconsolidated, stiff, fissured clay.

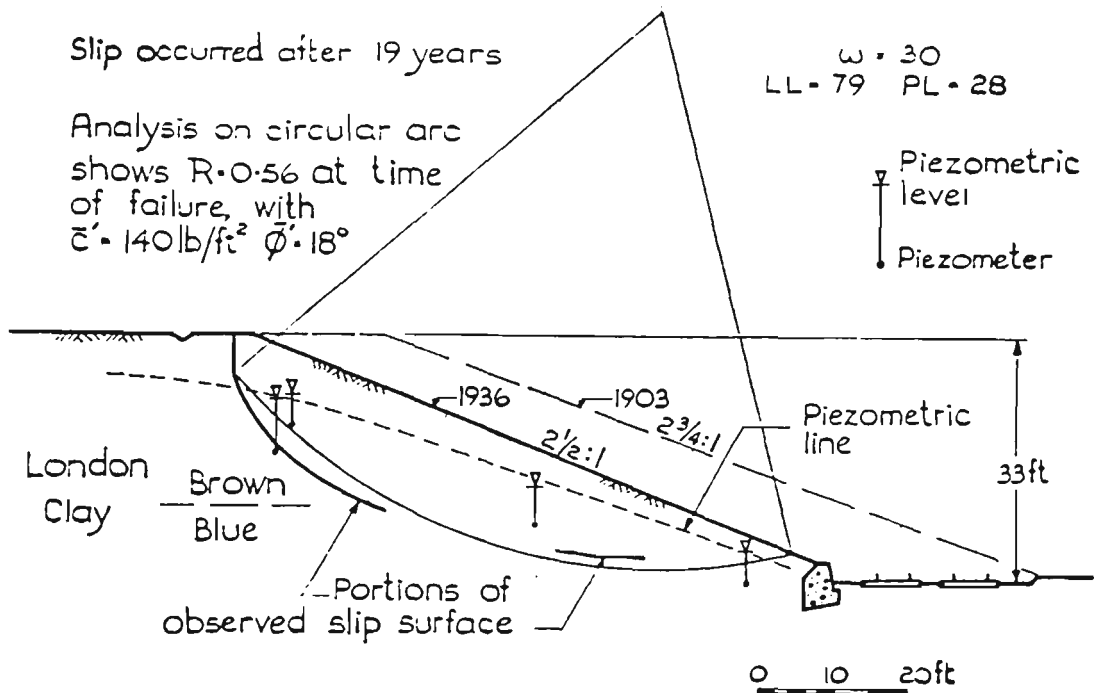


Figure A.1 Northolt Slip in Cutting

The cutting has a maximum depth of 10.06 metres and was made with 2.5:1 slopes rising from a small toe wall about 1 metre high. A cross-section of the Northolt slip is shown in figure A.1. For the purposes of the research, it is necessary to obtain the peak and residual shear strength parameters for the soil in the slope, as well as other necessary soil data.

- The slope geometry is taken from Skempton [88].
- The unit weight  $\gamma$  for the soil is given by Law and Lumb [58] as  $18.8 \text{ kN/m}^3$ .

- The peak value of the cohesion intercept,  $c'_p$ , is given as 250 lb/ft<sup>2</sup> (or 11.97 kPa), for weathered London clay by Skempton, and 1.6 tons/m<sup>2</sup> (or 15.94 kPa), for London clay by Bjerrum [18]. There seems to be some discrepancy between the value of the cohesion intercept for weathered London clay given by Henkel and Law and Lumb and that given by Skempton and Bjerrum. For this research, the former value of 12 kPa is assumed.
- The peak value of the angle of shearing resistance is given as 20°.
- The residual value of the angle of shearing resistance is given by Skempton and Bjerrum as 16°. Law and Lumb, however, assumed it to be equal to the peak value of 20°.
- The pore-pressure ratio is taken as 0.25 by Law and Lumb. Skempton [88], on the other hand, presented an outline for the phreatic surface and this can be seen in figure A.1. By making a back-analysis of this phreatic surface, a pore-pressure ratio of 0.34 is arrived at.

Summarising the above soil data, we obtain,

Assumed soil parameters.

$$\begin{aligned}
 \gamma &= 18.8 \text{ kN/m}^3 \\
 c'_p &= 12.0 \text{ kPa} \\
 c'_r &= 0 \\
 \phi'_p &= 20^\circ \\
 \phi'_r &= 16^\circ \\
 r_u &= 0.34 \text{ or phreatic surface given.}
 \end{aligned}$$

Parameters used by Law and Lumb [58].

$$\begin{aligned}
 \phi'_r &= 20^\circ \\
 r_u &= 0.25
 \end{aligned}$$

## A.2 SELSET LANDSLIDE.

The Selset slide took place in a boulder clay slope of the River Lune Valley in north Yorkshire, England. The boulder clay was remarkably uniform, without fissures or joints and showed little, if any, signs of weathering, except in the very shallow zone of seasonal variations [88]. Skempton also noted that, while the location of the slip surface was not determined, the tension crack near the top of the slope was clearly visible. Figure A.2 shows a cross-section of the Selset landslide (taken from Skempton's paper) with a typical slip circle.

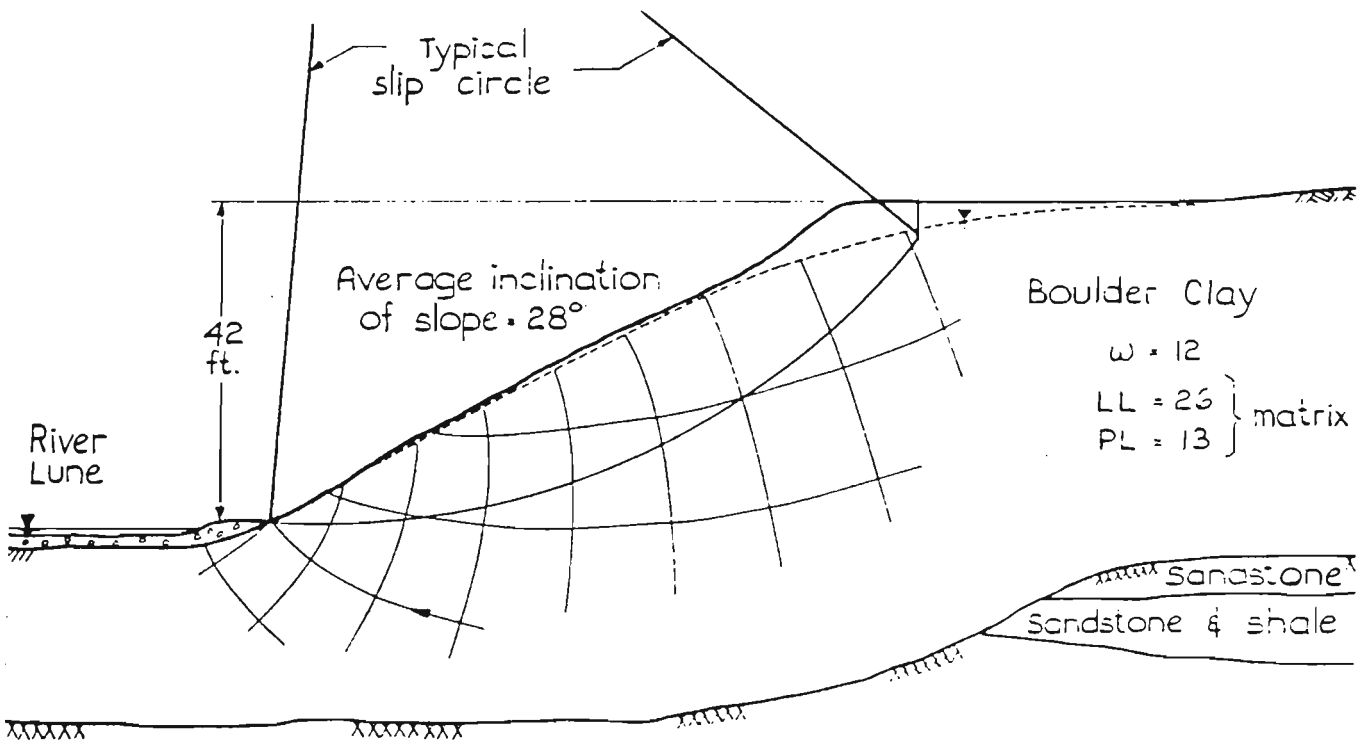


Figure A.2 Selset Landslide (Skempton)

Following is a summary of soil parameters obtained for the slope.

$$\gamma = 21.8 \text{ kN/m}^3$$

$$c'_p = 8.62 \text{ kPa} \quad (\text{Skempton, Law and Lumb})$$

$$c'_r = 0 \quad (\text{Skempton, Law and Lumb})$$

$$\begin{aligned}
 \phi'_p &= 32^\circ && \text{(Skempton, Law and Lumb)} \\
 \phi'_r &= 30^\circ && \text{(Skempton)} \\
 r_u &\text{ obtained from phreatic surface} && \text{(Skempton)} \\
 \phi'_r &= 32^\circ && \text{(Law and Lumb)} \\
 r_u &= 0.35 && \text{(Law and Lumb)}
 \end{aligned}$$

### A.3 SUDBURY HILL SLIP IN CUTTING.

The Sudbury Hill slip took place in 1949 in weathered London clay in a cutting excavated at Sudbury Hill in 1900 [88]. Figure A.3 (again taken from Skempton's paper), shows a cross-section of the slip, with the slope profile after failure indicated by the dashed line.

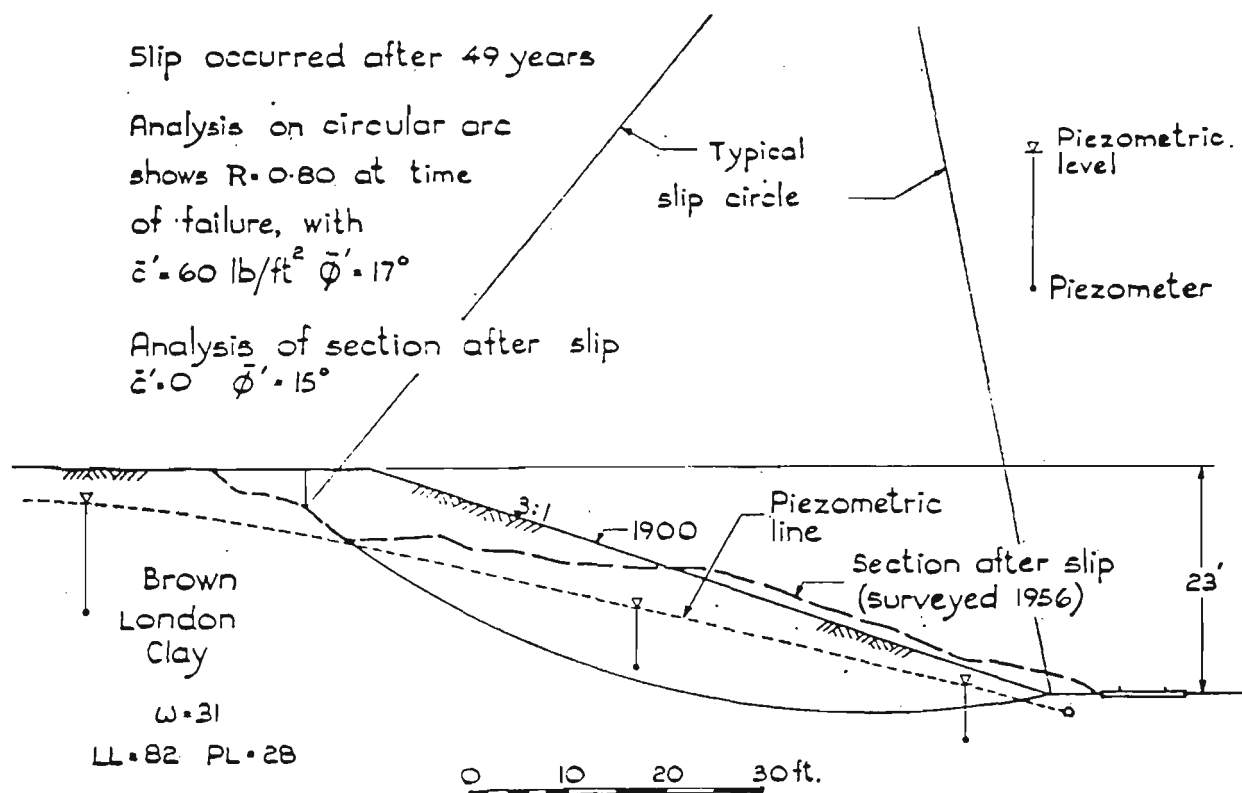


Figure A.3 Sudbury Hill Slip in Cutting

The following is a summary of soil parameters obtained for the slope.

$$\gamma = 18.8 \text{ kN/m}^3$$

$$c'_p = 12.0 \text{ kPa}$$

$$\phi'_p = 20^\circ$$

$$\phi'_r = 16^\circ \quad (\text{Skempton, Bjerrum})$$

$$r_u = 0.30 \text{ (Law and Lumb, Delory [39], James [49])}$$

Phreatic surface given by Skempton [88].

#### A.4 THE JACKFIELD SLIDE.

This slide, which took place in England in 1952, exhibited a very small rate of advance and was preceded by creep movements. Movements were first noticed in 1950, continued in 1951 and developed alarmingly during January of 1951 [18]. The total downhill displacement amounted to 18.3 metres. The slide had the characteristic shape of a flake with the dimensions 198 metres by 213 metres and the average depth of the slip plane was 5.5 metres.

According to Bjerrum [18], the slide was confined wholly within the upper zone of disintegrated and weathered clay. The sliding surface ran parallel to the slope and followed closely the boundary of the lower intact shale. It was found that the failure zone consisted of a soft clay layer only 5 centimetres thick.

Both Bjerrum [18] and Skempton [88] remarked that the shear stresses along the failure surface due to gravity forces were well below the drained peak shear strength of the clay and practically equal to the residual shear strength. Bjerrum stated that it was clear that the shear strength of the clay had been gradually exceeded by a mechanism of progressive failure.

Figure A.4, taken from Bjerrum's paper [18], shows a cross-section of the Jackfield slide.

The following soil data was obtained from Skempton [88] and Bjerrum [18].



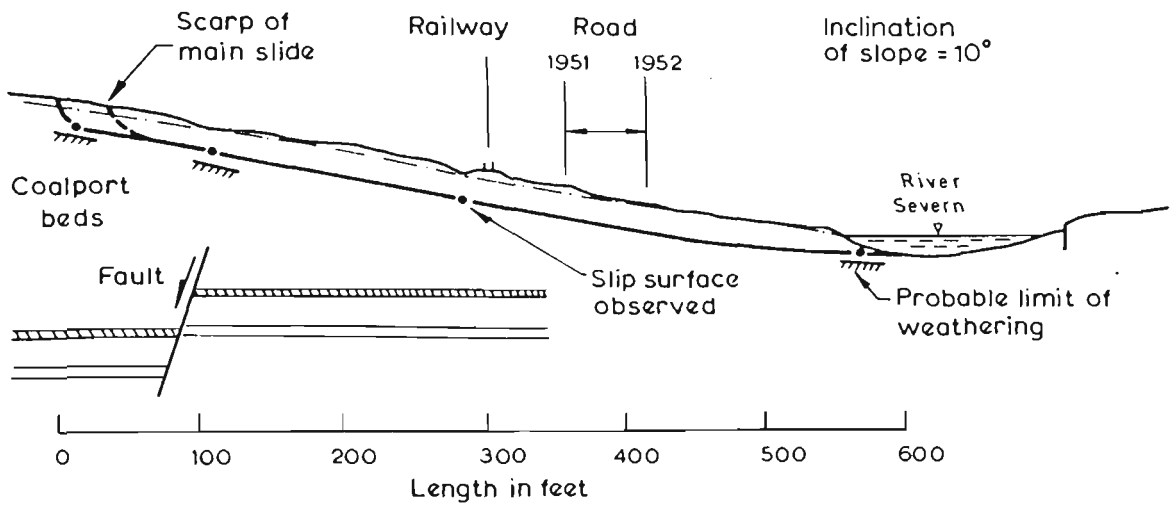


Figure A.4 Jackfield Slide

$$\begin{aligned}
 \gamma &= 19.32 \text{ kN/m}^3 && \text{(assumed)} \\
 c'_p &= 10.53 \text{ kPa (Skempton) and } 10.96 \text{ kPa (Bjerrum)} \\
 &= 10.75 \text{ kPa (average assumed value)} \\
 c'_r &= 0 \\
 \phi'_p &= 25^\circ \\
 \phi'_r &= 19^\circ \\
 \text{Phreatic surface is given (see figure A.4)}
 \end{aligned}$$

#### A.5 THE BALGHEIM SLIDE.

The slide at Balgheim, Germany, in 1957 took place on a gentle slope in the upper, weathered zone of heavily over-consolidated shales with strong diagenetic bonds (according to Bjerrum [18]). The slide had the characteristics of a flake with a large extent, compared to the thickness. It was the result of an excavation of a trench for a

water main and had occurred a few days after the excavation. The dimensions of the slide are about 30 metres by 60 metres and the thickness of the flake is about 4.3 metres. Figure A.5 shows the cross-section of the slide (taken from Bjerrum's paper).

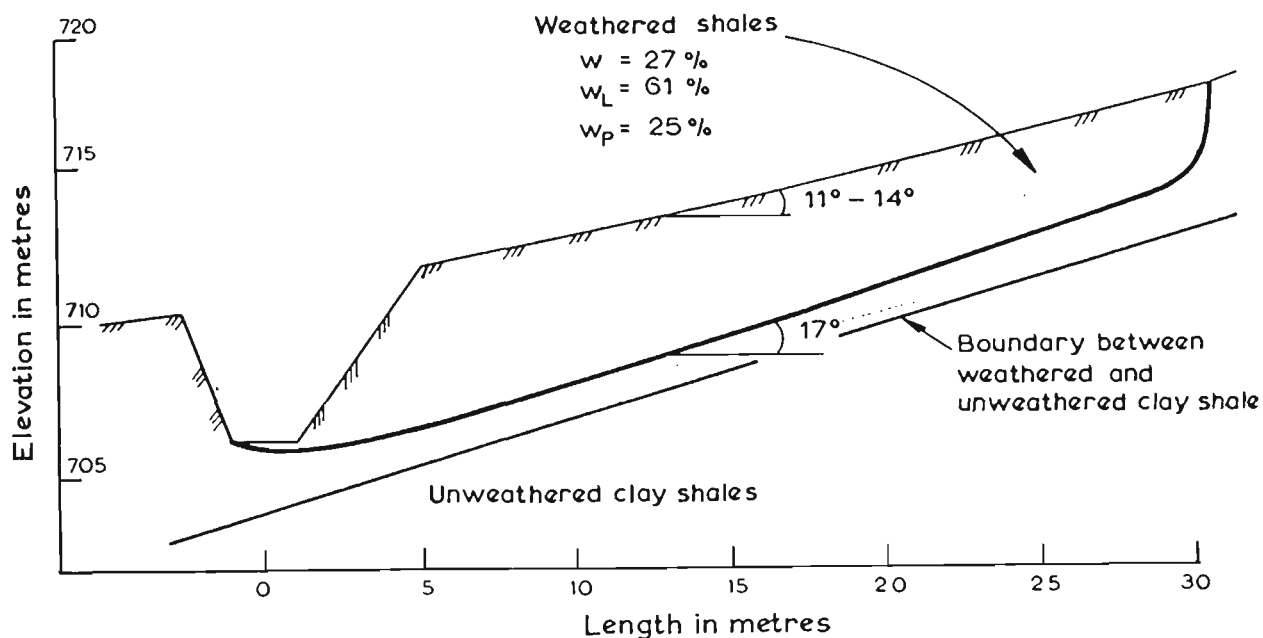


Figure A.5 Balgheim Slide

The following is a summary of the soil data used for the Balgheim slide.

$$\begin{aligned}
 \gamma &= 20 \text{ kN/m}^3 && \text{(assumed)} \\
 c'_p &= 15 \text{ kPa} && \text{(Bjerrum)} \\
 c'_r &= 0 && \text{(Bjerrum)} \\
 \phi'_p &= 18^\circ && \text{(Bjerrum)} \\
 \phi'_r &= 17^\circ && \text{(Bjerrum)} \\
 r_u &= 0.3 && \text{(assumed)}
 \end{aligned}$$

## A.6 THE VAJONT SLIDE.

The Vajont slide is a well known slide which occurred in Italy in 1963 and has been analysed and documented by various authors. It involved a mass of rock having a volume of about 250 million cubic metres, which plunged into the Piave River in Italy on the upstream slide of the Vajont dam.

Much discussion has been made regarding the presence of clay layers to account for the low  $\phi$  values of the order of  $20^\circ$ . Broilli [21], found that clay seams of considerable extent were not present and that failure occurred mainly in the limestones, for which residual  $\phi$  values below  $28^\circ$ , have never been measured around the world [64].

Lo, Lee and Gelinas [64], carried out a stability analysis using a  $\phi_r$  value of  $28^\circ$  and a  $c_r$  value of 0.

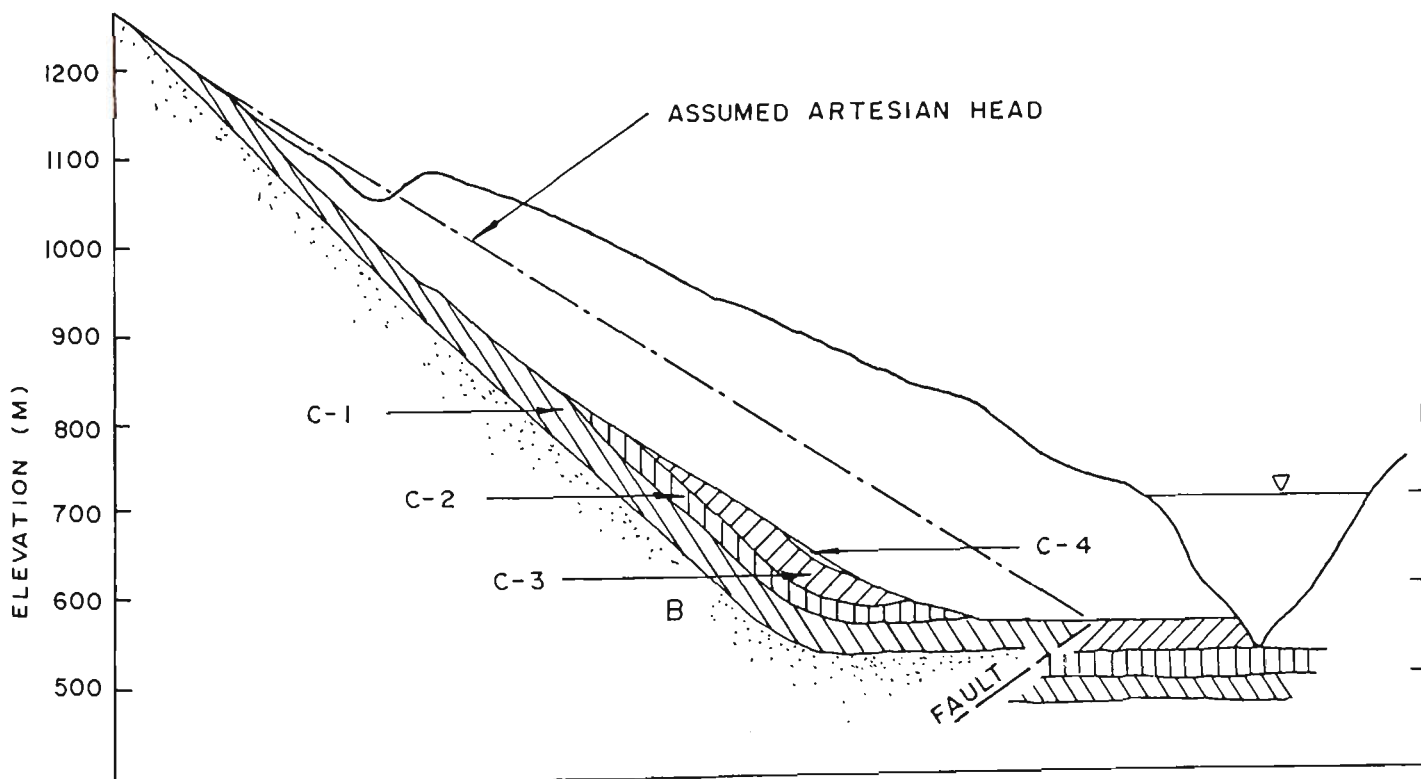


Figure A.6 Vajont Slide Eastern Central Slope

Various cross-sections of this massive slide were analysed by Lo, Lee and Gelinas, but for the purpose of this research, only the eastern-central slope designated as section E-E by Lo, Lee and Gelinas will be considered. This cross-section is shown in figure A.6.

The soil parameters associated with the Vajont slide are shown below,

$$\gamma = 18.8 \text{ kN/m}^3$$

$$c'_p = 6.7 \text{ kPa}$$

$$c'_r = 0$$

$$\phi'_p = 35^\circ$$

$$\phi'_r = 28^\circ$$

Phreatic surface given (Lo, Lee, Gelinas)

#### A.7 THE SASKATCHEWAN SLIDE.

The slide at South Saskatchewan in Canada, is one of the best documented slides in weathered clay. It is one of about 60 closely studied cases, in which the majority of the slides (about 55%), had occurred in the weathered zone of very stiff clays or clay shales, that is, in clays with strong, diagenetic bonds (Bjerrum [18]). Bjerrum stated that this fact seems to prove that, this type of clay has the greatest potential for the development of progressive slope failures, if subjected to disintegration.

Figure A.7 shows a cross-section of the Saskatchewan slide (obtained from Bjerrum [18]).

The soil parameters for the slope are given as,

$$\gamma = 20 \text{ kNm/m}^3 \quad (\text{assumed})$$

$$c'_p = 40.0 \text{ kPa} \quad (\text{Bjerrum})$$

$$c'_r = 0 \quad (\text{Bjerrum})$$

$$\phi'_p = 20^\circ \quad (\text{Bjerrum})$$

$$\phi'_r = 6^\circ \quad (\text{Bjerrum})$$

A phreatic surface is given as shown in figure A.7

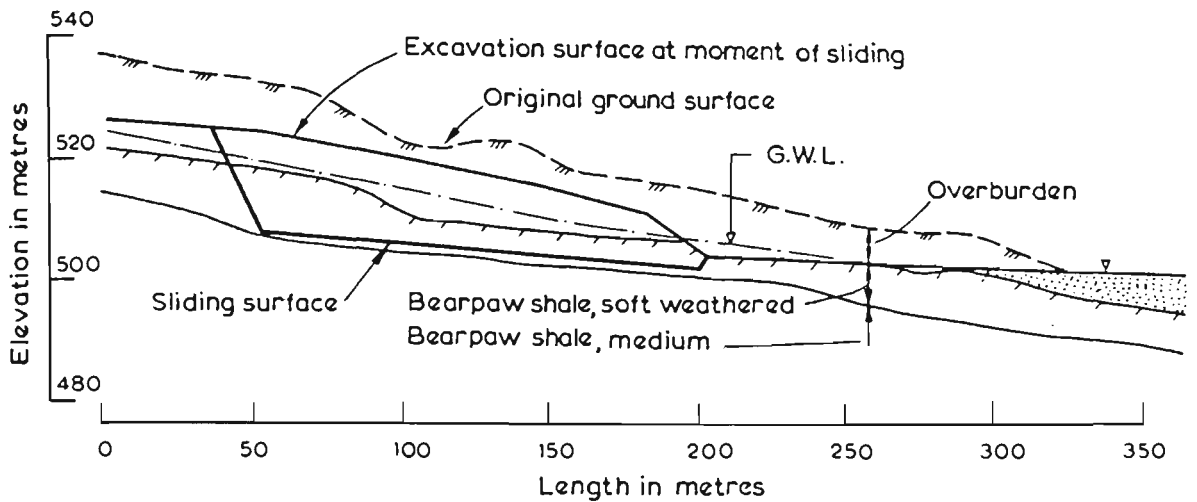


Figure A.7 Saskatchewan Slide

#### A.8 THE BRILLIANT CUT SLIDE.

The Brilliant Cut slide is described by Ackenheil [1] and again described and analysed by Hamel [46],[45]. The failure surface of the Brilliant Cut slide passed through a bed of soft clay and indurated rock to an open vertical joint in the overlying shale. The slide was triggered by high water pressures in the slope. Natural drainage outlets at the face of the slope were plugged by ice and the open joint was probably full of water [45]. The slope cross-section is shown in figure A.8.

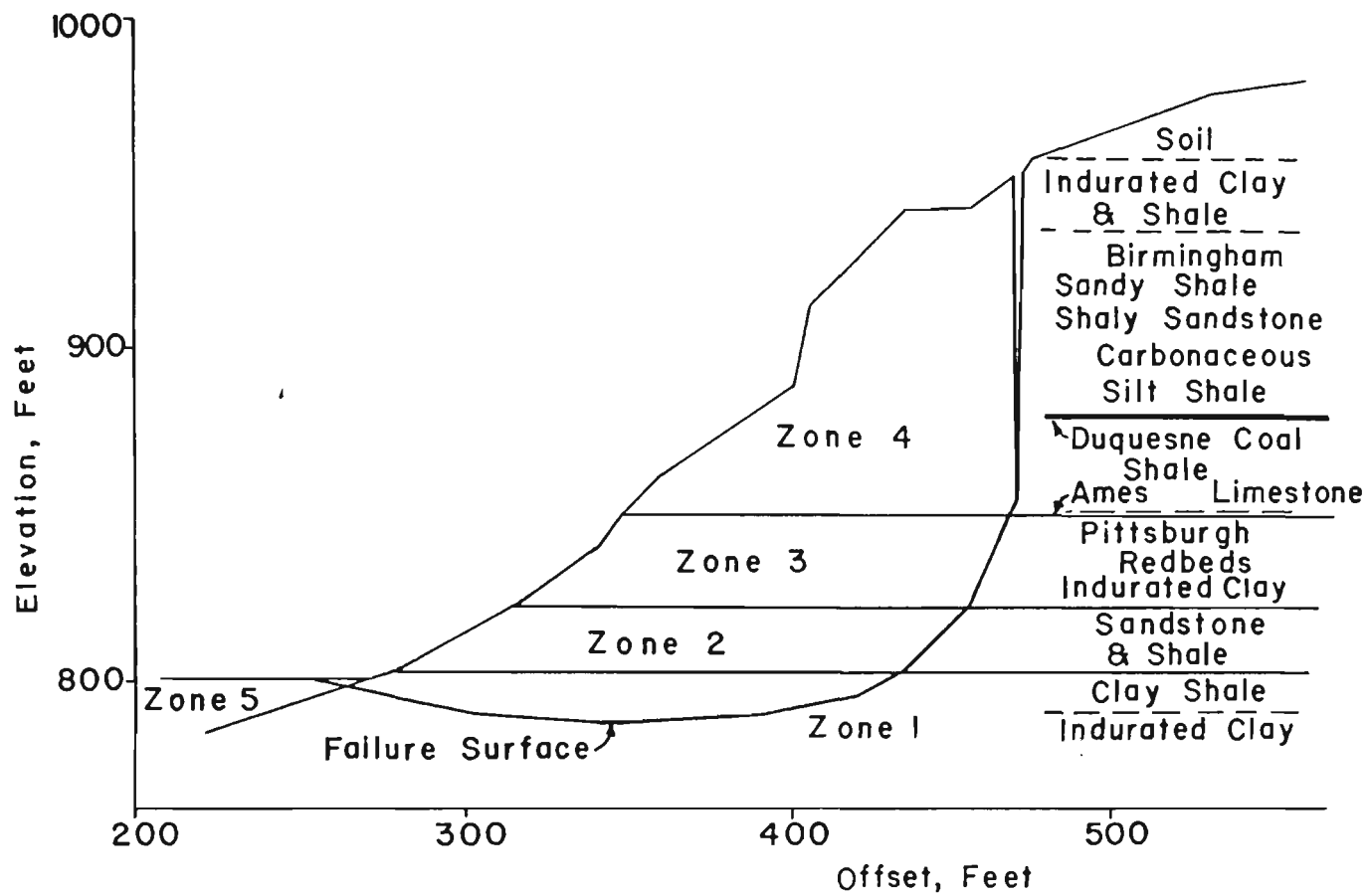


Figure A.8 Brilliant Cut Slide

The parameters for the five soil (or rock) layers are as shown below.

Material	$\gamma$	$c'_p$	$c'_r$	$\phi'_p$	$\phi'_r$	$r_u$
1	25.13	0.	0.	32°	15°	.39
2	25.13	95.8	0.	35°	20°	.39
3	25.13	47.9	0.	28°	12°	.39
4	25.13	95.8	0.	35°	15°	
5	25.13	0.	0.	30°	18°	

NOTE: The units for  $\gamma$  are kN/m<sup>3</sup> and those for  $c'$  are kPa. Also, the values of  $r_u$  for materials 4 and 5 are obtained from the phreatic surface.

### A.9 HYPOTHETICAL SLIP NUMBER 1.

An inspection of the slope profiles described in this section will show various irregularities in the slope geometries. These geometric irregularities may be the cause of unexpected results when performing stability analyses on the slopes. Therefore, the following hypothetical slope has been constructed with the aim of obtaining some stability analysis results which are free from the effects of geometric irregularities. The soil mass consists of a simple slope uniformly inclined at an angle of  $30^\circ$  to the horizontal as shown in figure A.9.

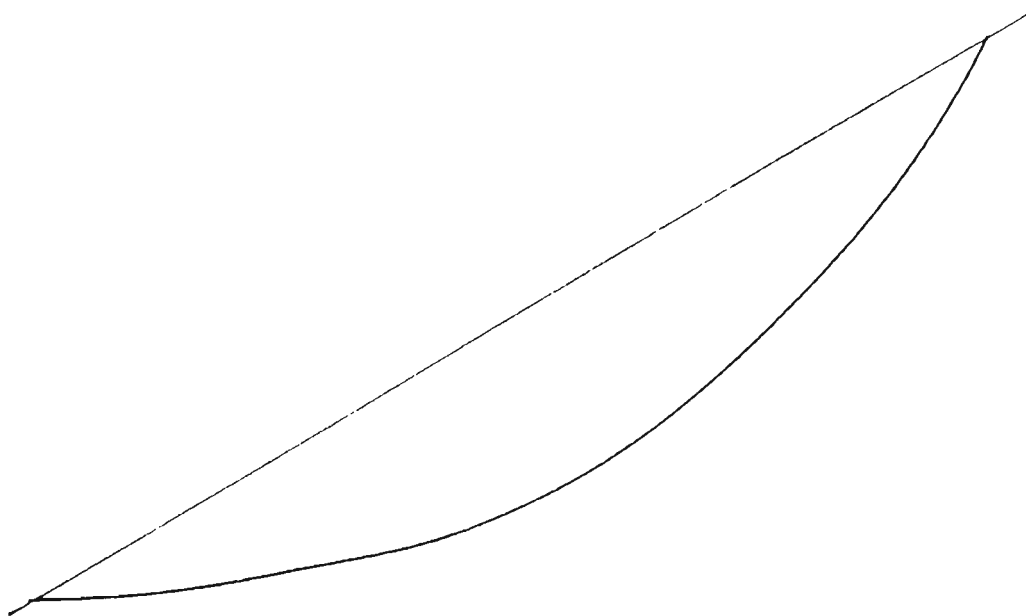


Figure A.9 Hypothetical Slip Number 1

The surface of sliding is assumed to be circular, with a radius  $R$  of 3.05 metres. For simplicity, the soil is assumed to be homogeneous and the following soil properties assumed to be true for the entire mass. A second reason for assuming a circular failure surface is, to test the accuracy of Bishop's simplified method in progressive failure

simulation techniques, described in this text.

The soil and slope parameters are assumed to be as follows.

$$\begin{aligned}\gamma &= 18.8 \text{ kN/m}^3 \\ c'_p &= 6 \text{ kPa} \\ c'_r &= 0 \\ \phi'_p &= 26^\circ \\ \phi'_r &= 22^\circ \\ r_u &= 0\end{aligned}$$

#### A.10 HYPOTHETICAL SLIP NUMBER 2.

For reasons similar to those described above, a second hypothetical soil mass is described here. In this case, however, a planar failure surface is chosen. This planar (actually bi-planar) surface and the slope profile, are shown in figure A.10.

The assumed soil parameters associated with this soil mass are as given below.

$$\begin{aligned}\gamma &= 20 \text{ kN/m}^3 \\ c'_p &= 12.0 \text{ kPa} \\ c'_r &= 0 \\ \phi'_p &= 22^\circ \\ \phi'_r &= 18^\circ \\ r_u &= 0.32\end{aligned}$$



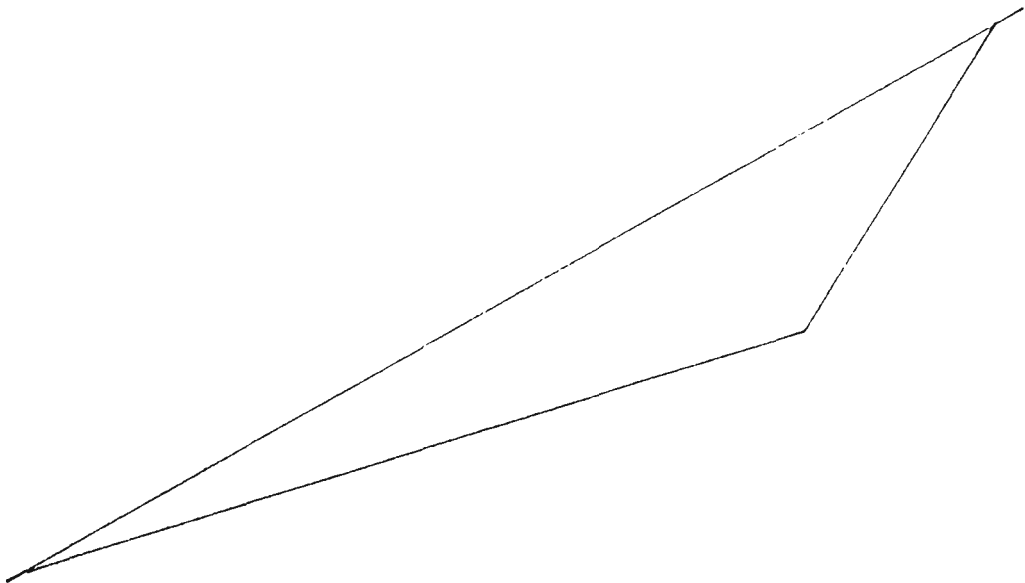
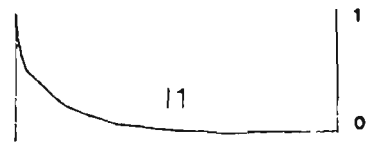
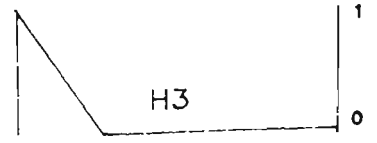
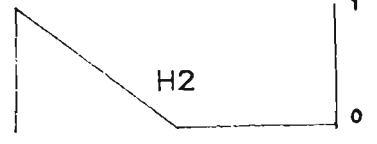
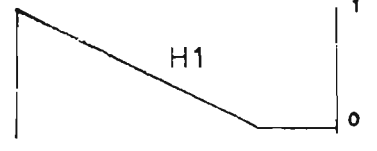
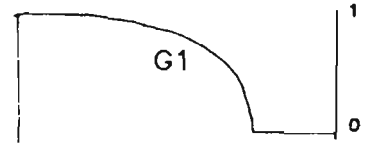
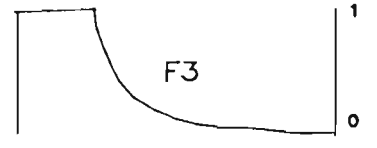
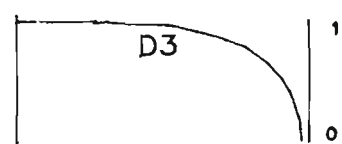
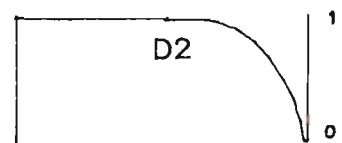
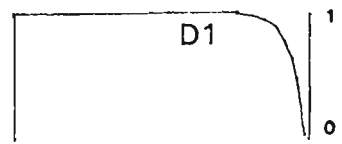
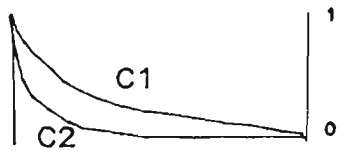
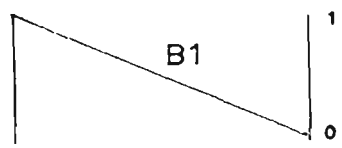
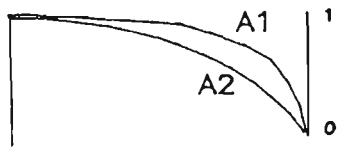


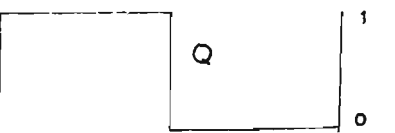
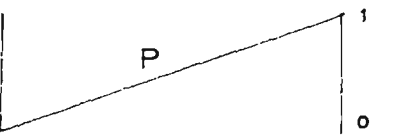
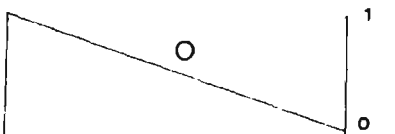
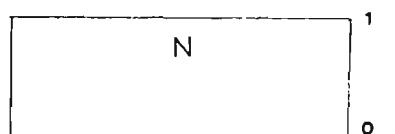
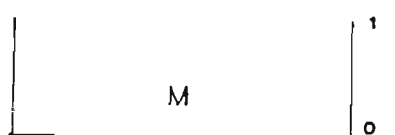
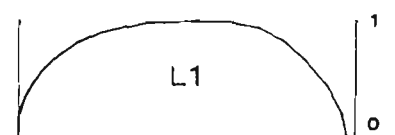
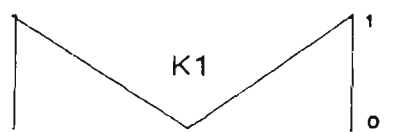
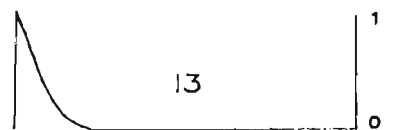
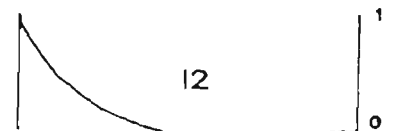
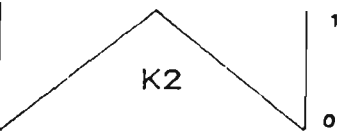
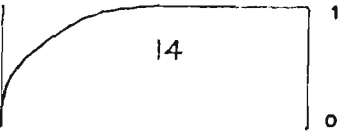
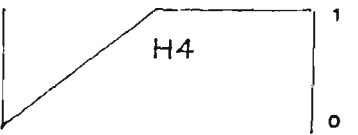
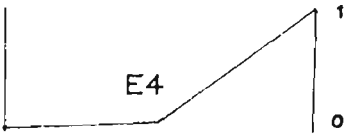
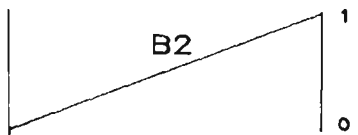
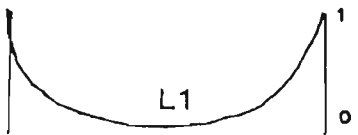
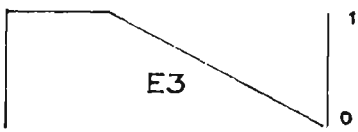
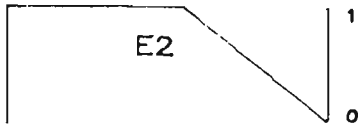
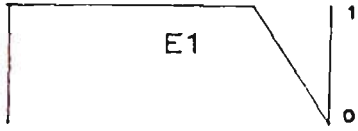
Figure A.10 Hypothetical Slip Number 2

## APPENDIX B

### RESIDUAL FACTOR DISTRIBUTIONS USED IN CHAPTER 4.

#### B.1 PROFILES OF RESIDUAL FACTOR DISTRIBUTIONS.





## B.2 RESIDUAL FACTOR COEFFICIENTS USED IN EQUATION (4.3).

	a	b	c	d
A1	-0.06	2.96	0.05	1.06
A2	-0.08	2.28	-0.29	1.08
B1	0.	0.	-1.	1.
C1	0.79	-2.28	-0.29	0.21
C2	1.11	-2.96	0.05	-0.12
D1	0.	0.	0.	1.
	-2.1E-12	26.80	-0.38	1.29
D2	0.	0.	0.	1.
	-3.3E-5	10.16	-0.31	1.17
D3	0.	0.	0.	1.
	-4.6E-3	5.27	-0.16	1.06
E1	0.	0.	0.	1.
	0.	0.	-4.	4.
E2	0.	0.	0.	1.
	0.	0.	-2.	2.
E3	0.	0.	0.	1.
	0.	0.	-1.33	1.33
F3	0.	0.	0.	1.
	3.50	-5.27	-0.16	0.14
G1	-0.02	5.27	-0.16	1.02
	0.	0.	0.	0.
H1	0.	0.	-1.33	1.
	0.	0.	0.	0.
H2	0.	0.	-2.	1.
	0.	0.	0.	0.
H3	0.	0.	-4.	1.
	0.	0.	0.	0.
I1	0.90	-5.27	-0.16	0.10
	0.	0.	0.	0.
I2	0.85	-10.16	-0.31	0.14
	0.	0.	0.	0.
I3	0.89	-26.80	-0.38	0.09
	0.	0.	0.	0.

K1	0.	0.	-2.	1.
	0.	0.	2.	-1.
L1	0.85	-10.16	-0.31	0.14
	3.3E-5	10.16	0.31	-0.17
M	0.	0.	0.	0.
N	0.	0.	0.	1.
O	0.	0.	-1.	1.
P	0.	0.	1.	0.
Q	0.	0.	0.	1.
	0.	0.	0.	0.
R	0.	0.	0.	0.
	0.	0.	0.	1.
B2	0.	0.	1.	0.
D4	0.	0.	0.	0.
	3.3E-5	10.16	0.31	-0.17
E4	0.	0.	0.	0.
	0.	0.	2.	-1.
H4	0.	0.	2.	0.
	0.	0.	0.	1.
I4	-0.85	-10.16	0.31	0.86
	0.	0.	0.	0.
K2	0.	0.	2.	0.
	0.	0.	-2.	2.
L2	-0.85	-10.16	0.31	0.86
	-3.3E-5	10.16	-0.31	1.17

## APPENDIX C

### ADDITIONAL INFORMATION ON COMPUTER PROGRAM MGSTRN.

#### C.1 BRIEF DESCRIPTION OF SUBROUTINES.

CNSTNT computes and stores values for the Gaussian integration constants used later when the moment equilibrium equations are solved. It is called once at the beginning of each new problem.

MTYPIN reads in the data describing the slope cross-section. Four sets of data are required.

- (a) Point data: points used to outline the slope profile or topline.
- (b) Line data: joins sets of two points to form lines and includes the assigned number of the soil underlying these lines.
- (c) Soil data: includes the total unit weight  $\gamma$ , the cohesion intercept  $c$ , friction angle  $\phi$ , pore pressure ratio  $r_u$  and the capillary head ratio  $r_c$ .
- (d) Phreatic Surface data:  $x$  and  $y$  co-ordinates of points forming the phreatic surface. Pore pressures will be calculated from this phreatic surface data if the value of  $r_u$  above is specified as 1.1.

MSLOPE sorts out randomly input point and line data and reassembles it into orderly arrays.

FRBODY reads in the x and y co-ordinates of the failure surface and divides the potential sliding mass into about 24 slices. Vertical slice boundaries are erected at the x co-ordinates of each of the following points:

- (a) All point data on or within the potential sliding mass.
- (b) All points where soil zone boundaries intersect the failure surface.
- (c) All points where the phreatic surface intersects the failure surface.
- (d) All points defining the failure surface.

If the number of slices created by this method is less than 24, boundaries will be erected at the centre of each slice which is wider than 7 percent of the overall width of the sliding mass. This process begins at the left end and stops when the number of slices equals 24 or when the right end is reached.

FBGEOM computes for each slice, the constants in Morgenstern and Price's equations and also determines the pore pressure ratio on the base of each slice. If pore pressure is represented by a phreatic surface, the subroutine NEUTRAL is called to compute  $r_u$  at each slice interface. The pore pressure ratio on each slice base is then taken as the average of the  $r_u$  values at the two sides of the slice.

JUNCTN is used by FBGEOM and OUTPUT to identify the soil boundaries which intersect each vertical slice interface. The soil on the right hand side of the interface is used as the effective soil type.

NEUTRL is used by FBGEOM and OUTPUT to compute the pore pressure ratio on slice bases in cases where the phreatic surface is used to define the piezometric head. The capillary head for points above the phreatic surface is computed as the vertical distance down to the phreatic surface, times the capillary head ratio.

FUNCTN reads in the side-force assumption and computes the values of

side-force constants. Several 'canned' side-force assumptions are available in the program. An arbitrary side-force assumption may also be input.

SOLUTN computes the boundary conditions  $E(N)$  and  $M(N)$  to be satisfied by the equations for  $E$  and  $M$ . The main task of this subroutine is the evaluation of the incremented values of  $F$  and  $\lambda$ . It also prints out each successive set of  $F$ ,  $\lambda$ ,  $E(N)$ ,  $M(N)$ , until convergence ( $\Delta F$  and  $\Delta \lambda$  less than 0.0001) occurs. If convergence does not occur within a designated number of iterations, control is transferred back to the main program.

NEWFSZ is called by SOLUTN to calculate increments for  $F$  and  $\lambda$ . It performs most of the detailed numerical calculations involved in the solution of Morgenstern's equations.

OUTPUT is called by the main program to compute and print detailed information on internal forces within the sliding mass.

C.2 INPUT DATA REQUIRED FOR PROGRAM.

Input Quantity	Symbol	Format
Point Data:		
point number	N	F4.0
x coordinate	X	F8.0
y coordinate	Y	F8.0
(999. at end of N column)		
Line Data:		
first point number	P1	F4.0
second point number	P2	F4.0
number of underlying soil	S	F4.0
(999. at end of P1 column)		



## Soil Data:

soil number	N	F4.0
total unit weight	G	F8.3
cohesion intercept	C	F8.3
angle of shearing resistance	P	F5.0
pore pressure ratio	ru	F5.1
capillary head ratio	rc	F5.1

(99. at end of N column)

## Phreatic Surface Points:

x coordinate	X	F8.0
y coordinate	Y	F8.0

(9999999. at end of X column)

## Failure Surface Points:

x coordinate	X	F8.0
y coordinate	Y	F8.0

(9999999. at end of X column)

## Side Force Assumption

ICHK	I1
------	----

A number corresponding to one of the side force assumptions presented later in this appendix must be entered here.

If assumptions 4 or 7 are used, the following additional data is required.

amplitude at left	F6.5
amplitude at right	F6.5

If assumption 8 is used, the function value, along with its corresponding x coordinate must be entered as follows.

x coordinate	X	F8.0
function value	FX	F8.0

(9999999. at end of X column)

## Factor of Safety estimate

F	F70.0
---	-------

Program control code

ICHK

I1

The program control code controls the operation of the program.  
The options available are as follows.

ICHK	Option
1	Change side-force assumption
2	Adjust failure surface
3	Input entirely new failure surface
4	Change soil properties
5	Change phreatic surface
6	Both (4) and (5)
7	Whole new problem
8	Terminate program

NOTE: After entering the factor of safety estimate, the program will attempt to obtain a solution for the problem. If the solution does not converge, the program expects a value of the constant  $\lambda$  to be entered (see chapter 2), followed by another estimate for the factor of safety. This procedure continues until the solution has converged or the program is aborted. The format of these two inputs is F70.0.

Also, in reply to yes/no questions when using the MGSTRN1 version of the program, enter the value 1 for YES and the value 0 for NO.

## C.3 COLUMN HEADINGS FOR DETAILED FORCE OUTPUT.

<u>Heading</u>	<u>Output Quantity</u>
No.	number of slice interface (from left to right).
X-COORD	x coordinate of slice interface.
SOIL	soil number at slice interface along failure surface.
RU	pore-pressure ratio on slice interface base.
F(X)	value of $f(x)$ at slice interface.
Q(I)	overburden stress at slice interface.
E(I)	total stress normal force at slice interface.
M(I)	moment (about centre-line of base of slice with left side at X-coordinate) of E(I) at slice interface.
YT	elev. of pt. of application of E(I) at slice interface.
YTL	elevation of topline at slice interface.
YTBAR	elev. of pt. of application of EBAR at slice interface.
YFS	elevation of failure surface at slice interface.
EBAR	effective stress normal force at slice interface.
NBAR	effective stress normal force on base of slice with right side at X-COORD.
XN	x coordinate of point of application of NBAR.
PHI	average friction angle required along slice interface when full cohesion is mobilized.

## NOTE:

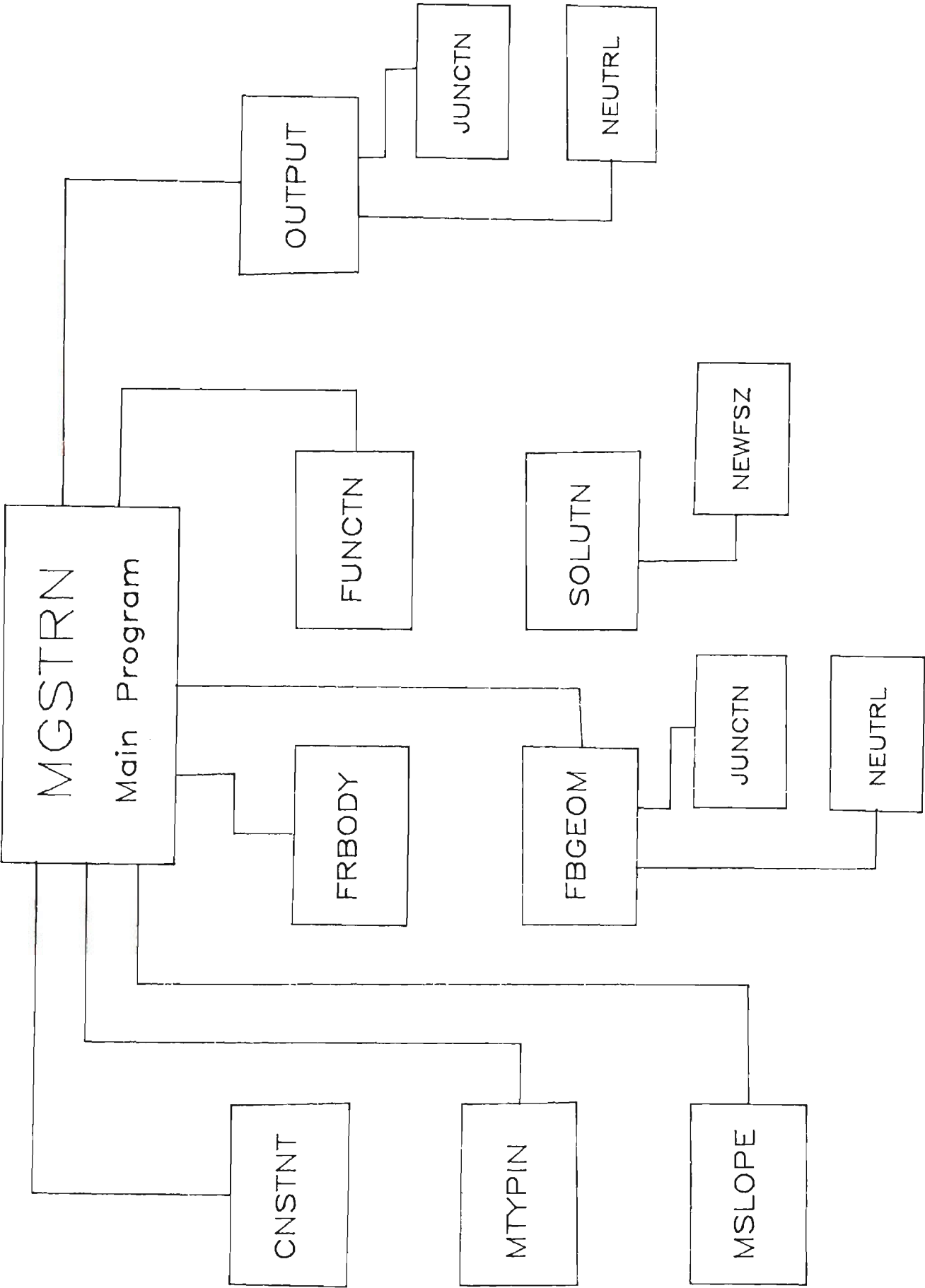
All distances are in feet or metres ;

All forces are in kips or tonnes ;

All moments are in kip-feet or tonne-metres ;

(depending on input units.)

C.4 SCHEMATIC LAYOUT OF MGSTRN PROGRAM.



## APPENDIX D

### BIBLIOGRAPHY

1. Ackenheil,A.C., 1954, 'A Soil Mechanics and Engineering Geology Analysis of Landslides in the Area of Pittsburgh, Pennsylvania', unpublished Ph.D. dissertation, University of Pittsburgh, pp. 83-87.
2. Alonso,E.E., 1976, 'Risk Analysis of Slopes and its Application to Slopes in Canadian Sensitive Clays', Geotechnique, Vol. 26, No. 3, pp. 453-473.
3. Andrei,S and Athanasiu,R., 1980, 'Stress Relation in Slope Stability Analysis', Proceedings of the International Symposium on Landslides, New Delhi, Vol. 1, pp. 105-108.
4. Athanasium,C., 1980, 'Non-Linear Slope Stability Analysis', Proceedings of the International Symposium on Landslides, Delhi, Vol. 1, pp. 259-262.
5. Azzouz,A.S., Baligh,M.M. and Ladd,C.C., 1981, 'Three-Dimensional Stability Analyses of Four Embankment Failures', Proceedings of the 10th International Conference on Soil Mechanics and Foundation Engineering, Stockholm, Vol. 3, pp. 343-346.
6. Barker,R. and Garber,M., 1978, 'Theoretical Analysis of the Stability of Slopes', Geotechnique, Vol. 28, No. 4, pp. 395-411.
7. Bailey,W.A., 1966, 'Stability Analysis by Limit Equilibrium', C.E. Thesis, Massachusetts Institute of Technology.
8. Barton,N., 1972, 'Progressive Failure of Excavated Rock Slopes', 13th Symposium for Rock Mechanics, Urbana (Illinois), Ed. E.J.Cording, ASCE, pp. 139-171.
9. Bell.,J.M., 1968, 'General Slope Stability Analysis', Journal of the Soil mechanics and Foundation Division, ASCE, Vol. 94, No. SM6, pp. 1253-1270.
10. Bernander,S., 1985, 'On Limit Criteria for Plastic Failure in Strain Rate Softening Soils', Proceedings of the 11th International Conference on Soil Mechanics and Foundation Engineering, San Francisco, Vol. 2, pp. 397-400.
11. Bernander,S. and Olofsson,I., 1981, 'On Formation of Progressive Failure in Slopes', Proceedings of the 10th International Conference on Soil Mechanics and Foundation Engineering, Stockholm, Vol. 3, pp. 357-362.

12. Bishop, A.W., 1955, 'Use of the Slip Circle in the Stability Analysis of Slopes', *Geotechnique*, Vol. 5, pp. 7-17.
13. Bishop, A.W., 1967, 'Progressive Failure with Special Reference to the Mechanism Causing It', *Proceedings of the Geotechnical Conference, Oslo*, Vol. 2, pp. 142-150.
14. Bishop, A.W., 1971, 'The Influence of Progressive Failure on the Choice of the Method of Stability Analysis', *Geotechnique*, Vol. 21, pp. 168-172.
15. Bishop, A.W. and Bjerrum, L., 1960, 'The Relevance of the Triaxial Test to the Solution of Stability Problems', *Proceedings of the ASCE Research Conference on the Shear Strength of Cohesive Soils, Boulder, Colorado*, pp. 437-501.
16. Bishop, A.W. et.al., 1971, 'A New Ring Shear Apparatus and its Application to the Measurement of Residual Strength', *Geotechnique*, Vol. 21, No. 4, pp. 273-328.
17. Bishop, A.W. and Morgenstern, N.R., 1960, 'Stability Coefficients for Earth Slopes', *Geotechnique*, Vol. 10, pp. 129-150.
18. Bjerrum, L., 1967, 'Progressive Failure in Slopes in Overconsolidated Plastic Clays and Clay Shales', *Terzaghi Lecture, Journal of the Soil Mechanics and Foundation Division, ASCE*, Vol. 93, No. SM5, pp. 3-49.
19. Bjerrum, L., 1969, 'Discussion of Main Session 5, Stability of Natural Slopes and Embankment Foundations', *Seventh International Conference on Soil Mechanics and Foundation Engineering, Mexico City, Mexico*, Vol. iii, pp. 377-414.
20. Booker, J.R., 1977, 'Introduction to the Finite Element Method', *Geotechnical Analysis and Computer Applications, University of Sydney School of Civil Engineering Course Notes*.
21. Broili, L., 1967, 'New Knowledge on the Geomorphology of the Vajont Slide Slip Surface', *Rock Mechanics and Engineering Geology*, Vol. 5, pp. 38-88.
22. Brown, C.B. and King, I.P., 1966, 'Automatic Embankment Analysis: Equilibrium and Instability Conditions', *Geotechnique*, Vol. 16, No. 3, pp. 209-219.
23. Chandler, R.J., 1977, 'Back Analysis Techniques for Slope Stabilisation Works: A Case Record', *Geotechnique*, Vol. 27, No. 4, pp. 479-495.
24. Chandler, R.J., 1984, 'Recent European Experience of Landslides in Overconsolidated Clays and Soft Rocks', *Proceedings of the 4th International Symposium on Landslides, Toronto*, Vol. 1, pp. 61-68.
25. Ching, R.K.H. and Fredlund, D.G., 1983, 'Some Difficulties Associated with the Limit Equilibrium Method of Slices', *Canadian Geotechnical Journal*, Vol. 20, pp. 661-672.

26. Chowdhury, R.N., 1976, 'Initial Stresses in Natural Slope Analysis', Rock Engineering for Foundations and Slopes, ASCE, Geotechnical Engineering Specialty Conference, Boulder (Colorado), Vol. 1, pp. 404-415.
27. Chowdhury, R.N., 1977, 'A New Approach to Slope Stability Studies', Research Report, Department of Civil Engineering, University of Wollongong, N.S.W., Australia.
28. Chowdhury, R.N., 1977, 'Propagation of Failure Surfaces in Natural Slopes', Research Report, Department of Civil Engineering, University of Wollongong, N.S.W., Australia.
29. Chowdhury, R.N., 1978, 'Slope Analysis', Elsevier Scientific Publishing Company, Amsterdam and New York.
30. Chowdhury, R.N., 1984, 'Recent Developments in Landslide Studies: Probabilistic Methods - State of the Art Report', Proceedings of the 4th International Symposium on Landslides, Toronto, Vol. 1, pp. 209-228.
31. Chowdhury, R.N., 1985, 'Successive Failures: A Probabilistic Approach', Proceedings of the 11th International Conference on Soil Mechanics and Foundation Engineering, San Francisco, Vol. 2, pp. 819-824.
32. Chowdhury, R.N. and A-Grivas, D., 1982, 'Probabilistic Model of Progressive failure of Slopes', Journal of the Geotechnical Engineering Division, ASCE, No. GT6, pp. 803-819.
33. Chowdhury, R.N. and DeRooy, E.R., 1985, 'Progressive Reliability of a Strain Softening Slope', Civil Engineering Transactions, Institution of Civil Engineers Australia, Vol. CE27, No. 1, pp. 79-94.
34. Chugh, A.K., 1986, 'Variable Factor of Safety in Slope Stability Analysis', Geotechnique, Vol. 36, No. 1, pp. 57-64.
35. Clough, R.W. and Woodward, R.J., 1967, 'Analysis of Embankment Stresses and Deformations', Journal of the Soil Mechanics and Foundation Division, ASCE, Vol. 93, No. SM4, pp. 529-549.
36. Crawford, C.B. and Eden, W.J., 1967, 'Stability of Natural Slopes in Sensitive Clays', Journal of the Soil Mechanics and Foundation Division, ASCE, Vol. 93, July, pp. 419-436.
37. Davis, E.H., 1977, 'Geotechnical Analysis and Computer Applications', University of Sydney School of Civil Engineering Course Notes.
38. Deere, D.U. and Patton, F.D., 1971, 'Slope Stability in Residual Soils', Proceedings of the Fourth Conference on Soil Mechanics for the Foundation of Engineers, State of the Art Report, 1, pp. 88-171.
39. DeLory, F.A., 1957, 'Long Term Stability of Slopes in Overconsolidated Clays', PH.D. Thesis, University of London.

40. Duncan, J.M. and Dunlop, P., 1969, 'Slopes in Stiff-fissured Clays and Shales', Journal of the Soil Mechanics and Foundation Division, ASCE, Vol. 95, No. SM2, pp. 467-491.
41. Dunlop, P. and Duncan, J.M., 1970, 'Development of Failure Around Excavated Slopes', Journal of the Soil Mechanics and Foundation Division, ASCE, Vol. 96, No. SM2, pp. 471-495.
42. Fellenius, W., 1936, 'Calculation of the Stability of Earth Dams', Transactions of the Second Congress on Large Dams (Washington), Vol. 4, p. 445.
43. Foerster, W. and Georgi, P., 1981, 'Application of a Stress-Strain-Time Relation', Proceedings of the 10th International Conference on Soil Mechanics and Foundation Engineering, Stockholm, Vol. 3, pp. 405-408.
44. Fredlund, D.G., 1984, 'Analytical Methods for Slope Stability Analysis', Proceedings of the 4th International Symposium on Landslides, Toronto, Vol. 1, pp. 229-250.
45. Hamel, J.V., 1968, 'Morgenstern and Price Method of Slope Stability Analysis', Report by the Department of Civil Engineering, University of Pittsburgh, to the U.S. Bureau of Mines, p. 149.
46. Hamel, J.V., 1972, 'The Slide at Brilliant Cut', Proceedings of the Thirteenth Symposium on Rock Mechanics, Urbana (Illinois), Edited by E.J. Cording, ASCE, pp. 487-510.
47. Hast, N., 1974, 'The State of Stress in the Upper Part of the Earths Crust as Determined by Measurements of Absolute Rock Stresses', Naturwissenschaften, Vol. 61, pp. 468-475.
48. Henkel, D.J., 1957, 'Investigations of Two Long-term Failures in London Clay Slopes at Woodgreen and Northolt', Proceedings of the Fourth International Conference on Soil Mechanics, London, Vol. 2, pp. 315-320.
49. James, P.M., 1970, 'Time Effects and Progressive Failure in Clay Slopes', PH.D. Thesis, University of London.
50. James, P.M., 1971, 'The Role of Progressive Failure in Clay Slopes', Proceedings of the First Australia - New Zealand Conference on Geomechanics, Vol. 1, pp. 344-348.
51. Janbu, N., 1954, 'Stability Analysis of Slopes with Dimensionless Parameters', Harvard Soil Mechanics Series, No. 46, p. 811.
52. Janbu, N., 1957, 'Earth Pressure and Bearing Capacity Calculations by Generalised Procedure of Slices', Proceedings of the Fourth International Conference and Foundation Engineering, Vol. 2, pp. 207-212.
53. Janbu, N., 1973, 'Soil Stability Computations', Embankment Dam Engineering, Casagrande Volume, Edited by R.C. Hirschfeld and S.J. Poulos, Wiley, New York, pp. 47-87.



54. Kenney,T.C., 1963, 'Stability of Cuts in Soft Soils', Journal of the Soil Mechanics and Foundation Division, ASCE, Vol. 89, No. SM5, pp. 17-37.
55. Kenney,T.C., 1967, 'The Influence of Mineral Composition on the Residual Strength of Natural Soils', Proceedings of the Geotechnical Conference, Oslo, Vol. 1, pp. 123-129.
56. Kirkpatrick,W.M., Khan,A.J. and Mirza,A.A., 1986, 'The effects of Stress Relief on some Overconsolidated Clays ', Geotechnique, Vol. 36, No. 4, pp. 511-525.
57. Langer,K., 1963, 'Discussion on Field Observations reported by K.Terzaghi', Proceedings 1st International Conference on Soil Mechanics and Foundation Engineering, Vol. 3, pp. 152-155.
58. Law,K.T. and Lumb,P., 1978, 'A Limit Equilibrium Analysis of Progressive Failure in the Stability of Slopes', Canadian Geotechnical Journal, Vol. 11, pp. 113-122.
59. Lo,K.Y., 1965, 'Stability of Slopes in Anisotropic Soils', Journal of the Soil Mechanics and Foundation Division, ASCE, Vol. 90, No. SM4, pp. 85-106.
60. Lo,K.Y., 1972, 'An Approach to the Problem of Progressive Failure', Canadian Geotechnical Journal, Vol. 9, p. 407.
61. Lo,K.Y., 1978, 'Regional Redistribution of In-situ Horizontal Stresses in Rocks of Southern Ontario', Canadian Geotechnical Journal, Vol. 15, pp. 371-381.
62. Lo,K.Y. and Lee,C.F., 1973, 'Stress Analysis and Slope Stability in Strain-softening Materials', Geotechnique, Vol. 23, No. 1, pp. 1-11.
63. Lo,K.Y. and Lee,C.F., 1973, 'Analysis of Progressive Failure in Clay Slopes'
64. Lo,K.Y., Lee,C.F. and Gelinas,P., 1972, 'An Alternative Interpretation of the Vajont Slide, Stability of Rock Slopes', Proceedings of the 13th Symposium on Rock Mechanics, ASCE, pp. 597-625.
65. Meyerhof,G.G., 1965, Discussion on paper 'Stability of Slopes in Anisotropic Soil', Journal of the Soil Mechanics and Foundation Division, ASCE, Vol. 91, No. SM6, p. 132.
66. Meyerhof,G.G. and Brown,J.D., 1967, Discussion on paper 'Boundary Conditions of Footings on Layered Clays', Journal of the Soil Mechanics and Foundation Division, ASCE, Sept. 1967, No. SM5.
67. Morgenstern,N.R., 1968, ''Ultimate Behaviour of Rock Structures', Rock Mechanics in Engineering Practice, Edited by O.C.Zienkiewicz and K.G.Stagg, Wiley, pp. 321-346.
68. Morgenstern,N.R. and Price,V.E., 1965, 'The Analysis of the Stability of General Slip Surfaces', Geotechnique, Vol. 15, No. 1, pp. 79-93.

69. Nelson, J.D. and Thompson, E.G., 1977, 'A Theory of Creep Failure in Overconsolidated Clay', Journal of the Geotechnical Engineering Division, ASCE, Vol. 103, No. GT11, pp. 1281-1294.
70. Nonveiller, E., 1965, 'The Stability Analysis of Slopes with a Slip Surface of General Shape', Proceedings of the 6th International Conference on Soil Mechanics and Foundation Engineering, Vol. 2, pp. 522-525.
71. Peck, R.B., 1967, 'Stability of natural Slopes', Journal of the Soil Mechanics and Foundation Division, ASCE, Vol. 93, No. SM4, pp. 403-417.
72. Pells, P.J.N., 1977, 'Slope Stability Analysis', Geotechnical Analysis and Computer Applications, University of Sydney School of Civil Engineering Notes.
73. Peterson, R., 1954, 'Studies of Bearpaw Shale at a Dam Site in Saskatchewan', Proceedings of the Soil Mechanics and Foundation Division, ASCE, Vol. 80, Separates No. 476 and 759.
74. Peterson, R., 1955, Closure of 'Studies of Bearpaw Shale at a Dam Site in Saskatchewan', Proceedings of the Soil Mechanics and Foundation Division, ASCE, paper No. 759, pp. 1-2.
75. Peterson, R., Jasper J.L., Rivard, P.J. and Iverson, N.L., 1960, 'Limitations of Laboratory Shear Strength in Evaluating Stability of Highly Plastic Clays', ASCE Research Conference on Shear Strength of Cohesive Soils, Boulder, Colorado, pp. 765-791.
76. Reddy, A.S. and Srinivasan, 1967, 'Boundary Conditions of Footings on Layered Clays', Journal of the Soil Mechanics and Foundation Division, ASCE, March 1967, pp. 83-99.
77. Reddy, A.S. and Venkatakrishna Rao, K.N., 1982, 'Stability of Slopes by Method of Characteristics', Journal of the Geotechnical Engineering Division, ASCE, No. GT9, pp. 1182-1186.
78. Rivard, P.J. and Lu, Y., 1978, 'Shear Strength of Soft Fissured Clays', Canadian Geotechnical Journal, Vol. 15, pp. 382-390.
79. Romani, F., Lovell, C.W. and Barr, M.E., 1972, 'Influence of Progressive Failure on Slope Stability', Journal of the Soil Mechanics and Foundation Division, ASCE, Vol. 98, No. SM11, pp. 1209-1223.
80. Sallfors, G.B. and Larsson, R., 1984, 'State of the Art report: Soft Clays in Sweden', Proceedings of the 4th International Symposium on Landslides, Toronto, Vol. 1, pp. 131-140.
81. Sarma, S.K., 1973, 'Stability Analysis of Embankments and Slopes', Geotechnique, Vol. 23, pp. 423-433.
82. Sarma, S.K. and Bhawe, M.V., 1974, 'Critical Acceleration vs. Static Factor of Safety in Stability Analysis of Earth Dams and Embankments', Geotechnique, Vol. 24, pp. 661-665.

83. Sevaldson, R.A., 1956, 'The Slide in Lodalen, October 6th 1954', *Geotechnique*, Vol. 6, No. 4, pp. 167-182.
84. Sidharta, A.S., 1985, 'Prediction of Creep Failure of Excavations in Overconsolidated Clay with Pore Pressure Dissipation', Postgraduate Research Thesis, Department of Civil Engineering, Colorado State University.
85. Skempton, A.W., 1945, 'A Slip in the West Bank of the Eau Brink Cut', *Journal of the Institute of Civil Engineers*, London, Vol. 24, No. 7, pp. 267-289.
86. Skempton, A.W., 1948, 'The  $\phi=0$  Analysis of Stability and its Theoretical Basis', *Proceedings of the 2nd International Conference on Soil Mechanics and Foundation Engineering*, Rotterdam, Vol. 1, pp. 145-150.
87. Skempton, A.W., 1961, 'Horizontal Stresses in Over-consolidated Eocene Clay', *Proceedings of the 5th International Conference on Soil Mechanics and Foundation Engineering*, Paris, Vol. 1, pp. 351-357.
88. Skempton, A.W., 1964, 'Long Term Stability of Clay Slopes', Rankine Lecture, *Geotechnique*, Vol. 14, pp. 77-101.
89. Skempton, A.W., 1970, 'First Time Slides in Over-consolidated Clays', *Geotechnique*, Vol. 20, pp. 320-324.
90. Skempton, A.W., 1977, 'Slope Stability in Cuttings in Brown London Clay', *Proceedings of the 9th International Conference on Soil Mechanics and Foundation Engineering*, Tokyo, Vol. 3, pp. 261-271.
91. Skempton, A.W., 1985, 'Residual Strength of Clays in Landslides, Folded Strata and the Laboratory', Special Lecture, *Geotechnique*, Vol. 35, No. 1, pp. 3-18.
92. Skempton, A.W. and Brown, J.D., 1961, 'A Landslide in Boulder Clay at Selset, Yorkshire', *Geotechnique*, Vol. 1, No. 4, pp. 280-293.
93. Skempton, A.W. and Delory, F.A., 1957, 'Stability of Natural Slopes in London Clay', *Proceedings of the 4th International Conference on Soil Mechanics and Foundation Engineering*, London, Vol. 2, pp. 378-381.
94. Skempton, A.W. and Hutchinson, J.N., 1969, 'Stability of Natural Slopes and Embankment Foundations, State of the Art Report', *Proceedings of the 7th International Conference on Soil Mechanics and Foundation Engineering*, Mexico, pp. 291-335.
95. Skempton, A.W. and LaRochelle, P., 1965, 'The Bradwell Slip: A Short-term Failure in London Clay', *Geotechnique*, Vol. 15, No. 3, pp. 221-242.
96. Skempton, A.W. and Petley, D.J., 1967, 'The Strength Along Structural Discontinuities in Stiff Clays', *Proceedings of the European Conference on Soil Mechanics and Foundation Engineering*, Vol. 2, pp. 29-46.

97. Sotiropoulos,E. and Cavounidis,S., 1981, 'Irregular Stress-Strain and Progressive Failure', Proceedings of the 10th International Conference on Soil Mechanics and Foundation Engineering, Stockholm, Vol. 3, pp. 527-531.
98. Spencer,E., 1968, 'Effect of Tension on Stability of Embankments', Journal of the Soil Mechanics and Foundation Division, ASCE, Vol. 94, No. SM5, pp. 1159-1173.
99. Spencer,E., 1968, 'Stability of Earth Embankments', Reprint from Civil Engineering journal.
100. Tang,W.H., Chowdhury,R.N. and Sidi, 1985, 'Progressive Failure Probability of Soil Slopes', Proceedings of ICOSSAR, Kobe, Japan, T34B, III, pp. 363-372.
101. Tavenas,F. and Leroueil,S., 1981, 'Creep and Delayed Failure of Slopes in Clays', Canadian Geotechnical Journal, Vol. 18, pp. 106-120.
102. Taylor,D.W., 1937, 'Stability of Earth Slopes', J. Boston Society of Civil Engineering, Vol. 24, p. 197.
103. Taylor,D.W., 1948, 'Fundamentals of Soil Mechanics', John Wiley and Sons, N.Y.
104. Ter-Stepanian,G., 1977, 'Behaviour of Clays Close to Failure', Proceedings of the 9th International Conference on Soil Mechanics and Foundation Engineering, Tokyo, Vol. 1, pp. 327-328.
105. Terzaghi,K., 1936, 'Stability of Slopes in Natural Clay', Proceedings of the 1st International Conference on Soil Mechanics and Foundation Engineering, Harvard, Vol. 1, pp. 161-165.
106. Terzaghi,K. and Peck,R.B., 1948, 'Soil Mechanics in Engineering Practice', John Wiley and Sons, N.Y.
107. Thompson,S. and Tweedie,R.W., 1978, 'The Edgerton Landslide', Canadian Geotechnical Journal, Vol. 15, pp. 510-521.
108. Vaughan,P.R. and Kwan,C.W., 1984, 'Weathering, Structure and In-situ Stress in Residual Soils', Geotechnique, Vol. 34, No. 1, pp. 43-59.
109. Whitman,R.V. and Bailey,W.A., 1967, 'Use of Computers for Slope Stability Analysis, Journal of the Soil Mechanics and Foundation Division, ASCE, Vol. 93, No. SM4, pp. 475-498.
110. Whitman,R.V. and Moore, 1963, 'Thoughts Concerning the Mechanics of Slope Stability Analysis', Proceedings of the 2nd Pan American Conference on Soil Mechanics and Foundation Engineering, Vol. 1, pp. 391-411
111. Wilson,S.D., 1970, 'Observational Data on Ground Movements Related to Slope Instability', Sixth Terzaghi Lecture, Journal of the Soil Mechanics and Foundation Division, ASCE, Vol. 96, No. SM5

112. Wright, S.G., 1975, 'Evaluation of Slope Stability Analysis Procedures', Preprint 2616, ASCE National Conference, Denver, Colorado.
113. Wright, S.G., Kulhawy, E.D. and Duncan, J.M., 1973, 'Accuracy of Equilibrium Slope Stability Analysis', Journal of the Soil Mechanics and Foundation Division, ASCE, Vol. 99, No. SM10, pp. 783-793.
114. Wu, T.H., Williams, R.L., Lynch, J.E. and Kulatilake, P.H.S.W., 1987, 'Stability of Slopes in Red Conemaugh Sale of Ohio', Journal of the Geotechnical Engineering Division, ASCE, Vol. 113, No. 3, pp. 248-264.
115. Yucemen, M.S., Tang, W.H. and Ang, A.H., 1973, 'A Probabilistic Study of Safety and Design of Earth Slopes', Civil Engineering Studies, Structural Research Series No. 402, University of Illinois, Urbane, Illinois.